POLITECNICO DI TORINO

Department of Structural, Geotechnical and Building Engineering

Master of Science in Civil Engineering

Master Thesis

Analysis of the optimal diagrid geometry for tall buildings based on the desirability function

Supervisor
Prof. Alberto Carpinteri

Candidate
Bonierose Albitos

Co-supervisors
Prof. Giuseppe Lacidogna
Dr. Ing. Domenico Scaramozzino PhD

December 2021

Abstract

The evolution of tall buildings has taken place worldwide, starting in the United States in the twentieth century, from the conventional moment resisting frame to more effective structural systems, such as braced tubes and diagrid structures. In this Thesis, attention has been paid on diagrid structures. Despite the lack of conventional vertical columns along the exterior of the building, their capacity to withstand lateral loads has made the diagrids highly appreciated in the fields of structural engineering and architecture. In particular, many researchers have emphasized their enhanced structural performance and ground-breaking aesthetic characteristics.

The main purpose of the study is to identify the optimal diagrid geometry able to ensure simultaneously a good structural behaviour, in terms of lateral and torsional stiffness, low consumption of material and easiness of construction. In the existing literature, this investigation has usually been carried out through optimization processes where some geometrical parameters, like the diagonal inclination and floor plan shape, are changed and the building performance is assessed. However, when the population of the geometrical solutions is wide, this procedure can hardly be implemented manually, or within a Finite Element Method (FEM) environment due to onerous computational costs. In this Thesis, the analysis has been performed by using the matrix-based method (MBM) coupled with the desirability function approach. The MBM allows to perform the structural analysis of the diagrid system considering fewer degrees of freedom than FEM. The desirability function approach is an optimization method, that leads to the selection of the optimal design parameters within a multi-response framework. The analysis had the goal of selecting the optimal geometry, out of a set of both uniform- and varying-angle diagrid structures, optimizing multiple responses. The outcomes of this analysis demonstrated the usefulness and the simplicity of the presented approach for the optimization of diagrid structures for the preliminary design.

Acknowledgments

Before entering in detail about my Thesis, I would like to express my deep gratitude to all people who have contributed to achieve this important goal at the end of my university journey at Politecnico of Turin.

First of all, I would like to thank my supervisors. Thanks to prof. Alberto Carpinteri for giving me the possibility to carry out this Thesis on topic that interests me as student in structural engineering. Thanks to prof. Giuseppe Lacidogna for guiding me through thought-provoking suggestions and advice. Thanks to PhD Domenico Scaramozzino for supporting me step by step during the development of the Thesis, for patience and for motivation by sharing his knowledge on the Thesis topic.

Now, I would like to give a special thanks to my beloved family starting from my parents, Rosario and Bonifacio, who have unconditionally supported me from the beginning and always encourage me on every decision I have made in my life. This achievement is mainly thanks to them who have worked hard to lead me to a better future. Thanks to my older brothers, Arsent and Albert, for moral support and for pleasant and memorable moments shared together.

Thanks to my best friend, Francesca, and to my friends, Andrea, Serena, Federica M., Federica C. and Ethan, who I have met at middle and high school, for spending lots of cheerful and carefree days between laughter and karaoke nights and for helping me to face my university journey. Thanks to all colleagues who I have met at university but especially to Paola, Annalisa, Gianbattista, Marisa and Giulia for making my journey more stimulating among several projects, lessons, breaks and exams and for invaluably constructive exchange of ideas, ensuring my professional growth.

Last but not least, I would also like to thank all people who have believed in me.

Bonierose Albitos

CONTENTS

LIST OF TABLES

LIST OF FIGURES

Chapter 1

1. INTRODUCTION

In the 18th century a significant tall building development begun, especially in United States, to cope with the rapid growth of urban population and consequent reduction of the land. The first tall buildings consisted of simple structural systems based on the conventional moment resisting frame, but over time new typologies have been emerged such as diagrid systems. The latter has been recognized as efficient structural system with high aesthetic potential able to resist better to lateral loads without vertical columns. The Chapter 1.1 summarizes the evolution of tall buildings until diagrid systems, underlying their main features. In Chapter 1.3.1 an overview of researches on diagrid are described regarding the preliminary design, the structural analysis in Chapter 1.3.2 and, finally, the application of optimization process in Chapter 1.3.3.

1.1. THE HISTORY OF HIGH-RISE BUILDINGS

A tall building can be defined as a high-rise structure having multiple floors. Its structural design is highly influenced by lateral forces, as wind and earthquake actions due to considerable height. The tall building development started in the 1880s for commercial and residential purposes. The necessity of having adjacent business activities in the city centre as near as possible, the necessity to provide peculiar landmarks for commercial organizations and to satisfy the business and tourist community demand led to a rapid growth of tall commercial buildings [1]. The urban cities advancement has been greatly determined by an accelerated increasing of the world population moving from rural areas to cities. The desire to limit the urban expansion on land without reducing agricultural production and the high land cost are the main causes of an upward building evolution in 18th and 19th centuries. In order to guarantee the high-rise building development, three important factors have to be considered: available materials, the level of construction technology and the types of service purposes necessary for the use of the building [1]. For these reasons, the advancement proceeded step by step whenever new material, construction method or computer technology was introduced.

In the 19th century, the Second Industrial Revolution, leading to socioeconomic issues and high demand for land, especially in the United States, created a boost to promote tall buildings growth, that was possible only thanks to two essential technical innovations: the introduction of new material able to resist more and be more efficient, steel, and the introduction of the elevator ensuring to get easily to upper floors. The first high-rise tall building characterized by steel frame was the 11-story Home Insurance Building in Chicago in 1883, but in 1931 one of the most important American skyscrapers was built, the Empire State Building, whose 102-story braced steel frame reached 381 m of height (Figure 1.2a). Moreover, at that time this height was considered considerable, and it was achieved not through technological evolution, but through excessive material consumption leading to an over-designed structure [2].

During the 1930s a severe worldwide economic depression, the Great Depression, stopped the skyscraper evolution, but after the World War II new structural systems different from the conventional rigid frames were proposed by means of modernized design and construction techniques. Furthermore, in the 1960s Fazlur Khan developed the "premium-for-height" framework that constituted a ground-breaking step for tall building design. According to Khan, the structural design of high-rise building was controlled by the lateral sway due to wind load and therefore different structural systems are necessary for increasing heights [3]. Consequently, the higher is the number of stories, the higher is the premium for height. Figure 1.1 shows the steel consumption, which increases linearly with the number of stories if the building is subjected only to gravity loads, but it increases drastically for buildings under lateral loads. The design aim is to minimize the weight of steel by choosing an appropriate structural system [3]. As a matter of fact, in 1973 the Empire State Building was beaten by the twin towers of the 110-story, 412 m high World Trade Center in New York, using framed-tube construction. The necessity to reflect different function requirements, such as providing large column-free open areas, led to different structural systems.

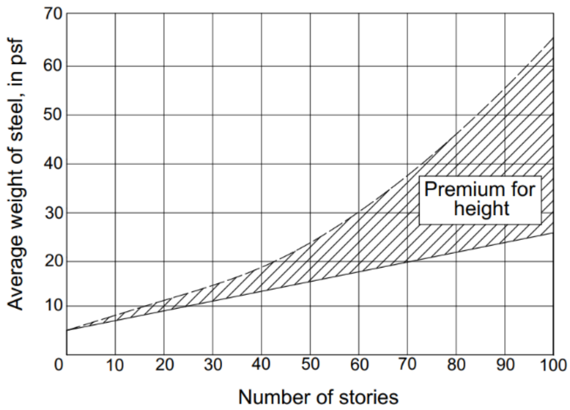

Figure 1.1 - Premium for height

1.2. EMERGING DEVELOPMENTS FOR DIAGRID STRUCTURES

In the late 19th century, diagonal bracing structural members were acknowledged as efficient to withstand lateral actions arising from wind and earthquake actions in high-rise building design. Thus, the taller the building, the more critical the lateral drifts and the necessity of diagonals in the structure becomes fundamental to carry properly lateral forces. Moreover, a taller building leads to a sudden rise of material consumption. Although the presence of diagonals was recognized as an improvement for the structural behaviour, the diagonals constituted an obstruction to the outside view limiting the aesthetic image. Thus, diagonals were usually installed within the building cores which were placed internally.

In the late 1960s a new structural solution in tall building design was emerged and it was based on the use of a braced tube system. One of the most important examples was the John Hancock Building in Chicago which is characterized by external perimeter diagonals with a X configuration that cross several stories (Figure 1.2b). This structural system allowed to reach considerable heights, to reduce the steel consumption, to resist higher lateral forces and to open internal spaces with increased usable surface. All these features made the braced tube system an architectural symbol at that time. The braced tube system derives from the framed tube, in which the lateral stiffness is provided by closely spaced perimeter columns. However, framed tubes ensured a lower structural performance and higher material usage than braced tubes.

(a)

(b)

Figure 1.2 - Tall buildings structural system: (a) Empire State Building in New York: moment resisting frame (Source: myusa.it) (b) John Hancock Center in Chicago: braced tube system (Source: wikipedia.org/wiki/John_Hancock_Center)

The use of external diagonals developed a such strong interest in tall building design from an architectural and engineering point of view that a further step occurred in tall building design concerned the introduction of an innovative structural system called diagrid. The term ‘diagrid’ was obtained by the combination of two words: “diagonal” and “grid”. It means that both vertical and horizontal loads are carried by only the external perimeter diagonals without the help of vertical columns that are present in the conventional braced tube solution. Furthermore, diagrid structures, where diagonal members carry shear by axial action, are more efficient in minimizing shear deformation than conventional braced frame structures, where shear is carried by the bending of vertical columns [4].

The first diagrid structure was built before the realization of the John Hancock Center, in the 1970, by the Russian architect Vladimir Shukhov in Moscow (Figure 1.3a). The structure is a broadcasting tower 160 m tall made of steel. It is a hyperboloid structure, and the diagrid structure allows to minimize the wind load and the required material [5]. The first construction of high-rise building using diagrid system was the IBM Building in Pittsburgh built in 1963 (Figure 1.3b). The building is constituted by a steel exoskeleton lean on eight piers and an internal central core. Moreover, the façades have a peculiar aesthetic effect given by stainless steel and glass panels. Nevertheless, the diagrid system was not recognized until the 21st century when other diagrid structures have been constructed like the Swiss Re’s Building in London and the Hearst Tower in

New York. Both have been designed by Sir Norman Foster. The Swiss Re's Building (also known as 30 St Mary Axe or the Gherkin) is a 40-story steel framed office building with a circular plan of varying size and it reaches 180 m (Figure 1.3c). The double curvature of the building façade provides an aerodynamic behaviour limiting wind actions and open space offices [6] [7]. Similarly, the Hearst Tower is a 46-story building, 183 m tall (Figure 1.3d). The diagrid structure provides stability requirement under vertical and horizontal loads increasing both lateral stiffness and strength. Moreover, this innovative structural system allows to reduce 20% of the steel consumption with respect to an equivalent conventional moment frame structure [8] [9]. After a few years many diagrid buildings have been built throughout the world, mainly in American and in Asian countries. Some main examples are the CCTV Headquarters and the Guangzhou West Tower in China, the Bow in Canada, the Capital Gate in United Arab Emirates, and the Tornado Tower in Qatar [10]. These buildings are made of steel because of speed of construction and cheap formworks. Nonetheless, there are few examples of concrete diagrid structures as the O-14 Building in Dubai and the Doha Tower in Doha [3].

(a) (b) (c) (d)

Figure 1.3 - Diagrid structures: (a) Shukhov Tower in Moscow (Source: http://www.skyscrapercenter.com/) (b) IBM Building in Pittsburgh (Source: ©Natalia Melikova The Constructivist Project) (c) Swiss Re Tower in London (Source: © 2019 Michael Tessler) (d) Hearst Tower in New York (Source: https://www.swissre.com/)

Diagrid structure developments have been rapidly increasing worldwide due to the main following features summarized as:

1) Lesser amount of structural material than conventional structural systems composed of orthogonal members. Figure 1.4 shows the difference between the orthogonal structure and the three-dimensional model of a diagrid structure;

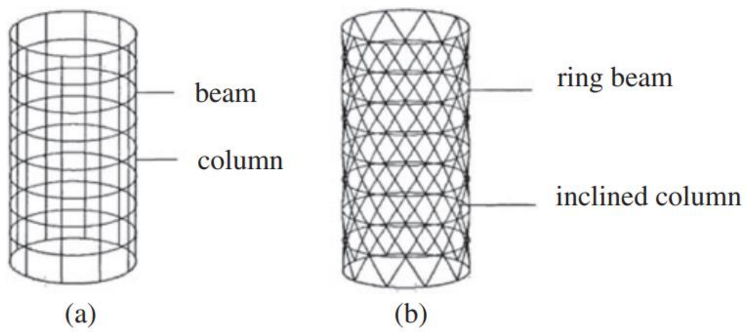

Figure 1.4 - 3D model and structural members: (a) orthogonal structure (b) diagrid structure [11]

2) Easy prefabrication and construction techniques thanks to the modularity and repetitive operations;
3) Able to address most of the designing requirements in terms of lateral stiffness and strength reaching enhanced structural performance;
4) Peculiar aesthetic appearance and remarkable architectural effect provided by the outer arrangement of diagonal columns and beams, which gives to the building a unique diamond shape pattern, interior column-free floor spaces and flexibility on the plan design.

As known in tall building design, the dominant design factor is the lateral force due to wind and seismic loads and therefore in order to resist to these actions internal and external resisting systems have to be considered. In the case of the diagrid system the external system, located along the building perimeter, is made up of repetitive triangular units constituted by diagonal columns and a ring beam, providing an efficient performance [10]. These structural members are hinged at nodes, as illustrated in Figure 1.5. Generally, when the diagrid structure is subjected to both vertical and horizontal loads, axial forces mainly arise in diagonals. However, shear and bending stresses could be present in diagonals that extend over multiple stories because of the supported floor beams at intermediate floors. Nonetheless, these stresses can be disregarded in the preliminary design. By observing the existing diagrid structures, it can be also found that the internal resisting system is typically provided by an internal core. Thus, the external diagrid system, coupled with the internal core, assumes the so-called tube in tube configuration. Note that in preliminary design the diagrid structure is designed under gravity and lateral loads, whereas the internal core only under gravity load [10].

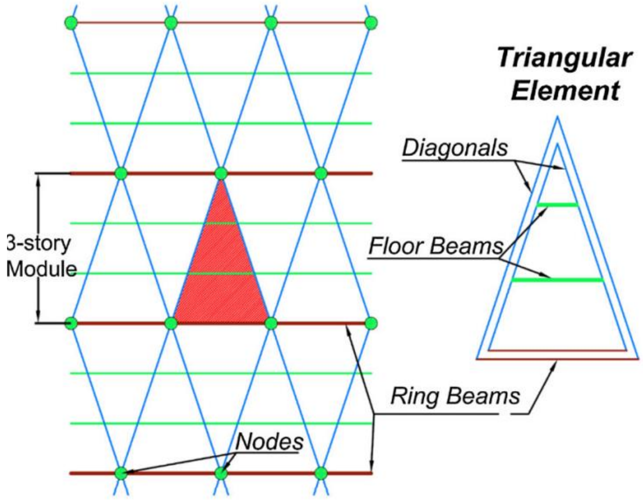

Figure 1.5 - Three 3-story diagrid modules and a sample triangular element [12]

1.3. OVERVIEW OF THE EXISTING LITERATURE RELATED TO DIAGRID SYSTEMS

The structural, architectural and economic advantages described in the previous Chapter 1.2 allowed diagrid structures to be recognized as emerging innovative solutions in recent years, therefore several research works have been developed in order to promote advanced design strategies and make diagrid system more efficient and more economical [13]. These studies underline the diagrid structural behaviour in function of different but important parameters like the height, the numbers of stories for each module and the diagonal inclinations. Differently from traditional structural types, few design methodologies have been developed and therefore many researchers tried to carry out investigations as a means to provide guidelines and provisions to engineers and architects for diagrid structure design [14].

1.3.1. METHODOLOGY FOR THE PRELIMINARY DESIGN

The preliminary design of diagrid structure is necessary in order to determine the preliminary diagonal sizes rapidly and this procedure is useful to make decisions at the early stage of design for both architects and engineers. For these reasons many researchers have carried out many investigations on this problem for determining a simplified and approximate method. Among all the researchers it is worth to note Moon et al. [4] and Montuori et al. [14].

According to Moon's research, in the preliminary design, the internal core lateral stiffness is neglected because its contribution is only 15-20% of the total despite both diagrid structure and internal core provide lateral stiffness to lateral action. The design methodology proposed in [4] presents an empirical guideline for assessing diagonal cross-sectional areas necessary to limit the lateral displacement, starting from the evaluation of the relative contribution of bending and shear deformations to the total lateral displacement of a diagrid structure with rectangular plan, vertical facades and constant diagonal inclination along the height of the building. The Moon's methodology of preliminary design of diagrid structures is a stiffness-based approach that considers the building as a beam divided into modules. In the case of this study, the module is defined by two triangular elements covering a height h as shown in Figure 1.6 and the diagonals are inclined with an angle θ. The tall building façade can act as either web or flange elements in function of the loading direction. Moreover, the diagonals are subjected only to axial forces as they are assumed to be pin ended [4].

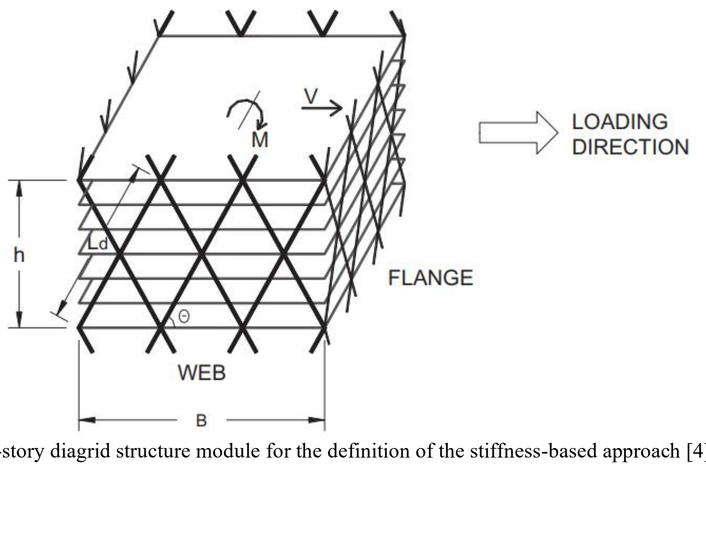

Figure 1.6 - Six-story diagrid structure module for the definition of the stiffness-based approach [4]

The assessment of cross-sectional areas for each module is carried out determining equations that correlate shear force V and bending moment M respectively to relative displacement Δu and relative rotation $\Delta\beta$:

$$V = K_T \Delta u \tag{1.1}$$

$$M = K_B \Delta\beta \tag{1.2}$$

The relative displacement and rotation are calculated as the product of module height and transverse shear γ and bending deformation χ, respectively.

By means of compatibility, constitutive and equilibrium equations, it is possible to evaluate the bending and shear stiffnesses as:

$$K_T = 2N_w \left(\frac{A_{d,w}E}{L_d} \cos^2\theta\right) \tag{1.3}$$

$$K_B = (N_f + \delta) \left(\frac{B^2 A_{d,w} E}{2L_d}\right) \sin^2\theta \tag{1.4}$$

Where N_w and N_f are the total number of diagonals in the web and façade, respectively, $A_{d,w}$ and $A_{d,f}$ the cross-sectional area of the web and flange members, E the elastic modulus, B the web dimension, L_d the diagonal length and δ is the web diagonals contribution for bending rigidity. At that point, fixing the desired transverse shear and bending deformations, γ^* and χ^*, and for given V and M, the preliminary cross-sectional areas expressions in the web and flange are obtained:

$$A_{d,w} = \frac{VL_d}{2N_w E_d h \gamma^* \cos^2\theta} \tag{1.5}$$

$$A_{d,f} = \frac{2ML_d}{(N_f + \delta)\, B^2 E_d \chi^* h sin^2\theta} \tag{1.6}$$

As specified before, the lateral load can be applied in different directions, thus each diagonal can act as either a web or flange member and its cross-sectional area would be evaluated as the maximum value from Equations (1.5) and (1.6).

According to stiffness-based approach, in order to define γ^* and χ^* the top deflection is expressed in function of them assuming the building as a cantilever beam:

$$u(H) = \gamma^* H + \frac{\chi^* H^2}{2} \tag{1.7}$$

Where $\gamma^* H$ and $\frac{\chi^* H^2}{2}$ are the contribution from shear and bending deformation, respectively. Each contribution can be determined by introducing a dimensionless factor s, defined as the ratio between the top displacement due to bending and the top displacement due to shear [4]:

$$s = \frac{\left(\frac{\chi^* H^2}{2}\right)}{\gamma^* H} = \frac{H\chi^*}{2\gamma^*} \tag{1.8}$$

Imposing the maximum allowable displacement as $u(H) = \frac{H}{\alpha}$, the desired transverse shear and bending deformations expressions are:

$$\gamma^* = \frac{1}{(1+s)\alpha} \tag{1.9}$$

$$\chi^* = \frac{2\gamma^* s}{H} = \frac{2s}{H(1+s)\alpha} \tag{1.10}$$

The dimensionless factor s governs the preliminary cross-sectional areas of diagonal members. Indeed, if s assumes high values, the top displacement contribution due to bending is dominant with respect to the one due to shear and the design of diagonal area is mainly affected by shear deflection. On the contrary, if s assumes low values, the shear contribution prevails and the design is governed by bending deflection. Moreover, Moon et al. carried out further studies on the optimal value of s in function of the height to width ratio H/B and the proposed empirical expression is $s = \left(\frac{H}{B} - 3\right)$ valid for $\frac{H}{B} \geq 5$ and $60° \leq \theta \leq 70°$.

Another geometrical attribute considered major in preliminary design is the diagonal angle θ since it influences the structural behaviour. In this article [4] the authors highlight the influence of the diagonal angle on the structural behaviour of tall buildings. As a matter of fact, they have found that the optimal angle for maximum shear rigidity is about 35° for the case of 60-story structure, meanwhile the optimal angle for maximum bending rigidity is 90°. It means that in diagrid system the optimal angle will fall between these two extreme values. From a structural perspective, shear behaviour prevails in short buildings and bending behaviour prevails in tall buildings. As a consequence, the higher is the building, the higher will be the optimal diagonal angle.

In the following year Moon published another research paper [15] in which the previous stiffness-based approach is applied to braced tube systems. Differently from diagrid structure, in the braced tube solution the mega-diagonals are subjected to shear force and the perimeter vertical columns to bending moment. In this study Moon proposed another empirical expression for the optimal s value, $s_{opt} = H/2B - 1$, obtained considering height to width ratio higher than 6 and diagonal angle between 40° and 50°. The same models were also employed for diagrid tall building analysis and a new empirical equation was suggested, $s_{opt} = H/B - 2$, valid for height to width ratio higher than 6 and θ between 60° and 70°.

Although tall building design is mainly influenced by stiffness requirement, consisting into limiting the lateral displacement at the top of the building, in some cases the strength requirement can become primary in the design criteria. This methodology is called strength-based approach and it is proposed by Montuori et al. in [14]. The investigations are focused on the assessment of simplified formulae for determining rapidly cross-sectional area of diagonals according to the strength-based design. At the end the results were compared to the ones obtained from the stiffness-based design proposed by Moon in order to understand which one governs the design in specific conditions. The research paper analyses a 100-story building whose shaft is divided into diagrid modules. Each module m is subjected to three actions, i.e. the gravity load Q_m, the shear force V_m and the overturning moment M_m, that generate compression and tension axial forces in the diagonals as shown in Figure 1.7.

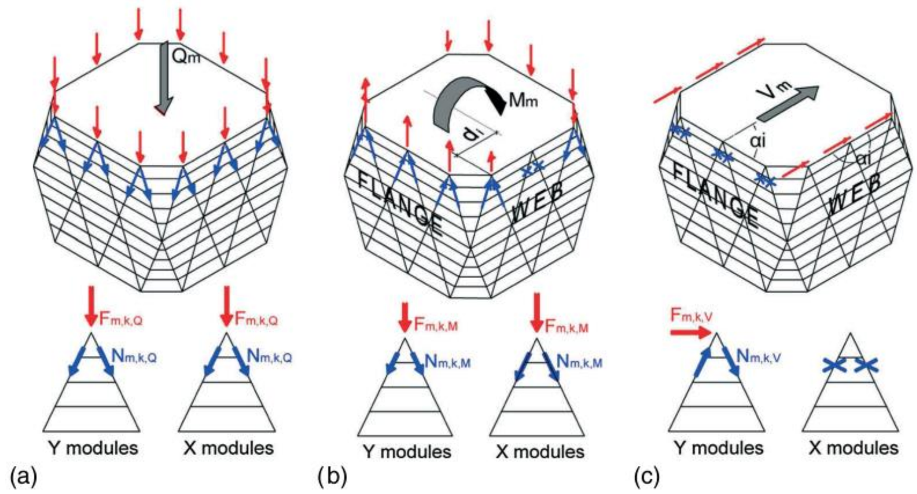

Figure 1.7 - Diagrid module scheme for the strength-base preliminary design. Axial force in diagonals of the k-th triangular scheme of the m-th module due to: (a) gravity loads Q_m (b) overturning moment M_m (c) global shear V_m [14]

The gravity loads produce a global downward force $F_{m,k,G}$ on each module equal to the 37.5% of the total floor load supposing that the internal core holds the 25% of the total floor area. Thus, the compressive axial force in each diagonal is assessed as follows:

$$N_{m,k,Q} = \frac{0{,}375\ Q_m}{n_k} \frac{sen\theta}{2} \tag{1.11}$$

The wind load gives rise to overturning moment and shear force. The overturning moment generates uniform compression and tension state in the diagonals of leeward and windward façade, respectively, and a linear distribution in the webs, arising the following axial force:

$$N_{m,k,M} = \pm \frac{M_m d_k}{\sum_{i=1}^{n_k} d_i^2} \frac{sen\theta}{2} \tag{1.12}$$

Where d_i is module distance from plan shape centroid

The global shear force leads to horizontal force causing compression and tension forces in diagonals belonging to web facades.

$$N_{m,k,V} = \pm \frac{V_m cos\alpha_k}{\sum_{i=1}^{n_k} cos\alpha_i} \frac{cos\theta}{2} \tag{1.13}$$

Where α is the angle between module and wind direction.

By summing all the previous contributions from Equations (1.11)(1.12)(1.13), it is possible to calculate the total axial force in each diagonal of each module and to assess the minimal cross-sectional area necessary to guarantee strength and stability requirements.

In a second step, the strength and stiffness-based approaches are applied to the 100-story diagrid building with rectangular plan considering different diagonal angle ($\theta = 64°, \theta = 69°$ and $\theta = 79°$) and then the results are compared. Of course, the height to width ratio is different in function on which side (larger/shorter) is considered. On the basis of the results, it is worth to note that the design can be governed by only the strength-, only the stiffness-based approach or both of them in function of which façade and module is examined. In fact, for the larger side the strength demand prevails at the upper modules, whereas the stiffness demand at the lower ones. On the other hand, on the shorter side the strength governs the design for the whole building height for θ=64° and stiffness for $\theta = 79°$. In the case of $\theta = 69°$ both methodologies lead to the same results. In addition, the comparison between the two approaches is carried out in terms of horizontal displacements, interstory drifts and DCR[1] in order to highlight the structural performance by changing the diagonal angle. With regard to the stiffness design, the top displacement is always lower than the target limit value for all three geometries. Conversely, the

[1] DCR stands for demand capacity ratio, and it is obtained as axial force to yield/buckling capacity ratio

maximum value of the interstory drift d_h is not satisfied mainly at upper modules and it is possible to note that the higher is the diagonal angle, the higher is the maximum value of d_h because the diagonal member become longer and so more flexible. Concerning the strength verification, unsatisfactory performance is observed for solutions $\theta = 64°$ and $\theta = 69°$ for which 25% of elements have DCR higher than 1, whereas for solution $\theta = 79°$ only 0.3% of elements collapse. On the contrary, in the case of strength design, the top displacement exceeds the limit value only for $\theta = 79°$ due to higher flexibility and the interstory drift is not fulfilled as in the previous approach. Regarding the DCR, almost no diagonals reach DCR=1. Generally, in both methodologies interstory drift problem is found, and this can be resolved by introducing a secondary bracing system (SBS) as it is shown in [16]. The study performed in this research paper is also carried out by Mele in [17] considering a 90-story tall diagrid building with different diagonal angles and the investigations confirm the previous results.

Further research work is published by Mele et al. [18] underlying th effect of slenderness on the diagrid structures design by means of both stiffness- and strength-based approaches. Considering a tall building with varying angle from 50° to 80° and slenderness from 2 to 8, it is possible to note that the strength requirement governs the design for aspect ratio between 2 and 4 without the influence of the diagonal angle and the weight is linearly proportional to H/B, whereas the stiffness prevails for aspect ratio higher than 6 and the weight is more than linearly proportional to H/B. The solution with H/B=5 represents instead a transition between the two previous behaviours and it emphasizes the condition in which both approaches return comparable weight.

In conclusion, all the studies described previously always confirm the dominant role of diagonal angle in design, but they also point out that stiffness and strength requirements must be considered complemental and not independent in order to achieve a complete design process [14]. Although at the early stage of design it is impossible to establish which one will govern the design, it has been underlined that the strength criteria prevail in buildings with low diagonal angle and the stiffness criteria prevails in buildings with steep diagonal angle.

1.3.2. METHODS FOR THE STRUCTURAL ANALYSIS

As a means to solve various project-specific complex design of diagrid structures, simplified methodologies are requested for performing the structural analysis in the preliminary design in terms of displacements, rigidity and diagonal axial forces. As the Finite Element Analysis is mandatory for detailed models in the ultimate design stages, at the early stage of design a simplified analysis is a requisite to understand the overall structural behaviour in function of the fundamental diagrid parameters. As a matter of fact, the final model depends strongly on the decisions made in the preliminary stage and therefore it is necessary to define a reliable and effective method alternative to FEM. As follows, two methods are described: the modular method (MM) and the matrix-based method (MBM).

1.3.2.1. MODULAR METHOD (MM)

Despite diagrid structures have been recognized from an aesthetic perspective thanks to the flexible arrangement of plane layout, several researchers have developed studies mainly on diagrid tall buildings with rectangular plan such as Moon in [4] and Guo in [19]. The former has proposed a lateral stiffness calculation for only rectangular diagrid structures neglecting web contribution in bending rigidity, whereas the latter has performed the same Moon’s study but considering web contribution in the bending stiffness. On the contrary, few works have been published regarding arbitrary polygonal diagrid structures. The first research paper providing a simplified calculation model of lateral stiffness of arbitrary polygonal diagrid buildings is [20] by Liu and Ma. The proposed method is called modular method. It consists into dividing the structure into modules along the entire height in order to generate a simplified structure constituted by nodes and elastic rods as it is shown in Figure 1.8. Each node represents a module considering its relative lateral stiffness, whereas the rods connect nodes with each other.

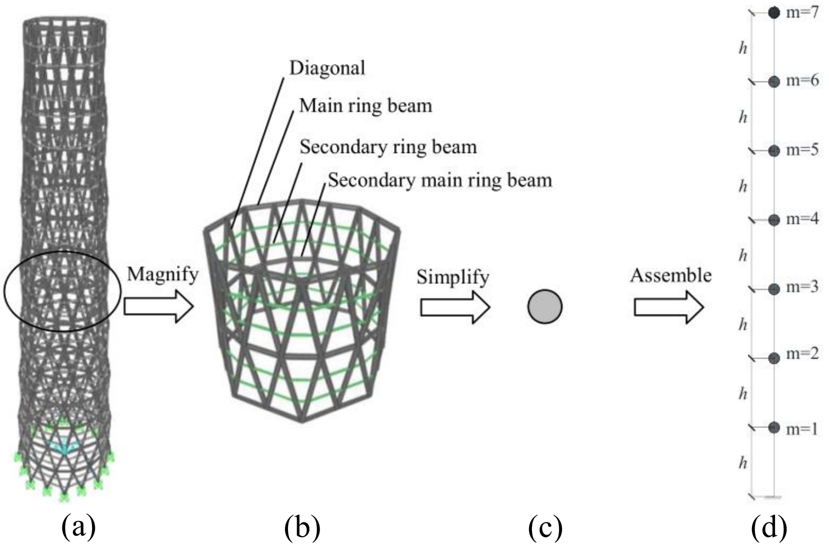

Figure 1.8 - Schematic scheme for the applicability of modular method in diagrid structures: (a) diagrid structure (b) modularization (c) nodes with stiffness (d) simplified structure [20]

In order to evaluate the lateral displacement, it is necessary to distinguish shear and bending contribution for lateral stiffness as well as for lateral displacement. It means that the total lateral displacement will be given by applying the superposition principle:

$$u_{vi} = \frac{V_1}{K_{v1}} + \frac{V_2}{K_{v2}} + \cdots + \frac{V_i}{K_{vi}} \tag{1.14}$$

$$u_{mi} = \frac{M_1}{K_{m1}} h_i + \frac{M_2}{K_{m2}} h_{i-1} + \cdots + \frac{M_i}{K_{mi}} h_{i-(i-1)} \tag{1.15}$$

$$u_i = u_{vi} + u_{mi} \tag{1.16}$$

Where u_{vi} and u_{mi} are shear and bending lateral displacements of the i-th module, respectively, V_i and M_i are the shear and bending forces at i-th module, respectively, K_{vi} and K_{mi} are the shear and bending rigidities of i-th module, respectively. Known the lateral stiffness of the structure, the lateral displacement can be calculated. The modular method is based on the following hypothesis: (a) diagonals are only subjected to axial force; (b) linear elastic behaviour of diagonals; (c) the section planarity after deformation [20]. Therefore, the expressions of shear and bending stiffnesses are obtained by applying horizontal displacement Δv and rotation $\Delta\beta$ to each module, respectively, and by means of compatibility, constitutive and equilibrium equations and geometrical considerations, Liu and Ma have provided these following equations for the calculation of shear and bending stiffnesses:

$$K_V = \frac{EAcos^2\theta\ sin\theta\ sin\gamma}{h}\sum_{i=1}^{N}\cos^2\alpha_i + \frac{EA\sin^3\theta\cos^2\gamma\ \ sin\gamma}{h}\sum_{i=1}^{N}\sin^2\alpha_i \tag{1.17}$$

$$K_m = \frac{EA\sin^3\theta\sin^3\gamma}{h}\sum_{i=1}^{N}B_i^2 \tag{1.18}$$

Where E is the Young modulus, A the diagonal cross-sectional area, θ the angle between diagonals and main ring beams in the façade, γ the façade inclination with respect to the horizontal plane, α_i the angle between main ring beam and shear direction, h the module height, B_i the distance of diagonals to neutral axis in the main ring beam plane. All the geometrical parameters are shown in Figure 1.9. Differently from K_m which is constituted only by one term, the shear stiffness K_V is obtained by the sum of two contributions. The first part is related to the effect of shear parallel to the main ring beam, the second part is instead related to the effect of shear orthogonal to the main ring beam. These equations represent a generalization of Moon formulae in [4] because they include the effect of inclined facades and polygonal planar shapes. Further studies are carried out in order to confirm the validity of the modular method by comparing the results with the ones obtained from FEM analysis. The results show a good agreement and the possible relative errors are on the safe side.

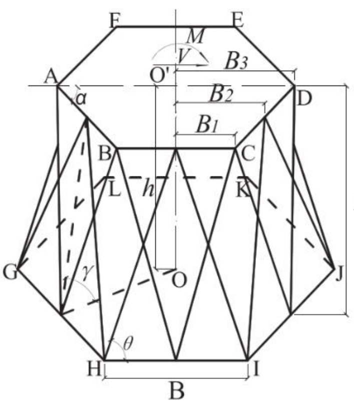

Figure 1.9 - Scheme of diagrid module and representation of geometrical properties for the definition of shear and bending stiffness in the modular method [20]

1.3.2.2. MATRIX-BASED METHOD (MBM)

Another methodology for the structural analysis of a generic freeform diagrid was suggested, the so-called matrix-based method proposed by Lacidogna et al. in [21]. It consists into the direct assessment of the complete structure stiffness matrix, differently from the modular method that considers only bending and shear stiffnesses. Thus, from the structural analysis it is possible to assess the overall structural behaviour not only in terms of vertical and lateral deformability, but also in terms of out-of-plane and in-plane floor rotations.

The main hypotheses of the MBM are the same ones employed by Moon et al. in [4] and Montuori et el. in [14]: (a) linear elastic behaviour of diagonals subjected only to axial force; (b) the floor planarity assumption after structure deformation, so the floors are assumed rigid in-plane; (c) the intra-module floors are neglected. By means of these assumptions the system is constituted by only six degrees of freedom related to the displacements and the rotations of each floor for a three-dimensional structure. For this reason, this procedure is more convenient than the Finite Element Method from a computational perspective since FEM assembles the local stiffness matrices of single elements and therefore it considers a huge number of DOFs. In order to assess the global stiffness matrix of the structure that correlates the inputs (external forces) and the outputs (floor displacements), each matrix coefficient k_{ij} has been defined in the Matlab code as the total reaction force (or moment) on the ith floor due to an imposed unitary floor displacement (or rotation) on the jth floor [21]. Thus, the diagrid stiffness matrix, the displacements, the rotations of the floors and the diagonal axial forces are calculated by the proposed model for a given diagrid geometrical configuration and external forces.

For the sake of clarity as a means to understand the main methodology theory, the analysis of two-dimensional system has been carried out and therefore each floor has two degrees of freedom. The diagrid structure is subjected to lateral load causing lateral displacement and out-of-plane rotation. The relationship between external forces and displacement can be defined as Hooke's law:

$$\begin{Bmatrix} \{F\} \\ \{M\} \end{Bmatrix} = \begin{bmatrix} [K_{F\delta}] & [K_{F\varphi}] \\ [K_{M\delta}] & [K_{M\varphi}] \end{bmatrix} \begin{Bmatrix} \{\delta\} \\ \{\varphi\} \end{Bmatrix} \tag{1.19}$$

Where N is the number of floors, $\{F\}$ and $\{M\}$ are N x 1 forces and moments vectors, respectively; $\{\delta\}$ and $\{\varphi\}$ are N x 1 floor displacements and rotations vectors; $[K_{F\delta}]$, $[K_{F\varphi}]$, $[K_{M\delta}]$ and $[K_{M\varphi}]$ are N x N stiffness matrices that correlate floor forces to floor displacements, floor forces to floor rotations, floor moments to floor displacements and floor moments to floor rotations, respectively. Each stiffness coefficient k_{ij} is computed by means of the analytical definition according to which an imposed unitary horizontal displacement or rotation to jth floor generates diagonal deformations, diagonals axial force and the total reaction force on the ith floor. The schematic schemes are shown in Figure 1.10.

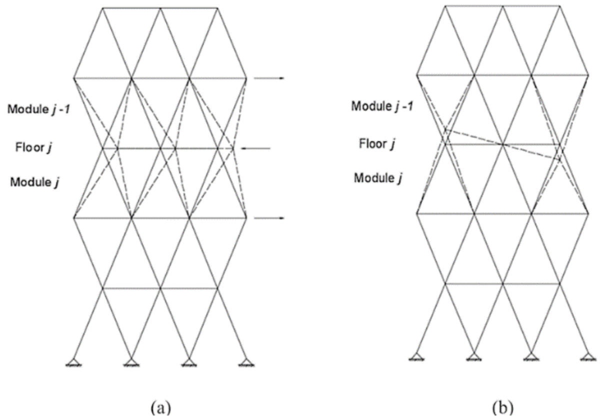

Figure 1.10 -Two-dimensional diagrid structural system for the definition of the matrix-based method MBM. Calculation of the stiffness coefficients: (a) unitary horizontal displacement applied to the jth floor; (b) unitary rotation applied to the jth floor [21]

The expressions of k_{ij} are provided in [21] and they are reported as follow:

- Matrix $[K_{F\delta}]$:

$$k_{i,i}^{F\delta} = \sum_{d=1}^{n_{i-1}} E_{d,i-1} A_{d,i-1} \frac{\Delta x_{d,i-1}^2}{L_{d,i-1}^3} + \sum_{d=1}^{n_i} E_{d,i} A_{d,i} \frac{\Delta x_{d,i}^2}{L_{d,i}^3} \tag{1.20}$$

$$k_{i-1,i}^{F\delta} = -\sum_{d=1}^{n_{i-1}} E_{d,i-1} A_{d,i-1} \frac{\Delta x_{d,i-1}^2}{L_{d,i-1}^3} \tag{1.21}$$

$$k_{i+1,i}^{F\delta} = -\sum_{d=1}^{n_i} E_{d,i} A_{d,i} \frac{\Delta x_{d,i}^2}{L_{d,i}^3} \tag{1.22}$$

- Matrix $[K_{F\varphi}]$:

$$k_{i,i}^{F\varphi} = -\sum_{d=1}^{n_{i-1}} E_{d,i-1}A_{d,i-1}\frac{\Delta x_{d,i-1}\Delta y_{d,i-1}}{L_{d,i-1}^3}\left(x_{d,i-1,i} - x_{C,i}\right) - \sum_{d=1}^{n_i} E_{d,i}A_{d,i}\frac{\Delta x_{d,i}\Delta y_{d,i}}{L_{d,i}^3}\left(x_{d,i,i} - x_{C,i}\right) \tag{1.23}$$

$$k_{i-1,i}^{F\varphi} = \sum_{d=1}^{n_{i-1}} E_{d,i-1}A_{d,i-1}\frac{\Delta x_{d,i-1}\Delta y_{d,i-1}}{L_{d,i-1}^3}\left(x_{d,i-1,i} - x_{C,i}\right) \tag{1.24}$$

$$k_{i+1,i}^{F\varphi} = \sum_{d=1}^{n_i} E_{d,i}A_{d,i}\frac{\Delta x_{d,i}\Delta y_{d,i}}{L_{d,i}^3}\left(x_{d,i,i} - x_{C,i}\right) \tag{1.25}$$

- Matrix $[K_{M\delta}]$:

$$k_{i,i}^{M\delta} = -\sum_{d=1}^{n_{i-1}} E_{d,i-1}A_{d,i-1}\frac{\Delta x_{d,i-1}\Delta y_{d,i-1}}{L_{d,i-1}^3}\left(x_{d,i-1,i} - x_{C,i}\right) - \sum_{d=1}^{n_i} E_{d,i}A_{d,i}\frac{\Delta x_{d,i}\Delta y_{d,i}}{L_{d,i}^3}\left(x_{d,i,i} - x_{C,i}\right) \tag{1.26}$$

$$k_{i-1,i}^{M\delta} = \sum_{d=1}^{n_{i-1}} E_{d,i-1}A_{d,i-1}\frac{\Delta x_{d,i-1}\Delta y_{d,i-1}}{L_{d,i-1}^3}\left(x_{d,i-1,i-1} - x_{C,i-1}\right) \tag{1.27}$$

$$k_{i+1,i}^{M\delta} = \sum_{d=1}^{n_i} E_{d,i}A_{d,i}\frac{\Delta x_{d,i}\Delta y_{d,i}}{L_{d,i}^3}\left(x_{d,i,i+1} - x_{C,i+1}\right) \tag{1.28}$$

- Matrix $[K_{M\varphi}]$:

$$k_{i,i}^{M\varphi} = -\sum_{d=1}^{n_{i-1}} E_{d,i-1}A_{d,i-1}\frac{\Delta y_{d,i-1}^2}{L_{d,i-1}^3}\left(x_{d,i-1,i} - x_{C,i}\right)^2 + \sum_{d=1}^{n_i} E_{d,i}A_{d,i}\frac{\Delta y_{d,i}^2}{L_{d,i}^3}\left(x_{d,i,i} - x_{C,i}\right)^2 \tag{1.29}$$

$$k_{i-1,i}^{M\varphi} = -\sum_{d=1}^{n_{i-1}} E_{d,i-1}A_{d,i-1}\frac{\Delta y_{d,i-1}^2}{L_{d,i-1}^3}\left(x_{d,i-1,i} - x_{C,i}\right)\left(x_{d,i-1,i-1} - x_{C,i-1}\right) \tag{1.30}$$

$$k_{i+1,i}^{M\varphi} = -\sum_{d=1}^{n_i} E_{d,i} A_{d,i} \frac{\Delta y_{d,i}^2}{L_{d,i}^3} \left(x_{d,i,i} - x_{C,i}\right)\left(x_{d,i,i+1} - x_{C,i+1}\right) \tag{1.31}$$

Where L is the diagonal length, E the Young's modulus, A the diagonal cross-sectional area, Δx and Δy are the differences in the X- and Y-coordinates of the diagonal nodes belonging to each diagonal, respectively, n_i and n_{i-1} are the number of diagonals included within the modules i and i-1, $x_{d,i-1,i}$ is the diagonal x-coordinate included within the (i-1)th module and referred to the ith floor, $x_{C,i}$ is the ith floor centroid coordinate [21]. For each parameter, the first subscript refers to the diagonal and the second one to the diagonal module. After the calculation of all the stiffness coefficients, the diagrid global stiffness matrix can be obtained by inverting the linear equation (1.19):

$$\begin{Bmatrix} \{\delta\} \\ \{\varphi\} \end{Bmatrix} = \begin{bmatrix} [K_{F\delta}] & [K_{F\varphi}] \\ [K_{M\delta}] & [K_{M\varphi}] \end{bmatrix}^{-1} \begin{Bmatrix} \{F\} \\ \{M\} \end{Bmatrix} \tag{1.32}$$

This procedure was implemented in Matlab code and it solves automatically the two-dimensional structural problem. Further investigations have been carried out regarding the analysis of three-dimensional diagrid systems following the same procedure. In this case the system has six degree of freedom per floor and the equation (1.19) is generalized as follows:

$$\begin{Bmatrix} \{F_x\} \\ \{F_y\} \\ \{M_z\} \\ \{M_x\} \\ \{M_y\} \\ \{F_z\} \end{Bmatrix} = \begin{bmatrix} [K_{F_x\delta_x}] & [K_{F_x\delta_y}] & [K_{F_x\varphi_z}] & [K_{F_x\varphi_x}] & [K_{F_x\varphi_y}] & [K_{F_x\delta_z}] \\ [K_{F_y\delta_x}] & [K_{F_y\delta_y}] & [K_{F_y\varphi_z}] & [K_{F_y\varphi_x}] & [K_{F_y\varphi_y}] & [K_{F_y\delta_z}] \\ [K_{M_z\delta_x}] & [K_{M_z\delta_y}] & [K_{M_z\varphi_z}] & [K_{M_z\varphi_x}] & [K_{M_z\varphi_y}] & [K_{M_z\delta_z}] \\ [K_{M_x\delta_x}] & [K_{M_x\delta_y}] & [K_{M_x\varphi_z}] & [K_{M_x\varphi_x}] & [K_{M_x\varphi_y}] & [K_{M_x\delta_z}] \\ [K_{M_y\delta_x}] & [K_{M_y\delta_y}] & [K_{M_y\varphi_z}] & [K_{M_y\varphi_x}] & [K_{M_y\varphi_y}] & [K_{M_y\delta_z}] \\ [K_{F_z\delta_x}] & [K_{F_z\delta_y}] & [K_{F_z\varphi_z}] & [K_{F_z\varphi_x}] & [K_{F_z\varphi_y}] & [K_{F_z\delta_z}] \end{bmatrix} \begin{Bmatrix} \{\delta_x\} \\ \{\delta_y\} \\ \{\varphi_z\} \\ \{\varphi_x\} \\ \{\varphi_y\} \\ \{\delta_z\} \end{Bmatrix} \tag{1.33}$$

Where $\{F_x\}$, $\{F_y\}$ and $\{F_z\}$ are N x 1 vectors of floor forces along X, Y and Z direction, $\{M_x\}$, $\{M_y\}$ and $\{M_z\}$ are N x 1 vectors of out-of-plane floor moments along X and Y direction and in-plane floor torque moment along Z direction. In analogy, $\{\delta_x\}$, $\{\delta_y\}$ and $\{\delta_z\}$ are N x 1 vectors of floor displacements along X, Y and Z direction, $\{\varphi_x\}$, $\{\varphi_y\}$ and $\{\varphi_z\}$ are N x 1 vectors of out-of-plane floor rotations along X and Y direction and in-plane floor rotations along Z direction. The global stiffness matrix of 3D spatial diagrid structure has 6N x 6N dimensions and it contains submatrices N x N that correlate floor force-moment vector to floor displacement-rotation vector [21]. For the symmetry property of [K] only 21 sub-matrices have to be calculated and the following sub-matrices $[K_{F_x\varphi_x}]$, $[K_{F_y\varphi_y}]$, $[K_{M_x\delta_x}]$ and $[K_{M_y\delta_y}]$ point out the connection between bending and shear stiffnesses that define the lateral deflection [10]. From the equation (1.33) it is possible to evaluate displacements and rotations knowing the external acting forces or to evaluate the axial forces in the diagonals by means of compatibility and constitutive equations.

1.3.3. OPTIMIZATION OF DIAGRID GEOMETRY

As explained in the previous chapters, the preliminary design is a fundamental step in diagrid design since it greatly influences the structural behaviour. According to the preliminary design, it is necessary to assess the diagonal cross sections in function of many geometrical parameters and several constraints, such as stiffness, strength and constructability requirements. Thus, this process can be onerous from a computational point of view. For this reason, this Chapter presents some research papers that have provided optimization techniques for diagrid structures to identify the optimal solution among a huge number of possibilities.

In the research paper [4] Moon et al. emphasize the major role of the diagonal angle in the diagrid structural design in function of the height. As a matter of fact, employing 20-, 42- and 60-story tall buildings and dimensioning diagonal cross-sectional area through displacement requirement, it is found that the optimal angle increases with increasing story height since bending deformation prevails. In particular, the optimal angle has a range between 65° and 75° for 60-story building and around 10° lower for 42-story one. Moreover, it was found that the lateral stiffness is dominant for high aspect ratio, i.e. from 5 to 7, whereas the strength is prevalent for low aspect ratio, i.e. 2.

In the following year Moon published another work paper [15] investigating the structural behaviour of diagrid structures with varying angle compared to those with uniform angle. Based on shear and bending moment trends along the building height under uniform lateral load, the bending stiffness is mainly required at the base because it increases quadratically towards the base, whereas the shear stiffness is requested at the top due to its linear trend. Thus, Moon has supposed that diagrid structures with gradually stepper angle towards the base would have better structural efficiency than those with uniform angle. In order to demonstrate that, the author has carried out several analyses employing three different diagrid heights, precisely 40-, 60- and 80-story buildings. For each of them three different angle configurations have been considered: (a) varying angle with steeper angle at the base (b) uniform-angle (c) varying angle with steeper angle at the top, as it is shown in Figure 1.11.

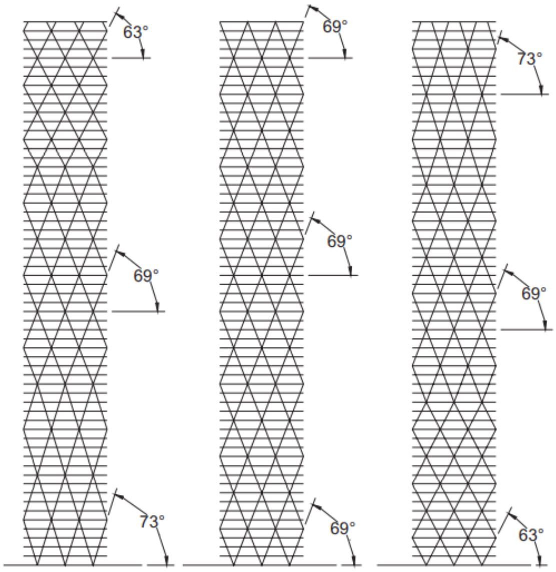

(a) (b) (c)

Figure 1.11 - Three diagrid angle configurations: (a) varying angle with steeper angle at the base (b) uniform angle (c) varying angle with steeper angle at the top [15]

According to the results, it is found that uniform angle configuration leads to the most economical solution in terms of material consumption with respect to the varying angle pattern, but it is valid only for aspect ratio lower than 7 because short buildings act similarly to shear beams and therefore the varying-angle solutions results to be inefficient. Conversely, the structural behaviour is opposite for aspect ratio higher than 7. In taller buildings the bending governs the design and therefore the varying-angle diagrid with steeper angle towards the base seems to be the best economical design [15]. The analysis related to varying angle with steeper angle towards the top is performed only for completeness even if these solutions are the worst ones independently from the aspect ratio.

Although Moon has demonstrated the structural efficiency of varying angle pattern, his proposed models are not really efficient because the diagonal does not remain straight in its whole length over the total building height, but its direction changes in correspondence of the passage from one module to another one. In fact, Zhou et al. in [22] underline the importance of diagonal continuity and directness of load path through straight diagonals in order to guarantee an enhanced structural performance of tall building. The first authors that have performed investigations on the optimal diagrid geometries considering straight diagonals with gradually varying angles are Zhang et al. in [23]. In the research paper an approximate methodology for performing the preliminary design based on stiffness and strength requirements and expressions of the optimal diagonal angle in function of aspect ratio ranging from 3.6 to 9 are provided:

$$\theta_{2,opt} = \arctan \frac{H/B}{1 + 0.475\sqrt{\frac{H/B}{4.75}}} \tag{1.34}$$

$$\begin{cases} \theta_{1,opt} = \theta_{2,opt} & for\ H/B \leq 3.5 \\ \theta_{1,opt} = \dfrac{1}{\left(1 + \dfrac{\ln(H/B)}{3.5}\right)^{\frac{H/B}{2}}} \left(\theta_{2,opt} - arsin\dfrac{1}{\sqrt{3}}\right) + arsin\dfrac{1}{\sqrt{3}} & for\ H/B > 3.5 \end{cases} \tag{1.35}$$

Zhang et al. define two geometrical parameters, namely the top angle θ_1 and the bottom angle θ_2 (Figure 1.12a). The typical values can be presumed by considering that in tall buildings gravity load and bending moment prevail in the lower part, and the shear in the upper part. Consequently, the lower limit of θ_1 is 35° in order to maximize shear rigidity at the top levels and the value of θ_2 will be greater in function of the aspect ratio to maximize bending rigidity at lower levels. The main aim of the study on the optimal geometry was to identify the best combination of $\theta_1 - \theta_2$ resulting in less material consumption according to strength and stiffness criteria. Based on the results, it is found the critical value of the aspect ratio, i.e. H/B=5, representing the optimal solution transition from the uniform-angle configuration for short structures to the varying angle one for tall structures. In fact, the optimal value of θ_2 increases with the aspect ratio and the correspondent optimal value of θ_1 decreases with the aspect ratio. Furthermore, for short structures with the aspect ratio lower than 5 the solutions with $\theta_{2,opt}$ are all structurally acceptable independently from θ_1. Conversely, for tall buildings the number of acceptable solutions is drastically reduced having fewer $\theta_1 - \theta_2$ possible combinations [23]. Out of the optimal range of θ_2, the influence of θ_1 has much more effect and the uniform-angle diagrid is more economical than the varying angle one.

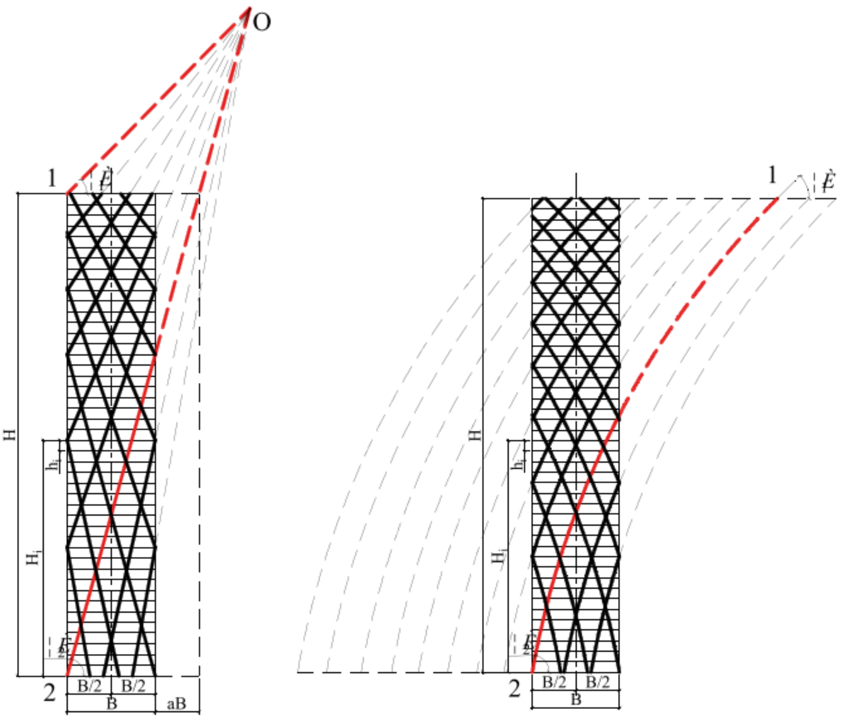

Figure 1.12 - Varying-angle diagrid configurations for the definition of optimal solution in terms of material consumption: (a) straight diagonals (b) curved diagonals [24]

Zhao et al. have performed further studies in [24] regarding varying-angle straight diagonals under seismic action. By comparing the results to the ones obtained with wind action [23], the formulation of the optimal value of $\theta_{2,opt}$ is the same Equation (1.34), whereas the optimal value of θ_1 is not affected by either the aspect ratio or $\theta_{2,opt}$. In fact, it is very close to 35° or precisely to $arsin(1/\sqrt{3})$. Moreover, the authors have proposed an alternative diagrid pattern made up of curved diagonals defined by the top tangent angle θ_1 and the bottom tangent angle θ_2 (Figure 1.12b). In this case considering a set of models from 30- up to 75- story with curved diagonals under wind and seismic loads, the paper provides empirical equations for the optimal values of the top and bottom angles:

$$\theta_{2,opt} = \arctan(H/B) \tag{1.36}$$

$$\theta_{1,opt} = 0.8 \left(\frac{H/B}{8}\right)^{\frac{1}{8}} \theta_{2,opt} \tag{1.37}$$

It is found out that under seismic action if θ_2 is lower than $\theta_{2,opt}$, the optimal value of θ_1 increases close to θ_2 and therefore the uniform-angle diagrid is the preferable economical solution. However, if θ_2 is greater than $\theta_{2,opt}$, the optimal value of θ_1 decreases until

35°. In addition, the admissible value of θ_1 ranging from 50° to 70° is greater in contrast to varying-angle straight diagonals.

Another scientific contribution in diagrid literature has been developed by Montuori et al. in [25] exploring alternative design strategies from the structural perspective. For this purpose, eight alternative geometrical patterns, namely 3 patterns of regular diagrid, 3 patterns of variable angle and 2 patterns of variable density (Figure 1.13a), of 90-story diagrid building have been investigated under vertical and wind loads. The latter pattern represents a new diagonal layout proposed by the authors consisting into increasing the number of diagonals from the top to the building base to follow the variable stiffness and strength demands along the height. These models have been compared in terms of horizontal displacement, interstory drift ratio and DCR after performing the structural analysis using FEM. In order to identify the optimal solution among the different patterns, a structural efficiency parameter has been defined as the inverse of the top displacement multiplied by the structural weight [25]. Figure 1.13b shows the results for the optimized patterns. It is found that the optimal pattern is VA1. Conversely, the solutions 80° and VA3 are the least efficient and the regular patterns 60° and 70° and the variable ones VA2, VD1 and VD2 have slight differences.

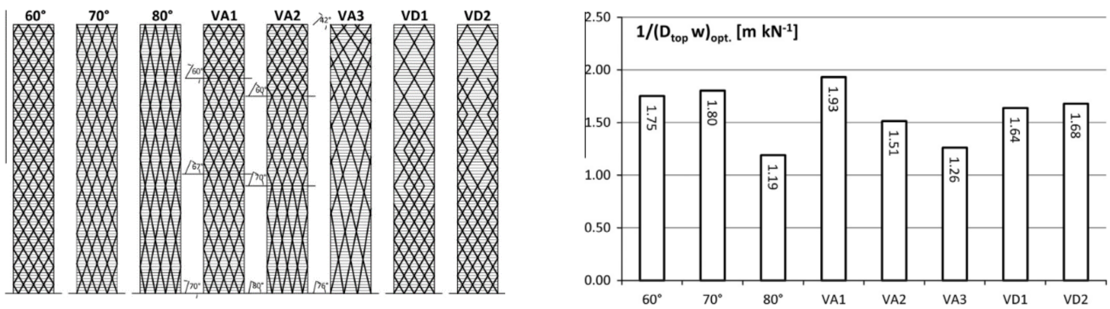

(a) (b)

Figure 1.13 - (a) Eight alternative geometrical patterns of diagrid structures: regular, varying angle and varying density (b) Efficiency parameter for the optimized solutions [25]

In the following paper, Angelucci and Mollaioli [26] have investigated a regular diagrid building 351 m tall with optimal (69°) and non-optimal (82°) diagonal angles under gravity and wind loads to assess the effectiveness of the stiffness-based methodology proposed by Moon in [4], comparing the outcomes with the ones evaluated by means of the iterative strength-based and displacement-based optimization. Based on results, it is found that the Moon stiffness-based approach is valid only for a range of diagonal angle between 60°-70° because the method leads to excessive material usage for steeper angles. Furthermore, the authors have analysed the performance of different density configurations for the case of 82° diagonal angle in order to ensure the stiffness demand. To this aim, two typologies of design pattern are considered: diagrid-outrigger system, thickening the pattern density at fixed levels (Figure 1.14a) and varying density diagrid system, decreasing gradually the number of diagonals towards upper levels (Figure 1.14b). These studies have pointed out that the varying density diagrid is more effective in limiting lateral drift than the diagrid-outrigger system, though the latter ensures a drastic weight reduction.

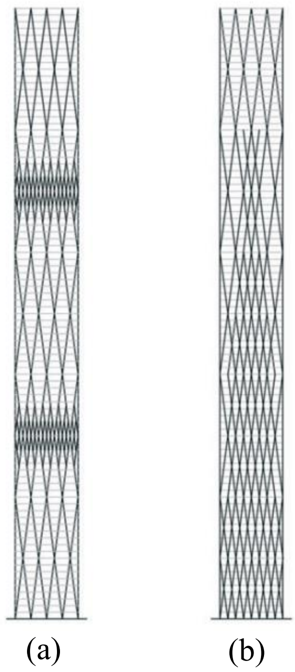

Figure 1.14 - Non-uniform diagrid configurations to ensure stiffness requirement: (a) concentrated outrigger at fixed levels (b) gradual varying density system [26]

Another important contribution in literature worth of note is [27] by Tomei et al. regarding the optimization of structural patterns for diagrid structures. The paper proposed an alternative design strategy based on structural optimization, employing the mono-objective genetic algorithm. The latter consists in the definition of the objective function OF, i.e. the structural weight, that has to be minimize ensuring the lateral stiffness and strength requirements. This procedure has been applied to different patterns for the 90-story tall diagrid building. Besides employing the conventional regular, variable-angle, Tomei et al. have introduced a double-density regular pattern, obtained by doubling the diagonal layout, a variable-density patter and an ISO pattern, made up of diagonals along the principal stress lines considering the building as equivalent cantilever beam. The main study purpose is the assessment of the structural efficiency of the different diagrid patterns in terms of unit structural weight, diagonal cross section distribution, lateral displacements, interstory drift ratio and DCR besides the confirmation of simplified design methodologies validity. All of them have been also treated in the abovementioned papers. The emerging topic is related to the definition of the construction complexity index in order to predict the best solution in terms of efficiency and economics. This parameter has been defined as the sum of the following normalized parameters: the weighted number of nodes, the number of different cross sections, the number of slices considering a maximum diagonal length of 12 m, the number of diagonals and the number of different lengths [27]. Figure 1.15 shows that the patterns 80° and VD1 are characterized by the lowest value of the complexity index although the great structural weight. On the contrary, both complexity index and structural weight are low for the patterns 60°, 70° and VA.

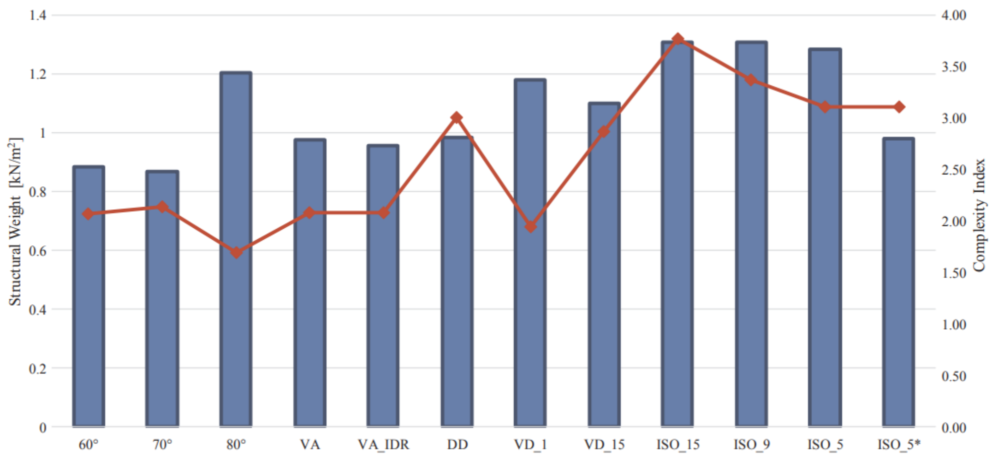

Figure 1.15 - Structural efficiency and economic assessment through the comparison between structural weight and complexity index for different diagrid patterns [27]

The previous genetic algorithm-base optimization is also employed in the research of Mirniazmandan et al. [28] to assess the structural efficiency of various non-extruded forms different from the usual square and rectangular plans. Unlike the previous study, the optimization process is a multi-objective optimization since it has to minimized two objectives, i.e. the unit structural weight and the top displacement. These two objectives are conflicting as the reduction of the total weight leads to the increase of lateral displacement and therefore the optimization returns the average best solution instead of the optimum one. To this purpose, 64 parametric models of 180 m height with different geometric plans configurations generated by increasing the numbers of sides at the top and base plans, ranging from 3 to 12 in addition to circle, are employed. From the iteration of polygonal cross-sections plans and diagrid angle, it is found that, fixing circle base plan, the displacement decreases and the weight increases for lower number of top plan's sides, while both displacement and weight increases for lower base plan's sides with fixed top circular plan. For these reasons, the models with best performance are those with base circular plan and 8-to-12-sided top plan in addition to circle. Under these considerations, the authors affirm that the efficiency grows with the number of polygonal cross sections. It is also found that the optimal diagonal angle range is between 53° and 70° in accordance with [4].

As can be found out in diagrid literature, most of research projects carried out in recent decades are concerned various diagrid configurations, starting from regular diagrid to varying floor plans, considering only lateral actions. However, it is necessary to take into account also torque actions, especially when the mass and stiffness distributions are not uniform due to asymmetrical conditions. This issue has been recently investigated in [29] by Lacidogna et al. The investigation of the influence of the diagonal inclination and the floor plan shape on the structural performance has been performed by means of the MBM described in Chapter 1.3.2.2. To this aim, a total of 96 diagrid models are employed combining four different heights (126, 168, 210 and 252 m), four different floor plan shapes (square, hexagon, octagon and circle) and six different numbers of intra-module floors (1, 2, 3, 4, 6 and 12), subjected simultaneously to uniformly distributed horizontal and torque loads [29]. Based on the results, it is evident that the structural behaviour is mainly affected by the diagonal angle, confirming the previous studies. Unlike the lateral stiffness for which it is maximized for diagonal angle ranging from 64° to 72° or greater values for taller buildings, the torsional stiffness is maximized for lower diagonal inclinations, 35°-38°, because the torsional behaviour depends only on the shear rigidity. Regarding the influence of floor plan shape on lateral displacement, slight differences are found among different models for diagonal inclination in the optimal range, whereas more accentuated dissimilarities far from the optimal condition. As far as torsional behaviour is concerned, the circular plan shape with optimal inclination minimizes torsional rotation.

The diagrid tall building models proposed in [29] are also used in another research paper [30] by Lacidogna et al. In this case the desirability function approach has been applied for the first time in order to find the best diagrid configuration in terms of stiffness, structural weight, performance and construction complexity. This procedure is based on the definition of two parameters, namely the individual $d_{i,p}$ and overall desirability OD_i (Eq. (1.38)). The former has a range between 0 and 1 and it is evaluated for each solution referred to each response variable; the latter has also a range from 0 to 1 and it is a global score for each diagrid geometry. In particular, the authors have considered twenty-four different diagrid geometries with different floor shapes and diagonal angles and four response parameters, i.e. top lateral displacement, top torsional rotation, mass and complexity index.

$$d_{i,p} = \left(\frac{max_i p_i - p_i}{max_i p_i - \min_i p_i}\right)^{r_p} \qquad OD_i = \prod_{p\_=1}^{k} \left(d_{i,p}\right)^{1/k} \tag{1.38}$$

The proposed methodology has been employed on 126-, 168-, 210- and 252-meter-tall buildings assuming a unitary r_p for each response parameter. From the analysis, it is obtained that the best solution is always the three intra-module floors geometry with circular floor shape. Moreover, it is worth of note that the overall desirability is mainly affected by the diagonal angle, whereas both structure height and floor shape have minor contribution. Conversely, it is found that the worst diagrid geometries have one intra-module floor due to the highest value of complexity index. The study has been completed with a parametric analysis by considering 4096 simulations obtained from different values of r_p and the results show a slight influence of the exponent on the outcomes.

Besides the typical geometrical parameters, there are other factors that can contribute to improve the structural performance of a diagrid building. For example, the geometry plan and the building cross-section can affect the structural behaviour. Their influence has been investigated in [31] by Ardekani et al. through a FEM analysis. In this research work a 160-meter steel diagrid structure has been employed under wind and earthquake actions. The geometry modifications are related to different number of shape sides from triangle to circle and two tapered building sections (concave and convex). As far as plan shape is concerned, it can be noted that the roof displacement increases with the number of plan sides with maximum value for the hexagonal plan, whereas the structural weight has an opposite trend because it decreases with minimum value for the circular plan. Regarding section modification, the tapered geometry results to be more efficient than the normal one. In particular, the concave model provides an enhanced performance in terms of roof displacement and structural weight for any plan shape. Indeed, the concave sections have 20% less weight than normal structures.

Recently, the structural design workflow has been enhanced through the Computational Design (CD) based on the generative design (GD). This procedure has been employed in [32] by Cascone et al. investigating structural efficiency and feasibility of optimal solutions. The generative design algorithm creates various and complex models by means of triangular units and it is based on the use of structural grammar, which is constituted by a shape grammar and structural optimization processes. The former generates infinite geometries discretizing the design domain in triangular units through diagonals, while the latter selects the optimal solution minimizing the unit structural weight by means of structural analysis and genetic algorithm. In particular, in the research work the generative design has been applied to three prismatic building models with different slenderness ratio H/B, namely 3, 5 and 6.6. Once the optimal diagrid pattern (TO) for each H/B are evaluated, the authors provide a comparison with regular (RE) diagrids and Principal Direction Inspired [2] (PDI) pattern in terms of performance indexes. The novelty of the grammar approach is offering the possibility of integrating non-quantitative criteria in the selection process [32]. From the Figure 1.16a it is evident that in the case of TO solutions the diagonal density is greater at the façade edges and the inclination is less inclined at the centre. Further, the proposed methodology has demonstrated its efficiency since it has returned a solution similar to the PDI pattern for H/B=6.6 due to the dominating stiffness demand. From the performance assessment, the comparative parameters have been defined, precisely the relative strength efficiency ratio E_{STR}, the relative stiffness efficiency ratio E_{STF} and the global efficiency parameter $E = E_{STR} \cdot E_{STF}$. Figure 1.16b shows that the TO patterns have the best performance and the best efficiency for each slenderness and they tend to behave similarly to PDI ones for H/B≥ 5.

[2] The Principal Direction Inspired pattern corresponds to ISO pattern employed in [28]

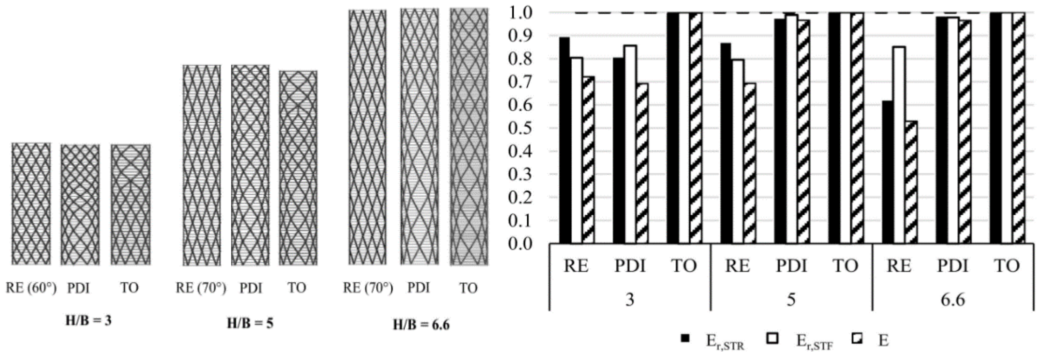

Figure 1.16 - Results of the structural gramma approach: (a) structural patterns: (RE) regular, (PDI) Principal Direction Inspired, (TO) topology optimisation (b) comparison among patterns in terms of efficiency parameters [32]

Further investigations have been carried out in [33] by Orhan et al. regarding the genetic algorithm optimization applied to uniform- and varying-angle diagrid as in [15]. Three rectangular plan buildings with different heights, namely 30, 60 and 90 stories, and two base module shapes, namely Type 1 (Figure 1.17a) and Type 0 (Figure 1.17b), are manually modelled in FEM software in order to transfer in MATLAB a SAP2000 model file containing the model geometry (node coordinates, load patterns, loads and material properties). The optimization process has been performed on the basis of strength and stiffness-based approaches adopting simplified formulas proposed in literature [14, 23] to minimize the structural weight. In the case of uniform-angle structures, the optimal solution for each slenderness has been found minimizing the structural weight in function of the diagonal angle and based on results, it can be seen that the optimal angle increases with the aspect ratio independently from the type 0 or 1, as it has been studied in [2].

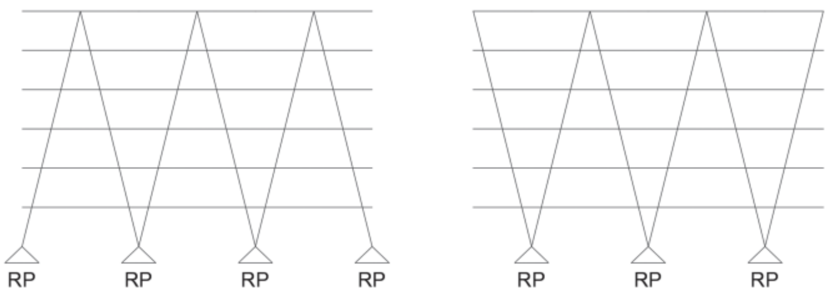

Figure 1.17 - Diagonal geometry types due to base module shape for application of optimization process in unifom- and varying-angle diagrid: (a) Type 1 (b) Type 0 [33]

In the case of varying-angle diagrid, the genetic optimization has been employed and coupled with MATLAB code. Once the optimal models have been defined for each height and type, the structural analysis has been performed in terms of DCR, displacements, weight and complexity index CI. The results of the analyses confirm again the abovementioned literature studies and highlight that varying-angle models have better performance than uniform-angle ones although the latter have instead lower complexity index values. In addition, type 1 model shows to have greater weight than type 0 model in any case due to different load pattern [33].

Recently, a new design optimization algorithm has been proposed by Ashtari et al. in [34], the so-called accelerated fuzzy-genetic algorithm with bilinear membership function, modified cross over and penalty function ensuring better convergence rate with respect to the simple genetic algorithm. The reference models used in this study are obtained by considering a diagrid tall building with five different stories from 24 to 60-stories, three different numbers of bays (4, 6 and 8) and three different building dimensions (15, 21 and 27 m). Thus, a total of 30 models are considered. The purpose of the study is to assess the optimal solution for each slenderness and building dimension by varying diagrid angles and cross-sectional areas in order to ensure strength, constructability and serviceability requirements. From the results shown in Figure 1.18 it can be seen that the optimum weight decreases for big plan dimensions because the lateral stiffness is increased and this is more evident for taller structures. Indeed, the weight reduction is respectively of 1% and 33% for 36- and 56-story structures. Moreover, the effect of the bay number on the weight is visible especially for taller buildings because fewer bays correspond to wider openings and consequently reduced material consumption.

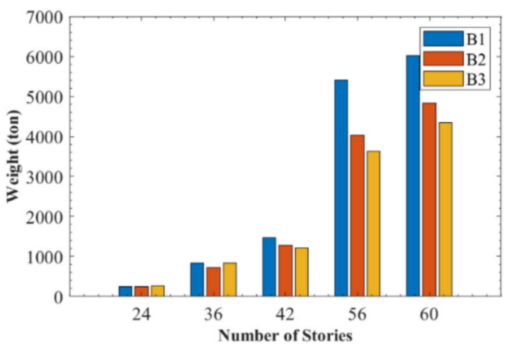

(a)

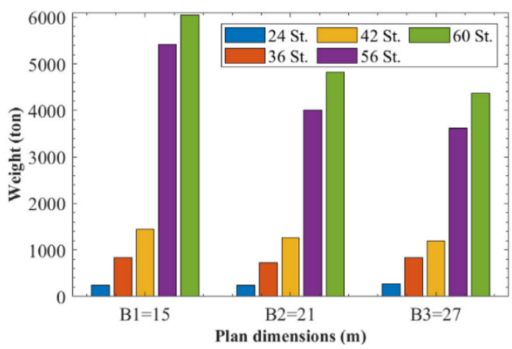

(b)

Figure 1.18 - Results of the accelerated fuzzy-genetic algorithm with bilinear membership function on diagrid structures: (a) Effect of plan dimension on the weight (b) Effect of height on the weight [34]

Although the previous studies are mainly focused on the structural performance optimization aiming to minimize top displacement and material consumption in function of geometrical parameters, over the last two decades machine learning techniques have been applied on computational optimization for designing sustainable tall buildings in order to cope with the rapid worldwide tall building development and the consequent significant increasing of energy consumption. In particular, many studies have been carried out employing a general approach based on a single-floor level, but the proposed procedure requires a great amount of time to investigate an enormous number of design parameters. To overcome the computational problem, Ekici et al in [35] [36] have proposed a novel multi-zone optimization (MUZO) methodology consisting in subdivisions, called zones, of the high-rise building considered as separate design problems. In the research paper [36] the multi-zone optimization has been used on quad-grid and diagrid scenarios to optimize the spatial daylight autonomy (sDA) and annual sunlight exposure (ASE), varying more than 200 design parameters for each scenario, such as glazing type, number, and rotation of diagonals [36]. By applying Illuminating Engineering Society (IES) recommendations ($sDA_{300/50\%,min} = 55\%$ and $ASE_{1000,250h,max} = 10\%$), the results show that in the optimal models the sDA have greater values at the lower zones and lower values at upper zones due to the dense close environment. In addition, the quad-grid buildings provide better daylight performance than diagrid buildings.

Chapter 2

2. DIAGRID MODELS, EXTERNAL ACTIONS AND STRUCTURAL ANALYSIS

This Chapter describes the diagrid building models employed in this Thesis highlighting the different geometrical parameters investigated, namely slenderness, diagonal inclination and floor plan shape. In Chapter 2.2 wind load assessment according to ASCE recommendation is provided. In Chapter 2.3 strength and stiffness expressions are reported.

2.1. DIAGRID MODELS FOR TALL BUILDINGS ANALYSED IN THIS STUDY

The proposed models in [29] [30] are employed in this study. In particular, four different building heights were investigated, precisely 126, 168, 210 and 252 m. For each height, twenty-four unform-angle diagrid structures were considered, obtained by varying the plan shape, i.e. square, hexagon, octagon and circle, and the diagonal inclination to which a different number of intra-module floors corresponds, i.e. 1, 2, 3, 4, 6 and 12, as it is shown in Figure 2.1. Thus, a total of ninety-six models of uniform-angle diagrid structures are obtained. These are analyzed in order to understand the influence of the geometrical parameters on the structural behaviour and to identify the best geometry able to minimize simultaneously lateral displacement, torsional rotation, mass and construction complexity. Note that each solution will be named with an acronym, constituted by a letter for the floor plan shape (S=square, H=hexagon, O=octagon, C=circle) and a number for the number of intra-module floors (1, 2, 3, 4, 6, 12). For example, S6 is the model with square floor plan shape and six intra-module floors. In Chapter 5 varying-angle diagrid structures will be also investigated.

In these models certain geometrical parameters are set constant along the building height, such as the inter-story height and total floor area. The diagrid structure is assumed to be made up of steel hollow circular section CHS with an elastic modulus of 210 GPa, steel density of 7.8 $\mathrm{ton/m^3}$ and yielding strength of 275 MPa.

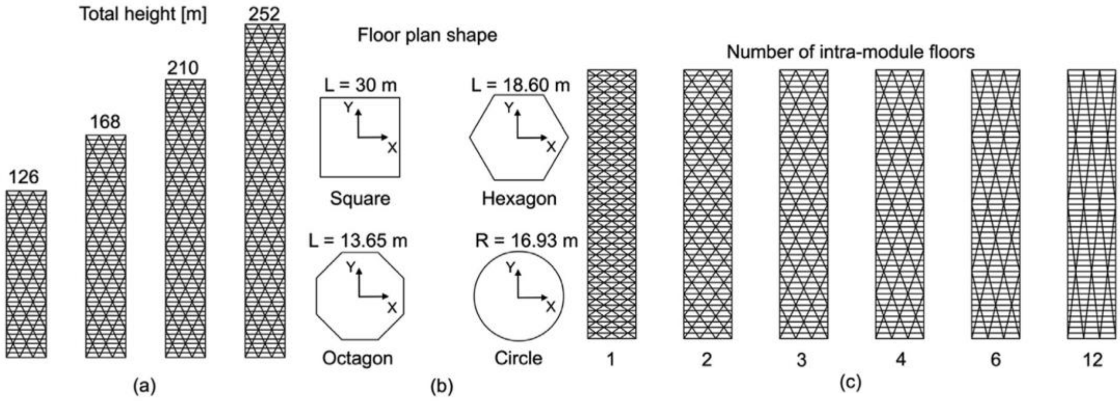

Figure 2.1 - Diagrid tall building models with (a) four different building heights, (b) four different floor plan shapes, (c) six different diagonal inclinations [29]

These structures are assumed to be subjected to both vertical and horizontal loads. The former is assessed by combining 7 $\mathrm{kN/m^2}$ of dead load and 4 $\mathrm{kN/m^2}$ of live load. However, it is fundamental to remember that the vertical load is not entirely applied on the diagrid structure, since the load is mainly carried by the internal central core. Indeed, assuming that the core occupies 25% of the total area, as Montuori et al. have done in [14], only 37.5% of the gravity load is carried by the diagrid structure and therefore the total vertical load considered is equal to 4.125 $\mathrm{kN/m^2}$. As far as the horizontal load is concerned, this is generated by the wind and its effect is dual since it induces not only a horizontal action, but also a torque moment action. The assessment of these lateral actions is carried out through ASCE as it will be explained in the next Chapter 2.2.

The following Table 2.1 and Table 2.2 summarize the main parameters of the diagrid structures.

Inter-story height	3,5	m
Total floor area	900	$\mathrm{m^2}$
Diagonals' elastic modulus	210	GPa
Steel density	7,8	$\mathrm{ton/m^3}$

Table 2.1 - Main parameters of the diagrid buildings

		Number of intra-module floors					
		1	2	3	4	6	12
Floor plan shape	Square	34,99	54,46	64,54	70,35	76,61	83,21
	Hexagon	36,97	56,4	66,11	71,63	77,51	83,68
	Octagon	37,57	56,98	66,57	72	77,77	83,82
	Circle	38,37	57,73	67,17	72,48	78,11	83,99

Table 2.2 - Diagonal angle [°] in function of the floor plan shape and the number of intra-module floors [29]

2.2. WIND LOAD

2.2.1. INTERACTION BETWEEN TALL BUILDINGS AND WIND ACTIONS

The design of low-rise buildings with low slenderness is mainly governed by gravitational loads, whereas the wind load provides minor effects on the structural behaviour. Thus, for rigid structures the expected response under vertical and wind loads is static. On the contrary, in the case of tall buildings the wind load plays a major role in structural design producing a dynamic response. In particular, in tall buildings with aerodynamic shape susceptible to wind action the interaction between wind and structure becomes so significant that it modifies the response itself due to high lateral displacements. Generally, the wind load induces two important effects, namely aerodynamic and aeroelastic actions on the structure [37]. For this reason, the assessment of wind loads on slender building is essential. To this aim, various methods can be employed, but generally in the preliminary design engineers can refer to practice codes to evaluate the wind action. However, in specific and particular cases it is necessary to have a more accurate assessment: the typical approaches simulating the impact of the geometrical shape of the building on the wind-structure interaction are the wind tunnel test and the computational fluid dynamics (CFD) aiming to define the optimal profile of tall buildings, as well as to suggest local shape modifications (e.g. building corners or top), which ensure better aerodynamic performance [27]. In addition, the proposed standard procedures do not consider many issues, such as shielding effect due to the interference from other structures, wind directionality, across-wind response and dynamic effects including acceleration [38]. Nevertheless, the wind evaluation through National regulations is admissible for buildings in which higher modes have slight contribution in displacement response [39] and in the preliminary design because the building geometry and properties are still unknown variables.

2.2.2. ASCE 7-10 PROCEDURE FOR EVALUATING WIND LOADS

In this Chapter it is shown how to calculate the lateral load due to wind on tall buildings according to ASCE 7-10 recommendation [40] in order to perform the preliminary design of diagrid structures.

The basic wind speed V is assumed to be equal to 40 m/s supposing the tall building location in New York as Mele et al. have done in [41] for the Hearst Tower. The velocity pressure at height z is evaluated as follows:

$$q_z = 0.613\, K_z\, K_{zt}\, K_d V^2 \left[\frac{\mathrm{N}}{\mathrm{m}^2}\right] \text{ for V in } \frac{\mathrm{m}}{\mathrm{s}} \tag{2.1}$$

Where K_d is the wind directionality factor depending on the structure type and in the case of main wind force resisting system of enclosed and partially enclosed buildings ASCE recommends $K_d = 0.85$, K_z is the velocity pressure exposure coefficient, K_{zt} is the topographic factor assumed unitary and V is the basic wind speed. In order to evaluate the velocity pressure exposure K_z, it is necessary to define the surface roughness and the exposure categories. Supposing that the building is in an urban area, the exposure category is B and K_z is calculated as follows:

$$K_z = 2.01 \left(\frac{z}{z_g}\right)^{\frac{2}{\alpha}} [-] \text{ for } 15 \text{ ft.} \leq z \leq z_g \tag{2.2}$$

Where z is the height above ground level, z_g and α are tabulated in Table 2.3.

Exposure	α	z_g [ft]	$\hat{a}$	$\hat{b}$	$\bar{a}$	$\bar{b}$	c	l [ft]	$\bar{\epsilon}$	z_{min} [ft]*
B	7.0	1200	1/7	0.84	1/4	0.45	0.30	320	1/3.0	30

*z_{min} = minimium height used to ensure that the equivalent height $\bar{Z}$ is greater of 0.6h or z_{min}.

Table 2.3 - Terrain exposure constant for definition of wind loads according to ASCE 7-10 [40]

Thus, the design wind pressure for the main wind force resisting system of enclosed flexible buildings can be calculated as:

$$p = q\, G_f C_p - q_i\left(G C_{pi}\right) \left[\frac{\mathrm{N}}{\mathrm{m}^2}\right] \tag{2.3}$$

Where q is the velocity pressure at height z, q_i is the internal pressure equal to q evaluated at z=h for sake of safety, G_f is the gust-effect factor, C_p is the external pressure coefficient and GC_{pi} is the internal pressure coefficient. The evaluation of the design wind pressure for tall buildings is based on the definition of the gust-effect factor because it considers the interaction between the high-rise building and wind action. To this aim, it is necessary the fundamental frequency assessment for flexible building. The approximate fundamental frequency n_1 for tall buildings greater than 400 ft (122 m) is given by the following expression:

$$n_1 = \frac{150}{h} \quad [\mathrm{Hz}] \quad (\mathrm{h\ in\ ft}) \tag{2.4}$$

Where h is the total building height. For flexible buildings the dimensionless gust-effect factor shall be calculated by the following Equation:

$$G_f = 0.925 \left(\frac{1 + 1.7 I_{\bar{z}} \sqrt{g_Q^2 Q^2 + g_R^2 R^2}}{1 + 1.7\, g_v I_{\bar{z}}} \right) \tag{2.5}$$

Where $I_{\bar{z}}$ is the intensity of turbulence at height $\bar{z}$ where $\bar{z}$ is the equivalent height of the structure defined as 0.6h (h in ft), but not less than z_{min} for all building heights h. z_{min} and c are listed in Table 2.3.

$$I_{\bar{z}} = c \left(\frac{33}{\bar{z}} \right)^{\frac{1}{6}} \tag{2.6}$$

g_Q and g_v are the peak factor for background and wind response, respectively, and they are equal to 3.4. g_R is the peak factor for resonant response and it is given by:

$$g_R = \sqrt{2 \ln (3600\, n_1)} + \frac{0.577}{\sqrt{2 \ln (3600\, n_1)}} \tag{2.7}$$

R is the resonant response factor given by:

$$R = \sqrt{\frac{1}{\beta} R_n R_h R_B (0.53 + 0.47 R_L)} \tag{2.8}$$

$$R_n = \frac{7.47 N_1}{(1 + 10.3 N_1)^{\frac{5}{3}}} \tag{2.9}$$

$$N_1 = \frac{n_1 L_{\bar{z}}}{\bar{V}_{\bar{z}}} \tag{2.10}$$

$$R_l = \begin{cases} \frac{1}{\eta} - \frac{1}{2\eta^2}(1 - e^{-2\eta}) & for\, \eta > 0 \\ 1 & for\, \eta = 0 \end{cases} \tag{2.11}$$

where the subscript l in Equation (2.11) shall be taken as h, B and L. B and L are plan dimension measured normal and parallel to the wind direction, respectively. Thus, n_1 is the fundamental natural frequency, $R_l = R_h$ setting $\eta = 4.6 n_1 h/\overline{V_{\bar{z}}}$, $R_l = R_B$ setting $\eta = 4.6 n_1 B/\overline{V_{\bar{z}}}$, $R_l = R_L$ setting $\eta = 4.6 n_1 L/\overline{V_{\bar{z}}}$, β is the damping ratio assumed equal to 1% and $\overline{V_{\bar{z}}}$ is the mean hourly wind speed in ft/s at height $\bar{z}$:

$$\overline{V_{\bar{z}}} = \bar{b}\left(\frac{\bar{z}}{33}\right)^{\bar{\alpha}}\left(\frac{88}{60}\right)V \quad \left[\frac{\text{ft}}{\text{s}}\right] \text{ for } \bar{z} \text{ in ft and V in mph} \tag{2.12}$$

Where $\bar{b}$ and $\bar{\alpha}$ are constant listed in Table 2.3.

The background response Q is given by:

$$Q = \sqrt{\frac{1}{1 + 0.63\left(\frac{B+h}{L_{\bar{z}}}\right)^{0.63}}} \tag{2.13}$$

Where $L_{\bar{z}}$ is the integral length scale of turbolence at the equivalent height:

$$L_{\bar{z}} = l\left(\frac{\bar{z}}{33}\right)^{\bar{\epsilon}} \tag{2.14}$$

Where l and $\bar{\epsilon}$ are reported in Table 2.3.

The internal pressure coefficient GC_{pi} for enclosed buildings is ± 0.18 and it has been chosen the sign that increases the wind pressure for safety condition, whereas the external coefficients C_p are reported in Table 2.4 for the case of square plan.

Surface	L/B	C_p	Use with
Windward Wall	All values	0.8	q_z
Leeward Wall	0-1	-0.5	q_h
Side Wall	All values	-0.7	q_h

Table 2.4 - External Wall Pressure Coefficients for main wind force resisting system [40]

Note that the design wind pressure is evaluated considering the wind pressure only on windward and leeward walls neglecting the effect on side wall. Moreover, it is fundamental for the analysis to take into account the torsional effect due to the wind effect on high-rise building, that is considered by applying an eccentricity of 15% with respect to plan dimension normal to load direction. Thus, for 30 m plan dimension, $e = 4.5\ m$.

2.2.3. RESULTS OF WIND LOAD CALCULATION

Considering the four different heights, precisely 126, 168, 210 and 252 m, the abovementioned parameters are reported in the Table 2.5.

			Tall building height h [m]			
			126	168	210	252
Velocity pressure exposure	K_h	-	1,48	1,61	1,72	1,81
Fundamental natural frequency	n_1	Hz	0,36	0,27	0,22	0,18
Intensity of turbulence	$I_{\bar{z}}$	-	0,21	0,20	0,20	0,19
Peak factor for resonant response	g_R	-	3,94	3,87	3,81	3,76
Mean hourly wind speed at height $\bar{z}$	$\bar{V}_{\bar{z}}$	$\frac{\text{ft}}{\text{s}}$	97,78	105,07	111,10	116,28
Integral length scale of turbulence	$L_{\bar{z}}$	ft	626,83	689,91	743,19	789,75
Reduced frequency	N_1	-	2,33	1,79	1,46	1,23
	η_h	-	7,06	6,57	6,21	5,93
	η_B	-	1,68	1,17	0,89	0,71
	η_L	-	5,62	3,93	2,97	2,36
	R_h	-	0,13	0,14	0,15	0,15
	R_B	-	0,42	0,52	0,60	0,66
	R_L	-	0,16	0,22	0,28	0,33
	R_n	-	0,08	0,10	0,11	0,12
Resonant response factor	R	-	0,53	0,67	0,79	0,91
Background response factor	Q	-	0,80	0,79	0,78	0,77
Gust effect factor for flexible buildings	G_f	-	0,93	0,97	1,01	1,05
Velocity pressure at height h	q_h	$\frac{\text{N}}{\text{m}^2}$	1235,83	1341,70	1430,03	1506,50

Table 2.5 - Calculation of wind load parameters according to ASCE for different building heights

In Table 2.5 it is important to note that the gust effect factor increases with the building height as the wind load effect is greater on the structural behaviour.
In the case of the 168-m tall building, Table 2.6 shows the lateral load F and the torque moment M_T values along the building height considering a step of 3.5 m for the interstory height. All the calculations are repeated for the other heights. In particular, the maximum lateral forces F obtained at the building top are 203, 229, 251 and 273 kN for the 126-, 168-, 210- and 252 m tall buildings, respectively. The lateral loads are applied to the building independently from the plan shape. In order to perform the structural analysis, the horizontal and torque actions are converted to concentrated horizontal and torque loads to be applied at each rigid floor of the diagrid structure. Note that at the top floor of the building the wind force is given only by the wind pressure acting on the upper half of the top module.

Forces along the height due to wind load on the 168-m tall building					
z [m]	F [kN]	M_T [kNm]	z [m]	F [kN]	M_T [kNm]
3,5	155	700	88	210	946
7	163	735	91	211	950
10,5	169	760	95	212	955
14	173	779	98	213	959
17,5	177	795	102	214	964
21	180	809	105	215	968
24,5	182	821	109	216	972
28	185	832	112	217	976
31,5	187	842	116	218	980
35	189	852	119	219	983
38,5	191	860	123	219	987
42	193	868	126	220	991
45,5	195	876	130	221	994
49	196	883	133	222	998
52,5	198	890	137	223	1001
56	199	897	140	223	1005
59,5	201	903	144	224	1008
63	202	909	147	225	1011
66,5	203	915	151	225	1014
70	205	921	154	226	1018
73,5	206	926	158	227	1021
77	207	931	161	228	1024
80,5	208	936	165	228	1027
84	209	941	168	229	1030

Table 2.6 - Lateral force and torque moment distributions for the 168-m tall building due to wind load

The distributions of the lateral force and torque moment for different building heights are reported in Figure 2.2. It is evident that both lateral force and torque moment increase with the building height. In addition, Table 2.7 shows values of wind base shear, wind overturning moment and wind base torque moment for different heights.

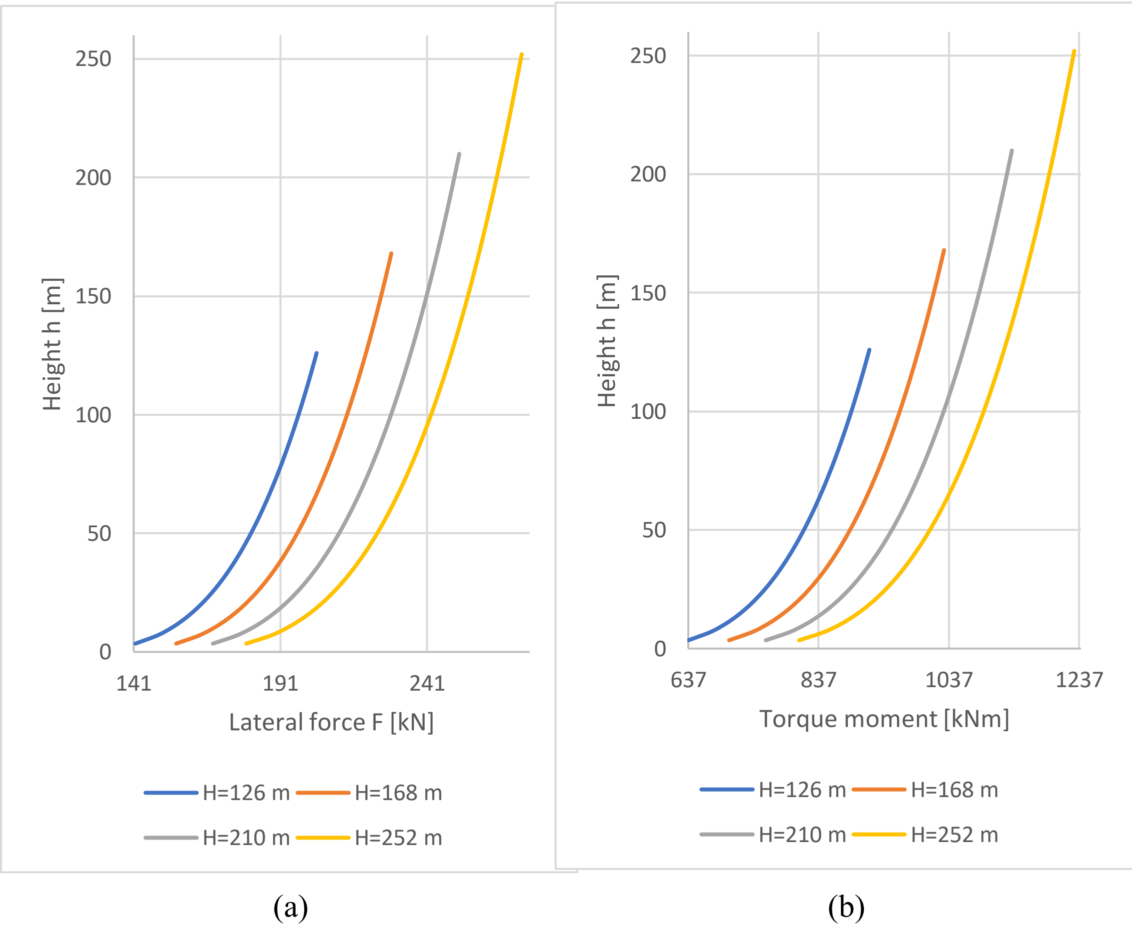

Figure 2.2 - Forces distribution for different building heights due to wind action: (a) Lateral force F in kN (b) Torque moment M in kNm

	126	168	210	252
Wind base shear [MN]	7	10	14	18
Wind overturning moment [MNm]	447	887	1518	2363
Wind base torque moment [MNm]	30	44	61	79

Table 2.7 - Wind base shear, wind overturning moment and wind base torque moment for different heights

The results reported in Table 2.7 demonstrate that the wind effect increases with the building height, the overturning moment increases by five times when the height is doubled, whereas the base shear and base torque moment increase almost linearly with the height. This observation implies that the bending behaviour prevails on the shear one for taller buildings and therefore steeper diagonals should be needed to ensure lateral stiffness, as mentioned in Chapter 1.3.

2.3. STRENGTH AND STIFFNESS REQUIREMENTS

In tall building design is fundamental to ensure two requirements, namely the strength and the stiffness. As mentioned in Chapter 1.3, it is not possible to predict a priori which one will govern the design and therefore both strength and stiffness have to be taken into account. As far as the global stiffness of the structure is concerned, it consists in limiting the lateral displacement, especially at the top of the building, in order to cope with the lateral load due to wind action. To this aim, the stiffness requirement is simply given by imposing the limit target top displacement equal to H/500. Regarding the strength, since the diagrid system is made up of the diagonals subjected only to tensile or compressive axial forces, the strength requirement is based on the assessment of tensile and compressive strengths, as it is shown in the following Chapter. However, in the case of compressed diagonal the buckling strength must be defined in order to prevent instability phenomena. Strength values are evaluated referring to Eurocode 3 [42] for the case of steel structures.

2.3.1. TENSILE STRENGTH

The verification of a diagonal in traction subjected to the design axial force N_{Ed} is satisfied when its bearing capacity $N_{t,Rd}$ is not exceeded:

$$N_{Ed} \leq N_{t,Rd} \tag{2.15}$$

The term $N_{t,Rd}$ is assumed to be equal to the design plastic strength of a gross section by neglecting the presence of holes in the structural members:

$$N_{t,Rd} = \frac{A \cdot f_y}{\gamma_{M0}} \tag{2.16}$$

Where A is the gross transversal section area, f_y is the yielding strength and γ_{M0} is a safety factor. In the study case γ_{M0} is not considered for sake of simplicity.

2.3.2. COMPRESSIVE STRENGTH

The verification of a diagonal in compression subjected to the design axial force N_{Ed} is satisfied when its bearing capacity $N_{c,Rd}$ is not exceeded:

$$N_{Ed} \leq N_{c,Rd} \tag{2.17}$$

The design compression strength $N_{c,Rd}$ is defined in function of cross section classification:

- Sections of class 1, 2 or 3:

$$N_{c,Rd} = \frac{A \cdot f_y}{\gamma_{M0}} \tag{2.18}$$

- Sections of class 4:

$$N_{c,Rd} = \frac{A_{eff} \cdot f_y}{\gamma_{M0}} \tag{2.19}$$

where A is the gross transversal section area, A_{eff} is the effective transversal area, f_y is the yielding strength and γ_{M0} is a safety factor. The local instability reduces the bearing capacity of compression elements in class 4 as their crisis occurs when the axial force is lower than the yielding force evaluated with reference to the gross section area.

2.3.3. BUCKLING

The state of stress of a compressed element, especially for steel members, is always associated to buckling phenomena. Thus, the strength verification has to be coupled with buckling verification which is often the most critical one for the design, especially in slender structural elements. In this Chapter the assessment of Euler load by equilibrium analysis and buckling strength calculation through EC3 are described.

2.3.3.1. THE EULER CRITICAL LOAD BY EQUILIBRIUM ANALYSIS

The assessment of Euler load has been carried out for the first time by Euler in 1744. In order to evaluate the Euler's critical load a simply supported (pin-ended) beam with length l is considered (Figure 2.3a). This system is assumed to be ideal without any imperfection and subjected to a positive compression axial force N. For small values of N, the beam remains in equilibrium, but for greater values the system reaches an instability condition. In particular, the load N produces a bending moment $M = -Nv$ along the beam length, where v represents the lateral deflection. Thus, it is possible to define the second order differential equation of bending considering the effect of deflection on the equilibrium conditions (second-order theory [43]) as:

$$v'' + \alpha^2 v = \frac{M}{EI} \tag{2.20}$$

$$v'' + \alpha^2 v = 0 \qquad with\ \alpha^2 = \frac{N}{EI} \tag{2.21}$$

The Equation (2.21) is an ordinary linear differential equation. By imposing the boundary conditions, precisely lateral deflection null at the ends ($v(0) = v(l) = 0$), the general solution for N>0 is:

$$v(z) = A\ cos\alpha z + B\ sin\alpha z \tag{2.22}$$

Where A and B are arbitrary constants obtained by the boundary conditions:

$$A = 0 \qquad Bsin\alpha l = 0 \tag{2.23}$$

The last equation is satisfied only if $\alpha l = n\pi$ for any value of the coefficient B, where n is a natural number, and substituting in α^2 definition the following critical loads are obtained:

$$N_{cn} = \frac{n^2\pi^2}{l^2} EI \qquad (n = 1,2,3, \dots) \tag{2.24}$$

N_{cn} are the eigenvalues of the buckling problem and are called critical loads. The corresponding eigenmodes or deflection shapes at critical loads are:

$$v_n(z) = B \sin\left(\frac{n\pi z}{l}\right) \tag{2.25}$$

Where B is arbitrary constant. The deformed shape is constituted by n sinusoidal half-waves as shown in Figure 2.3b.

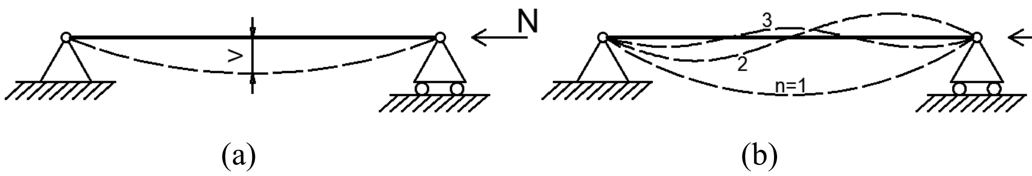

Figure 2.3 - Euler's critical load definition: (a) Static scheme of compressed beam with hinge ends (b) Deformed configurations

The lowest critical load is the first eigenvalue (n=1):

$$N_{c1} = \frac{\pi^2}{l^2} EI \tag{2.26}$$

N_{c1} is also called the Euler's critical load and it represents the load beyond which a perfect elastic beam fails due to buckling. Indeed, for $N < N_{c1}$ the equilibrium is stable; for $N = N_{c1}$ the equilibrium is neutral; for $N > N_{c1}$ the equilibrium is unstable. Further, it can be seen that the Euler's critical load is proportional to the beam rigidity EI, whereas it is inversely proportional to the beam length [44]. In case of different restraints, the deformed shape of the system can be obtained by the following forth order differential equation:

$$EIv^{IV} + Nv^{II} = 0 \tag{2.27}$$

The integral of Equation (2.27) is

$$v(z) = A\,cos\alpha z + B\,sin\alpha z + Cz + D \tag{2.28}$$

Equation (2.28) has four arbitrary constants A, B, C and D because there are four degrees of freedom (two deflections and two rotations). These are partly kinematic (or essential) conditions and partly static (or natural) conditions [44]. Thus, it is possible to evaluate the critical load in function of the basic schemes of different restraints. Analysing the critical formulations for different restraints, the more general Euler's critical load formulation can be obtained for any case as follows:

$$N_{c1} = \pi^2 \frac{EI}{l_0^2} \tag{2.29}$$

where l_0 is the free length of deflection, which represents the distance between two successive inflection points in the critical deformed configuration [44].

2.3.3.2. EVALUATION OF THE BUCKLING CRITICAL LOAD

Assuming no presence of geometrical imperfections and linear-elastic behaviour of the material, namely the ideal bar, it is possible to demonstrate that exists a critical load value N_{cr} beyond which the global buckling phenomena is activated. There are three types of buckling: flexural, torsional and flexural-torsional [45]. For circular hollow cross section (CHS) the typical instability is the flexural one because the section is characterized by two symmetry axes. In case of flexural instability, the critical value would be given by the minimum among two values evaluated in function of geometrical and mechanical parameters:

$$N_{cr} = \min\left\{\frac{\pi^2 EI_y}{L_{0,y}^2}, \frac{\pi^2 EI_z}{L_{0,z}^2}\right\} \tag{2.30}$$

Where E is the Young modulus, I second moment of inertia, L_0 effective length and y and z subscripts are referred to principal axes.

From a design perspective, it could be convenient to have an expression in terms of tension:

$$\sigma_{cr} = \frac{N_{cr}}{A} = \min\left\{\frac{\pi^2 E \rho_y^2}{L_{0,y}^2}, \frac{\pi^2 E \rho_z^2}{L_{0,z}^2}\right\} = \min\left\{\frac{\pi^2 E}{\lambda_y^2}, \frac{\pi^2 E}{\lambda_z^2}\right\} \tag{2.31}$$

Where A is the cross-section area, ρ gyrator radius of inertia and λ is the slenderness $\lambda = L_0/\rho$. In the verification the slenderness choosen is the maximum between the one in y direction and the other in z direction. In general, an ideal bar is not considered for the structural design because it is valid for elements characterized by perfectly linear-elastic behaviour and without geometrical imperfections. Actually, the structural members used in construction field are characterized by non-linear behaviour limited by the strength and mechanical and geometrical imperfections due to manufacture and assembly processes. Indeed, considering an element with cross section area A without imperfections, the critical load cannot overpass the value at which there is the complete plasticization of section ($f_y A$). The associated stability curve is given in Figure 2.4 in terms of tension σ – slenderness λ.

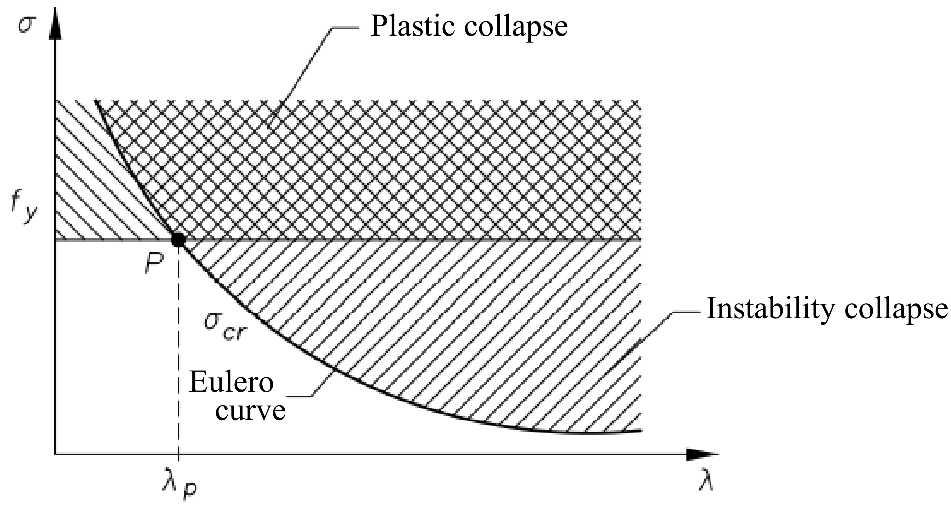

Figure 2.4 - Strength domain tension-slenderness for compressed element [45]

The intersection between Euler curve and the horizontal line in correspondence of f_y is the point P that has λ_P as abscissa. It is called proportionality slenderness and it is defined as:

$$\lambda_P = \pi \sqrt{\frac{E}{f_y}} \tag{2.32}$$

The definition of λ_P is important in order to define the type of structural collapse:

- If $\lambda < \lambda_P$ the cross section reaches the total plasticization due to strength failure;
- If $\lambda > \lambda_P$ the elastic instability phenomena would occur;
- If $\lambda = \lambda_P$ plastic and instability failure occur at the same moment.

The mechanical and geometrical imperfections are always present in a real structural element and they influence its bearing capacity. If the presence of an initial imperfection as an initial sinusoidal deformed shape is considered, the higher is the load applied N, the higher is the deflection δ and therefore the higher is the bending moment due to the eccentricity. The structural member response in terms of load – transverse displacement corresponds to the ideal system with initial imperfection and the curve reaches the asymptote N_{cr} because the material has an elastic behaviour as it is shown in Figure 2.5a. Furthermore, the deflection is approximated in function of the initial imperfection:

$$\delta = \delta_0 \cdot \frac{1}{1 - \frac{N}{N_{cr}}} \tag{2.33}$$

The section in midspan is in bending-compression and the maximum tension σ is evaluated as:

$$\sigma = \frac{N}{A} + \frac{N \cdot \delta}{W} = \frac{N}{A} + \frac{N \cdot \delta_0}{W} \cdot \frac{1}{1 - \frac{N}{N_{cr}}} \tag{2.34}$$

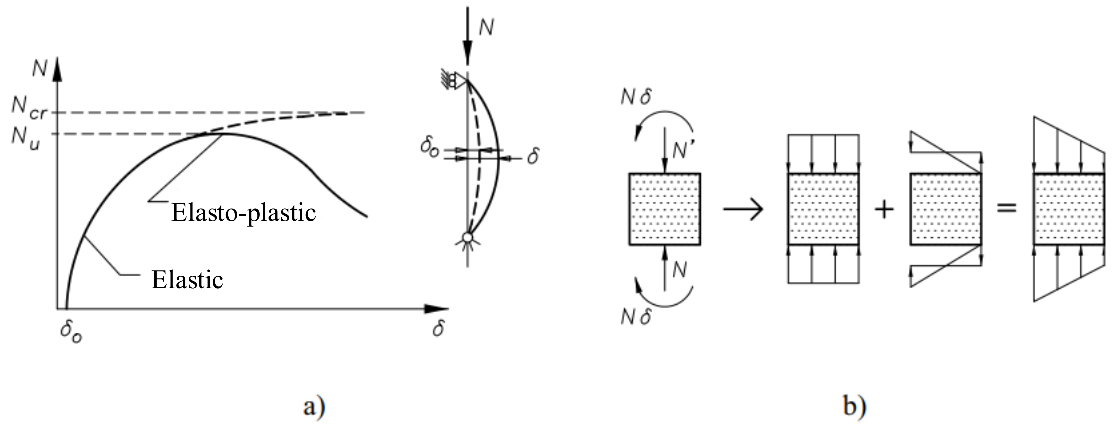

Figure 2.5 – Definition of buckling capacity: (a) Load-transverse displacement behaviour with initial imperfection and (b) state of stress in midspan [45]

When the yielding stress is reached, the stiffness of regions in post-elastic field is decreased. Therefore, there is a gradual increasing of flexural deformability after overpassing the maximum strength N_u that is lower than the critical load N_{cr}. From a comparison between the tension – slenderness curve of an element without imperfection and the one with imperfection it is evident that the latter has lower bearing capacity than the former due to the elasto-plastic behaviour and the defects (Figure 2.6). The transition from plastic collapse to instability one depends on instability phenomena and it starts from $0.2\lambda_P$ instead from λ_P.

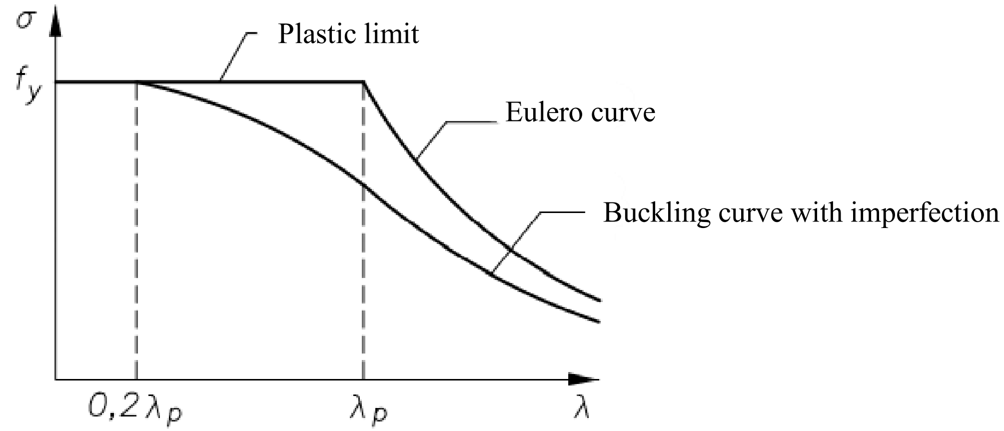

Figure 2.6 – Comparison of tension-slenderness curve with and without imperfection [45]

According to the Eurocode EC3 [42], the stability verification of a compressed element subjected to an axial force N_{Ed} is satisfied if it does not exceed the bearing capacity $N_{b,Rd}$:

$$N_{Ed} \leq N_{b,Rd} \tag{2.35}$$

The buckling strength is evaluated in function of cross section classification:

- Class 1,2 and 3 sections:

$$N_{b,Rd} = \chi \cdot A \frac{f_y}{\gamma_{M1}} \tag{2.36}$$

- Class 4 sections:

$$N_{b,Rd} = \chi \cdot A_{eff} \frac{f_y}{\gamma_{M1}} \tag{2.37}$$

Where A is the cross-section nominal area, A_{eff} section effective area, f_y yielding strength, χ is a reduction factor and γ_{M1} is the safety factor. The reduction factor is calculated in function of instability typology and it is given as:

$$\chi = \frac{1}{\phi + \sqrt{\phi^2 - \lambda^2}} \leq 1 \tag{2.38}$$

$$\phi = 0.5 \cdot \left[1 + \alpha\left(\bar{\lambda} - 0.2\right) + \bar{\lambda}^2\right] \tag{2.39}$$

Where α represents the imperfection coefficient and it depends on the stability curve (Table 2.8) that has to be selected in function of the transverse section, limits, axis of instability and steel quality.

Buckling curve	a_0	a	b	c	d
Imperfection factor α	0.13	0.21	0.34	0.49	0.76

Table 2.8 - Imperfection factor values in function of stability curve [42]

The relative slenderness $\bar{\lambda}$ depends on cross section classification:

- Class 1,2 and 3 sections:

$$\bar{\lambda} = \sqrt{\frac{A \cdot f_y}{N_{cr}}} \tag{2.40}$$

- Class 4 sections:

$$\bar{\lambda} = \sqrt{\frac{A_{eff} \cdot f_y}{N_{cr}}} \tag{2.41}$$

Where N_{cr} is the critical elastic force.

In the case of the problem examined, the stability curve chosen is related to hot finished circular hollow sections (CHS), as it is shown in Table 2.9. Thus, the correspondent buckling curve is a and the imperfection coefficient α is equal to 0.21.

Transverse section	Limits	Buckling about axis	Buckling curve	
			S 235 S 275 S 355 S 420	S 460
Hollow sections 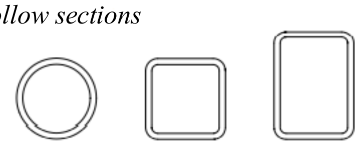	Hot finished	Any	*a*	a_0
	Cold formed	Any	*c*	*c*

Table 2.9 - Buckling curve for circular hollow sections CHS [42]

Chapter 3

3. STRENGTH- AND STIFFNESS-BASED PRELIMINARY DESIGN

Chapter 3 describes the proposed strength- and stiffness-base preliminary design developed within Matlab environment in order to define the geometrical properties of each model able to withstand vertical and horizontal loads ensuring both stiffness and strength requirements by minimizing the structural weight. Chapter 3.1 highlights step by step the methodology employed, while Chapter 3.2 summarizes the main outcomes.

3.1. METHODOLOGY

The methodology consists in the evaluation of diagonal sectional areas to ensure strength and stiffness requirements. From an engineering perspective, it is a better choice that these requirements are satisfied with minimum structural weight as related to sustainability problem. The proposed procedure is implemented within Matlab environment and it employed the matrix-based method (MBM) described in detail in [21] in order to perform the structural analysis of diagrid structures.

In order to carry out this analysis, it is necessary to define initial parameters to be introduced in the preliminary design and the MBM codes. Based on the diagrid models described in Chapter 2.1, there are parameters that are assumed constant independently from the building height, diagonal angle and floor plan shape: diagonals' elastic modulus E, steel density ρ, inter-story height and total floor area. The correspondent values are reported in Table 2.1. In the next step, the definition of the base module geometry has been determined in function of the floor plan shape (square, hexagon, octagon and circle) and the number of intra-module floors. Moreover, it is assumed that each module is made up of diagonals with same cross-section. Since the diagonals' cross section areas have to be provided for performing the structural analysis, in the preliminary stage the cross-section areas are initially assumed equal to $0.1\ \mathrm{m}^2$ and $0.01\ \mathrm{m}^2$ for the base and the top module, respectively, while a linear interpolation is used for the intermediate modules. The obtained values are compared to a vector of cross-section areas provided by handbooks of profiles available in commerce in order to consider a real and not fictitious cross-sections in the analysis. In particular, Table 3.1 shows circular hollow sections (CHS) with different outer diameters and thicknesses used in this study. These values refer to cross sections belonging to class 1, 2 and 3. Specifically, the sections of class 4 with diameter and thickness ratio higher than $90 \cdot 235/f_y$ have been excluded as the local instability problem occurs before reaching the yielding resistance, remaining in the elastic range. The cross-sections reported are sorted in ascending order in terms of diameters and areas. The diagonal area distribution along the height has been verified through the MBM for the structural analysis, ensuring strength and stiffness demands. Before performing the analysis, it is fundamental to define another input data, i.e. the load. From Chapter 2.1, the vertical load has been set equal to $4.125\ \mathrm{kN/m}^2$ by combining dead and live loads; while in Chapter 2.2, the lateral forces in kN and torque moments in kNm are obtained for each rigid floor. Since the intra-module floors are neglected in the MBM for hypothesis, the lateral actions are exclusively carried by the rigid floors and these actions are evaluated by means of an isostatic repartition. In particular, the lateral force and torque moment resultant are respectively result of the sum of lateral forces and torque moments acting on the upper half of the lower module and on the lower half of the upper module, except for the top floor where there is only the contribution of half of the top module. Thus, given all the above-mentioned parameters the analysis can be performed and for each model with different height, floor plan shape and diagonal angle, the MBM provides the structure response in terms of lateral displacements parallel and orthogonal to wind direction, torsional rotation, structural weight and axial diagonal forces.

CHS section [mm]			A $[cm^2]$	CHS section [mm]			A $[cm^2]$
70	×	16	27	194	×	60	252
70	×	18	29	219	×	50	266
70	×	20	31	219	×	55	284
76	×	18	32	219	×	60	300
76	×	20	35	219	×	65	315
83	×	18	36	219	×	70	328
83	×	20	39	245	×	60	348
83	×	22	42	245	×	65	367
83	×	25	45	245	×	70	384
89	×	22	47	245	×	80	413
89	×	25	50	245	×	90	437
102	×	20	51	267	×	80	470
102	×	22	55	267	×	90	500
102	×	25	60	267	×	100	525
102	×	28	65	273	×	100	543
102	×	30	67	299	×	80	549
108	×	28	70	299	×	90	590
108	×	30	74	299	×	100	624
114	×	28	76	324	×	90	661
114	×	30	79	324	×	100	703
114	×	32	83	356	×	90	751
114	×	36	89	356	×	100	803
127	×	30	91	368	×	100	842
127	×	32	96	406	×	90	895
127	×	36	103	406	×	100	963
127	×	40	109	419	×	100	1002
127	×	45	116	457	×	90	1038
140	×	36	117	457	×	100	1122
140	×	40	125	508	×	90	1182
140	×	45	134	508	×	100	1282
140	×	50	141	559	×	90	1326
152	×	40	141	559	×	100	1442
152	×	45	152	610	×	90	1470
152	×	50	161	610	×	100	1602
159	×	45	161	660	×	90	1612
159	×	50	171	660	×	100	1759
159	×	60	187	711	×	100	1920
168	×	60	204	1620	×	40	1985
178	×	55	212	1820	×	36	2018
178	×	60	222	1820	×	40	2237
194	×	50	226	2020	×	36	2244
194	×	55	240	2020	×	40	2488
				2220	×	40	2739

Table 3.1 - Steel structural circular hollow section (outer diameter × thickness in mm) and area for diagrid structures [46]

As mentioned before, the diagrid structure has to be designed in order to fulfill not only the global stiffness, but also the strength. To this aim, the demand capacity ratio (DCR) has been introduced as indicator of diagonal capacity under axial force. It is computed as the ratio between the design value of acting axial force and the diagonal strength. However, a diagonal can be in compression or in tension and therefore the expression of DCR is given by Equation (3.1):

$$DCR = \begin{cases} \dfrac{|\mathrm{N_{Ed}}|}{\min(\mathrm{N_{c,Rd}}, \mathrm{N_{b,Rd}})} & \text{if } \mathrm{N_{Ed}} < 0 \text{ (compression)} \\ \dfrac{\mathrm{N_{Ed}}}{\mathrm{N_{t,Rd}}} & \text{if } \mathrm{N_{Ed}} > 0 \text{ (tension)} \end{cases} \tag{3.1}$$

Where N_{Ed} is the axial force acting in the diagonal evaluated from the MBM: it is positive if diagonal is in tension and negative if diagonal is in compression; $N_{t,Rd}$ and $N_{c,Rd}$ are the tensile and compressive strength evaluated in Eq. (2.16)(2.18), respectively; $N_{b,Rd}$ is the buckling strength evaluated in Eq. (2.36) for compressed diagonals due to instability issue. Note that the safety factor is not considered for sake of simplicity. The DCR is calculated for each diagonal of a diagrid module. However, the preliminary design deals with the maximum value of DCR of each module in order to ensure greater diagonal exploitation and lower structural weight.

The proposed methodology is constituted by three fundamental steps. As follows, there is a detailed description of each step underlying the main aim of each of them:

STEP 1 – Initialization: for a given diagonal cross-section distribution chosen by the user in function of the initial diagonal cross section area of the base and top module, each module is analysed by means of the MBM and the strength calculation in order to evaluate the maximum value of DCR among diagonals of ith module. Supposing to start from the top module, for each module the undersized diagonal cross section area is assessed until obtaining DCR greater than the unit. This step is fundamental to minimize the diagrid structural mass. In addition, this iteration leads to a diagrid structure in failure condition, not being able to bear vertical and horizontal load.

STEP 2 – Strength: this step is opposite to the previous one because the diagonal cross section area is increased instead of decreasing it in order to ensure the resistance of each module. In general, the starting point is given by the diagonal area distribution along the building height obtained from STEP 1. Thus, the DCR is evaluated by performing the structural analysis and the strength calculation. If its value is greater than unit, it means that the strength demand is not fulfilled and consequently it is necessary to further increase the diagonal cross section area of the ith module until the DCR is less than or equal to 1. After, this operation is repeated for all lower modules step by step. Moreover, it is also essential to specify that the top lateral displacement is checked at each iteration. Indeed, if at the end of STEP 2 the top displacement is lower than the target limit value evaluated as H/500, the structure satisfies both strength and stiffness requirements and the STEP 3 does not have to be implemented. Conversely, in case of greater value the preliminary design is not concluded and the STEP 3 must be performed to ensure the global stiffness as described next. To sum up, STEP 2 allows to define a diagrid structure able to cope with the external load without yielding and buckling issues for all diagonals of each module.

It should be noted that it would have been possible to develop a code in Matlab that considered simultaneously STEP 1 and STEP 2, but with the difference that at each iteration cycle the diagonal cross section area can be increased or decreased according to DCR value with respect to the unit. Consequently, in this Thesis the distinction between STEP 1 and STEP 2 has been made aimed at obtaining clearer graphs and keeping the iterative process under control.

STEP 3 – Stiffness: this step is implemented only when the STEP 2 returns a structure that is too flexible and deformable due to the excessive top displacement. Differently from the first two steps, the diagonal cross section area is increased starting from the base module to fulfill stiffness requirements. The purpose is to proceed the iteration process until stiffening the structure enough to limit the global top lateral displacement. In case of flexible structure with high slenderness the final geometry may not satisfy the stiffness demand due to the limited maximum diagonal cross section area, i.e. $A_{max} = 0.2739\, m^2$ obtained from Table 3.1. Thus, in this particular case the algorithm returns a structure with constant stiffness along the building height and with huge structural weight.

The whole iterative process is schematized in Figure 3.1. The flow chart is divided into four parts: definition of input parameters, initialization step, strength step and stiffness step.

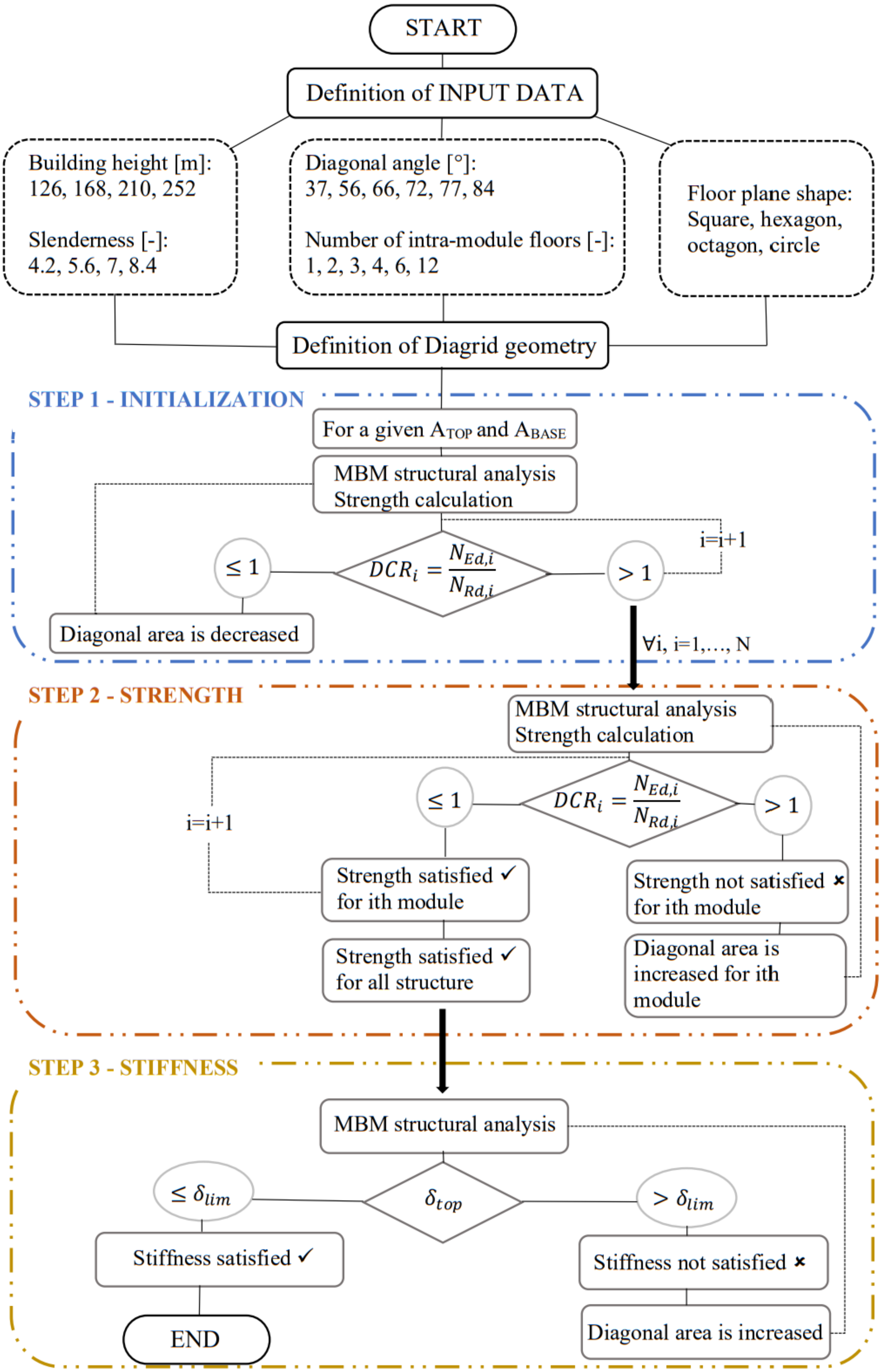

Figure 3.1 - Flow chart of the preliminary design; DCR = Demand to capacity ratio, δ_{top}= top lateral displacement, $\delta_{\lim}$ = target limit top lateral displacement value

3.2. UNIFORM-ANGLE DIAGRID STRUCTURES: RESULTS AND DISCUSSION

The previous algorithm developed within the software Matlab is employed to define the distribution of diagonal cross section minimizing the structural weight and satisfying both strength and stiffness requirements. The analysis is carried out for a total of ninety-six models obtained by choosing building height, floor plan shape and number of intra-module floors (or diagonal angle). This Section is divided into three sub-sections aiming at describing the top lateral displacement trend during the preliminary design in Chapter 3.2.1, the effect of the building height and diagonal inclination on DCR in Chapter 3.2.2 and the effect of the floor plan shape in Chapter 3.2.3.

3.2.1. EVOLUTION OF THE TOP LATERAL DISPLACEMENT THROUGHOUT THE PRELIMINARY DESIGN STAGE

As mentioned in Chapter 3.1, the iterative preliminary design is based on three fundamental steps which have been distinguished with different colors in the following graphs. In particular, blue for the initialization step, red for the strength step and yellow for the stiffness step. Further, the graphs represented in Figure 3.2 are related only to diagrid structures with square floor plan shape because the curves follow similar trend for buildings with other plan shapes. The choice of representing the top lateral displacement trend instead of the torsional rotation or the structural weight trend is due to the stiffness constrain, expressed in terms of the target limit value H/500.

As regard the top lateral displacement, in the case of the 126-m tall building with an aspect ratio of 4.2 it can be seen that the strength demand governs the structure design. Indeed, as it is shown in Figure 3.2(a-f), it is found that all diagrid structures have a top lateral displacement lower that the target limit value (δ_{lim} =0.252 m) at the end of step 2 without the necessity of performing the step 3. Moreover, it is also evident that the diagonal angle influences the top lateral displacement since the minimum value (δ_{min} =0.149 m) is provided by diagonal angle of about 65°, corresponding to S3 solution. By increasing or decreasing the diagonal angle far from 65°, the lateral stiffness decreases, leading to greater top lateral displacement. Generally, all diagrid structures have good lateral behaviour except for the twelve intra-module floors solution because it is the unique geometry for which the step 3 is performed. In fact, in case of low slenderness, like in the case of the 126-m tall building, the shear contribution is greater than the bending one and therefore the twelve intra-module floors geometrical solution provides more bending stiffness than the shear rigidity because of steep diagonals. Nevertheless, it has been possible to increase diagonals inertia to ensure more rigidity. Further, it can be noted that the initial diagonal area distribution of $0.1\ m^2$ and $0.01\ m^2$ at the base and top module, respectively, oversizes the structure except for the S12 model.

By increasing the building height, the stiffness requirement tends to prevail for aspect ratio greater than 5 since the value of the top lateral displacement is very close to the limit value. In particular, the case of the 168-m tall building represents a transition condition in which both stiffness and strength provide same contribution in the structural design. In fact, according to Moon et al. in [4] the slenderness value of transition is 5 and, in the case examined, the slenderness is 5.6. From the results, it can be said that the stiffest structure is always provided by the geometrical solutions with three intra-module floors, whereas the most flexible is provided by solutions with one and twelve intra-module floors. This phenomenon is more accentuated in the case of the 210- and 252-m tall buildings because the structure with only one intra-module floor is so deformable that it is not able to guarantee the target limit value. Thus, the preliminary design returns geometries characterized by the highest structural weight with maximum inertia constant along the height. For this reason, in Figure 3.2m and Figure 3.2s the curves follow an asymptote.

As far as the torsional rotation is concerned, the curves are not reported since they have similar trends to the previous ones and in this case there is no target limit value to respect, as the torsional rotation tends to increase with the diagonal inclination. In particular, the maximum value is always provided by solutions with twelve intra-module floors for any height.

Regarding the structural weight, the graphs present curves similar to the previous ones, but they are flipped horizontally. Thus, it means that if the top lateral displacement or torsional rotation increases, the mass decreases to obtain flexible structure that is more susceptible to wind, whereas if the top lateral displacement decreases, the mass increases to stiffen the structure.

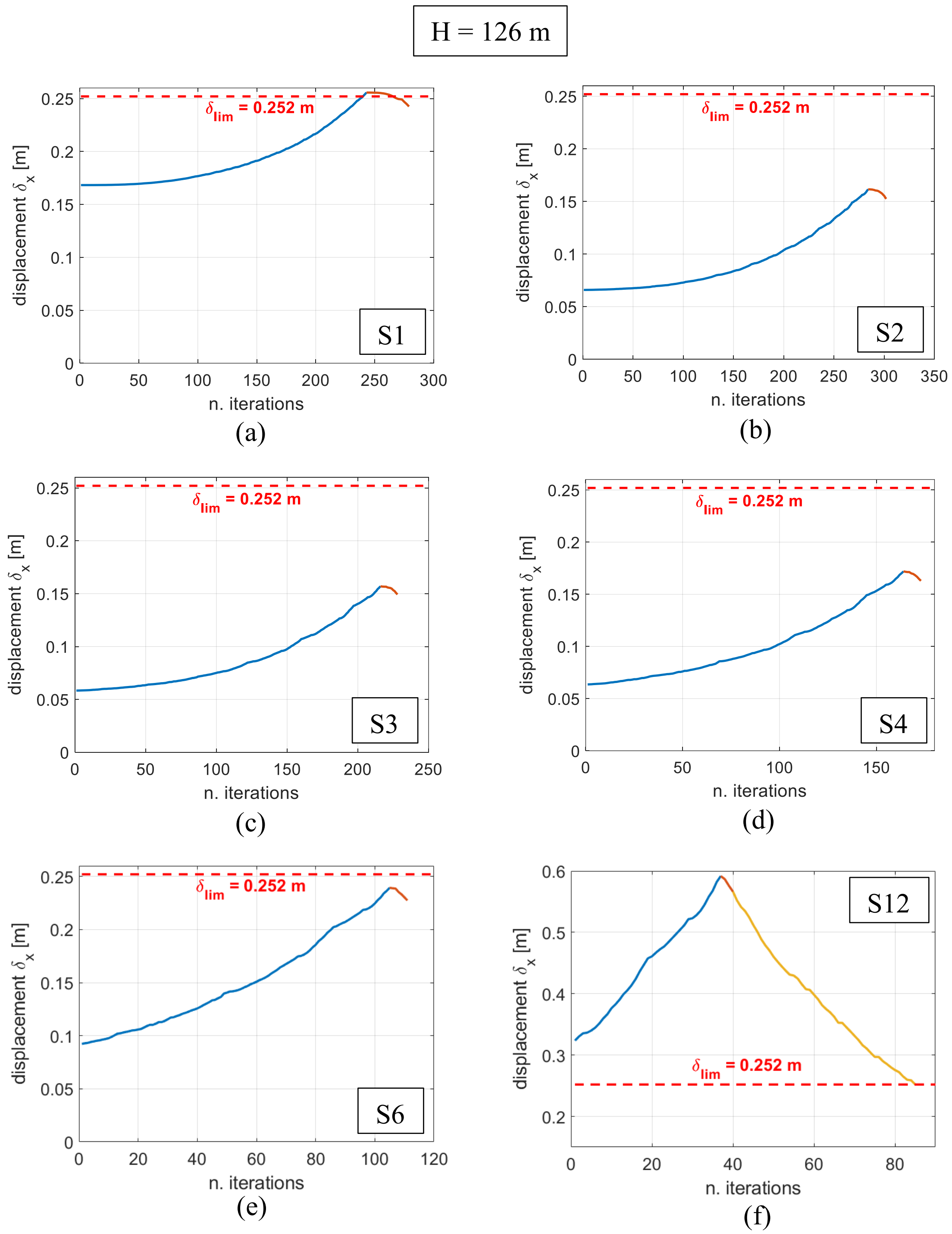
H = 126 m
displacement δx [m]
n. iterations
δlim = 0.252 m
S1
(a)
S2
(b)
S3
(c)
S4
(d)
S6
(e)
S12
(f)

H = 168 m

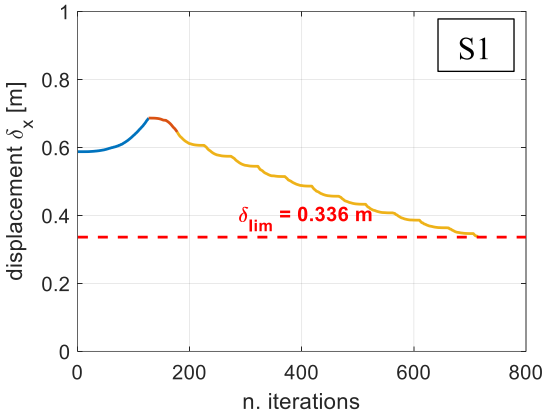

(g)

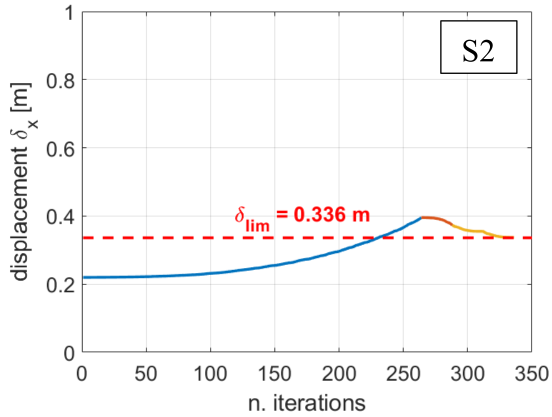

(h)

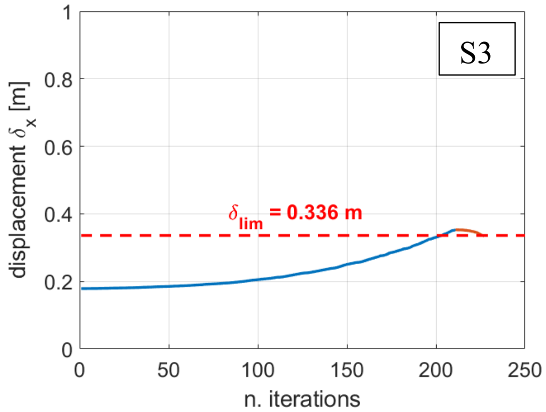

(i)

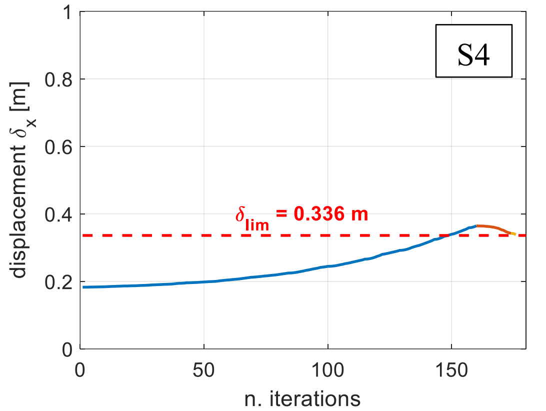

(j)

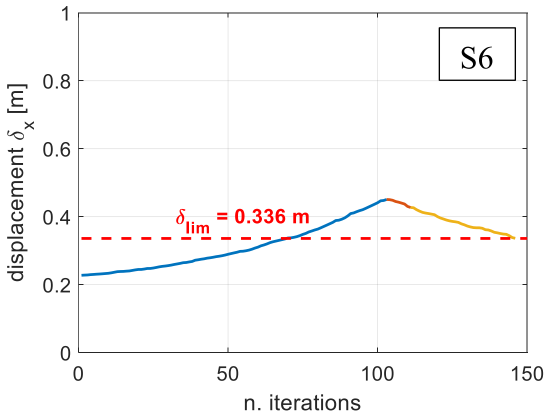

(k)

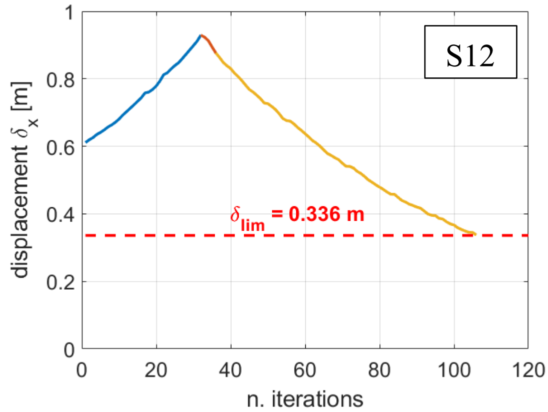

(l)

H = 210 m

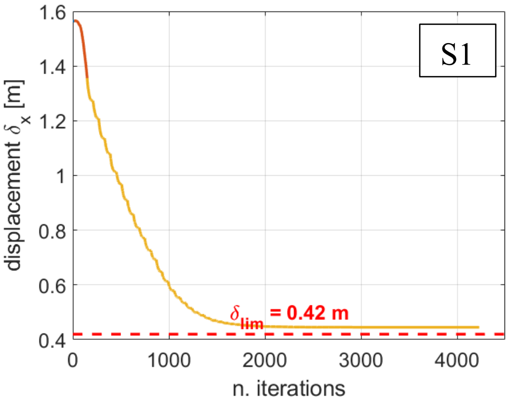

(m)

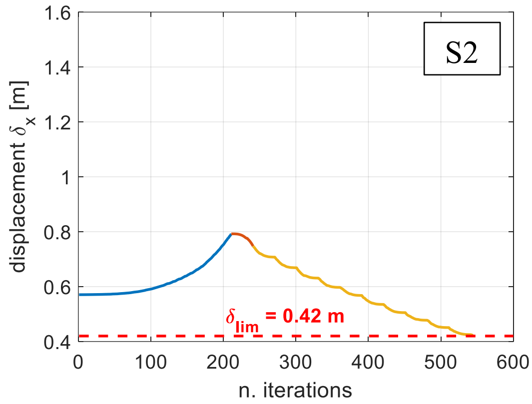

(n)

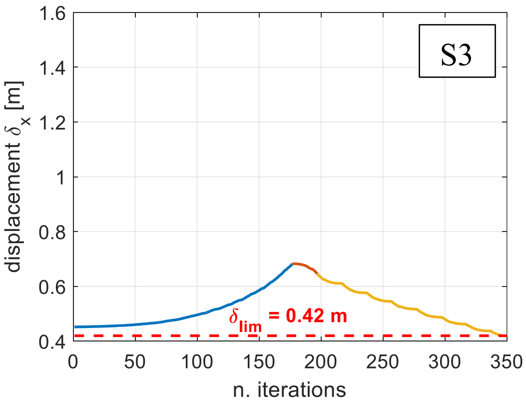

(o)

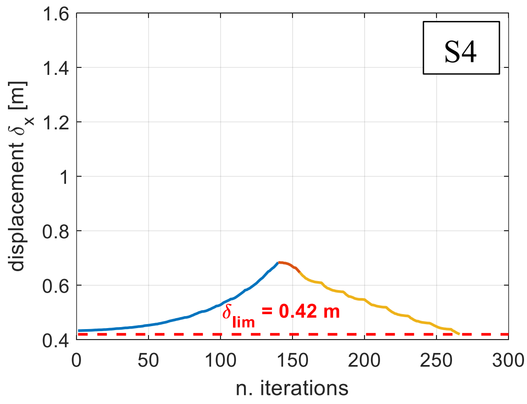

(p)

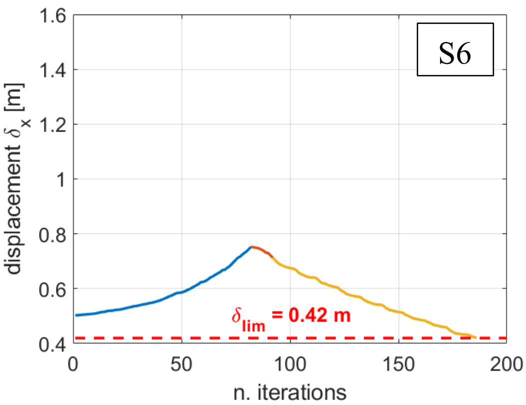

(q)

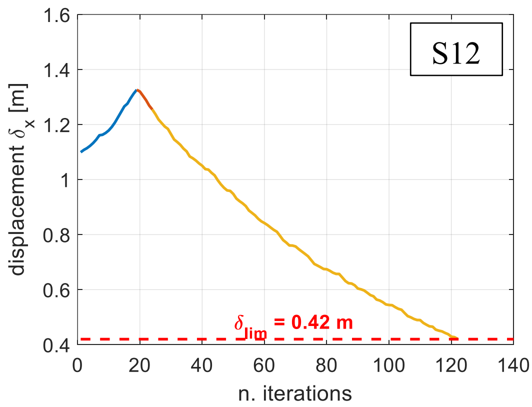

(r)

H = 252 m

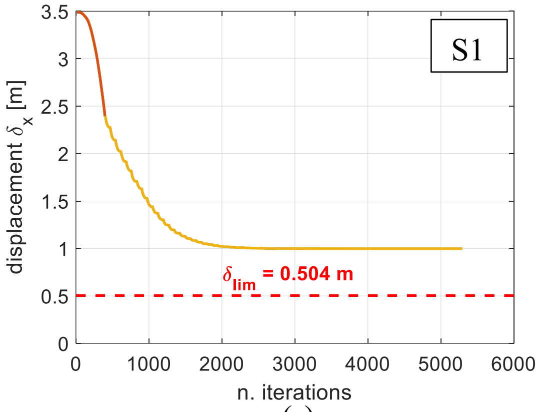

(s)

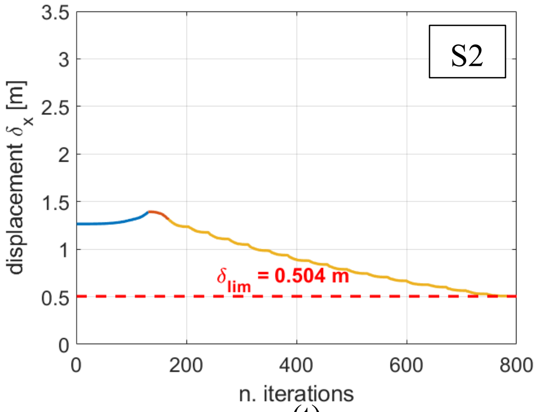

(t)

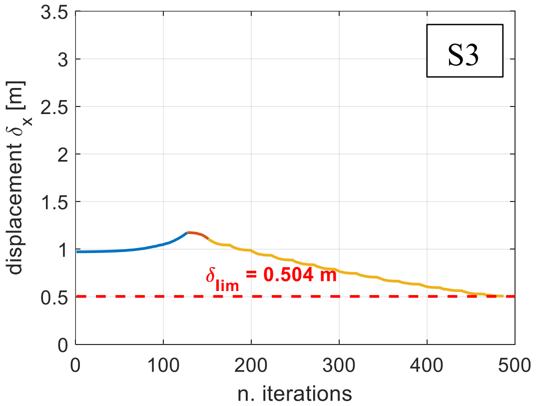

(u)

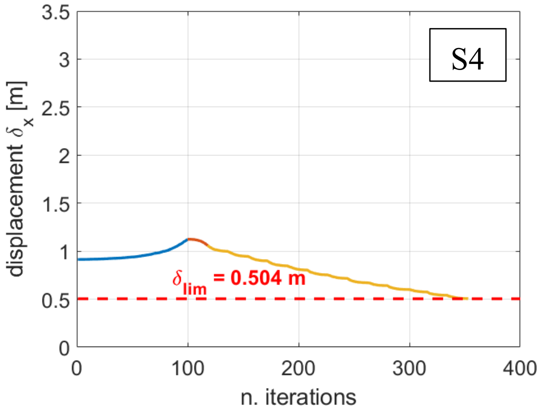

(v)

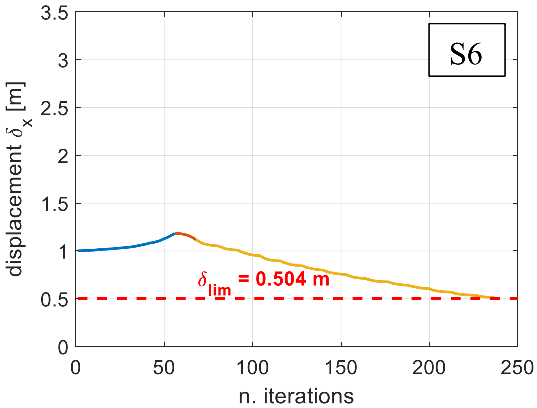

(w)

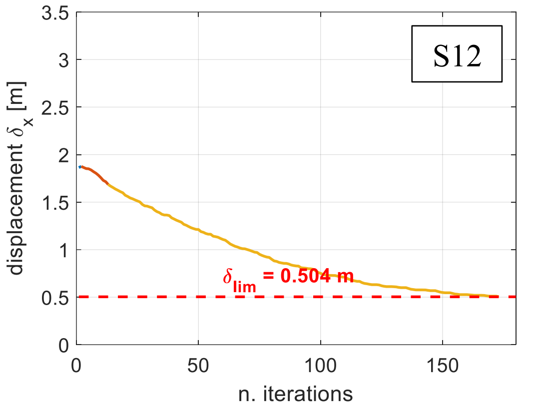

(x)

Figure 3.2 – Evolution of the top lateral displacement throughout the preliminary design stage: (a-f) H=126 m (g-l) H=168 m (m-r) H= 210 m (s-x) H=252 m

3.2.2. THE INFLUENCE OF THE BUILDING ASPECT RATIO AND DIAGONAL INCLINATION ON THE DEMAND CAPACITY RATIO (DCR)

After studying the parameters obtained by the structural analysis, it could be useful to carry out an investigation on DCR distribution. In Figure 3.3 there are graphs representing DCR values for each diagonal referred to each module. It can be seen that DCR distribution depends on the aspect ratio and specifically on the dominant requirement in the structural design. In fact, in the case of low slenderness of 4.2 in which strength demand prevails (Figure 3.3a-e), DCR range is from 0.2 to 1 for all the geometrical solutions, ensuring an enhanced strength performance. However, the S12 model which is characterized by steeper diagonals is not able to ensure sufficient shear rigidity to cope with the lateral load and therefore in this case DCR values drop below 0.4 (Figure 3.3f).

In the case of the 168-m tall building the DCR points are well distributed having maximum value close to 1 for all diagrid geometries except for S1 and S12 because the structural design is governed by the stiffness demand for slenderness greater than 5. In fact, for the latter solutions the DCR points are more concentrated within range between 0 and 0.4-0.45 (Figure 3.3g-l). This phenomenon of having low DCR values is strongly accentuated in slender structures, i.e. the 210-m and 252-m tall buildings, because the stiffness requirement is more important than the strength demand (Figure 3.3m-x). In particular, the cloud of points tends to move toward left below 0.6 for structures with slenderness of 7 and below 0.4 for the ones with slenderness of 8.4. Thus, it means that the diagonals are so oversized that their strength becomes much greater than the acting axial force, leading to a cloud of points more concentrated toward lower DCR values. By observing these graphs, it can be also found that there are two graphs in Figure 3.3m and Figure 3.3s with different trend with respect to others because the distribution is zero at the top of the structure and it increases almost linearly at the bottom. The reason is given by the diagonal cross section area distribution obtained from the preliminary design. As mentioned before, since the stiffness of these structures is constant along the height with the maximum diagonal area, the DCR increases as diagonal axial force increases toward the building base.

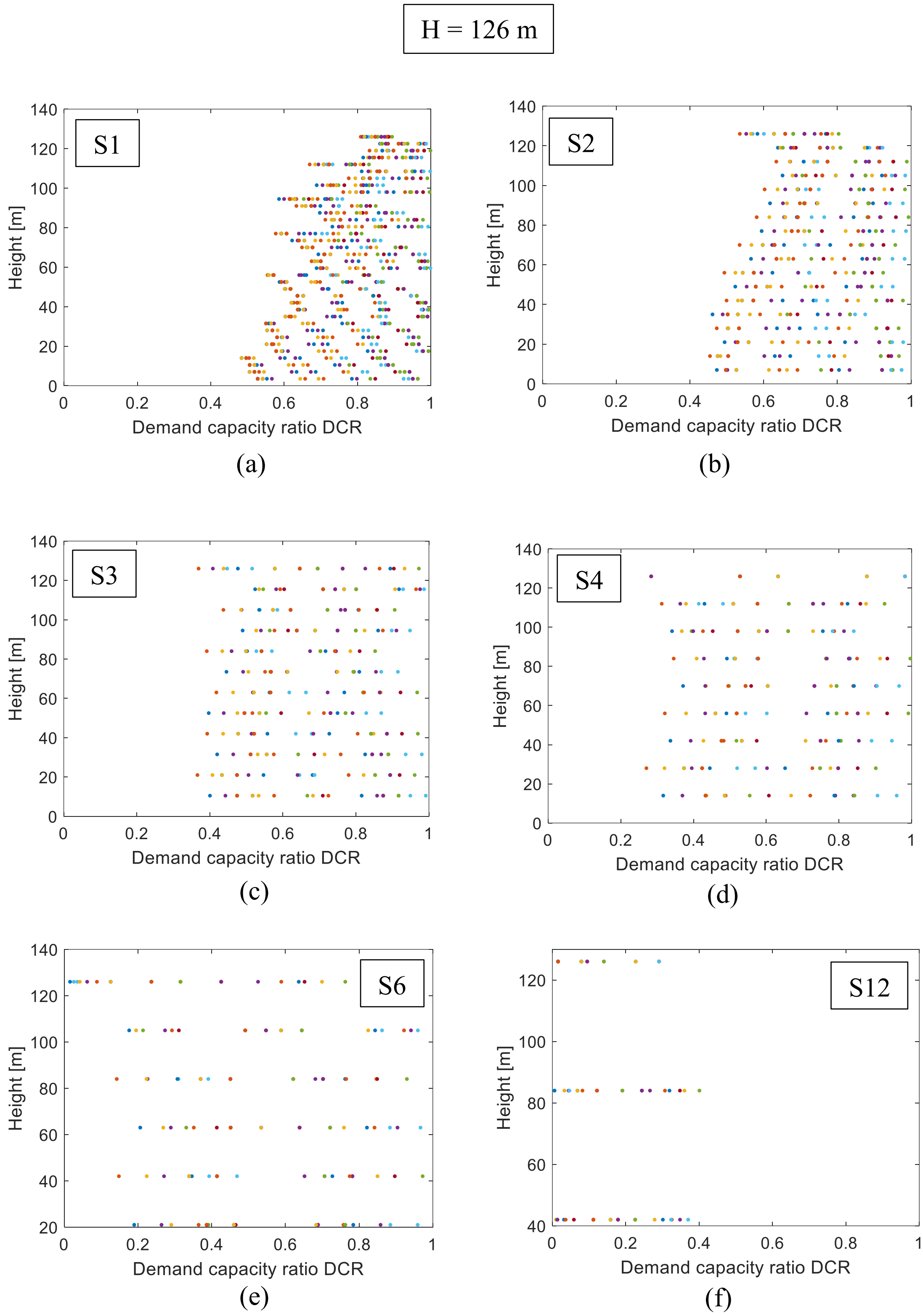
H = 126 m
S1
Height [m]
Demand capacity ratio DCR
(a)
S2
Height [m]
Demand capacity ratio DCR
(b)
S3
Height [m]
Demand capacity ratio DCR
(c)
S4
Height [m]
Demand capacity ratio DCR
(d)
S6
Height [m]
Demand capacity ratio DCR
(e)
S12
Height [m]
Demand capacity ratio DCR
(f)

H = 168 m

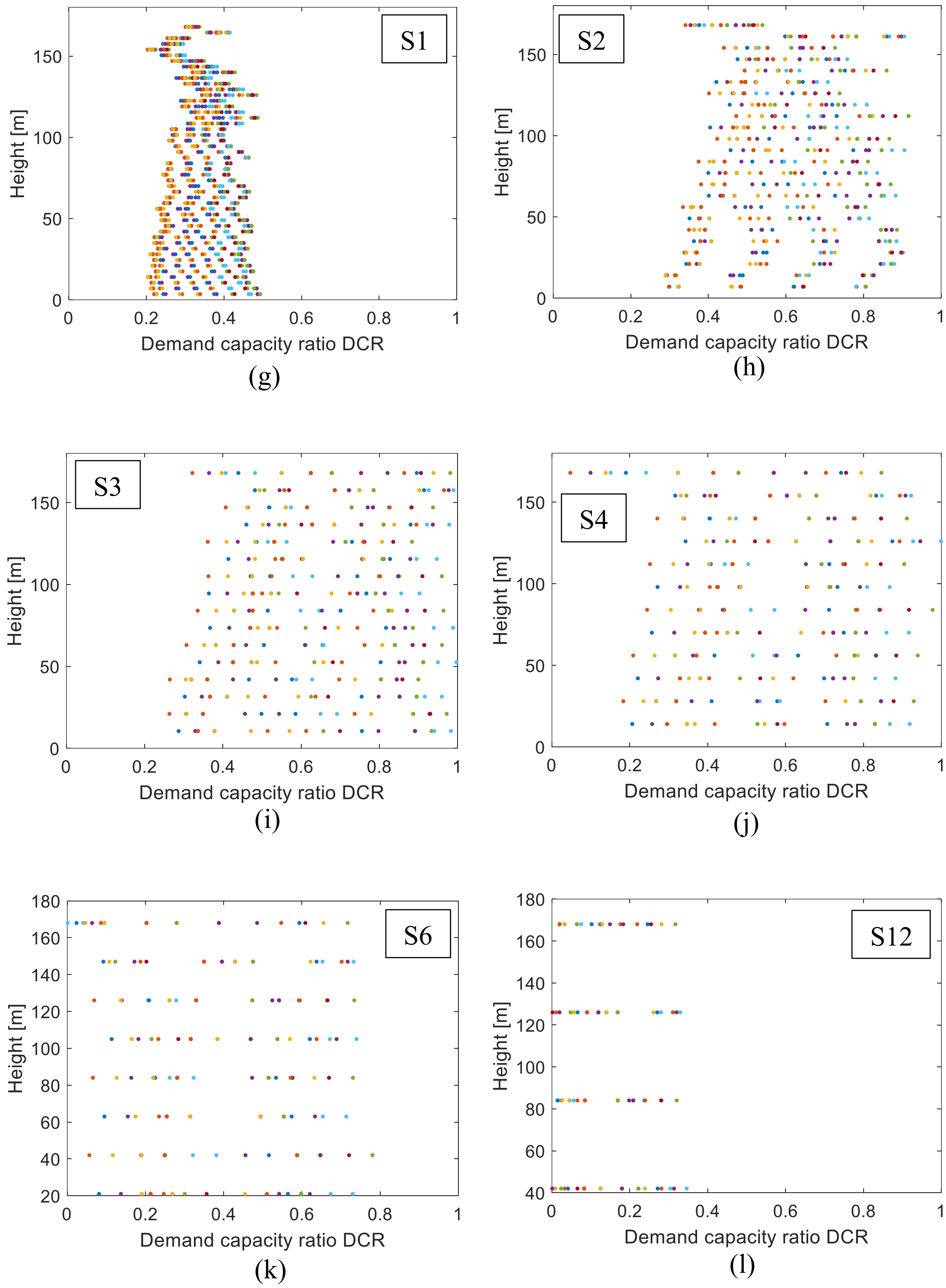
S1
Height [m]
Demand capacity ratio DCR
(g)
S2
Height [m]
Demand capacity ratio DCR
(h)
S3
Height [m]
Demand capacity ratio DCR
(i)
S4
Height [m]
Demand capacity ratio DCR
(j)
S6
Height [m]
Demand capacity ratio DCR
(k)
S12
Height [m]
Demand capacity ratio DCR
(l)

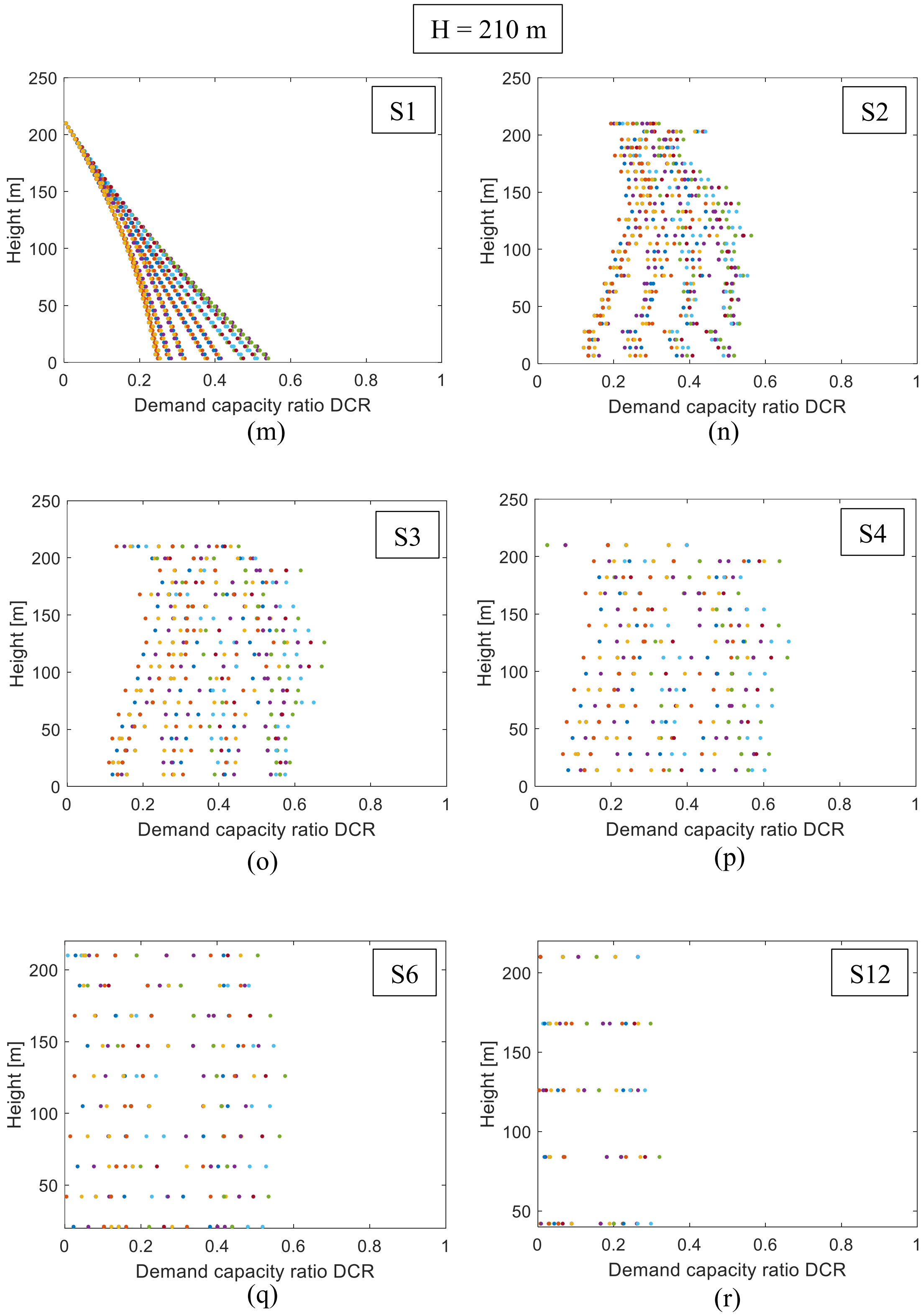
H = 210 m
S1
S2
S3
S4
S6
S12
Height [m]
Demand capacity ratio DCR
(m)
(n)
(o)
(p)
(q)
(r)

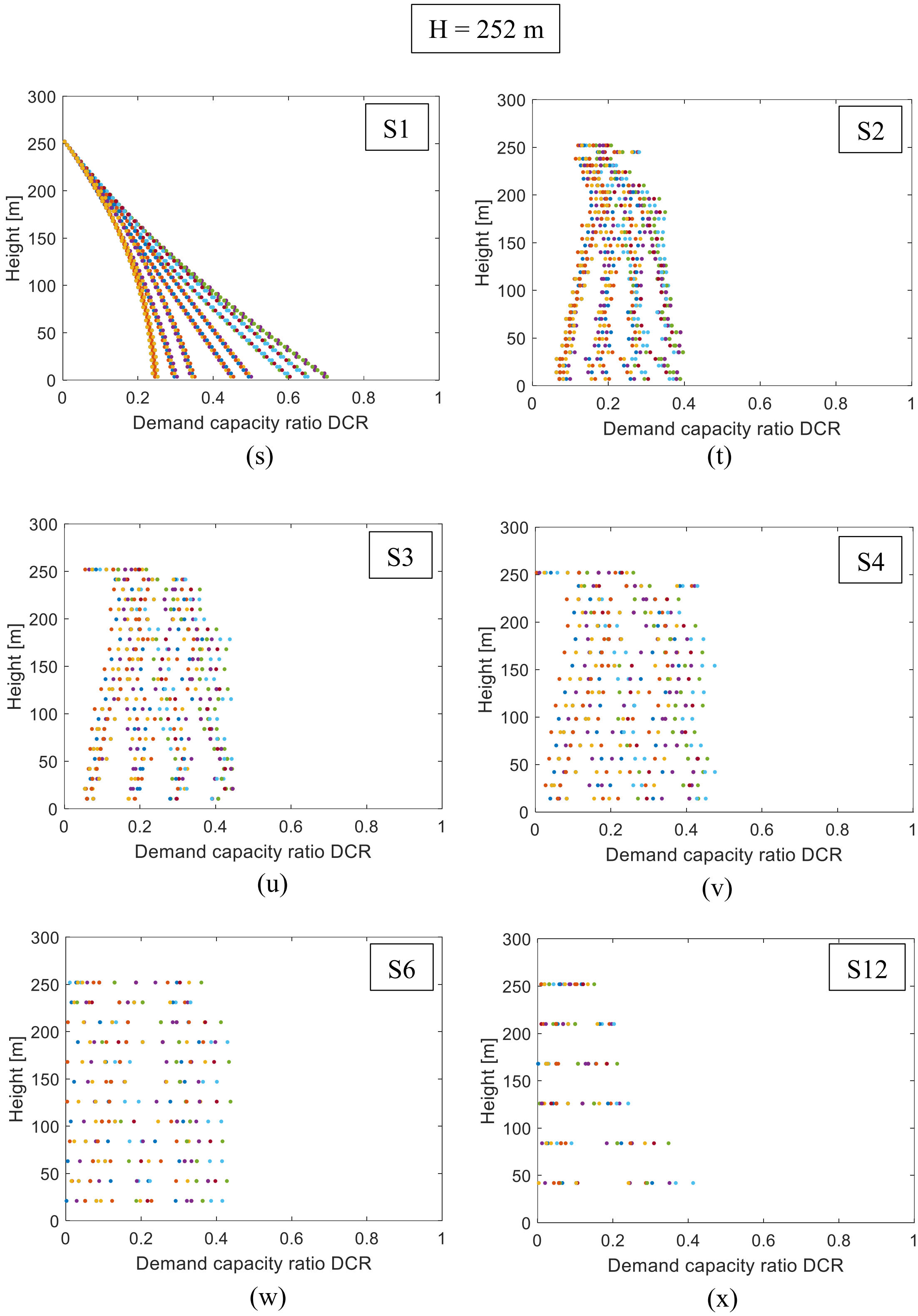

Figure 3.3 - DCR distribution for each diagonal in each module along height obtained from the preliminary design: (a-f) H=126 m (g-l) H=168 m (m-r) H= 210 m (s-x) H=252 m

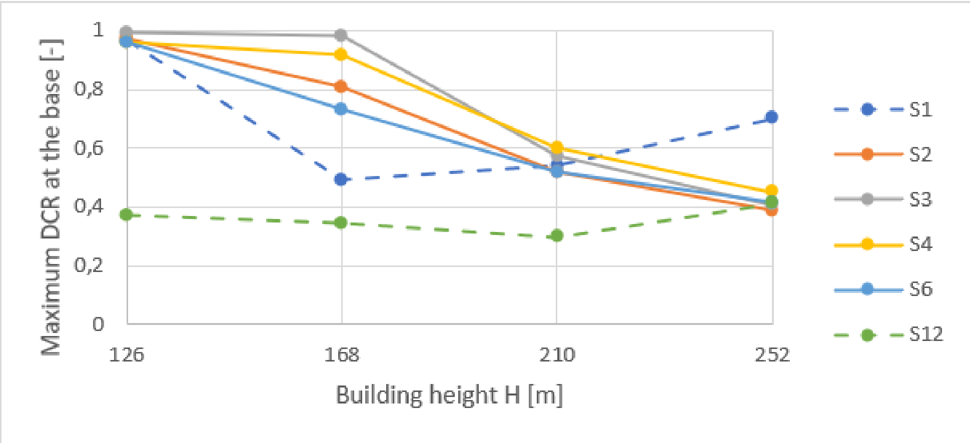

(a)

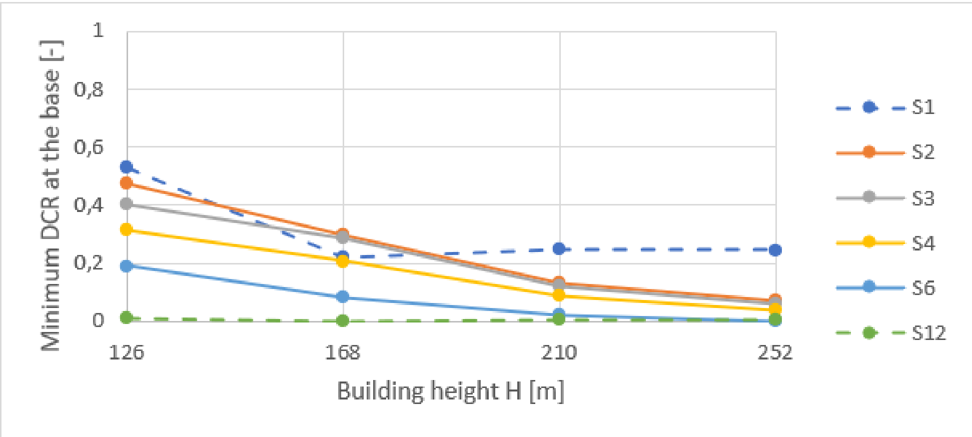

(b)

Figure 3.4 - DCR values at the base in function of building height and diagonal angle for structures with square floor plan shape: (a) Maximum values (b) Minimum values

In order to understand the effect of building height and diagonal angle on maximum and minimum value of DCR at the building base, Figure 3.4 has been provided aimed at summarizing the main aspects. Figure 3.4a shows that in the case of the 126-m tall building all geometries, except the S12 solution, tend to have maximum DCR values close to 1, and it means that the design is governed by the strength requirement, while in the case of the 168-m tall building, the geometrical solution providing highest DCR value is the one with three intra-module floors. Since the diagonal angle of 66° seems to be the optimal one in terms of strength for a slenderness of 5.6, in case of solutions with steeper or shallower diagonals maximum value of DCR decreases. As the structure height increases, the stiffness condition prevails. In fact, a further reduction of DCR value occurs due to oversized diagonals and as a consequence some diagonals even have null DCR, as it is shown in Figure 3.4b. Moreover, it can be noted that there are two types of curves, namely continuous and dashed. The dashed curves are related to more flexible structures, i.e. S1 and S12, and they start to go up starting from 168 and 210 m heights respectively because, as it can be seen in Figure 3.2s and Figure 3.2m, they do not satisfy the target limit value of the top lateral displacement even if characterized by the maximum inertia. Thus, DCR growth is mainly caused by the huge structural weight. Conversely, the continuous curves are referred to stiff structures that fulfil both strength and stiffness requirements at the end of the preliminary design. All these observations are in line with the studies carried out in literature reported in Chapter 1.3.

3.2.3. The influence of the different floor plan shapes

Until now structures with square floor plan have been analysed to point out the main results. As follow, instead, the results of all geometrical solutions with different floor plan shapes are provided in terms of diagonal cross section area and response parameters, namely top lateral displacement, torsional rotation and structural weight. The results related to diagonal cross section areas are reported in Figure 3.5. The graphs show diagonal cross section area at the top (blue curve) and at the base (red curve) of the building obtained from the preliminary design. In general, it is evident that diagonals are stiffer at the base than at the top and for each floor plan shape the curves follow the repetitive parabolic shape with minimum on solution with three or four intra-module floors. Thus, the effect of different floor plan shapes is more negligible than diagonal inclination and building height. Moreover, from the previous results it could have been predicted the diagonal cross section area growth with the building height because of the flexible behaviour. In fact, in the case of the 252-m tall building it is clear in Figure 3.5d that the structures with one intra-module floor provide constant diagonal area along the height since the two curves intersect.

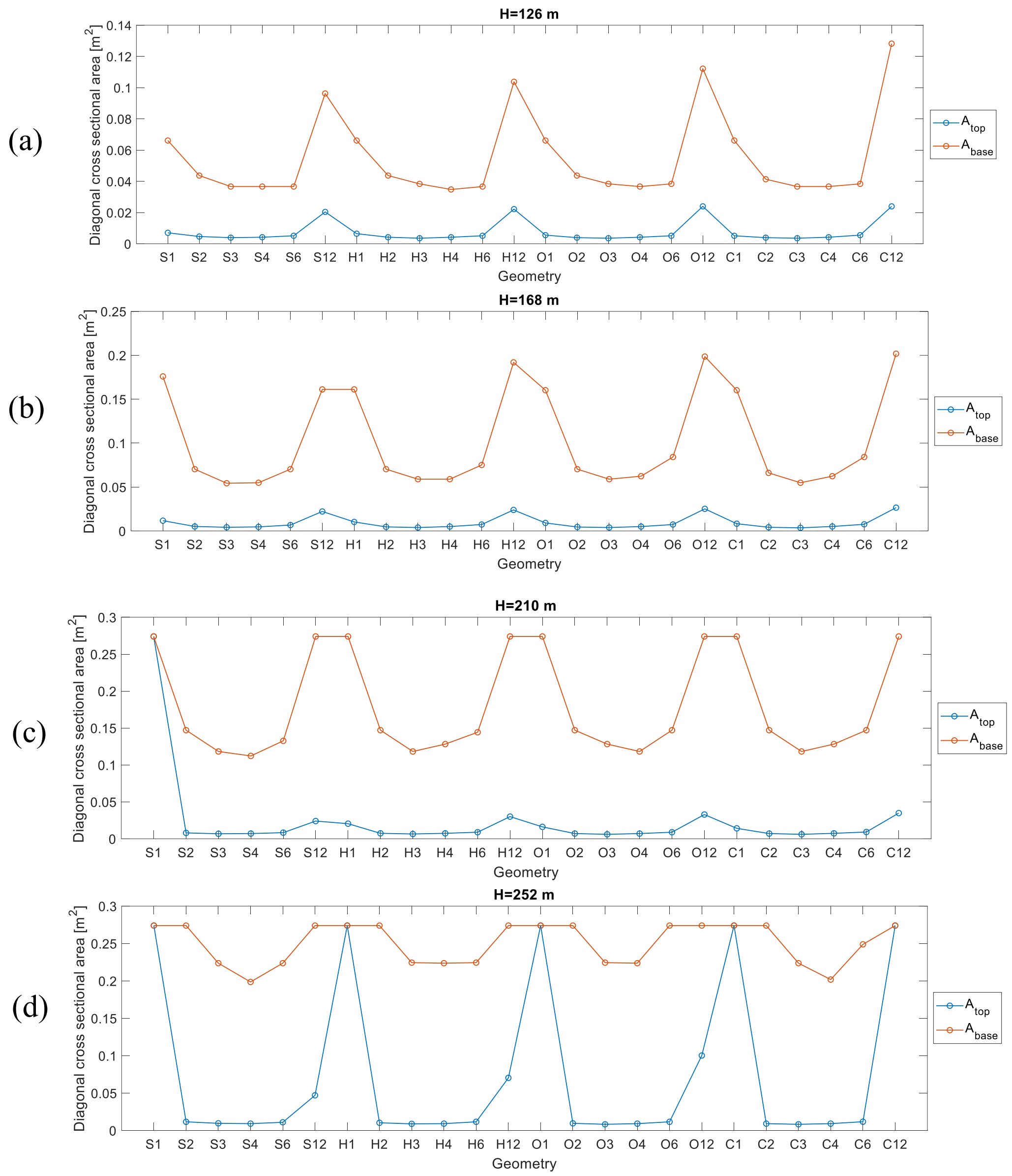

Figure 3.5 - Diagonal cross section area at the top and base module in function of floor plan shape and diagonal inclination for building with height of: (a) H=126 m (b) H=128 m (c) H=210 m (d) H=252 m

As far as the top lateral displacement is concerned, Figure 3.6a illustrates four curves for each building height and it also points out that for buildings with slenderness greater than 5 the top deflection is almost the same independently from the floor plan shape and the diagonal inclination due to the dominant stiffness demand. However, for the 252-m tall building the stiffness requirement is not always ensured due to the presence of peaks for one intra-module floor solutions. Conversely, in the case of the 126-m tall building the top displacement is not constant because the prevailing constraint is given by the strength requirement and furthermore the most efficient solutions are the ones with two or three intra-module floors.

Regarding the torsional rotation shown in Figure 3.6b, it can be noted that the effect of floor plan shape on structural behaviour is slight, but the effect of diagonal inclination is more evident. In fact, the minimum value is provided by the lowest diagonal angle and the maximum value by the steepest diagonals. The last but not least investigated parameter is the structural weight reported in Figure 3.6c. It has found that for each floor plan shape the curves are alike to parable and the best geometry which minimizes the mass is the one with intermediate diagonal inclinations. In addition, it is worth to note that the effect of floor plan shape is minor inside of the optimal diagonal inclination range (66°-72°) corresponding to three and four intra-module floors solutions, but it is major outside the optimal range, as it is illustrated in Figure 3.7. In particular, the one intra-module floor square building provides the highest mass, whereas the twelve intra-module square building provides the lowest one. Conversely, the circular structure with one intra-module floor is the lightest, whereas the heaviest is the one with twelve intra-module floors. These outcomes are in line with the ones obtained in [29].

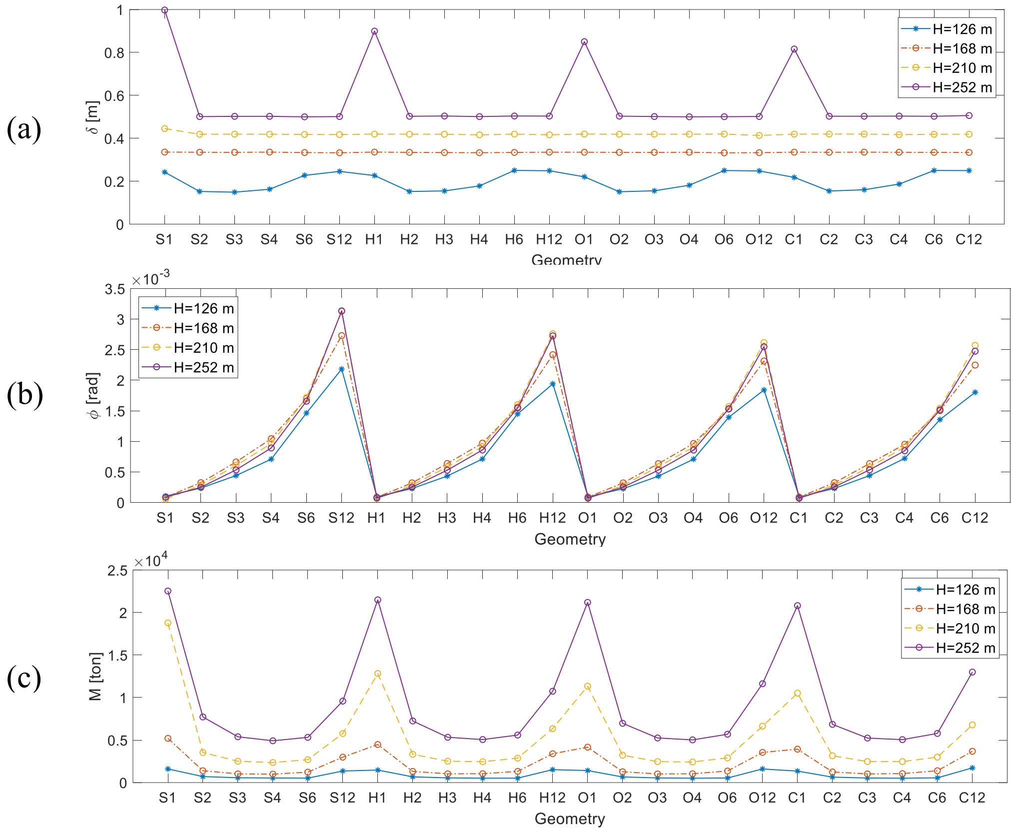

Figure 3.6 - Structural response parameters in function of floor plan shape, number of intra-module floors and building height: (a) top lateral displacement (b) torsional rotation (c) mass

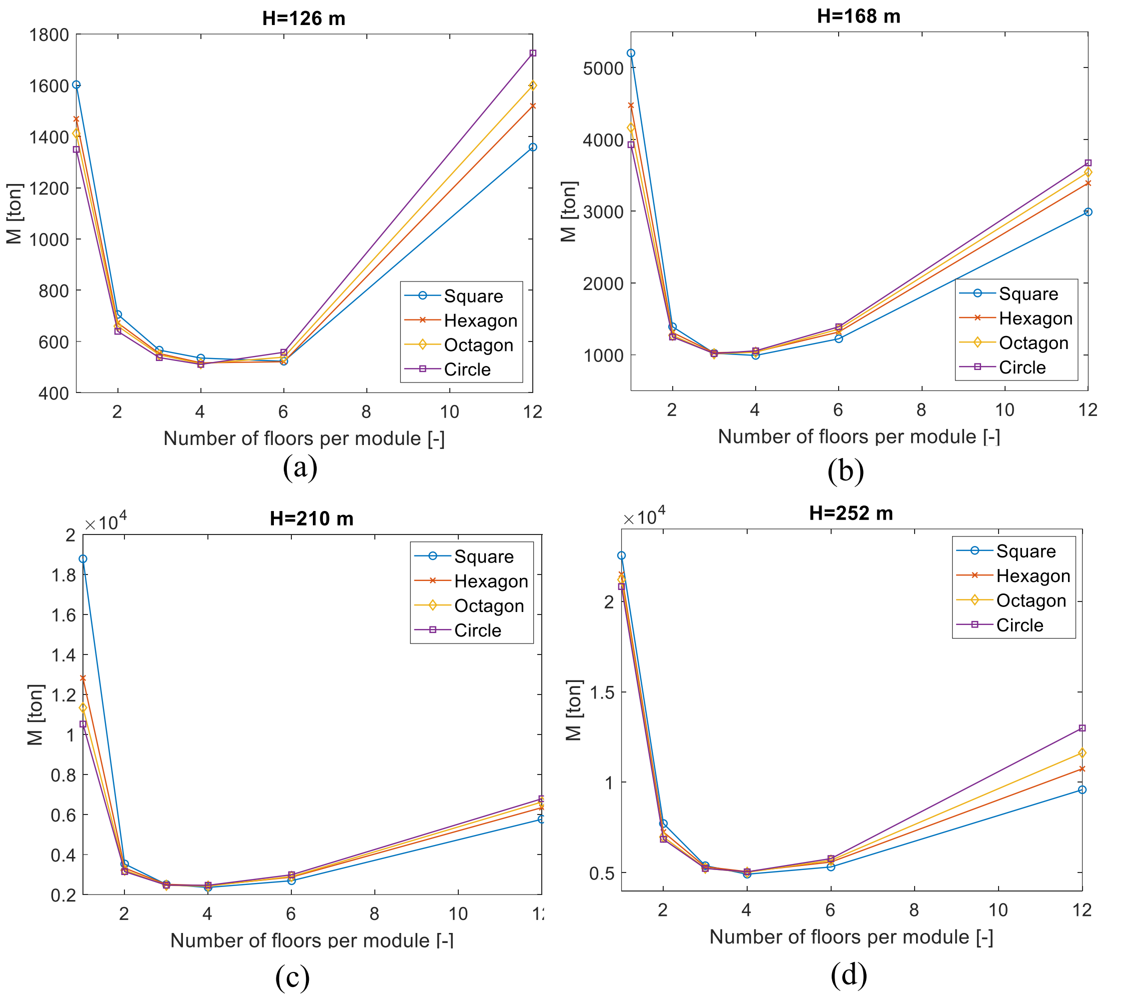

Figure 3.7 - Diagrid structure mass in function of the floor plan shape and the number of intra-module floors for building height of: (a) H=126 m (b) H=168 m (c) H=210 m (d) H=252 m

Finally, it can be concluded that for the 126-m tall building the strength requirement governs the structural design, whereas for the other heights the stiffness demand prevails. From the stiffness- and strength-based preliminary design it is found that the structural behaviour depends mainly on the building height and diagonal inclination. In fact, the minimum of torsional rotation and mass have often been obtained for one- and three-intra-module floors solutions, respectively. Regarding the top lateral displacement, it is a further restrain for tall buildings with slenderness greater than 5 since it tends to be close to the target value for different diagrid geometries. However, in the case of the 126-m tall building the top lateral displacement is variable. In fact, the two- and three-intra module floors models have provided the lower values of the parameter.

Chapter 4

4. MULTI-RESPONSE OPTIMIZATION BASED ON THE DESIRABILITY FUNCTION APPROACH

From Chapter 3 the structural response has been obtained in terms of top lateral displacement, torsional rotation and structural weight. It is evident that the best solution, able to minimize simultaneously and individually all parameters, does not exist. In fact, the geometrical model with the greatest torsional stiffness is the one with diagonal inclination of about 35° corresponding to one intra-module floor. Conversely, the lowest value of top lateral displacement has been provided by three and four intra-module floors solutions having diagonal angle range between 66° and 72° to ensure both shear and bending stiffness in case of the 126-m tall building. For this reason, it necessary to define a methodology that allows to select the optimal diagrid solution in terms of the response parameters. However, the engineer can choose other variables to be analysed, such as the maximum inter-story drift, the maximum acceleration under seismic action and the construction complexity. The latter has been used by Tomei et al. in [27] and Lacidogna et al. in [30] as further parameter besides the conventional ones, namely top lateral displacement, torsional rotation and structural weight, for investigating the optimal diagrid geometry. To this aim, these four parameters are sufficient to fully describe both structural behaviour and main features of tall building: capacity to withstand external loads by ensuring both strength and stiffness, reduction of material consumption to solve sustainability problem and feasibility of construction. Thus, in this Chapter a similar investigation is carried out in order to establish the optimal solution among the ones described in Chapter 2.1 providing simultaneously shear and bending stiffness, lightness and easiness of construction. To this purpose, the post-optimization process employed in this study is based on the desirability function and it is described in Chapter 4.1. The results are provided in Chapter 4.2.

4.1. DESIRABILITY FUNCTION APPROACH

The desirability function approach is a powerful tool widely used in industry. It has been firstly proposed by Harrington in [47] and developed by other authors as Derringer and Suich in [48] to define the optimal product or process that guarantees optimal quality cutting out the ones outside of a “desirable” limit [49]. According to Derringer and Suich, the proposed approach aims at reaching simultaneously the optimal value for all the evaluated variables by defining a unique function obtained by combining the individual responses [49]. In particular, the method starts from the definition of the individual desirability $d_i(y_i)$ for each response variable $y_i(x)$ and generally its typical range is between 0 and 1. The variable x represents the examined population. In case of unacceptable response, the individual desirability is null, while for the most desirable response it will be unitary. If the response is acceptable, the value falls between the two extreme values. The authors have proposed three individual desirability functions depending on the acceptable range of response $U_i - L_i$, where U_i and L_i are respectively the upper and the lower acceptable bounds, if the response must be minimized or maximized in that range or depending on the target value of the response T_i if the optimal response lies within $U_i - L_i$ [49].

If the response variable has to be maximized, the desirability function $d_i\big(y_i(x)\big)$ expression is provided as follows:

$$d_i\big(y_i(x)\big) = \begin{cases} 0 & y_i(x) < L_i \\ \left(\dfrac{y_i(x) - L_i}{U_i - L_i}\right)^{s_i} & L_i \le y_i(x) \le U_i \\ 1 & y_i(x) > U_i \end{cases} \tag{4.1}$$

Where s_i is a weight exponent defined by the user to distinguish the different importance of the response variable close to the optimal value U_i. Thus, if s_i is low, it means that the individual desirability tends to the unit also for a wider range of response values not close to the optimal range, whereas if s_i is greater, the individual desirability leans on 1 for a narrower range of response values very close to U_i. From Equation (4.1), it can be observed that the individual desirability is null for response values lower than the lower bound, while it is equal to one for response values greater than the upper bound. Within the acceptable range $U_i - L_i$, the response variable assumes intermediate values according to a trend that depends on the value of s_i. In particular, the linear trend is provided for $s_i = 1$ and the non-linear ones for $s_i \neq 1$, as it is represented in Figure 4.1a.

If the response variable has to be minimized, the equation of the individual desirability function is given by:

$$d_i(y_i(x)) = \begin{cases} 1 & y_i(x) < L_i \\ \left(\dfrac{U_i - y_i(x)}{U_i - L_i}\right)^{t_i} & L_i \leq y_i(x) \leq U_i \\ 0 & y_i(x) > U_i \end{cases} \tag{4.2}$$

Where t_i is the weight exponent as s_i. Equation (4.2) is similar to Eq.(4.1), but in this case the optimal value is the lower bound L_i instead of the upper one U_i. The function is illustrated in Figure 4.1b.

If the response variable has to be close to the target value, the individual desirability function is as follows:

$$d_i(y_i(x)) = \begin{cases} 0 & y_i(x) < L_i \\ \left(\dfrac{y_i(x) - L_i}{T_i - L_i}\right)^{s_i} & L_i \leq y_i(x) < T_i \\ 1 & y_i(x) = T_i \\ \left(\dfrac{y_i(x) - U_i}{T_i - U_i}\right)^{t_i} & T_i < y_i(x) \leq U_i \\ 0 & y_i(x) > U_i \end{cases} \tag{4.3}$$

The trend of Eq. (4.3) is represented in Figure 4.1c

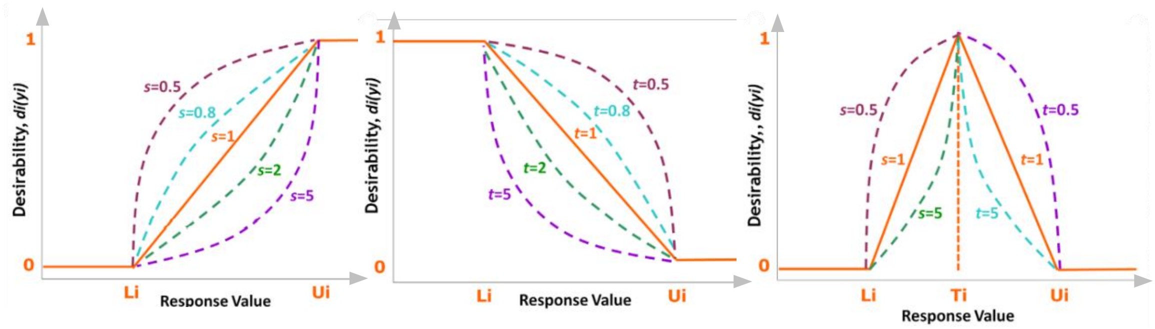

(a) (b) (c)

Figure 4.1 - Graphical representation of the individual desirability function in function of the optimization criteria adopted. The most desirable response value is: (a) the upper bound U_i (b) the lower bound L_i (c) the target value T_i [49]

The second step of the desirability function approach is the definition of a unique function, namely the overall desirability (OD), obtained by the combination of the n individual desirability function values as follows:

$$OD = [d_1(y_1) \cdot d_2(y_2) \cdot \dots \cdot d_n(y_n)]^{\frac{1}{n}} = \left[\prod_{i=1}^{n} d_i(y_i)\right]^{\frac{1}{n}} \quad (4.4)$$

The typical range of OD is between 0 and 1. It can be observed that it is sufficient to have only one null value among the individual desirability values to make OD null, whereas it is necessary to have all unitary values to obtain unitary OD. In intermediate cases, if all values of individual desirability are different from zero and at least one is non-unitary, OD is less than 1. Thus, the definition of the overall desirability allows the analyst to select the optimal process or product by simply identifying the best desirable one with the greatest value of OD.

As described in Chapter 1.3.3, the desirability function approach has been employed for the first time as multi-response diagrid optimization process in [30]. In this present Chapter a similar study has been carried out considering four response variables, namely the top lateral displacement, torsional rotation, structural weight and complexity index. The latter parameter is fundamental since it is correlated to construction issues that can lead to greater cost of the building. It has been proposed by Tomei et al. that defines the complexity index as the sum of each parameter normalized to the maximum value among the ones obtained for different patterns [27]:

$$CI_i = \sum_{j=1}^{5} \frac{N_j}{max_i N_j} \quad (4.5)$$

Where the subscript i refers to each geometrical solution and j to each metric, namely N_1, N_2, N_3, N_4 and N_5. Specifically, N_1 is the weighted number of nodes, N_2 is the number of different cross sections employed for the diagonals in the pattern, N_3 is the number of splices required for the diagonals in the pattern assuming a maximum diagonal length of 12 m, N_4 is the number of diagonals of the patterns and N_5 is the number of different lengths (distance between two nodes) of diagonal members in the pattern [27]. Regarding N_1 metric, it has been evaluated assuming that the nodes at rigid floors are more complex that nodes at intra-module floors because, respectively, six and four diagonals converge. Thus, a unit weight has been considered for the former joints and a weight of 4/6 (67%) for the latter ones.

The purpose of the study is to select the optimal solution that minimizes simultaneously four response variables. Under these considerations, the individual desirability function is defined as reported in Equation (4.2), where the upper bound is the maximum value of the responses among all geometrical solutions and the lower bound L_i is assumed zero:

$$d_i\big(y_i(x)\big) = \left(\frac{\max\limits_{\mathrm{x}} y_i(x) - y_i(x)}{\max\limits_{\mathrm{x}} y_i(x)}\right)^{r_i} \tag{4.6}$$

Where x represents the geometrical solutions with different diagonal inclinations and floor plan shapes, $y_i(x)$ is the response variable and r_i is the weight exponent. Note that the subscript i is related to each response variable. Equation (4.6) is applied to the top torsional rotation $\varphi(x)$ and the structural weight $\mathrm{M}(x)$ as follows:

$$d_{i,\varphi} = \left(\frac{\max\limits_{\mathrm{x}} \varphi_i - \varphi_i}{\max\limits_{\mathrm{x}} \varphi_i}\right)^{r_{i,\varphi}} \tag{4.7}$$

$$d_{i,M} = \left(\frac{\max\limits_{\mathrm{x}} M_i - M_i}{\max\limits_{\mathrm{x}} M_i}\right)^{r_{i,M}} \tag{4.8}$$

In the case of the evaluation of the individual desirability of the complexity index CI the upper bound of the Eq. (4.2) has been assumed equal to 5 and the $d_{i,CI}$ expression is given by:

$$d_{i,CI} = \left(\frac{5 - CI_i}{5}\right)^{r_{i,CI}} \tag{4.9}$$

Conversely, the definition of the individual desirability of the top lateral displacement is more complicated than the previous response parameters because the displacement is also used as a constraint to ensure building stiffness by imposing the target limit value of H/500. In general, three cases can be obtained: (a) $d_{i,\delta}$ is null if the top lateral displacement exceeds the limit value δ_{lim} (b) $d_{i,\delta}$ is unitary if the δ_i variation for a given height is low (c) if the variation range is wide the expression of $d_{i,\delta}$ is given by:

$$d_{i,\delta} = 0.5 + 0.5\left(\frac{\delta_{lim} - \delta_i}{\delta_{lim}}\right)^{r_{i,\delta}} = 0.5\left[1 + \left(1 - \frac{\delta_i}{\delta_{lim}}\right)^{r_{i,\delta}}\right] \tag{4.10}$$

The trend of Eq. (4.10) is reported in Figure 4.2.

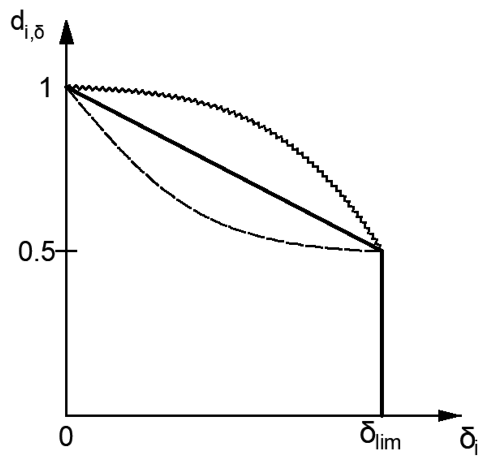

Figure 4.2 - The trend of the individual desirability for the lateral displacement at the top of the building. The continuous line is related to $r_{i,\delta} = 1$, the dashed line to $r_{i,\delta} > 1$ and the zig-zag line to $r_{i,\delta} < 1$

From a numerical point of view, the second and the third cases are implemented in function of the coefficient of variation CV_δ, defined as the ratio between the standard deviation σ_δ and the mean value μ_δ. Thus, assuming a limit value CV_{lim} of 10%, the individual desirability of the top lateral displacement is equal to 1 if the correspondent coefficient of variation CV_δ is lower than the limit value (case b). In particular, it means that the effect of the lateral displacement on the overall desirability (OD) is neglected. Conversely, for greater value than CV_{lim} Equation (4.10) is employed (case c). It can be noted that the range of $d_{i,\delta}$ is between 0.5 and 1 because for some diagrid structures, whose structural behaviour depends simultaneously on stiffness and strength requirements, the lateral displacement at the top increases getting closer to the limit value. Therefore, $d_{i,\delta}$ has to be decreased, but without reaching the zero value because the structures are considered acceptable in terms of rigidity and strength. The above-mentioned procedure has been repeated for each building height.

By combining the individual desirability for each response variable, the overall desirability (OD) can be obtained by applying Equation (4.4) considering n=4:

$$OD(x) = \left[\prod_{i=1}^{4} d_i(y_i)\right]^{\frac{1}{4}} = \left[d\big(\delta(x)\big) \cdot d\big(\varphi(x)\big) \cdot d\big(M(x)\big) \cdot d\big(CI(x)\big)\right]^{\frac{1}{4}} \qquad (4.11)$$

Based on OD values, it is possible to identify the optimal solution that minimizes simultaneously the four response variables.

4.2. UNIFORM-ANGLE DIAGRID STRUCTURES: RESULTS AND DISCUSSION

The desirability function approach described in the previous Chapter 4.1 has been applied to the twenty-four diagrid geometrical models for each building height reported in Chapter 2.1. For sake of simplicity, the 168-m tall building is firstly analysed in Chapter 4.2.1 with its correspondent twenty-four diagrid models in order to point out the main aspects. In Chapter 4.2.2 the study has been repeated for the other three buildings with different heights.

4.2.1. RESULTS FOR THE 168-M TALL BUILDING

4.2.1.1. SELECTION OF THE OPTIMAL GEOMETRY

In the case of the 168-m tall building the four response parameters $(\delta, \varphi, \mathrm{M}, \mathrm{CI})$ evaluated from the preliminary design and Equation (4.5) are reported in Table 4.1 for each i^{th} solution.

By investigating Table 4.1, the following considerations can be made. First of all, the second column related to the lateral displacement at the top of the building obtained from the preliminary design shows similar values to δ_{lim} independently from the considered diagrid geometry due to the prevalence of stiffness over strength demand in design. In fact, in this case the coefficient of variation CV_δ assumes lower value than CV_{lim}, namely $CV_\delta = 1.15\%$. Thus, the individual desirability $d_{i,\delta}$ is expected to be unitary for all geometries ($d_{i,\delta} = 1$ for $i = 1 \div 24$). Regarding the top torsional rotation reported in the third column of Table 4.1, the highest torsional rigidity is provided by the hexagonal structure with one intra-module floor H1, leading to the highest values of the individual desirability $d_{H1,\varphi}$. However, the other solutions with one intra-module floor (S1, O1, C1) have always a good torsional behaviour thanks to the low diagonal inclination (35°-38°). On the contrary, the solutions with highest torsional rotations are referred to the ones with steeper diagonals (S12, H12, O12, C12) having diagonal angle of about 83°. In particular, the S12 solution which is the worst one in terms of φ will have $d_{S12,\varphi} = 0$, based on Equation (4.7). By analysing the next column of Table 4.1 related to the structural weight of the external diagrid system, it can be noted that the lightest structure is the four intra-module floors structure with square plan (S4), corresponding to diagonal inclination of about 70°, whereas for the other plan shapes the minimum mass is provided by the three intra-module floors solution (H3, O3, C3) having diagonal angle of 66°- 67°. Conversely, the heaviest structures are the one intra-module floor solutions (S1, H1, O1, C1) due to greater diagonal density. Therefore, the most desirable structure S4 will have highest $d_{S4,M}$ and the least desirable one will have $d_{S4,M} = 0$, according to Equation (4.8).

i^{th} solution	δ $[m]$	φ $[10^{-4}rad]$	M [ton]	N1 [-]	N2 [-]	N3 [-]	N4 [-]	N5 [-]	CI [-]
S1	0,336	**0,88**	*5204*	**572**	*28*	**0**	*1152*	**1**	*3,70*
S2	0,335	3,24	1392	668	22	**0**	576	**1**	3,13
S3	0,335	6,62	1023	700	15	**0**	384	**1**	**2,77**
S4	0,336	10,44	**991**	716	12	*288*	288	**1**	3,61
S6	0,334	17,02	1224	732	8	192	192	**1**	3,08
S12	0,333	*27,30*	2990	*748*	**4**	*288*	**96**	**1**	3,22
H1	0,336	**0,85**	*4477*	**572**	*27*	**0**	*1152*	**1**	*3,66*
H2	0,335	3,20	1311	668	21	**0**	576	**1**	3,09
H3	0,334	6,37	**1029**	700	16	**0**	384	**1**	**2,80**
H4	0,333	9,71	1041	716	12	*288*	288	**1**	3,61
H6	0,334	15,57	1318	732	8	192	192	**1**	3,08
H12	0,335	*24,18*	3392	*748*	**4**	*288*	**96**	**1**	3,22
O1	0,335	**0,87**	*4165*	**572**	*26*	**0**	*1152*	**1**	*3,63*
O2	0,335	3,20	1272	668	22	**0**	576	**1**	3,13
O3	0,335	6,35	**1014**	700	15	**0**	384	**1**	**2,77**
O4	0,335	9,65	1036	716	11	*288*	288	**1**	3,57
O6	0,332	15,28	1359	732	8	192	192	**1**	3,08
O12	0,333	*23,15*	3545	*748*	**4**	*288*	**96**	**1**	3,22
C1	0,336	**0,87**	*3928*	**572**	*30*	**0**	*1152*	**1**	*3,76*
C2	0,335	3,24	1249	668	21	**0**	576	**1**	3,09
C3	0,336	6,36	**1018**	700	16	**0**	384	**1**	**2,80**
C4	0,335	9,51	1055	716	12	*288*	288	**1**	3,61
C6	0,335	15,02	1391	732	8	192	192	**1**	3,08
C12	0,334	*22,48*	3675	*748*	**4**	*288*	**96**	**1**	3,22

Table 4.1 - Response parameters (δ, φ, M, CI) for the twenty-four diagrid geometrical models in case of the 168-m tall building. Absolute minimum values are in **bold underlined**, minimum values for each floor shape are in **bold**, absolute maximum values are in *italic underlined*, maximum values for each floor shape are in *italic*.

The following five columns of Table 4.1 report the values of the five metrics needed to assess the complexity index (CI) for each geometry. N_1 is the weighted number of nodes that increases with the diagonal inclination since the number of nodes at intra-module floors is greater. In fact, the corresponding maximum value is 748 for all plan shapes and, specifically, it is related to twelve intra-module floors solutions (S12, H12, O12, C12), whereas the S1, H1, O1 and C1 solutions provide the least number of nodes. The number of different cross sections employed for the diagonals in the pattern is represented by N_2 which is always lower or equal to the number of diagrid modules. The employed diagonal cross-sections evaluated in the preliminary design are reported in Annex A. The minimum value of N_2 is provided by the twelve intra-module floors solutions (S12, H12, O12, C12), while the maximum value by the one intra-module floor geometries (S1, H1, O1, C1). N_3 is the number of splices required for the diagonals in the pattern assuming a maximum diagonal length of 12 m. Thus, N_3 is null for geometries with one, two and three intra-module floors because diagonal length is lower than 12 m, whereas it is maximum for solutions with greater diagonal inclination. N_4 is the total number of diagonals which is maximum for S1, H1, O1 and C1 solutions and minimum for S12, H12, O12 and C12 ones. Lastly, N_5 represents the number of different lengths of diagonal members in the pattern and it is always unitary for each geometry because the diagonal inclination is constant along the height of the building. By combining these five metrics according to Equation (4.5), the complexity index can be calculated and its values are reported in the tenth column of Table 4.1. It can be noted in Figure 4.3 that the complexity index decreases with the diagonal inclination from 35° to 65° due to N_2 and N_4, and it suddenly increases for four intra-module floors solutions due to N_3. Moreover, it is evident that the complexity index is minimum for solutions with diagonal angle between 65° and 67° (S3, O3), leading to greater value of the individual desirability. Conversely, it is maximum for the circular structure with the shallowest diagonals and in this case $d_{C1,CI} = 0$.

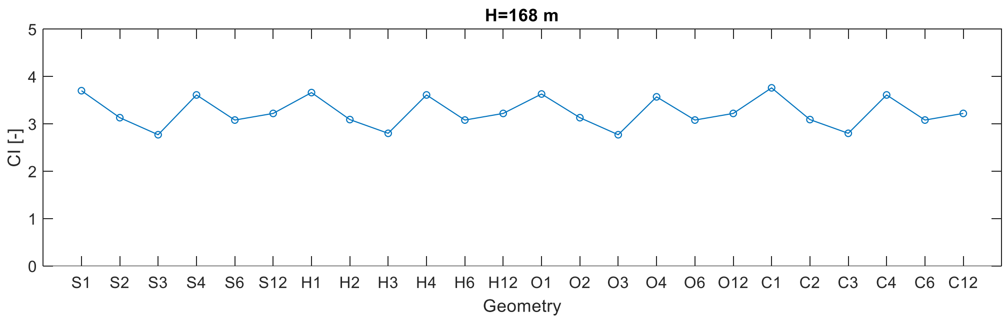

Figure 4.3 - Complexity index for different geometrical solutions in case of the 168-m tall building

Once the response parameters for each diagrid geometry have been evaluated according to Chapter 3, the individual desirability $d_{i,p}$ has been calculated by means of

Equations (4.7)-(4.10), assuming r_p equal to one for each response variable for sake of simplicity, namely $r_\delta = r_\varphi = r_M = r_{CI} = 1$. This assumption leads to consider each response parameter with the same weight. The values are shown in the first four columns of Table 4.2 and illustrated in Figure 4.4a. It has to be noted in Figure 4.4a that the individual desirability trend of each response variable is similar for each floor plan shape. Therefore, the effect of the plan shape on $d_{i,p}$ is very slight with respect to the effect of the diagonal angle, that leads to a more important variation of $d_{i,p}$.

At last, the final step of the desirability function approach consists into the assessment of the overall desirability (OD_i) of each i^{th} solution by combining together the four obtained individual desirabilities by applying Equation (4.11). The results are presented in last column of Table 4.2 and OD trend in Figure 4.4b. Based on the OD results, the most desirable solution is the three intra-module floors solution with octagonal floor plan shape because OD_{O3} assumes the highest value of 72.46% among all geometrical solutions. In particular, O3 solution is characterized by a unitary $d_{O3,\delta} = 1$, that does not affect the OD value, a good but not optimal torsional stiffness because $d_{O3,\varphi} = 76.73\%$ is not the highest value among all solutions ($d_{H1,\varphi,max} = 96.89\%$), a low structural weight ($d_{O3,M} = 80.51\%$) and the O3 solution is also the easiest structure to be constructed having the highest values of $d_{O3,CI} = 44.62\%$. However, similar values of OD for S3, H3 and C3 solutions, respectively $OD_{S3} = 72.18\%, OD_{H3} = 72.11\%$ and $OD_{C3} = 72.16\%$, demonstrate again the slight influence of the floor plan shape on the selection of the optimal geometry. Conversely, the diagonal inclination seems to be the predominant geometrical parameter that distinguishes the most and the least desirable solution, as it is evident in Figure 4.4b. In fact, as the diagonal inclination is increased or decreased with respect to 65°-67°, the overall desirability OD value tends to decrease. In particular, in case of S1 and S12 solutions OD is null because S1 is the heaviest structure ($d_{S1,M} = 0$) and S12 is the most torsionally flexible structure ($d_{S12,\varphi} = 0$). This consideration can be done also for the other floor plan shapes with the difference that OD reaches low and not null value. Indeed, for the H1, O1 and C1 solutions OD varies from 43.6% to 49.21% due to high torsional stiffness ($d_{i,\varphi} \cong 96.8\%$), huge steel consumption ($d_{i,M} \cong 13.97 - 24.53\%$) and difficult constructability ($d_{i,CI} \cong 24.71 - 26.71\%$), whereas for the H12, O12 and C12 solutions OD is between 34.52% and 36.89% due to high torsional flexibility ($d_{i,\varphi} \cong 11.44 - 17.66\%$), quite high weight ($d_{i,M} \cong 29.39 - 34.82\%$) and quite easy constructability ($d_{i,CI} = 35.67\%$). The solutions with two intra-module floors (S2, H2, O2, C2) corresponding to diagonal angle around 55° represent the second most desirable solutions having OD between 70.13% and 71.10%. These structures are characterized by a good torsional stiffness ($d_{i,\varphi} \cong$ 88%), good exploitation of steel material ($d_{i,M} \cong$ 73.26-76.01%) and easy constructability ($d_{i,CI} \cong 37.47 - 38.14\%$).

$i^{th}solution$	$d_{i,\delta}[-]$	$d_{i,\varphi}[-]$	$d_{i,M}[-]$	$d_{i,CI}[-]$	$OD_i[-]$
S1	**1**	0,9678	0	0,2604	0
S2	**1**	0,8813	0,7326	0,3747	0,7013
S3	**1**	0,7573	0,8035	**0,4462**	0,7218
S4	**1**	0,6177	**0,8095**	0,2786	0,6109
S6	**1**	0,3765	0,7649	0,3843	0,5767
S12	**1**	0	0,4254	0,3567	0
H1	**1**	**0,9689**	0,1397	0,2671	0,4360
H2	**1**	0,8826	0,7481	0,3814	0,7084
H3	**1**	0,7667	0,8022	0,4395	0,7211
H4	**1**	0,6444	0,8000	0,2786	0,6156
H6	**1**	0,4298	0,7467	0,3843	0,5926
H12	**1**	0,1144	0,3482	0,3567	0,3452
O1	**1**	0,9682	0,1997	0,2737	0,4796
O2	**1**	0,8827	0,7557	0,3747	0,7071
O3	**1**	0,7673	0,8051	**0,4462**	**0,7246**
O4	**1**	0,6465	0,8009	0,2852	0,6199
O6	**1**	0,4402	0,7389	0,3843	0,5946
O12	**1**	0,1521	0,3188	0,3567	0,3626
C1	**1**	0,9680	0,2453	0,2471	0,4921
C2	**1**	0,8815	0,7601	0,3814	0,7110
C3	**1**	0,7671	0,8044	0,4395	0,7216
C4	**1**	0,6515	0,7972	0,2786	0,6167
C6	**1**	0,4496	0,7328	0,3843	0,5965
C12	**1**	0,1766	0,2939	0,3567	0,3689

Table 4.2 -Individual desirability $d_{i,p}$ and overall desirability OD_i for each response variable assuming $r_p = 1$ in case of the 168-m tall building. Absolute maximum values are in **bold**

The overall desirability OD value drops to 62% for S4, H4, O4 and C4 solutions with diagonal angle around 70° because of low torsional stiffness ($d_{i,\varphi}$ ≅61.77-65.15%) and construction issues ($d_{i,CI} \cong 27.86 - 28.52\%$) despite the structure lightness ($d_{i,M} \cong$ 80%). Further reduction of OD values (57.67-59.65%) is found for the S6, H6, O6 and C6 solutions mainly due to lower torsional rigidity ($d_{i,\varphi} \cong$ 37.65-44.96%) in contrast with low mass ($d_{i,M} \cong 73.28 - 76.49\%$) and few constructability problems ($d_{i,CI} \cong 38.43\%$). Lastly, as mentioned before, the least desirable solutions are the ones with shallower and steeper diagonals.

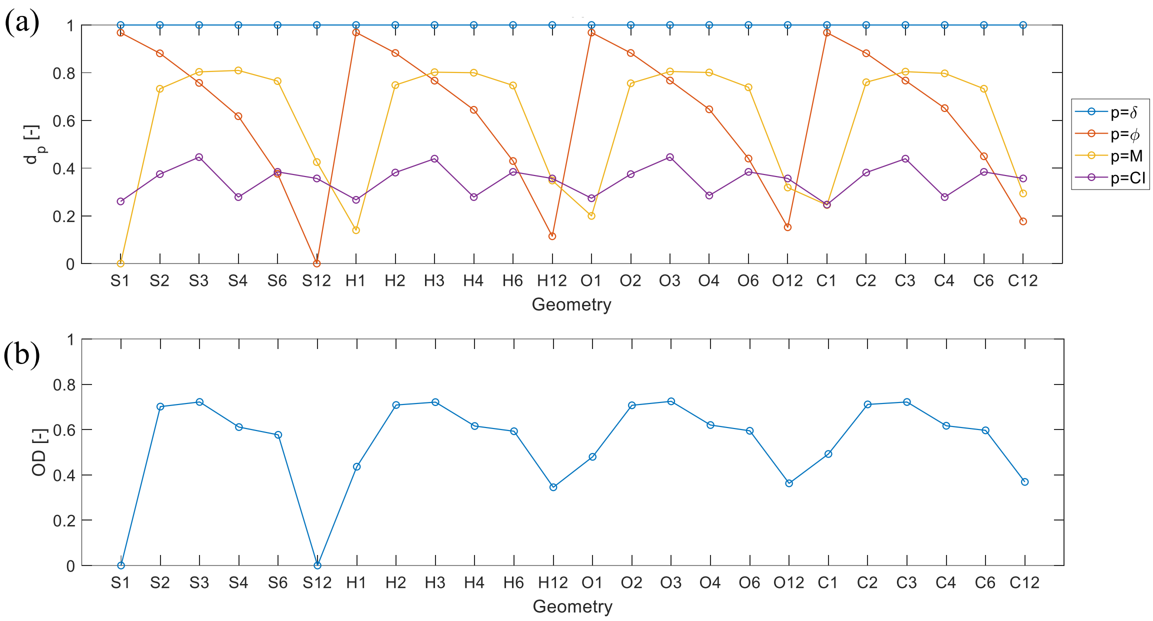

Figure 4.4 - Results of the desirability function approach in case of the 168-m diagrid tall building: (a) Individual desirability values for each response variable (b) Overall desirability values ($r_p = 1$)

4.2.1.2. Parametric analysis

The previous analysis has been carried out considering the same weight of the response parameters by means of the r_p exponent. As follows, another investigation is simulated by supposing different importance of each response parameter. To this aim, the exponent r_p presented in Equations (4.7) (4.10) assumes values varying between 0.25 and 2 with a constant step of 0.25, i.e. $r_p = (0.25, 0.5, 0.75, 1, 1.25, 1.5, 1.75, 2)$. Thus, since there are four response parameters, the total number of possible combinations to be performed is $8^4 = 4096$. In Table 4.3 some combinations are reported. Note that for structures with slenderness greater than 5, i.e. the 168, 210 and 252 m tall buildings, the individual desirability of the top lateral displacement is generally unitary for all geometrical solutions due to dominant stiffness demand and therefore the effect of r_δ is negligible. Nevertheless, 4096 combinations will always be employed for these buildings.

Combination	r_δ [−]	r_φ [−]	r_M [−]	r_{CI} [−]
1	0.25	0.25	0.25	0.25
2	0.25	0.25	0.25	0.5
3	0.25	0.25	0.25	0.75
⋮	⋮	⋮	⋮	⋮
1755	1	1	1	0.75
1756	1	1	1	1
1757	1	1	1	1.25
⋮	⋮	⋮	⋮	⋮
4094	2	2	2	1.5
4095	2	2	2	1.75
4096	2	2	2	2

Table 4.3 - Different values of the r_p exponent for each response parameter for application of the desirability function with 4096 simulations [30]

The assessment of the individual desirability of each response parameter is always provided by Equations (4.7) (4.10) applied to the obtained response variables shown in Table 4.1. In this case, it is not possible to predict a priori the most desirable solution, but it is expected that different geometrical solutions will be more desirable than others depending on the chosen combination. In particular, the most desirable solution with the greatest OD value has been selected for each combination and the relative frequency of occurrence has been evaluated as it is illustrated in Figure 4.5. Based on results, it is evident that the three intra-module floors solution with octagonal floor plan shape is preferable for 3040 out of 4096 combinations, leading to a relative frequency of about 74.22%. This outcome of O3 as optimal solution has been obtained also for the uniform-angle diagrid structure analysis with unitary r_p exponent with OD value of 72.46%. However, the final values of the overall desirability are a bit different. Generally, it can be noted that OD tends to decrease for greater value of r_φ, r_M and r_{CI}. Moreover, it is found that OD varies between 0.525 and 0.923. The minimum value is provided by combinations with highest value of r_p for the torsional rotation, structural weight and complexity index independently from the value of r_δ, i.e. $r_\varphi = r_M = r_{CI} = 2$, whereas the maximum value by combinations with $r_\varphi = r_M = r_{CI} = 0.25$. Figure 4.5 shows also that the two intra-module floors solution with circular floor plan shape is more desirable than the previous one when the weight related to the torsional rotation is greater than others ($r_\varphi > r_{CI}$ and $r_\varphi \geq r_M, \forall r_\delta$). In particular, 25.78% of the combinations corresponding to 1056 out of 4096 cases leads to C2 geometry as the most preferable solution. It is found that the overall desirability has a range between 0.632 and 0.911 corresponding respectively to $r_\varphi = 2, r_M = 0.5, r_{CI} = 1.5$ and $r_\varphi = 0.5,\ r_M = 0.25\ ,\ r_{CI} = 0.25$ combinations. Similarly, OD is equal to 71.10% for C2 solution with unitary r_p.

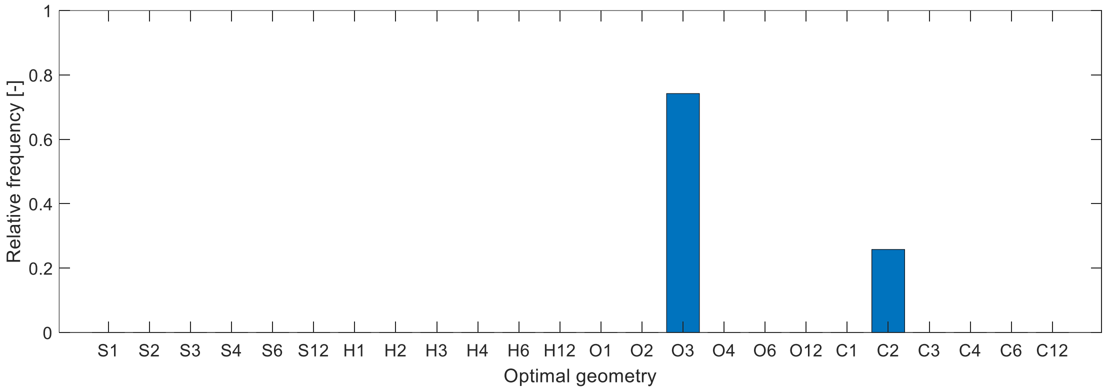

Figure 4.5 - Relative frequency of each geometrical solution for the 168-m tall building considering 4096 simulations

4.2.2. Results for the other building heights

Up to this point the analysis of the outcomes obtained from the desirability function for the 168-m tall building has been carried out, but the same procedure has been applied to the other three buildings with different heights, namely the 126, 210 and 252 m tall buildings, aimed at highlighting the influence of the building height on the selection of the optimal diagrid model. For sake of completeness, the values of the response parameters obtained from the preliminary design and Equation (4.5) are reported in Table 4.4, Table 4.5 and Table 4.6 for respectively 126, 210 and 252 m tall buildings. Based on the results, many considerations can be made and most of them have been pointed out in Chapter 3.2.2 referred to the top lateral displacement, torsional rotation and structural weight of the external diagrid system in function of the building height. Thus, attention is paid on the complexity index which is also illustrated graphically in Figure 4.6, Figure 4.7 and Figure 4.8. In general, it is found that the complexity index tends to assume slightly higher values with slender structures because the number of nodes and the number of diagonals employed are greater. However, in case of S1 geometry with 210 m height (Figure 4.7) and one intra-module floor solutions (S1, H1, O1, C1) besides C12 with 252 m height (Figure 4.8) the complexity index assumes the lowest value of 2.8 with respect to other solutions due to N_2. In fact, the latter parameter is unitary since the preliminary design has returned a structure with only one cross section for all diagonals characterized by the maximum area available in Table 3.1.

i^{th} solution	δ $[m]$	φ $[10^{-4}rad]$	M [ton]	N1 [-]	N2 [-]	N3 [-]	N4 [-]	N5 [-]	CI [-]
S1	0,243	**1,046**	*1603*	**428**	*20*	**0**	*864*	**1**	*3,60*
S2	0,153	2,354	705	500	17	**0**	432	**1**	3,10
S3	**0,149**	4,403	566	524	12	**0**	288	**1**	**2,77**
S4	0,163	7,092	535	536	9	*216*	216	**1**	3,58
S6	0,227	14,627	**523**	548	6	144	144	**1**	3,06
S12	*0,246*	*21,822*	1359	*560*	**3**	*216*	**72**	**1**	3,21
H1	0,227	**0,951**	1469	**428**	*20*	**0**	*864*	**1**	*3,60*
H2	0,152	2,277	672	500	16	**0**	432	**1**	3,06
H3	**0,155**	4,320	553	524	12	**0**	288	**1**	**2,77**
H4	0,178	7,115	517	536	8	*216*	216	**1**	3,54
H6	*0,251*	14,485	**521**	548	6	144	144	**1**	3,06
H12	0,249	*19,403*	*1520*	*560*	**3**	*216*	**72**	**1**	3,21
O1	0,221	**0,933**	1412	**428**	*23*	**0**	*864*	**1**	*3,72*
O2	**0,151**	2,255	660	500	16	**0**	432	**1**	3,06
O3	0,156	4,306	548	524	11	**0**	288	**1**	**2,73**
O4	0,182	7,087	**513**	536	9	*216*	216	**1**	3,58
O6	*0,250*	13,939	539	548	6	144	144	**1**	3,06
O12	0,248	*18,406*	*1600*	*560*	**3**	*216*	**72**	**1**	3,21
C1	0,218	**0,928**	1350	**428**	*24*	**0**	*864*	**1**	*3,76*
C2	**0,155**	2,290	640	500	15	**0**	432	**1**	3,02
C3	0,160	4,396	537	524	12	**0**	288	**1**	**2,77**
C4	0,187	7,207	**510**	536	9	*216*	216	**1**	3,58
C6	*0,250*	13,565	558	548	6	144	144	**1**	3,06
C12	*0,250*	*18,023*	*1726*	*560*	**3**	*216*	**72**	**1**	3,21

Table 4.4 - Response parameters (δ, φ, M, CI) for the twenty-four diagrid geometrical models in case of the 126-m tall building. Absolute minimum values are in **bold underlined**, minimum values for each floor shape are in **bold**, absolute maximum values are in *italic underlined*, maximum values for each floor shape are in *italic*.

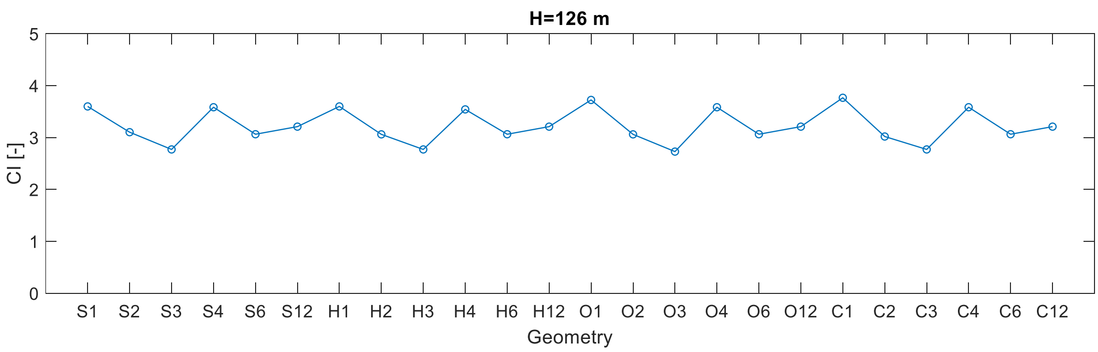

Figure 4.6 - Complexity index for different geometrical solutions in case of the 126-m tall building

i^{th} solution	δ $[m]$	φ $[10^{-4} rad]$	M [ton]	N1 [-]	N2 [-]	N3 [-]	N4 [-]	N5 [-]	CI [-]
S1	0,445	**0,56**	*18780*	**716**	**1**	**0**	*1440*	**1**	**2,80**
S2	0,419	2,84	3531	836	*24*	**0**	720	**1**	3,25
S3	0,419	6,04	2507	876	19	**0**	480	**1**	2,95
S4	0,419	9,63	**2358**	896	15	*360*	360	**1**	*3,74*
S6	0,418	17,15	2693	916	10	240	240	**1**	3,17
S12	0,418	*31,26*	5765	*936*	5	*360*	**120**	**1**	3,26
H1	0,420	**0,63**	*12826*	**716**	23	**0**	*1440*	**1**	3,59
H2	0,419	2,82	3323	836	*26*	**0**	720	**1**	3,32
H3	0,419	5,81	2513	876	18	**0**	480	**1**	**2,91**
H4	0,416	9,12	**2450**	896	15	*360*	360	**1**	*3,74*
H6	0,420	16,00	2873	916	10	240	240	**1**	3,17
H12	0,416	*27,60*	6348	*936*	**5**	*360*	**120**	**1**	3,26
O1	0,420	**0,68**	*11341*	**716**	*25*	**0**	*1440*	**1**	3,66
O2	0,419	2,81	3219	836	24	**0**	720	**1**	3,25
O3	0,419	5,86	2466	876	18	**0**	480	**1**	**2,91**
O4	0,419	9,06	**2421**	896	14	*360*	360	**1**	*3,71*
O6	0,420	15,69	2904	916	10	240	240	**1**	3,17
O12	0,413	*26,16*	6628	*936*	**4**	*360*	**120**	**1**	3,23
C1	0,419	**0,70**	*10521*	**716**	*28*	**0**	*1440*	**1**	3,76
C2	0,420	2,85	3149	836	*28*	**0**	720	**1**	3,39
C3	0,420	5,79	2471	876	20	**0**	480	**1**	**2,98**
C4	0,417	9,07	**2466**	896	15	*360*	360	**1**	*3,74*
C6	0,419	15,41	2992	916	10	240	240	**1**	3,17
C12	0,419	*25,70*	6790	*936*	**4**	*360*	**120**	**1**	3,23

Table 4.5 - Response parameters (δ, φ, M, CI) for the twenty-four diagrid geometrical models in case of the 210-m tall building. Absolute minimum values are in **bold underlined**, minimum values for each floor shape are in **bold**, absolute maximum values are in *italic underlined*, maximum values for each floor shape are in *italic*, in red unsatisfactory top lateral displacement

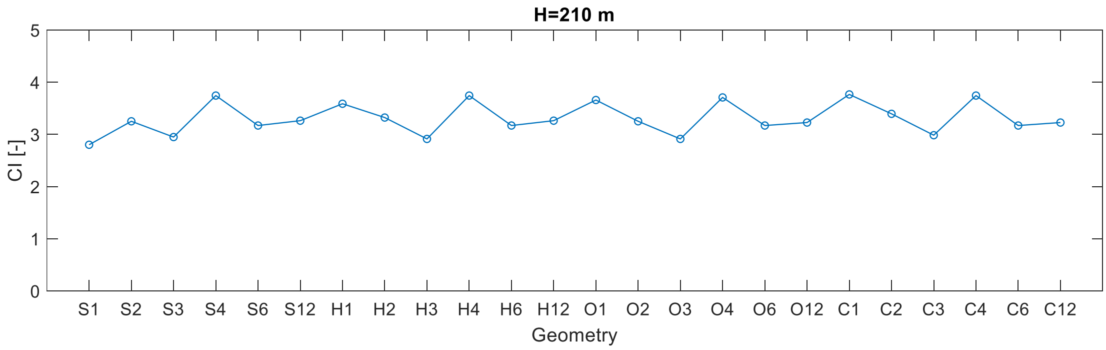

Figure 4.7 - Complexity index for different geometrical solutions in case of the 210-m tall building

i^{th} solution	δ [m]	φ [$10^{-4}rad$]	M [ton]	N1 [-]	N2 [-]	N3 [-]	N4 [-]	N5 [-]	CI [-]
S1	0,998	**0,88**	*22536*	**860**	**1**	**0**	*1728*	**1**	**2,80**
S2	0,501	2,48	7718	1004	*27*	**0**	864	**1**	3,21
S3	0,502	5,33	5387	1052	22	**0**	576	**1**	2,94
S4	0,502	8,92	**4916**	1076	17	*432*	432	**1**	*3,72*
S6	0,500	16,57	5316	1100	12	288	288	**1**	3,18
S12	0,501	*31,35*	9586	*1124*	4	*432*	**144**	**1**	3,20
H1	0,899	**0,76**	*21495*	**860**	**1**	**0**	*1728*	**1**	**2,80**
H2	0,503	2,50	7246	1004	*23*	**0**	864	**1**	3,09
H3	0,504	5,28	5327	1052	22	**0**	576	**1**	2,94
H4	0,501	8,58	**5059**	1076	17	*432*	432	**1**	*3,72*
H6	0,504	15,47	5588	1100	11	288	288	**1**	3,15
H12	0,504	*27,25*	10743	*1124*	3	*432*	**144**	**1**	3,17
O1	0,850	**0,73**	*21198*	**860**	**1**	**0**	*1728*	**1**	**2,80**
O2	0,503	2,52	6974	1004	*29*	**0**	864	**1**	3,27
O3	0,501	5,29	5248	1052	23	**0**	576	**1**	2,97
O4	0,500	8,57	**5019**	1076	16	*432*	432	**1**	*3,69*
O6	0,501	15,33	5685	1100	12	288	288	**1**	3,18
O12	0,502	*25,48*	11625	*1124*	2	*432*	**144**	**1**	3,14
C1	0,816	**0,71**	*20816*	**860**	**1**	**0**	*1728*	**1**	**2,80**
C2	0,503	2,54	6846	1004	*33*	**0**	864	**1**	3,39
C3	0,503	5,34	5235	1052	24	**0**	576	**1**	3,00
C4	0,504	8,46	**5048**	1076	18	*432*	432	**1**	*3,75*
C6	0,503	15,15	5780	1100	12	288	288	**1**	3,18
C12	0,506	*24,75*	12995	*1124*	**1**	*432*	**144**	**1**	3,11

Table 4.6 - Response parameters (δ, φ, M, CI) for the twenty-four diagrid geometrical models in case of the 252-m tall building. Absolute minimum values are in **bold underlined**, minimum values for each floor shape are in **bold**, absolute maximum values are in *italic underlined*, maximum values for each floor shape are in *italic*,in red unsatisfactory top lateral displacement

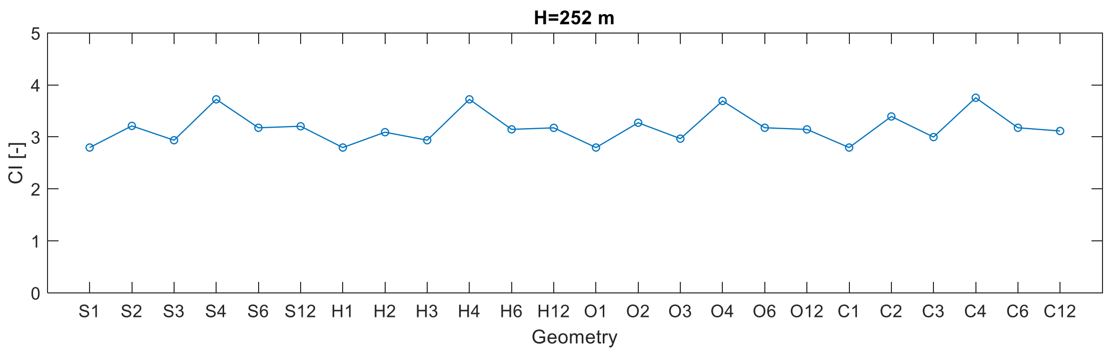

Figure 4.8 - Complexity index for different geometrical solutions in case of the 252-m tall building

By applying the desirability function approach to all geometrical solutions for each building height, the individual and overall desirabilities can be calculated considering initially same weight for each response parameter ($r_p = 1$). Regarding the 126-m tall building, it is evident in the first column of Table 4.7 that $d_{i,\delta}$ is not unitary since it varies from 0.5029 to 0.7038 because in case of strength-based preliminary design the top lateral displacement has greater variability. In fact, $CV_\delta = 20.86\%$ is higher than $CV_{lim} = 10\%$. In particular, the three intra-module floors solution with square floor plan provides the lowest lateral displacement at the top, leading to an individual desirability $d_{S3,\delta}$ equal to 70.38%. Conversely, the most flexible structure is the six intra-module floors solution with hexagonal plan ($d_{H6,\delta} = 50.29\%$). As far as the top torsional rotation, structural mass and complexity index are concerned, the trends are similar to the ones obtained in case of the 168-m tall building, as it is shown in Figure 4.9. In fact, the individual desirability of the torsional rotation reaches peak values for one intra-module floors solutions (S1, H1, O1, C1) ranging between 95.21-95.75% and it tends to decrease for steeper diagonals. On the contrary, $d_{i,M}$ and $d_{i,CI}$ are maximum for solutions with diagonal inclination of 65°-67° (S3, H3, O3, C3) and minimum for the shallowest and the steepest diagonals. In the last column of Table 4.7 the overall desirability values are reported. As for the 168-m tall building, the most desirable solution is always the three intra-module floors solution with octagonal floor plan corresponding to $OD_{O3} = 64.41\%$, whereas the least desirable ones are the twelve intra-module floors solutions with square and circular plans because of the greatest torsional deformability ($OD_{S12} = 0\%$) and highest structural mass ($OD_{C12} = 0\%$), respectively.

Based on the results of the 210-m tall building represented in Table 4.8 and Figure 4.10, the individual desirability of the top lateral displacement is unitary since $CV_\delta = 0.37\%$ is lower than CV_{lim}, except for the unique geometry that does not provide enough lateral stiffness ($d_{S1,\delta} = 0$). The optimal solution is always O3 ($OD_{O3} = 73.68\%$) thanks to good torsional behaviour, lightness and easiness of construction, whereas the worst ones are S1 and S12 due to excessive lateral displacement, torsional rotation and mass ($OD_{S1} = OD_{S12} = 0\%$).

Finally, in case of the 252-m tall building there are more structures that do not ensure the stiffness demand and therefore the S1, H1, O1, C1 and C12 solutions provide null $d_{i,\delta}$, whereas for the others $d_{i,\delta} = 1$ with $CV_\delta = 0.24\%$. In this case, the most desirable solution is H3 with $OD_{H3} = 71.55\%$ and the least desirable ones are S1, S12, H1, O1, C1 and C12 for unsatisfactory displacement, high torsional rotation and complexity index.

i^{th}solution	$d_{i,\delta}[-]$	$d_{i,\varphi}[-]$	$d_{i,M}[-]$	$d_{i,CI}[-]$	$OD_i[-]$
S1	0,5188	0,9521	0,0713	0,2805	0,3152
S2	0,6973	0,8921	0,5912	0,3798	0,6113
S3	**0,7038**	0,7983	0,6719	0,4462	0,6406
S4	0,6767	0,6750	0,6898	0,2836	0,5467
S6	0,5488	0,3297	0,6971	0,3876	0,4702
S12	0,5118	0	0,2127	0,3583	0
H1	0,5503	0,9564	0,1488	0,2805	0,3850
H2	0,6977	0,8957	0,6104	0,3881	0,6203
H3	0,6924	0,8020	0,6796	0,4462	0,6406
H4	0,6462	0,6739	0,7006	0,2919	0,5463
H6	0,5029	0,3362	0,6982	0,3876	0,4625
H12	0,5060	0,1109	0,1194	0,3583	0,2213
O1	0,5622	0,9572	0,1815	0,2555	0,3975
O2	0,7000	0,8967	0,6176	0,3881	0,6228
O3	0,6913	0,8027	0,6826	**0,4545**	**0,6441**
O4	0,6398	0,6752	0,7026	0,2836	0,5416
O6	0,5038	0,3613	0,6878	0,3876	0,4693
O12	0,5076	0,1566	0,0731	0,3583	0,2136
C1	0,5672	**0,9575**	0,2179	0,2471	0,4136
C2	0,6932	0,8951	0,6294	0,3964	0,6273
C3	0,6817	0,7986	0,6888	0,4462	0,6396
C4	0,6291	0,6697	**0,7042**	0,2836	0,5386
C6	0,5034	0,3784	0,6767	0,3876	0,4728
C12	0,5045	0,1741	0	0,3583	0

Table 4.7- Individual desirability $d_{i,p}$ and overall desirability OD_i for each response variable assuming $r_p = 1$ in case of the 126-m tall building. Absolute maximum values are in **bold**

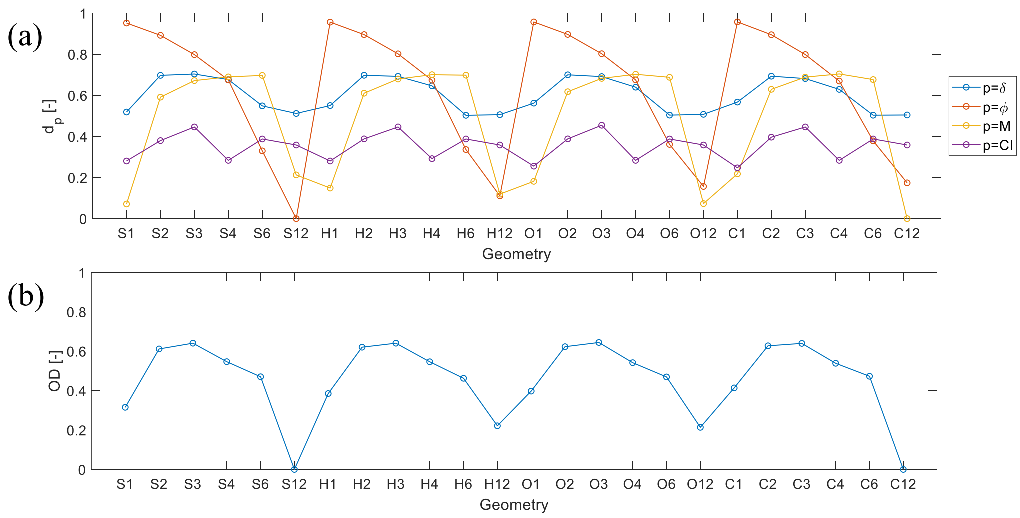

Figure 4.9- Results of the desirability function approach in case of the 126-m diagrid tall building: (a) Individual desirability values for each response variable (b) Overall desirability values ($r_p = 1$)

$i^{th}solution$	$d_{i,\delta}[-]$	$d_{i,\varphi}[-]$	$d_{i,M}[-]$	$d_{i,CI}[-]$	$OD_i[-]$
S1	0	**0,9820**	0	**0,4399**	0
S2	**1**	0,9093	0,8120	0,3499	0,7130
S3	**1**	0,8066	0,8665	0,4104	0,7319
S4	**1**	0,6918	**0,8744**	0,2514	0,6245
S6	**1**	0,4513	0,8566	0,3662	0,6134
S12	**1**	0	0,6930	0,3476	0
H1	**1**	0,9800	0,3170	0,2827	0,5444
H2	**1**	0,9097	0,8230	0,3357	0,7080
H3	**1**	0,8141	0,8662	0,4176	0,7366
H4	**1**	0,7081	0,8696	0,2514	0,6273
H6	**1**	0,4880	0,8470	0,3662	0,6237
H12	**1**	0,1169	0,6620	0,3476	0,4050
O1	**1**	0,9782	0,3961	0,2684	0,5679
O2	**1**	0,9101	0,8286	0,3499	0,7167
O3	**1**	0,8124	0,8687	0,4176	**0,7368**
O4	**1**	0,7102	0,8711	0,2585	0,6324
O6	**1**	0,4979	0,8454	0,3662	0,6266
O12	**1**	0,1632	0,6471	0,3548	0,4400
C1	**1**	0,9775	0,4398	0,2470	0,5708
C2	**1**	0,9087	0,8323	0,3214	0,7021
C3	**1**	0,8146	0,8684	0,4033	0,7308
C4	**1**	0,7099	0,8687	0,2514	0,6275
C6	**1**	0,5070	0,8407	0,3662	0,6285
C12	**1**	0,1779	0,6385	0,3548	0,4480

Table 4.8- Individual desirability $d_{i,p}$ and overall desirability OD_i for each response variable assuming $r_p = 1$ in case of 210-m tall building. Absolute maximum values are in **bold**

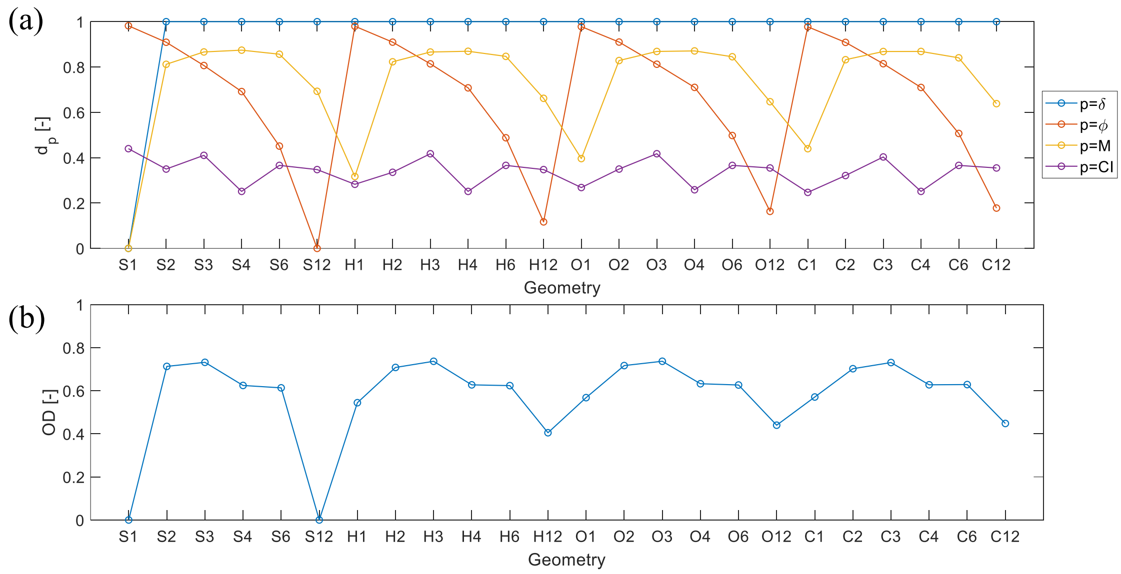

Figure 4.10- Results of the desirability function approach in case of 210-m diagrid tall building: (a) Individual desirability values for each response variable (b) Overall desirability values ($r_p = 1$)

$i^{th}solution$	$d_{i,\delta}[-]$	$d_{i,\varphi}[-]$	$d_{i,M}[-]$	$d_{i,CI}[-]$	$OD_i[-]$
S1	0	0,9720	0	**0,4409**	0
S2	**1**	0,9207	0,6575	0,3577	0,6822
S3	**1**	0,8299	0,7610	0,4128	0,7146
S4	**1**	0,7155	**0,7818**	0,2555	0,6149
S6	**1**	0,4714	0,7641	0,3649	0,6021
S12	**1**	0	0,5746	0,3591	0
H1	0	0,9757	0,0462	**0,4409**	0
H2	**1**	0,9202	0,6785	0,3820	0,6988
H3	**1**	0,8315	0,7636	0,4128	**0,7155**
H4	**1**	0,7261	0,7755	0,2555	0,6159
H6	**1**	0,5065	0,7520	0,3709	0,6131
H12	**1**	0,1307	0,5233	0,3652	0,3975
O1	0	0,9767	0,0594	**0,4409**	0
O2	**1**	0,9195	0,6905	0,3456	0,6844
O3	**1**	0,8313	0,7671	0,4068	0,7136
O4	**1**	0,7266	0,7773	0,2616	0,6200
O6	**1**	0,5109	0,7477	0,3649	0,6110
O12	**1**	0,1873	0,4841	0,3712	0,4283
C1	0	**0,9775**	0,0763	**0,4409**	0
C2	**1**	0,9188	0,6962	0,3214	0,6733
C3	**1**	0,8298	0,7677	0,4007	0,7108
C4	**1**	0,7302	0,7760	0,2495	0,6132
C6	**1**	0,5168	0,7435	0,3649	0,6119
C12	0	0,2105	0,4234	0,3773	0

Table 4.9- Individual desirability $d_{i,p}$ and overall desirability OD_i for each response variable assuming $r_p = 1$ in case of the 252-m tall building. Absolute maximum values are in **bold**

(a)

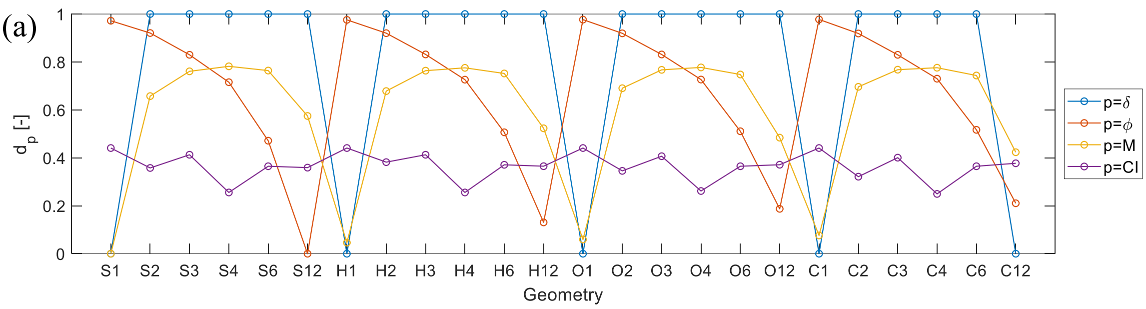

(b)

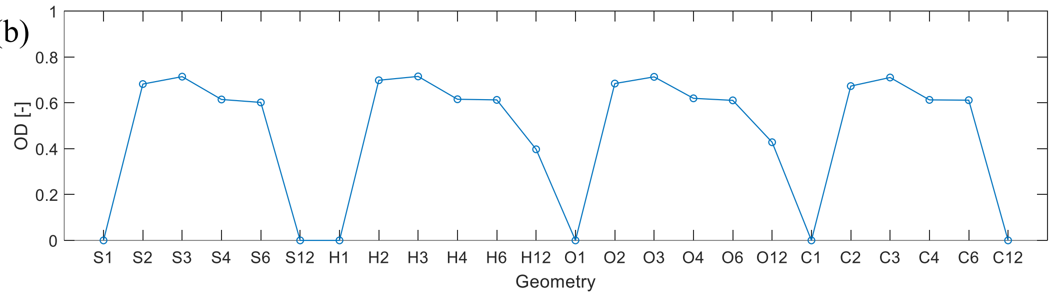

Figure 4.11- Results of the desirability function approach in case of the 252-m diagrid tall building: (a) Individual desirability values for each response variable (b) Overall desirability values ($r_p = 1$)

In Figure 4.12 the overall desirability OD is plotted in function of the two geometrical parameters, namely the diagonal inclination and the floor plan shape, for each building height, aimed at obtaining a three-dimensional surface. It is worth to note how the geometrical parameters have totally different effect on the selection of the most desirable solution. Specifically, it is evident that the influence of the floor plan shape is almost negligible. Conversely, as stated several times, the diagonal inclination has a stronger effect on the value of the overall desirability. This means that a variation of the diagonal angle can lead to a different structural behaviour in terms of lateral displacement and torsional rotation, structural weight and construction issues.

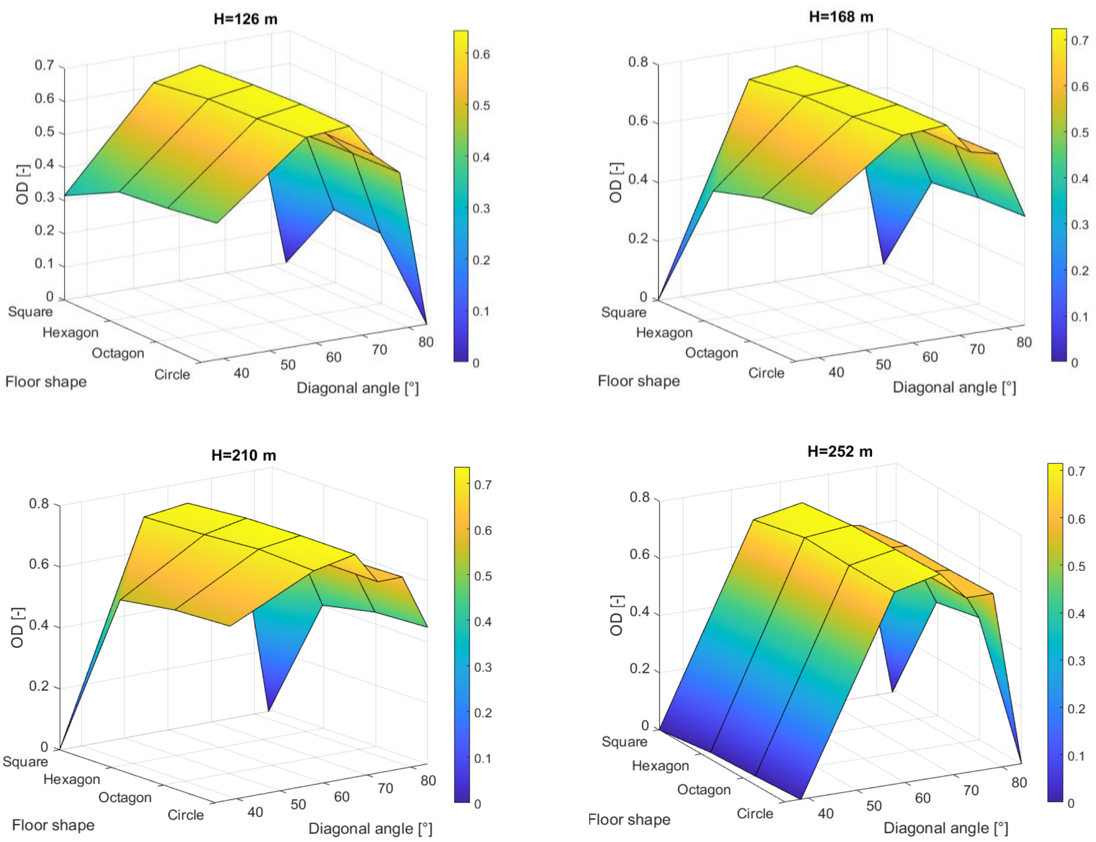

Figure 4.12 - Overall desirability (OD) in function of the diagonal angle and floor plan shape for each building height

For the 126, 210 and 252-m tall buildings the same analysis with different weights for different response parameters has been carried out. To this purpose, the combinations presented in Table 4.3 are employed. As for the 48-story building, the principal outcomes related to the optimal solution have been expressed in terms of the relative frequency of occurrence out of the total combinations for each geometrical solution, as shown in Figure 4.13. In case of the 36-story building, the most desirable solution in most combinations shown in Figure 4.13a is the three intra-module floors solution with octagonal plan for 3423 out of 4096 simulations, leading to a corresponding relative frequency of 83.57%. Based on the results, OD values varies between 0.434 and 0.891. Specifically, the minimum value is returned for $r_\delta = r_\varphi = r_M = r_{CI} = 2$ combination, whereas the maximum one for $r_\delta = r_\varphi = r_M = r_{CI} = 0.25$. In some other combinations where the torsional rotation exponent is greater ($r_\varphi > r_{CI}$ and $r_\varphi \geq r_M, r_\delta$) the two intra-module floors solution with circular plan is preferable in 574 out of 4096 combinations, leading to a relative frequency of occurrence equal to 14.01%. The overall desirability is between 0.582 ($r_\delta = r_\varphi = 2, r_M = r_{CI} = 1$) and 0.879 ($r_\delta = r_M = r_{CI} = 0.25$, $r_\varphi = 0.5$). Moreover, there are also other solutions with low relative frequency of occurrence: the S3, O2 and C3 geometries have greatest overall desirability in 46 (1.12%), 36 (0.88%) and 17 (0.42%) combinations, respectively.

Secondly, for the 60-story building the O3 solution is always the one most desirable in most combinations, namely 2440 out of 4096 (59.57%), having OD range between 0.543 ($r_\varphi = r_M = r_{CI} = 2$) and 0.927 ($r_\varphi = r_M = r_{CI} = 0.25$), whereas the H3 solution provides the greatest overall desirability in 936 cases (22.85%) where r_φ and r_{CI} prevail. In some other simulations the O2 geometry results to be the optimal one in 720 combinations (17.58%) where $r_\varphi \geq r_M$ and $r_\varphi > r_{CI}$. The results are presented in Figure 4.13b.

Lastly, regarding the 72-story building, the H3 geometry is the optimal solution in 3088 out of 4096 combinations (75.39%) with OD values from 0.512 ($r_\varphi = r_M = r_{CI} = 2$) to 0.9197 ($r_\varphi = r_M = r_{CI} = 0.25$), whereas the H2 solution results the best one in 624 simulations (15.23%) where the exponent related to torsional rotation r_φ is greater than the others. In some cases, 384 combinations (9.38%) return the O3 solution with highest overall desirability. Specifically, it occurs when the exponent referred to structural weight r_M is greater than r_φ and r_{CI}. Note that the 72-story building is the particular case that returns the H3 geometry as optimal solution in most of combinations instead of the O3 model. However, as mentioned before, it is expected a slight influence of the floor plan shape on the overall desirability, e.g. considering the combination given by $r_\varphi = r_M =$

$r_{CI} = 2$ the O3 geometry is characterized by $OD_{O3} = 50.52\%$ with a difference of 0.68% with respect to OD_{H3}. The results are shown in Figure 4.13c.

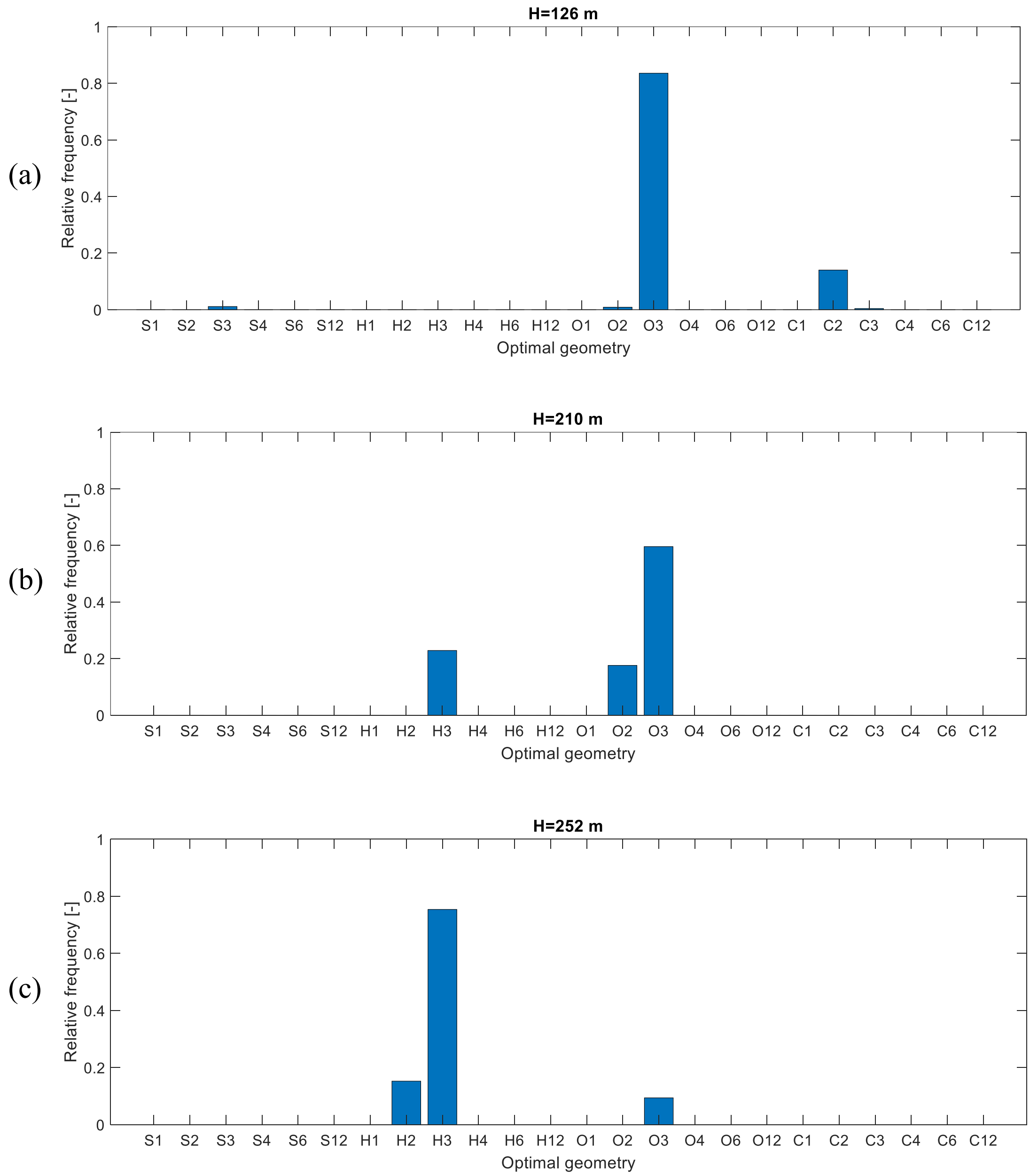

Figure 4.13 - Relative frequency of each geometrical solution considering 4096 simulations for: (a) the 126-m tall building (b) the 210-m tall building (c) the 252-m tall building

In conclusion, it is worth to note that the three intra-module floors solution results the most desirable geometry in terms of the top lateral displacement, torsional rotation, structural weight and complexity index for each building height. In fact, from the parametric analysis it was found that having diagonal inclination ranging between 65°-67° is optimal in 85.11%, 74.22%, 82.42% and 84.77% of the total number of combinations for the 36-, 48-, 60- and 72-story buildings, respectively. Conversely, the effect of exponent on the selection of the optimal geometry is slight as it also occurs for both building height and floor plan shape. However, the evidence that the building height is not significant in the choice of the optimal solution seems to contradict the studies in literature because many authors, like Moon, state that the optimal diagonal inclination increases with the height of the building as the bending moment prevails on the shear in slender structures. In the proposed study, instead, it was found that the three intra-module floors solution is almost always the optimal one independently from the building height. This phenomenon is caused by considering not only the lateral deflection, but also other response parameters, i.e. torsional rotation, structural weight of the external diagrid system and complexity index, in order to ensure an enhanced performance. Specifically, it is evident that the torsional rotation is the unique parameter that does not allow to obtain an optimal solution with steeper diagonals for taller buildings since the torsional stiffness is maximized by shallower diagonals (35°). On the contrary, the other parameters (δ, M, CI) reach minimum values for steeper inclinations: 65°-67° for the top deflection (only for the 126-m tall building) and the complexity index, whereas 70°-78° for the mass. Therefore, if the desirability function approach had been employed neglecting the torsional rotation, an optimal solution with steeper diagonals would have been expected for taller structures.

Up to this point, it has been demonstrated that the three intra-module floors solution is the most preferable solution among all geometries in the proposed study and in literature [29] [30]. However, this outcome may not necessarily be the same considering other response parameters, such as the maximum inter-story drift due to lateral actions, fundamental period of oscillation, fire resistance and many others. In any case the choice depends on the designer at the preliminary stage of the structural design.

Chapter 5

5. VARYING-ANGLE DIAGRID STRUCTURES

In literature many researchers such as Moon have affirmed a better performance of varying-angle diagrid structures than uniform-angle ones, mainly for taller buildings, as the bending moment increases quadratically towards the base of the building prevailing on the shear effect. Therefore, having steeper diagonals towards the base is expected to the structural behaviour despite greater construction complexity than unifom-angle structures. The interest of several authors into comparing uniform- and varying-angle diagrid structures leads to perform a similar investigation in the present Thesis. To this purpose, same geometrical models with different floor plan shapes, i.e. square, hexagon, octagon and circle, presented in Chapter 2.1 are employed in this study and same vertical and lateral loads are applied to tall buildings which are reported in Chapter 2.2. This Chapter is divided into the following sub-chapters: in Chapter 5.1 the diagrid geometry generation is described, whereas the outcomes obtained from the stiffness- and strength-based preliminary design and the desirability function approach are illustrated respectively in Chapter 5.2 and 5.3. Finally, Chapter 5.4 is related to the computational cost of the performed analysis.

5.1. VARYING-ANGLE DIAGRID GEOMETRY

In the previous Chapters the analysis has been performed on uniform-angle diagrid structures having diagonal inclination constant along the building height. Conversely, in the present Chapter attention is paid on varying-angle diagrid structures characterized by variable diagonal angles from the top to the base of the building. It means that the basic triangular module will be variable in the building spanning over different number of floors. Since in the analysis of uniform-angle diagrid structures it has been found that the twelve intra-module floors solution is the one of the least desirable geometries, in case of varying-angle structures, the considered diagonal inclinations correspond to number of intra-module floors varying from one to six, namely 1, 2, 3, 4, 5 and 6. Therefore, for a given building height with N stories, the external diagrid system can be obtained by combining different diagonal angles and it is also possible to have two or more consecutive modules with the same number of intermediate floors. In order to evaluate the total number of possible combinations, the following expression is provided:

$$\mathrm{n}_{\text{all combinations}} = \prod_{j=1}^{6} \left(\frac{\mathrm{N}}{\mathrm{j}} + 1 \right) \tag{5.1}$$

Where N is the number of the building stories, j is the number of intra-module floors ($j = 1, 2, 3, 4, 5, 6$). The term $(N/j + 1)$ in Equation (5.1) represents the probability that the j intra-module unit can occur in the varying-angle diagonal pattern, including the case where j intra-module unit is not present [50]. However, not all of these combinations are geometrically feasible because they have to ensure the following geometrical constraint equation [50]:

$$N = \sum_{j=1}^{6} M_j j \tag{5.2}$$

Where M_j is the number of modules with j intra-module floors. Moreover, it is possible to further reduce the number of combinations on the basis of the studies carried out in literature. Indeed, Moon in [15] has demonstrated that varying-angle pattern with steeper angle towards the top has the worst structural performance. Therefore, these geometrical models are also neglected in the present analysis. Based on these two considerations, the reduced value $\mathrm{n}_{\text{feasible comb}}$ can be assessed. At the end, the total number of diagrid structures that will be analysed in the preliminary design, coupled with the desirability function approach, will be $\mathrm{n}_{\text{feasible comb}} \times 4$ due to the four floor plan shapes. As follows, in Table 5.1 $\mathrm{n}_{\text{all combinations}}$ and $\mathrm{n}_{\text{feasible comb}}$ are reported for each building height.

Height [m]	126	168	210	252
$\mathrm{n}_{\text{all combinations}}$	5 117 840	24 365 250	90 858 768	256 851 595
$\mathrm{n}_{\text{feasible comb}}$	2 432	7 760	19 858	43 752
$\mathrm{n}_{\text{feasible comb}} \times 4$	9 728	31 040	79432	175 008

Table 5.1 - Total number of all combinations and feasible combinations in function of the building height for the generation of varying-angle diagrid geometry

Based on the values reported in Table 5.1, it is evident that for each building height the population is much wider than the twenty-four uniform-angle diagrid models. This huge difference is fundamental to demonstrate the efficiency of the two proposed methods, i.e. the matrix-based method (MBM) and the desirability function approach. In Figure 5.1 three examples of varying-angle diagrid structures are shown. Note that among all possible combinations some of them return uniform-angle pattern as it is illustrated in Figure 5.1a.

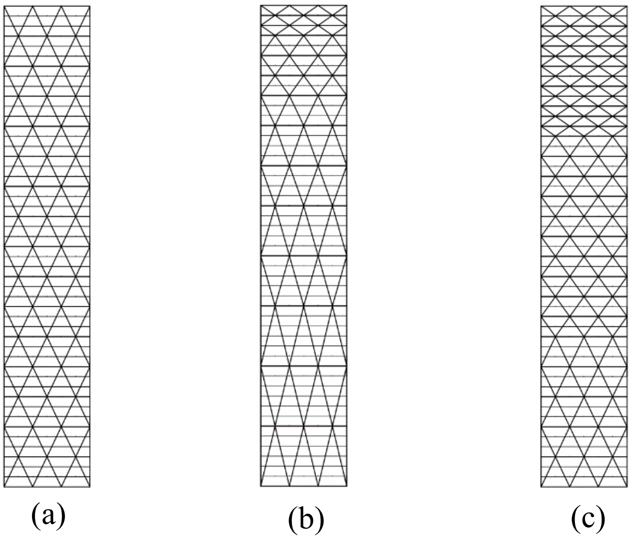

Figure 5.1 - Three varying-angle diagrid structures for the 168-m tall building: (a) combination #88: $M_1 = M_2 = M_4 = M_5 = M_6 = 0, M_3 = 16$ (b) combination #2023: $M_1 = 3, M_2 = 3, M_3 = 1, M_4 = 2, M_5 = 2, M_6 = 3$ (c) combination #5802: $M_1 = 13, M_2 = 10, M_3 = 5, M_4 = M_5 = M_6 = 0$

5.2. PRELIMINARY DESIGN: RESULTS AND DISCUSSION

Each geometrical solution defined by a specific combination of intra-module units is analysed by means of the strength- and stiffness-based preliminary design described in Chapter 3 applying both vertical and horizontal loads. Note that the assessment of the concentrated lateral force on each rigid floor is a bit more complicated due to different number of intra-module floors between two consecutive modules. In any case, the evaluation of these loads is always based on the isostatic load repartition. As in the previous Chapters related to uniform-angle diagrid structures, the 168-m tall building is firstly analysed in detail, whereas the others are discussed next for sake of completeness. Therefore, performing the structural analysis of all the 31040 structures for the 48-story tall building, the four response variables, i.e. top lateral displacement, top torsional rotation, diagrid structural mass and complexity index, can be evaluated. Their values for each diagrid geometry are shown in Figure 5.2 with their relative distribution curves illustrated in Figure 5.3.

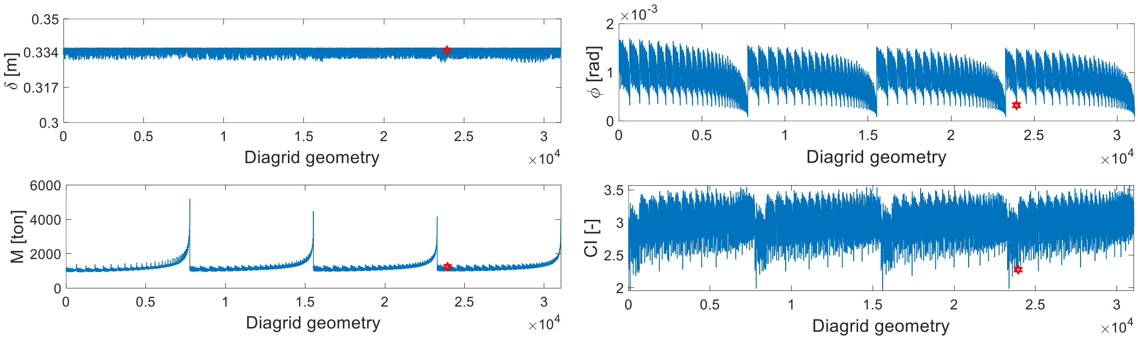

Figure 5.2 - Response variables, i.e. top lateral displacement, top torsional rotation, structural diagrid mass and complexity index, for the 168-m tall building with 31040 diagrid geometries. The optimal geometry (#23936) obtained from the desirability function approach with $r_\delta = r_\varphi = r_M = r_{CI} = 1$ is highlighted with the red star

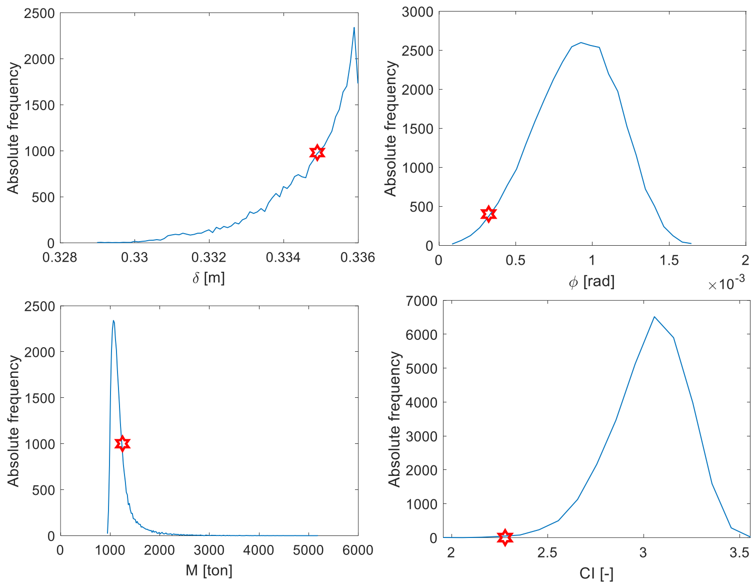

Figure 5.3 – Statistical distribution of response variables, i.e. top lateral displacement, top torsional rotation, structural diagrid mass and complexity index, for the 168-m tall building with 31040 diagrid geometries. The optimal geometry (#23936) obtained from the desirability function approach with $r_\delta = r_\varphi = r_M = r_{CI} = 1$ is highlighted with the red star

Based on results of Figure 5.2, it can be seen again the almost negligible effect of floor plan shape on the four response variables as the trend is repetitive for each plan shape. For the 168-m tall building the square, hexagonal, octagonal and circular plan shapes correspond respectively to diagrid geometries varying from 1 to 7760, from 7761 to 15520, from 15521 to 23280 and finally from 23281 to 31040. Conversely, the influence of diagonal inclination is more evident.

As far as the statistical distribution curves are concerned, Figure 5.3 shows values that are most and least frequent out of 31040 structures. In particular, the top lateral displacement curve seems to have exponential distribution. It reaches a maximum peak at 0.33589 m for 2340 structures, whereas the minimum value of 0.329 m is provided by only one diagrid geometry. By observing the limit of x axis, it is already evident that the maximum top lateral displacement variation is very small of 7 mm because of the stiffness-based design. Therefore, by performing the desirability function approach, it is expected to have unitary individual desirabilities for all geometries ($d_{i,\delta} = 1$). Moreover, it also important to point out that in case of the 48-story tall building all 31040 diagrid structures satisfy both strength and stiffness requirements. Regarding the statistical distribution curves of the top torsional rotation, structural mass and complexity index, they are more alike to Gaussian distribution as both minimum and maximum values are provided by few geometries, whereas most of structures lie within the extremes.

By analysing the trends in Figure 5.2 in function of inclinations of diagonals, it is found that for a given plan shape the top torsional rotation decreases as the number of modules with one or two intermediate floors increases, corresponding to shallower diagonals. Indeed, the maximum torsional stiffness is guaranteed by diagonal angle of 35°. In particular, the one intra-module floor geometry with hexagonal plan provides the minimum value of $8.482 \cdot 10^{-5}$ rad, which is the same one obtained in the uniform-angle structure analysis. Conversely, the greatest torsional stiffness is given to the six intra-module floors solution with square plan ($\varphi_{max} = 0.017$ rad). Conversely, the structural mass and the complexity index tend to increase for less steeper diagonals.

The slight increasing trend of the complexity index for each plan shape is mainly due to greater number of nodes (N_1) and greater number of diagonals with maximum length of 12 m (N_3), whereas the other metrics, i.e. number of different cross-sections N_2 and number of diagonals in the pattern N_4, increase of a small amount. The number of different lengths (N_5) does not follow a specific trend but assumes integer values between 1 and 6 in function of the number of different modules. This last aspect is different from the one obtained in uniform-angle structures as N_5 was always unitary for all geometries. The trends of these five metrics are graphically reported in Figure 5.4. Moreover, it can be noted that the six intra-module floors solution has the greatest number of nodes ($N_1 = 732$) and the least number of different cross-sections ($N_2 = 8$) and of diagonals ($N_4 = 192$). Conversely, the one intra-module floor geometry has the least number of nodes

($N_1 = 572$) and the greatest number of different cross-sections and diagonals ($N_2 = 30, N_4 = 1152$).

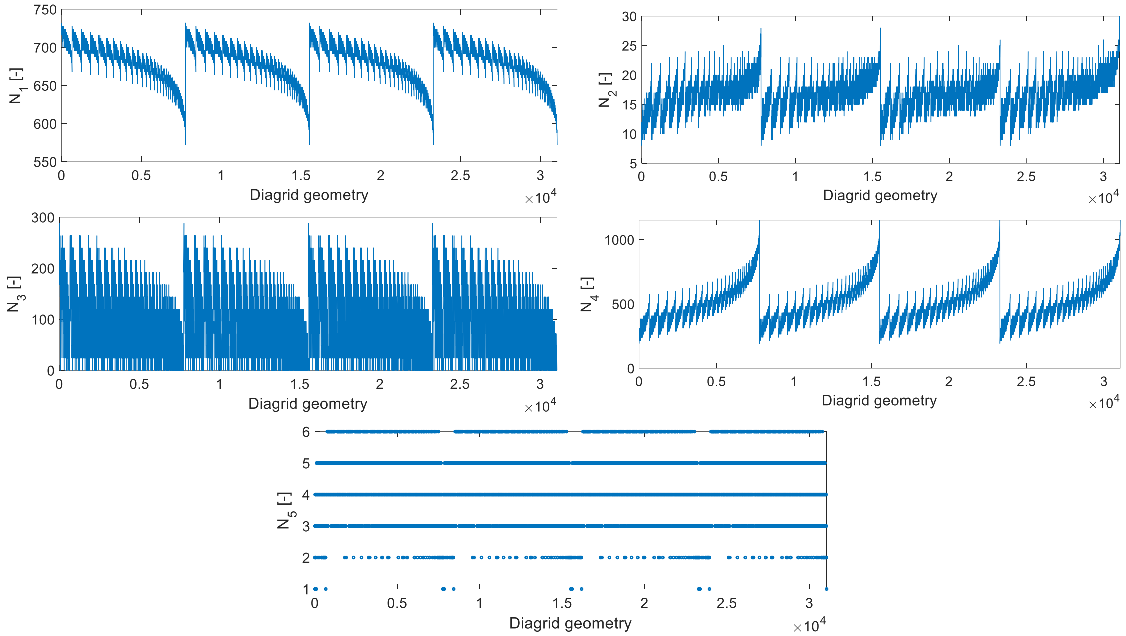

Figure 5.4 – Five metrics, N_1, N_2, N_3, N_4 and N_5, for the assessment of the complexity index for the 168-m tall building with 31040 diagrid geometries

		φ [rad]		M [ton]		CI [-]	
varying	min	$8.48 \cdot 10^{-5}$	H1	946	Varying (square)*	1,956	S3
	max	0,017	S6	5204	S1	3,568	Varying (square)**
uniform	min	$8.48 \cdot 10^{-5}$	H1	991	S4	2,769	S3, O3
	max	0,00273	S12	5204	S1	3,765	C1

* $M_1 = 1, M_2 = 4, M_3 = 6, M_4 = 4, M_5 = 1, M_6 = 0$ ** $M_1 = 10, M_2 = 2, M_3 = 1, M_4 = 5, M_5 = 1, M_6 = 1$

Table 5.2 - Maximum and minimum values of the top torsional rotation, structural mass and complexity index obtained from the structural analysis of 31040 structures (varying) and 24 structures (uniform) for the 168-m tall building

Another observation that can be made concerns the comparison between the maximum and minimum values of each response variables obtained from the analysis performed on 24 geometrical solutions for uniform-angle structures and 31040 for varying-angle ones. It can be observed that there is a good compatibility of the results. For example, as shown in Table 5.2, in both analysis the uniform-angle structure with one intra-module floor provides the least torsional rotation but the greatest diagrid mass, whereas the most deformable geometry from a torsional point of view is always the one with steeper diagonals. However, regarding the structural mass, the varying-angle structure with this combination of modules $M_1 = 1, M_2 = 4, M_3 = 6, M_4 = 4, M_5 = 1, M_6 = 0$ is lighter than S4 of about 45 tons. Note that this table will be fundamental for the definition of the individual desirability because $d_{i,p}$ will be null for geometries providing the maximum value of one parameter and it will be the greatest for the ones with minimum value.

Finally, a final observation is made on diagonal cross-section areas and on values of demand capacity ratio (DCR). The results are shown in Figure 5.5 where the values are referred to the top and the base of the building. In particular, Figure 5.5a points out a similar trend to the one illustrated in Figure 5.2 related to the structural mass as it increases for shallower diagonals. It is also evident that cross-section area at the top is almost equal for all geometries ($A_{top} \cong 0.0067\ m^2$), whereas at the base it reaches peaks in correspondence to the one intra-module floor solutions, which have the least lateral stiffness and therefore the diagonals cross-sections are bigger. Moreover, this leads to lower value of DCR ($DCR_{max,top} < 0.5$). Conversely, as presented in Figure 5.5b, for the other geometries there is a good exploitation of diagonals in terms of strength because DCR has a range between 0.6 and 1 and therefore this aspect ensures a reduction of steel consumption.

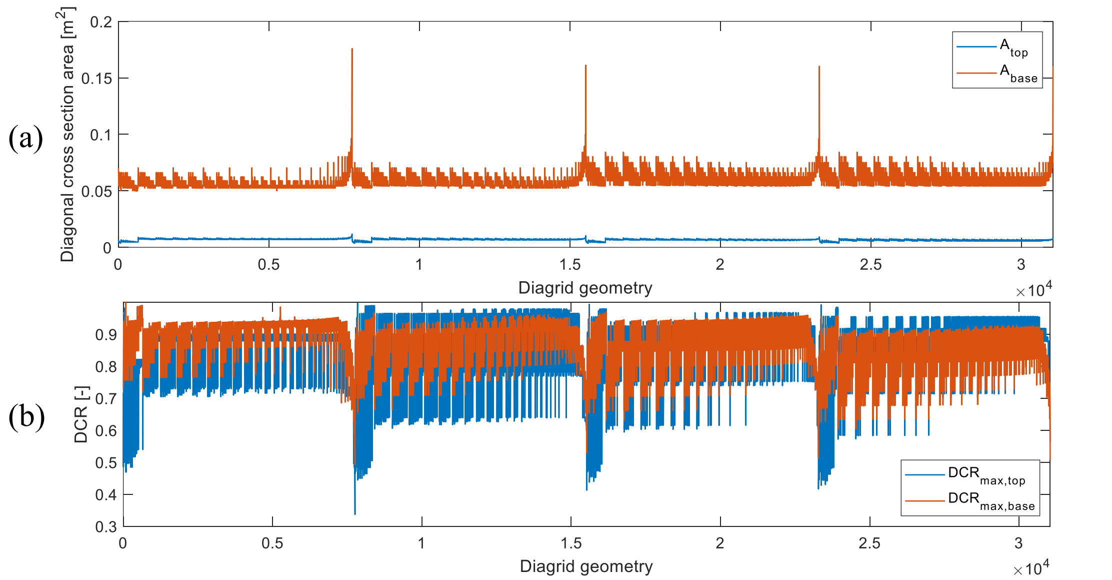

Figure 5.5 - 31040 varying-angle structures in function of: (a) diagonal cross section area (b) demand capacity ratio (DCR) for the 168-m tall building

Similarly, as mentioned before, now the 126-, 210- and 252-m tall buildings are analysed and the same graphs are proposed. By observing Figure 5.6-Figure 5.7, it is immediately evident from the repetitive trend for each plan shape that the structural behaviour of all diagrid geometries is more affected by diagonals inclinations rather than floor plan shape, independently from the building height.

Now, an individual analysis is carried out for each building height. Regarding the 36-story building, the graphs are plotted in such a way that geometries from 1 to 2432 are referred to square plan, from 2433 to 4864 to hexagonal plan, from 4865 to 7296 to octagonal plan and from 7297 to 9728 to circular plan. It is important to underline that the main difference with respect to the 168-m tall building is referred to the top lateral displacement. In fact, as shown in Figure 5.6a, the variation range is wider (δ =0.145÷0.252 m) as the design of less slender structures is governed by the strength demand instead of the stiffness one. Specifically, there is a reduction of the top lateral deflection for shallower diagonals in the upper modules, whereas the trend slightly grows up for shallower diagonals also in the lower modules. This is caused by the fact that the bending moment prevails in the lower part and the shear in the upper part. Moreover, the relative statistical distribution reported in Figure 5.6b does not have an exponential trend, but it is more similar to a Gaussian distribution as most values fall within the two extremes ($\delta_{min} = 0.145\ m, \delta_{max} = 0.252\ m$). For the other response variables, namely the top torsional rotation, structural mass and complexity index, no further considerations are made since graphs in Figure 5.6a-b show similar trends to the ones in Figure 5.2 and in Figure 5.3. As a matter of fact, the top torsional rotation decreases with shallower diagonals, whereas the structural mass and the complexity index increase for the same reasons mentioned before. However, two useful considerations on Figure 5.6d can be made. First of all, DCR curve at the top and at the base of the building are almost overlapped. Secondly, DCR is greater than 0.8 for most of the structures. These two considerations demonstrate that most of 9728 geometries are well dimensioned from strength perspective. Conversely, the uniform-angle structures with only one intra-module floors have instead the lowest DCR values. Finally, for the 36-story building it is also evident as in the previous case that the geometrical solutions providing maximum and minimum values of each response variable among 24 uniform-angle and 9728 varying-angle structures are compatible (Table 5.3).

		δ [m]		φ [rad]		M [ton]		CI [-]	
varying	min	0,145	Varying (square)*[1]	$9.28 \cdot 10^{-5}$	C1	454	Varying (hexagon)*[4]	1,9145	O3
	max	0,252	Varying (circle)*[2]	$1.53 \cdot 10^{-3}$	Varying (square)*[3]	1603	S1	3,5235	Varying (octagon)*[5]
uniform	min	0,149	S3	$9.28 \cdot 10^{-5}$	C1	510	C4	2,727	O3
	max	0,251	H6	0,002182	S12	1726	C12	3,764	C1

*[1] $M_1 = 0, M_2 = 1, M_3 = 6, M_4 = 0, M_5 = 8, M_6 = 0$
*[2] $M_1 = 6, M_2 = 1, M_3 = 1, M_4 = 4, M_5 = 3, M_6 = 3$
*[3] $M_1 = 1, M_2 = 0, M_3 = 0, M_4 = 0, M_5 = 1, M_6 = 5$
*[4] $M_1 = 0, M_2 = 1, M_3 = 0, M_4 = 7, M_5 = 0, M_6 = 1$
*[5] $M_1 = 12, M_2 = 1, M_3 = 1, M_4 = 2, M_5 = 1, M_6 = 1$

Table 5.3 - Maximum and minimum values of the top lateral deflection, top torsional rotation, structural mass and complexity index obtained from the structural analysis of 9728 structures (varying) and 24 structures (uniform) for the 126-m tall building

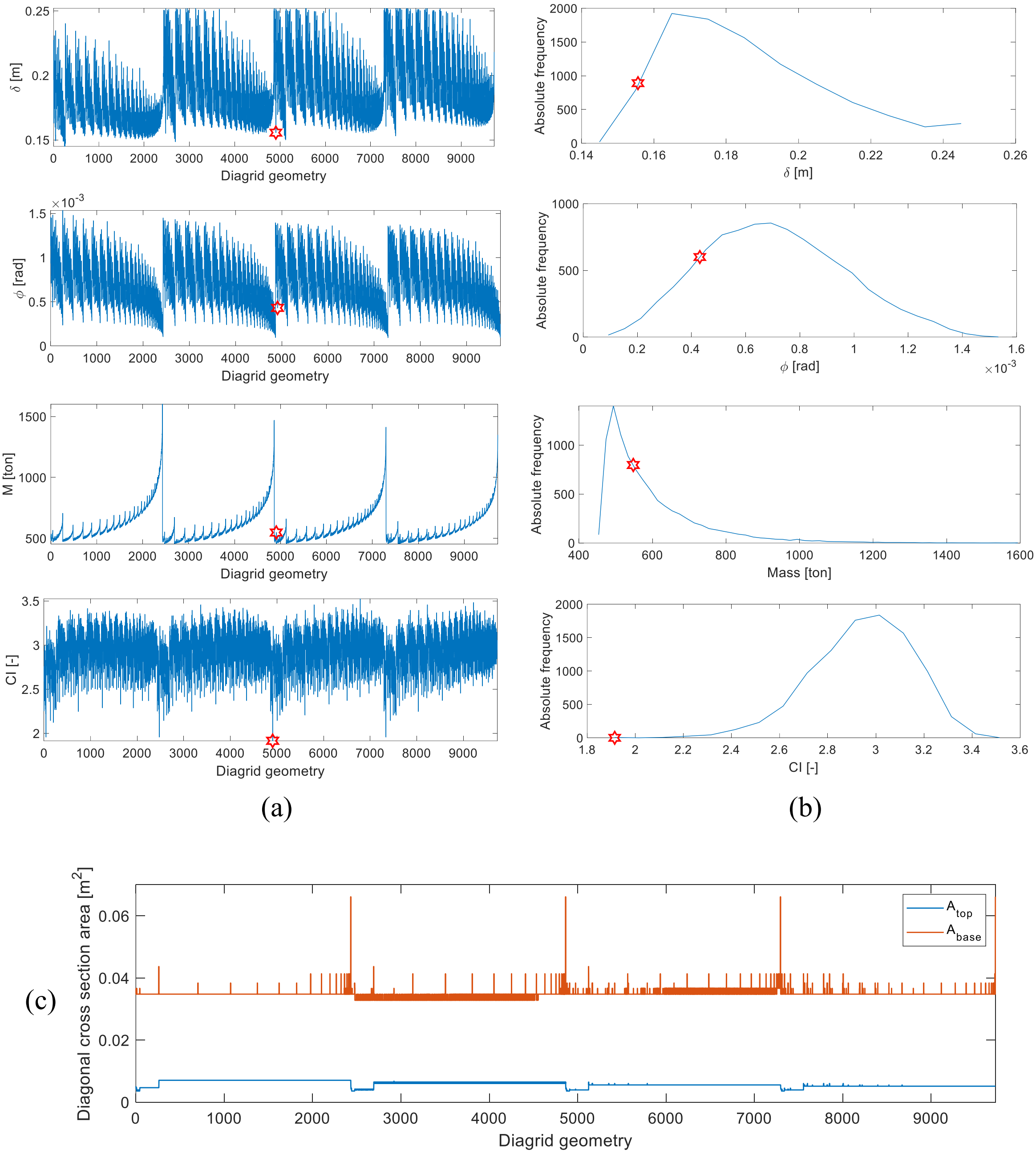

(d) 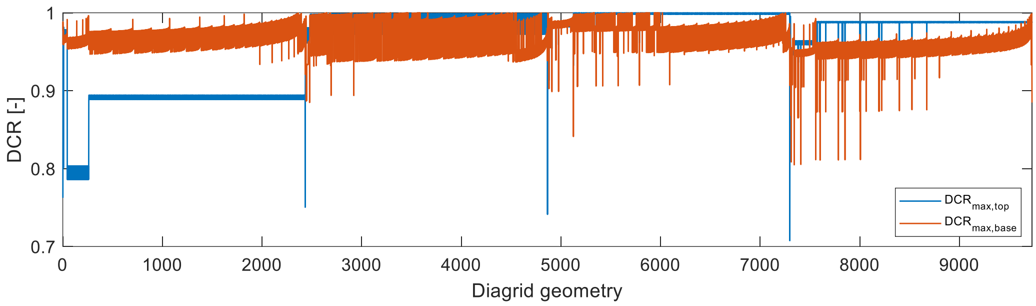

Figure 5.6 – Results of the preliminary design for the 126-m tall building with 9728 diagrid geometries: (a) Response variables, i.e. top lateral displacement, top torsional rotation, structural diagrid mass and complexity index (b) Statistical distribution of response variables. The optimal geometry (#4908) obtained from the desirability function approach with $r_\delta = r_\varphi = r_M = r_{CI} = 1$ is highlighted with the red star (c) diagonal cross section area (d) demand capacity ratio (DCR)

A further increasing of the building height, as for the 210-m tall building, leads to results with trends really close to the ones obtained for the 48-story building since the stiffness demand prevails on the strength one. Indeed, it is found that in Figure 5.7a the top lateral displacement has a small variation from 0.41 m to 0.42 m and in Figure 5.7b the relative statistical distribution has a cusp in correspondence of the target limit value of 0.42 m. However, there exists only one solution that is not able to ensure the stiffness requirement. In fact, as visible in Figure 5.7a, there is a sudden jump beyond the limit value. It is referred to #19858 solution having only one intra-module floors ($M_1 = 60, M_j = 0 \text{ for j} \neq 1$) as the top lateral displacement is equal to 0.445 m. This phenomenon has an impact on the diagonal cross sections and on DCR. In particular, from the preliminary design it has been obtained an oversized structure with so big diagonal cross sections that DCR tends to null value, as evident in Figure 5.7c-Figure 5.7d. Therefore, this case represents the worst condition for which, by applying the desirability function, the overall desirability will be null. Regarding the other response variables, the previous considerations hold valid. Note that in this case geometries from 1 to 19858 are referred to square plan, from 19859 to 39716 to hexagonal plan, from 39717 to 59574 to octagonal plan and from 59575 to 79432 to circular plan. Moreover, Table 5.4 is provided for sake of completeness.

		φ [rad]		M [ton]		CI [-]	
varying	min	$5.61 \cdot 10^{-5}$	S1	2257	Varying (square)**	1,9796	S1
	max	0,001727	Varying (square)*	18780	S1	3,7164	Varying (hexagon)***
uniform	min	$5.61 \cdot 10^{-5}$	S1	2358	S4	2,8007	S1
	max	0,003126	S12	18780	S1	3,7430	S4,H4,C4

* $M_1 = 1, M_2 = 0, M_3 = 0, M_4 = 0, M_5 = 1, M_6 = 9$
** $M_1 = 1, M_2 = 3, M_3 = 7, M_4 = 4, M_5 = 2, M_6 = 1$
*** $M_1 = 22, M_2 = 2, M_3 = 1, M_4 = 5, M_5 = 1, M_6 = 1$

Table 5.4 - Maximum and minimum values of the top torsional rotation, structural mass and complexity index obtained from the structural analysis of 79432 structures (varying) and 24 structures (uniform) for the 210-m tall building

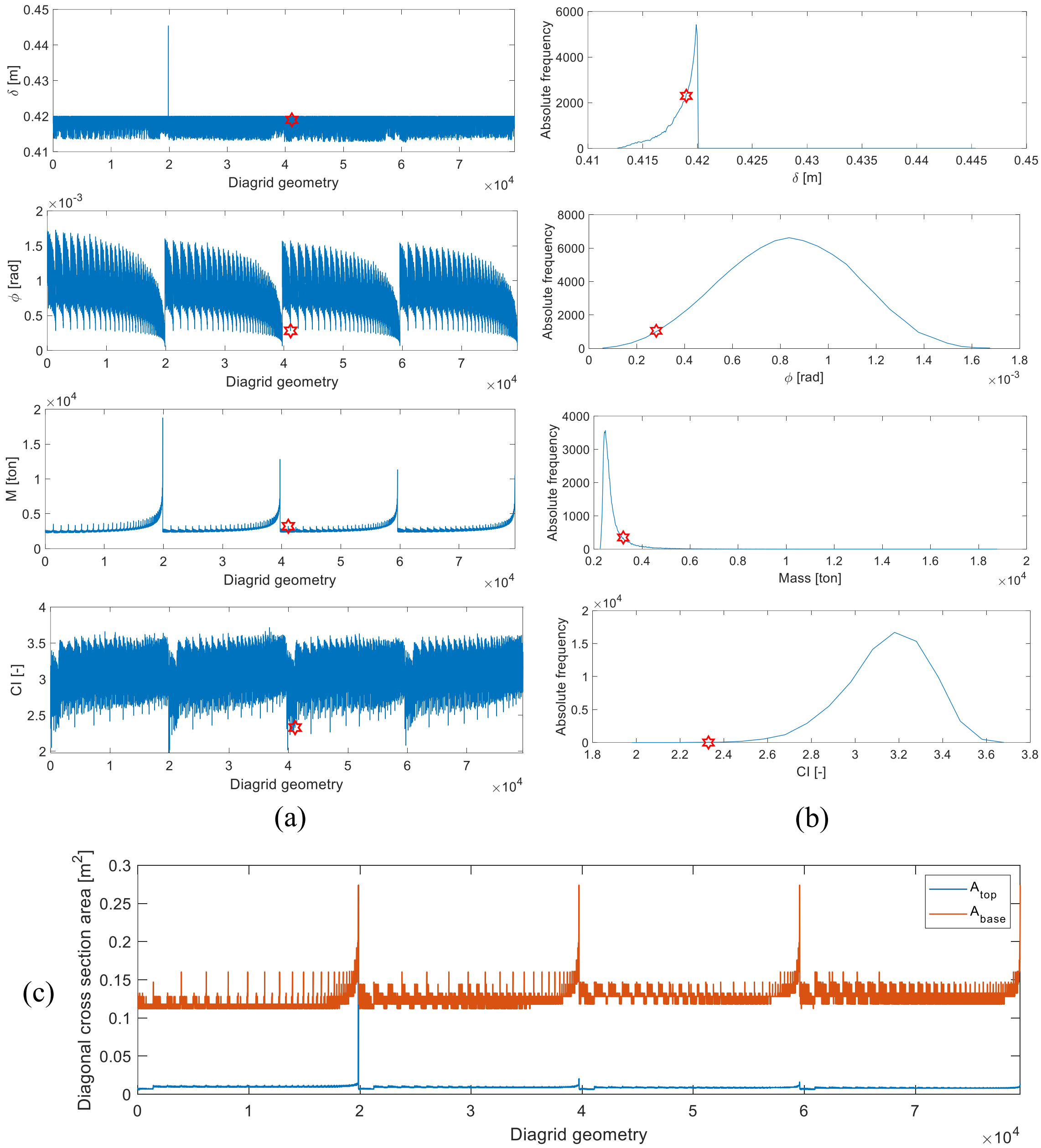

(d)
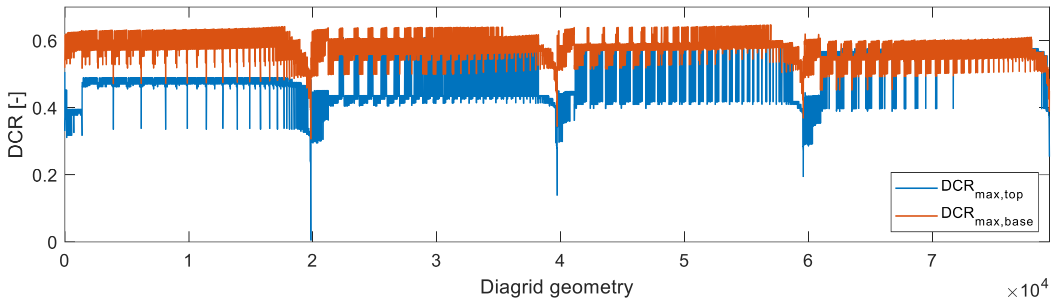

Figure 5.7 - Results of the preliminary design for the 210-m tall building with 79432 diagrid geometries: (a) Response variables, i.e. top lateral displacement, top torsional rotation, structural diagrid mass and complexity index (b) Statistical distribution of response variables. The optimal geometry (#41107) obtained from the desirability function approach with $r_\delta = r_\varphi = r_M = r_{CI} = 1$ is highlighted with the red star (c) diagonal cross section area (d) demand capacity ratio (DCR)

Finally, the 252-m tall building is analysed. Its structural behaviour is similar to the 60-story tall building since the stiffness requirement prevails. In fact, also in this case the top lateral deflection is almost equal to the target limit value ($\delta_{lim} = 0.504$ m) as it can be noted in Figure 5.8a. In particular, its correspondent statistical distribution, shown in Figure 5.8b, is characterized by a vertical jump at 0.504 m for most diagrid structures. Nevertheless, 480 geometries do not ensure the stiffness requirement since the top lateral displacement exceeds the limit value. Among these, there are uniform-angle diagrid geometries made up of one intra-module floor, i.e. #43752, #87504, #131256 and #175008 solutions ($M_1 = 72, M_j = 0$ for $j \neq 1$) as it is also shown in Chapter 4.2.2, and varying-angle ones with at least fifty base modules composed by one intra-module floor. For these geometries the expected overall desirability will be null for the unsatisfactory required stiffness. Regarding the top torsional rotation, the structural mass and the complexity index, same previous considerations are valid. Note that in this case geometries from 1 to 43752 are referred to square plan, from 43753 to 87504 to hexagonal plan, from 87505 to 131256 to octagonal plan and from 131257 to 175008 to circular plan. In Figure 5.8c and Figure 5.8d the distribution of diagonal cross sections and DCR are provided. In the former graph it is evident that for unsatisfactory geometries the stiffness of the building is constant along the height as all diagonals have the maximum area of 0.27 m^2. For this reason, the curve relative to the transversal area of diagonals at top module has sudden peaks. Moreover, it can be also noted that all structures have a great stiffness at the base in order to ensure a satisfactory performance. Consequently, these peculiarities influence DCR because its maximum value at base module drops below 0.5 for most geometries, whereas for the unacceptable models the minimum value at top is almost null and the maximum value at base is about 0.7. Thus, it can be concluded that increasing the height of the building leads to a heavier structure aimed at compensating its deformability. Also, in this case the difference of outcomes between the analyses of 24 uniform-angle and 175008 varying-angle structures is reported in Table 5.5.

		φ [rad]		M [ton]		CI [-]	
varying	Min	$7{,}06 \cdot 10^{-5}$	C1	4687	Varying (square)**	1,9779	S1
varying	Max	0,001673	Varying (square)*	22536	S1	3,7422	Varying (hexagon)***
uniform	Min	$7{,}1 \cdot 10^{-6}$	C1	4916	S4	2,80	S1,H1,O1,C1
uniform	max	$3{,}135 \cdot 10^{-3}$	S12	22536	S1	3,75	C4

* $M_1 = 1, M_2 = 0, M_3 = 0, M_4 = 0, M_5 = 1, M_6 = 11$

** $M_1 = 0, M_2 = 2, M_3 = 6, M_4 = 6, M_5 = 4, M_6 = 1$

*** $M_1 = 32, M_2 = 1, M_3 = 1, M_4 = 6, M_5 = 1, M_6 = 1$

Table 5.5 - Maximum and minimum values of the top torsional rotation, structural mass and complexity index obtained from the structural analysis of 175008 structures (varying) and 24 structures (uniform) for the 252-m tall building

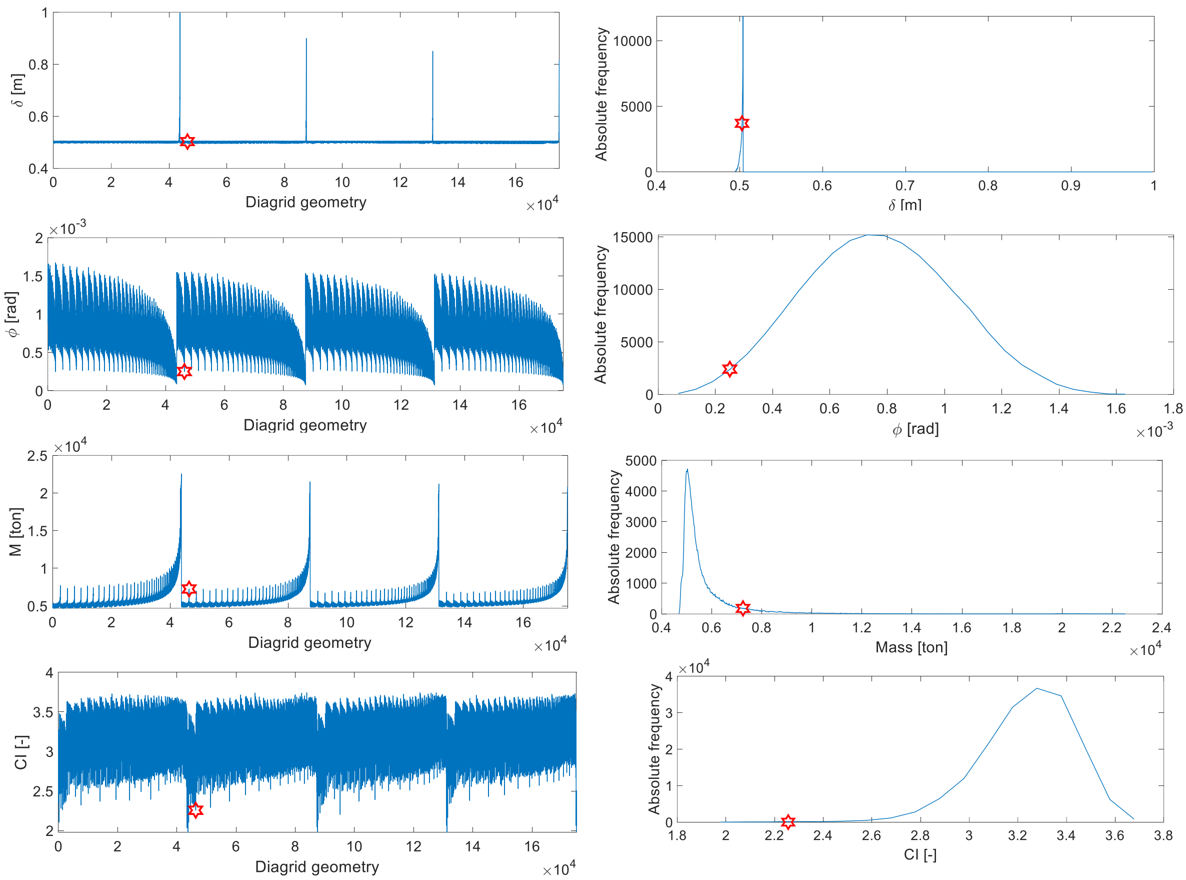

(a) (b)

(c)

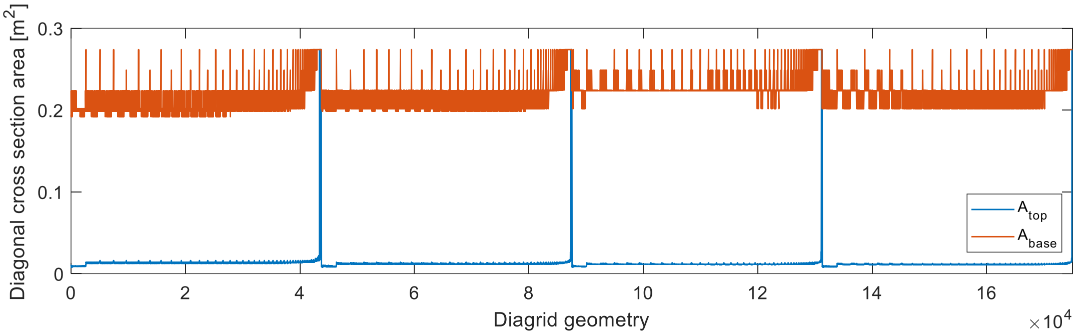

(d)

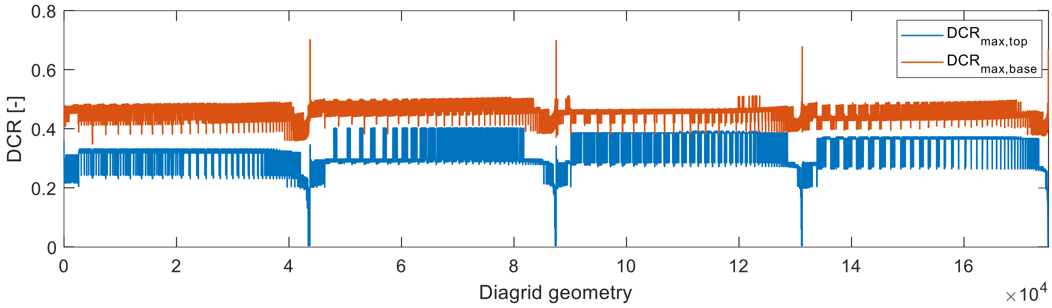

Figure 5.8 - Results of the preliminary design for the 252-m tall building with 175008 diagrid geometries: (a) Response variables, i.e. top lateral displacement, top torsional rotation, structural diagrid mass and complexity index (b) Statistical distribution of response variables. The optimal geometry (#46370) obtained from the desirability function approach with $r_\delta = r_\varphi = r_M = r_{CI} = 1$ is highlighted with the red star (c) diagonal cross section area (d) demand capacity ratio (DCR)

5.3. Desirability function approach: results and discussion

Once all the response variables have been obtained, the desirability function approach is applied to select the most desirable diagrid geometry among the varying-angle structures. To this purpose, the individual desirability of each structure referred to each parameter is assessed from Equations (4.7),(4.8),(4.9) and (4.10). In the following step the overall desirability is evaluated for each structure by applying Equation (4.11). The adopted procedure is exactly the one described in Chapter 4.1 but with one difference. Since the varying-angle population generated through combinations of triangular units is really wide, the selection of the optimal geometry with the greatest value of the overall desirability (OD_{max}) leads to neglect other geometries that have OD value close to the maximum one. Therefore, in order to solve this problem, besides identifying the optimal solution with OD_{max}, other geometrical solutions with OD ranging from $OD_{max} - 2\%$ and OD_{max} are selected and called "winners".

Now, the results of the desirability analysis, obtained with $r_\delta = r_\varphi = r_M = r_{CI} = 1$, for the 168-m tall building with 31040 diagrid geometries are represented. In Figure 5.9 the individual desirability of the top lateral displacement, top torsional rotation, structural mass and complexity index are shown. It is evident that the influence of the top lateral displacement on the overall desirability is null as it is always unitary for all geometries. In fact, in this case the coefficient of variation is equal to 0.0036.

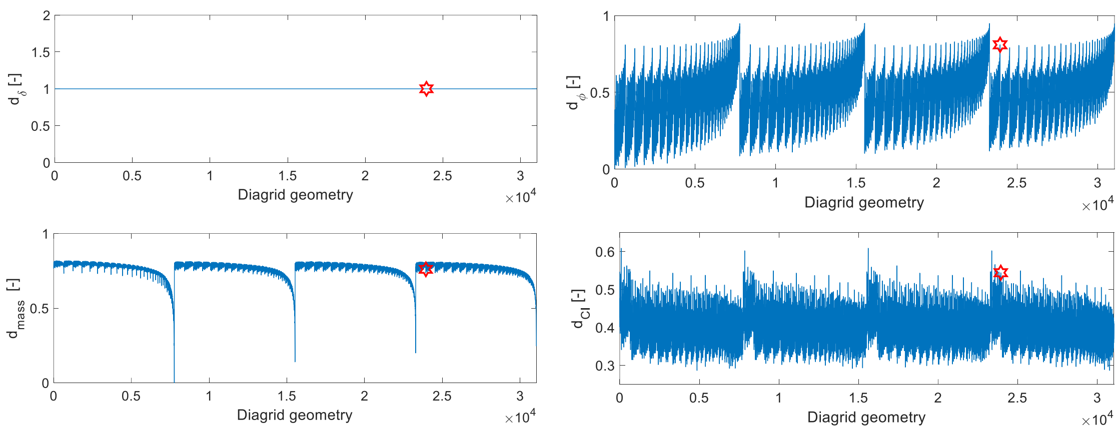

Figure 5.9 – Individual desirability of the top lateral displacement, top torsional rotation, diagrid structural mass and complexity index, for the 168-m tall building with 31040 diagrid geometries. The optimal geometry (#23936) obtained from the desirability function approach with $r_\delta = r_\varphi = r_M = r_{CI} = 1$ is highlighted with the red star

By applying Equation (4.11), the overall desirability can be evaluated. Figure 5.10 shows the obtained value of the overall desirability for each diagrid geometry with its relative statistical distribution among all geometries. Moreover, in both Figure 5.10a and Figure 5.10b the optimal solution #23936 is highlighted with a red star and the three-dimensional geometry is represented in Figure 5.10c.

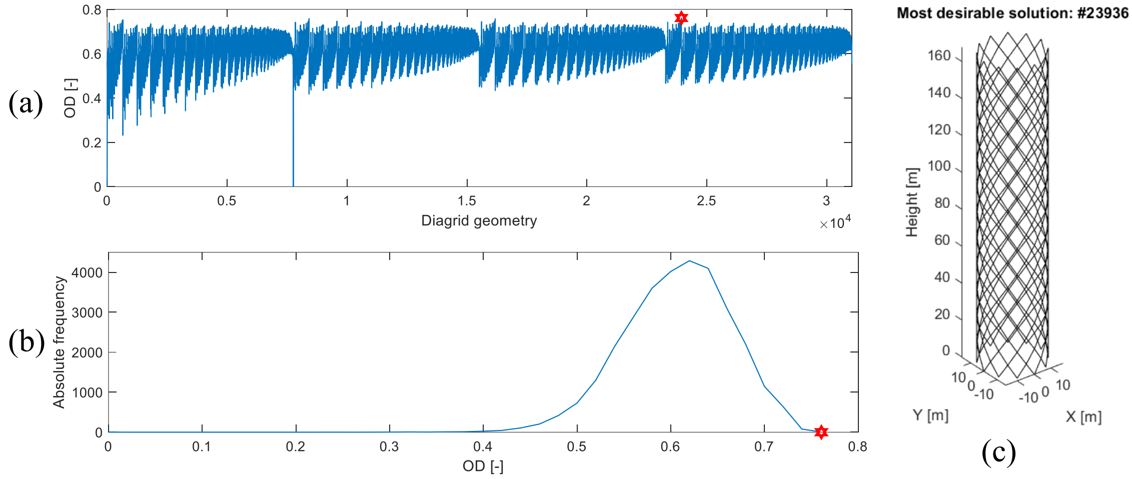

Figure 5.10 – Results of the desirability function approach for the 168-m tall building with 31040 geometries ($r_\delta = r_\varphi = r_M = r_{CI} = 1$): (a) overall desirability values for each geometry (b) statistical distribution of OD (c) 3-D representation of the optimal solution (#23936), which is highlighted with a red star

Based on the results, the greatest value of the overall desirability is 76.08% that is provided by #23936 solution. The latter is referred to a uniform-angle circular diagrid structure with two intra-module floors, corresponding to diagonal inclination of 57.73°. By analysing the individual desirability of each response variable of the optimal solution, it is clear that the optimal geometry has a good lateral and torsional behaviour ($d_\delta = 1, d_\varphi = 80.99\%$), reduced steel material consumption ($d_M = 76.01\%$) and quite low construction complexity ($d_{CI} = 54.42\%$). However, it is not the geometry that individually minimizes the top lateral displacement, top torsional rotation and structural mass. Specifically, based on the results shown in Table 5.2, the uniform-angle hexagonal structure with one intra-module floor (#15520) has the greatest torsional stiffness ($d_\varphi = 95.02\%$) but high structural mass ($d_M = 13.97\%$) and high construction complexity ($d_{CI} = 43.04\%$), leading to $OD = 48.89\%$. Conversely, the solution that minimizes the structural mass ($d_M = 81.83\%$) is the varying-angle square structure with $M_1 = 1, M_2 = 4, M_3 = 6, M_4 = 4, M_5 = 1$ and $M_6 = 0$ (#970) characterized by high torsional rotation ($d_\varphi = 45.95\%$) and many construction issues ($d_{CI} = 39.21\%$), leading to $OD = 61.96\%$. Similarly, the uniform-angle square structure with three intra-module floors is the least complex from construction perspective ($d_{CI} = 60.87\%$) but it has limited torsional rigidity ($d_\varphi = 61.08\%$) despite the reduced structural mass ($d_M = 80.35\%$), leading to $OD = 73.93\%$.

From Figure 5.10a it is worth to note that the repetitive trend of the overall desirability confirms the almost negligible effect of the floor plan shape. In fact, the two-intra-module floors uniform-angle solutions with respectively square, hexagonal and octagonal plan shape have in order $OD = 75.14\%$, $OD = 75.82\%$ and $OD = 75.78\%$, which are not too dissimilar to the maximum OD value of 76.08%, referred to the optimal geometry with circular shape. This slight difference is also evident in the individual desirability values, as reported in Table 5.6. Therefore, these geometries, i.e. #656, #8416 and #16176 beside to the optimal one #23936, can be considered as the most desirable solutions and thus as "winners".

#solution	d_δ [−]	d_φ[−]	d_M[−]	d_{CI}[−]	OD [−]	Model
656	1	0.8096	0.7326	0.5375	0.7514	S2
8416	1	0.8117	0.7481	0.5442	0.7582	H2
16176	1	0.8119	0.7557	0.5375	0.7578	O2
23936	**1**	**0.8099**	**0.7601**	**0.5442**	**0.7608**	**C2**

Table 5.6 – Individual desirability values of each response variable, i.e. top lateral displacement, top torsional rotation, structural mass and complexity index, and overall desirability for the 168-m tall building with two intra-module floors ($r_\delta = r_\varphi = r_M = r_{CI} = 1$). In **bold** the optimal solution

From the analysis presented in Chapter 4.2.1 that has been performed on the 168-m tall building with 24 uniform-angle structures considering always $r_p = 1$, it should be noted that the optimal solution is the three intra-module floors geometry with octagonal shape instead of the two intra-module floors solution as in this case. Therefore, apparently, the results obtained from considering 31040 varying-angle structures seem to be contradictory with respect to the results considering 24 uniform-angle structures because the corresponding optimal solutions have different diagonal inclinations. Actually, it is nothing like that. In fact, in both cases, i.e. 31040 varying-angle and 24 uniform-angle structures, the difference of the overall desirability between geometries with two and three intra-module floors is lower than 2%. In particular, in the case of 31040 varying-angle structures, these geometries, namely #88, #7848, #15608 and #23368, with three intra-module floors ($M_3 = 16, M_j = 0$ for $j \neq 3$) have respectively $OD = 73.93\%, OD = 74.15\%, OD = 74.45\%$ and $OD = 74.22\%$, whereas the two intra-module solutions ($M_2 = 24, M_j = 0$ for $j \neq 2$), i.e. #656, #8416, #16176 and

#23936, have respectively $OD = 75.14\%, OD = 75.82, OD = 75.78\%$ and $OD = 76.08\%$. These values are also reported in Table 5.7. Moreover, it is also evident that the two intra-module floors geometries are the most desirable because of greater d_{φ} despite lower value of d_M and d_{CI} . However, the three intra-module solutions are good candidates for the optimal geometry.

Further considerations can be made on results reported in Table 5.7. First of all, referring to Figure 5.10b, it can be seen that the OD values of "winners" correspond to the small right tail of the statistical distribution, that assumes a Gaussian shape distribution. Similarly, there are few solutions providing the lowest OD value. Conversely, most of 31040 structures lie around the OD average value of 60.66%. Among the "winners" there are not only uniform-angle structures but also varying-angle ones which are characterized by values of individual desirability and overall desirability between the values referred to the two and the three intra-module floors solutions. In addition, most of "winners" among varying-angle structures turns out to be more desirable than the three intra-module floors geometries even if OD difference is very slight. Secondly, 22 solutions out of 30 "winners" are varying-angle structures made up of diagonals with inclination varying from 35°-38° (one floor per module) at upper modules to 70°-72° (four floors per module) at lower modules. In particular, it is found that these geometrical models have a maximum of two different diagonal inclinations. Conversely, geometries with diagonal angles higher than 72°, corresponding to five or six intra-module floors, have lower OD due to low torsional stiffness. Finally, although the desirability function approach returns a total of 30 "winners", among these the uniform-angle diagonal pattern with two intra-module floors is the most preferable for each plan shape.

	#solution	d_δ $[-]$	$d_\varphi[-]$	$d_M[-]$	$d_{CI}[-]$	OD $[-]$	M_1	M_2	M_3	M_4	M_5	M_6
SQUARE	88	1	0,6108	0,8035	0,6087	0,7393	0	0	16	0	0	0
	630	1	0,7157	0,7855	0,5534	0,7468	0	15	6	0	0	0
	647	1	0,7462	0,7738	0,5236	0,7415	0	18	4	0	0	0
	654	1	0,7770	0,7563	0,5472	0,7530	0	21	2	0	0	0
	655	1	0,7637	0,7559	0,5239	0,7416	0	22	0	1	0	0
	656	1	0,8096	0,7326	0,5375	0,7514	0	24	0	0	0	0
HEXAGON	7848	1	0,6259	0,8022	0,6021	0,7415	0	0	16	0	0	0
	8390	1	0,7280	0,7901	0,5400	0,7465	0	15	6	0	0	0
	8407	1	0,7555	0,7809	0,5170	0,7432	0	18	4	0	0	0
	8414	1	0,7831	0,7665	0,5339	0,7524	0	21	2	0	0	0
	8415	1	0,7679	0,7671	0,5106	0,7405	0	22	0	1	0	0
	8416	1	0,8117	0,7481	0,5442	0,7582	0	24	0	0	0	0
	9578	1	0,8046	0,7498	0,5144	0,7464	2	23	0	0	0	0
	10585	1	0,8081	0,7460	0,5113	0,7451	4	22	0	0	0	0
	11450	1	0,8123	0,7412	0,5083	0,7438	6	21	0	0	0	0
	12189	1	0,8180	0,7355	0,4985	0,7400	8	20	0	0	0	0
OCTAGON	15608	1	0,6267	0,8051	0,6087	0,7445	0	0	16	0	0	0
	16116	1	0,6997	0,8006	0,5364	0,7404	0	12	8	0	0	0
	16150	1	0,7265	0,7953	0,5400	0,7474	0	15	6	0	0	0
	16167	1	0,7551	0,7857	0,5236	0,7466	0	18	4	0	0	0
	16174	1	0,7814	0,7735	0,5339	0,7537	0	21	2	0	0	0
	16176	1	0,8119	0,7557	0,5375	0,7578	0	24	0	0	0	0
	17338	1	0,8053	0,7573	0,4944	0,7410	2	23	0	0	0	0
CIRCLE	23368	1	0,6265	0,8044	0,6021	0,7422	0	0	16	0	0	0
	23876	1	0,6999	0,8013	0,5364	0,7406	0	12	8	0	0	0
	23910	1	0,7264	0,7961	0,5334	0,7453	0	15	6	0	0	0
	23927	1	0,7534	0,7879	0,5303	0,7490	0	18	4	0	0	0
	23934	1	0,7820	0,7756	0,5339	0,7543	0	21	2	0	0	0
	23935	1	0,7708	0,7728	0,5106	0,7426	0	22	0	1	0	0
	23936	**1**	**0,8099**	**0,7601**	**0,5442**	**0,7608**	**0**	**24**	**0**	**0**	**0**	**0**

Table 5.7 - Individual desirability values and overall desirability for geometrical solutions called "winners" among 31040 varying-angle structures of the 168-m tall building ($r_\delta = r_\varphi = r_M = r_{CI} = 1$). In **bold** the optimal solution

The previous analysis is referred to the case where all response variables have same weight, i.e. $r_\delta = r_\varphi = r_M = r_{CI} = 1$. As follows, the parametric analysis is performed considering a variation of r_p from 0.25 to 2 with a step of 0.25, leading to a total of 4096 combinations, which are already reported in Table 4.3. In this way it is possible to highlight the influence of weight exponents on the selection of the "winners". Note that for each combination the optimal solution among 31040 structures with the highest OD value is always identified, then the "winners" with OD value not different of 2%

compared to the maximum value will be selected. The results of the parametric analysis are reported in Figure 5.11 in terms of the probability of occurrence of each diagrid geometry. It can be seen that the desirability function selects a total of 3415 "winners" out of 31040 structures and the four geometries that appear to be the most desirable ones in most combinations are, in descending order: #23936 in 3616 cases, which is related to the uniform-angle circular structure made up of triangular unit of two intra-module floors ($M_2 = 24, M_j \neq 0$ for $j \neq 2$); #8416 in 3496 cases, which is referred to the uniform-angle hexagonal structure with two-intra module floors; #16176 in 3456 cases, which corresponds to the uniform-angle octagonal structure with always two intra-module floors; lastly, #654 in 3408 cases, which is related to the varying-angle square structure with $M_2 = 21, M_3 = 2, M_j \neq 0$ for $j \neq 2,3$. Moreover, based on the obtained results, other geometries with similar diagrid pattern provide slightly lower probability of occurrence than the previous ones and they are in descending order: #23934 in 3464 cases, which is related to the varying-angle circular structure with $M_2 = 21, M_3 = 2, M_j \neq 0$ for $j \neq 2,3$; #16174 in 3440 cases, which corresponds to the varying-angle octagonal structure with $M_2 = 21,\ M_3 = 2, M_j \neq 0$ for $j \neq 2,3$; #8414 in 3368 cases, which corresponds to the varying-angle hexagonal structure with $M_2 = 21,\ M_3 = 2, M_j \neq 0$ for $j \neq 2,3$; lastly, #656 in 3200 cases, which corresponds to the uniform-angle square structure with $M_2 = 24, M_j \neq 0$ for $j \neq 2$. In any case no geometrical solution is the optimal or "winner" in all 4096 combinations.

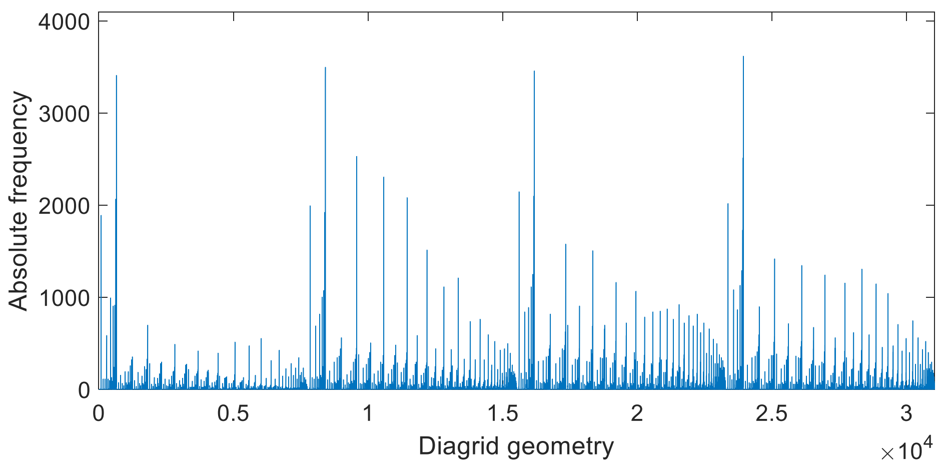

Figure 5.11 - "Winners" diagrid geometries based on 4096 combinations with different exponents r_p for the 168-m tall building

The other "winners" are mainly referred to varying-angle structures, i.e. 3407 geometries out of 3415, whereas there are only four uniform-angle structures with three intra-module floors as "winners" besides the previous four three intra-module floors solutions. Most of the varying-angle structures (2246 out of 3415) are made up of diagonals with inclination ranging from 35°-38° at upper modules, corresponding to one intra-module floor, to 70°-72° at lower modules, corresponding to four intra-module floors. The relative probability of occurrence varies from 8 to 2528. However, few solutions have steeper diagonals at lower modules, namely 875 and 294 varying-angle structures with diagonal inclination of 74°-76° and 77°-78°, respectively. Moreover, for these structures the maximum value of the probability of occurrence drops to lower value of 200-240. Generally, these steep inclinations occur in maximum two or three lower modules. Another aspect to highlight is that all "winner" structures have a maximum of four different diagonal inclinations.

Finally, it can be concluded that despite in 92.91% of cases the "winners" are varying-angle structures the preference is towards the uniform-angle diagrid pattern with two intra-module floors since they return the maximum value of the overall desirability. In fact, if the analysis had been performed by selecting only the optimal solution, it would have been obtained that 95.70% of cases (3920 out of 4096 combinations) are referred to uniform-angle structures. Moreover, there is a slight preference towards plan shapes with more sides, i.e. octagonal and circular shapes, as already shown in Table 5.6 and in Figure 5.11.

Similarly, based on the analysis performed for the 48-story tall building, the desirability function approach has been applied to other buildings with different heights, i.e. 126, 210 and 252-m tall buildings, in order to identify the optimal geometry and the "winners". First of all, Figure 5.12 shows the overall desirability values for each diagrid geometry obtained by Equation (4.11) considering $r_\delta = r_\varphi = r_M = r_{CI} = 1$. It is found that the optimal geometry is respectively #4908 solution corresponding to the uniform-angle octagonal structure made up of three intra-module floors with $OD = 67.04\%$ for the 36-story tall building, #41107 solution corresponding to the uniform-angle octagonal structure made up of two intra-module floors with $OD = 78.02\%$ for the 60-story tall building and #46370 solution corresponding to the uniform-angle hexagonal structure made up of two intra-module floors with OD =75.02% for the 72-story tall building. Also in these cases, it is evident the slight effect of the plan shape on the overall desirability, as shown graphically in Figure 5.12. In all three different heights the statistical distribution of the overall desirability is alike to Gaussian distribution. Also in this case "winners" are selected and the results are reported in Table 5.8 in terms of individual desirability for each response variable, overall desirability and combinations of triangular units. The results are similar to the ones obtained for the 168-m tall building. In fact, the "winners" among varying-angle structures have a maximum of two different diagonal inclinations lying between 35° at upper modules and 65° at lower modules. In addition, the overall desirability values of uniform-angle structures with two and three intra-module floors are very close since the difference is lower than 2%.

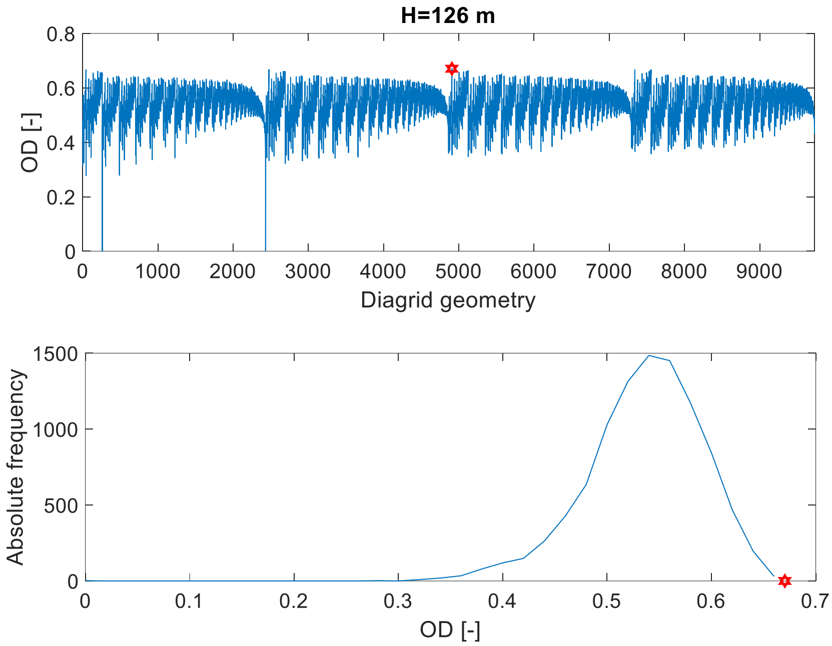

(a)

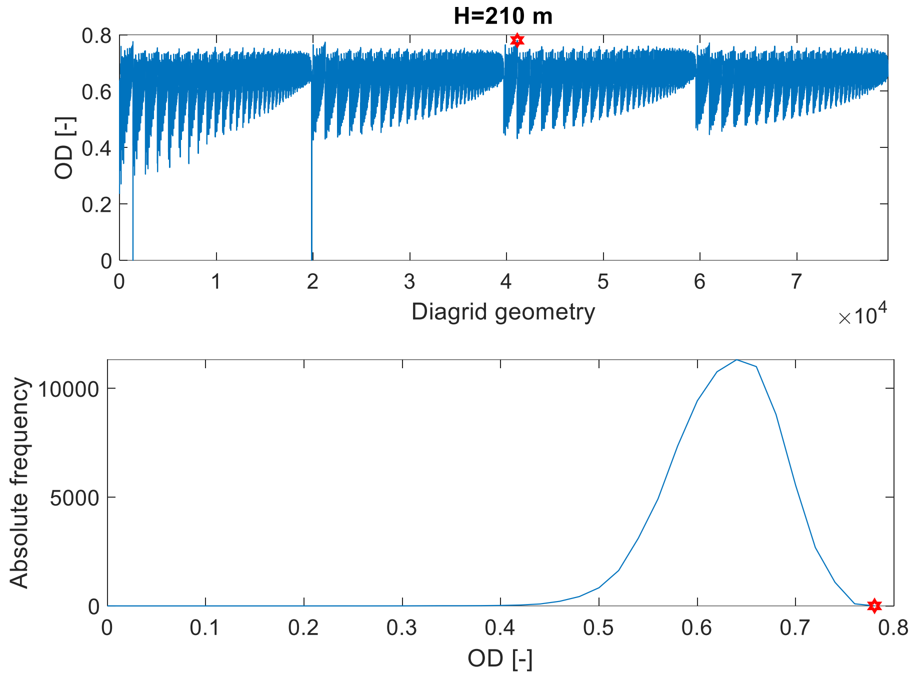

(b)

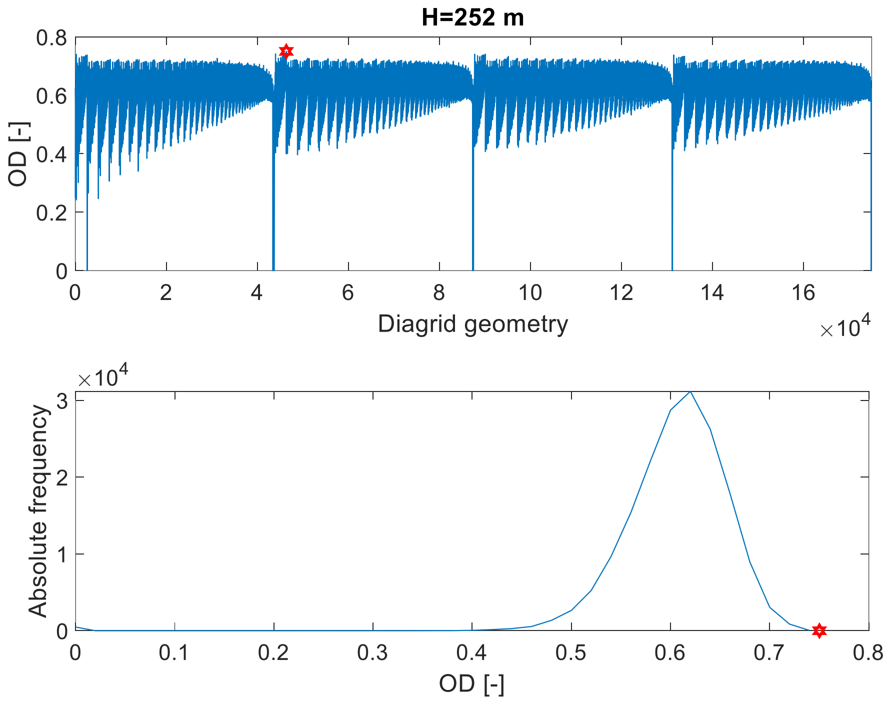

(c)

Figure 5.12 – Desirability function results in terms of the overall desirability values and its relative statistical distribution for each diagrid geometry in case of $r_\delta = r_\varphi = r_M = r_{CI} = 1$: (a) the 126-m tall building with 9728 geometries (b) the 210-tall building with 79432 geometries (c) the 252-m tall building with 175008 geometries. The optimal solution is highlighted with a red star

H=126 m												
	#solution	d_δ $[-]$	$d_\varphi[-]$	$d_M[-]$	$d_{CI}[-]$	OD $[-]$	M_1	M_2	M_3	M_4	M_5	M_6
SQUARE	44	0,7038	0,7129	0,6467	0,6088	0,6667	0	0	12	0	0	0
	140	0,6865	0,7012	0,6681	0,5713	0,6547	0	3	10	0	0	0
	200	0,6961	0,7319	0,6499	0,5756	0,6607	0	6	8	0	0	0
	234	0,7040	0,7620	0,6304	0,5465	0,6557	0	9	6	0	0	0
	251	0,7060	0,7901	0,6123	0,5424	0,6560	0	12	4	0	0	0
	258	0,7058	0,8195	0,5867	0,5466	0,6563	0	15	2	0	0	0
	260	0,6973	0,8465	0,5598	0,5425	0,6507	0	18	0	0	0	0
HEXAGON	2476	0,6924	0,7183	0,6550	0,6088	0,6673	0	0	12	0	0	0
	2572	0,6690	0,7024	0,6823	0,5713	0,6542	0	3	10	0	0	0
	2632	0,6797	0,7328	0,6688	0,5589	0,6569	0	6	8	0	0	0
	2666	0,6934	0,7659	0,6469	0,5548	0,6607	0	9	6	0	0	0
	2683	0,6987	0,7952	0,6296	0,5424	0,6600	0	12	4	0	0	0
	2690	0,7047	0,8261	0,6029	0,5299	0,6567	0	15	2	0	0	0
	2692	0,6977	0,8515	0,5805	0,5509	0,6602	0	18	0	0	0	0
OCTAGON	**4908**	**0,6913**	**0,7192**	**0,6582**	**0,6171**	**0,6704**	**0**	**0**	**12**	**0**	**0**	**0**
	5004	0,6710	0,7069	0,6822	0,5713	0,6557	0	3	10	0	0	0
	5064	0,6844	0,7382	0,6674	0,5589	0,6589	0	6	8	0	0	0
	5098	0,6957	0,7695	0,6486	0,5465	0,6600	0	9	6	0	0	0
	5115	0,7009	0,7979	0,6327	0,5424	0,6619	0	12	4	0	0	0
	5122	0,7024	0,8257	0,6132	0,5299	0,6589	0	15	2	0	0	0
	5124	0,7000	0,8529	0,5883	0,5509	0,6632	0	18	0	0	0	0
	5567	0,6699	0,8345	0,6259	0,5134	0,6510	2	17	0	0	0	0
CIRCLE	7340	0,6817	0,7134	0,6649	0,6088	0,6661	0	0	12	0	0	0
	7436	0,6565	0,6974	0,6922	0,5713	0,6523	0	3	10	0	0	0
	7496	0,6684	0,7279	0,6797	0,5589	0,6557	0	6	8	0	0	0
	7530	0,6847	0,7636	0,6572	0,5548	0,6608	0	9	6	0	0	0
	7547	0,6921	0,7935	0,6414	0,5507	0,6637	0	12	4	0	0	0
	7554	0,6963	0,8231	0,6215	0,5466	0,6643	0	15	2	0	0	0
	7555	0,6944	0,8099	0,6163	0,5161	0,6503	0	16	0	1	0	0
	7556	0,6932	0,8507	0,6009	0,5592	0,6672	0	18	0	0	0	0

	H=210 m											
	#solution	d_δ [−]	d_φ[−]	d_M[−]	d_{CI}[−]	OD [−]	M_1	M_2	M_3	M_4	M_5	M_6
SQUARE	1331	1	0,7521	0,8529	0,5231	0,7611	0	18	8	0	0	0
	1365	1	0,7721	0,8468	0,5207	0,7638	0	21	6	0	0	0
	1382	1	0,7956	0,8368	0,5120	0,7641	0	24	4	0	0	0
	1389	1	0,8134	0,8269	0,5095	0,7651	0	27	2	0	0	0
	1391	1	0,8358	0,8120	0,5341	0,7759	0	30	0	0	0	0
HEXAGON	20013	1	0,6634	0,8662	0,5962	0,7651	0	0	20	0	0	0
	21129	1	0,7384	0,8615	0,5319	0,7627	0	15	10	0	0	0
	21189	1	0,7574	0,8577	0,5356	0,7680	0	18	8	0	0	0
	21223	1	0,7779	0,8519	0,5144	0,7641	0	21	6	0	0	0
	21240	1	0,7998	0,8433	0,5120	0,7666	0	24	4	0	0	0
	21247	1	0,8170	0,8352	0,5033	0,7655	0	27	2	0	0	0
	21249	1	0,8366	0,8230	0,5216	0,7742	0	30	0	0	0	0
OCTAGON	39871	1	0,6604	0,8687	0,5962	0,7647	0	0	20	0	0	0
	40891	1	0,7187	0,8664	0,5406	0,7617	0	12	12	0	0	0
	40987	1	0,7379	0,8643	0,5256	0,7609	0	15	10	0	0	0
	41047	1	0,7579	0,8607	0,5294	0,7666	0	18	8	0	0	0
	41081	1	0,7770	0,8555	0,5082	0,7624	0	21	6	0	0	0
	41098	1	0,7998	0,8478	0,5182	0,7699	0	24	4	0	0	0
	41105	1	0,8164	0,8402	0,5033	0,7665	0	27	2	0	0	0
	41107	**1**	**0,8373**	**0,8286**	**0,5341**	**0,7802**	**0**	**30**	**0**	**0**	**0**	**0**
	54639	1	0,8573	0,8107	0,4811	0,7604	16	22	0	0	0	0
CIRCLE	59729	1	0,6644	0,8684	0,5837	0,7618	0	0	20	0	0	0
	60905	1	0,7589	0,8605	0,5169	0,7622	0	18	8	0	0	0
	60939	1	0,7791	0,8556	0,5082	0,7629	0	21	6	0	0	0
	60956	1	0,7972	0,8505	0,4995	0,7628	0	24	4	0	0	0
	60963	1	0,8145	0,8427	0,4970	0,7643	0	27	2	0	0	0
	60965	1	0,8347	0,8323	0,5091	0,7712	0	30	0	0	0	0

	H=252 m											
	#solution	d_δ [−]	d_φ[−]	d_M[−]	d_{CI}[−]	OD [−]	M_1	M_2	M_3	M_4	M_5	M_6
SQUARE	249	1	0,6812	0,7610	0,5793	0,7403	0	0	24	0	0	0
	1382	1	0,6931	0,7610	0,5478	0,7331	0	6	20	0	0	0
	1764	1	0,7085	0,7594	0,5339	0,7321	0	9	18	0	0	0
	2050	1	0,7234	0,7568	0,5260	0,7326	0	12	16	0	0	0
	2257	1	0,7396	0,7520	0,5298	0,7368	0	15	14	0	0	0
	2402	1	0,7549	0,7466	0,5160	0,7344	0	18	12	0	0	0
	2498	1	0,7710	0,7390	0,5140	0,7356	0	21	10	0	0	0
	2558	1	0,7895	0,7269	0,5002	0,7319	0	24	8	0	0	0
	2592	1	0,8029	0,7164	0,5158	0,7380	0	27	6	0	0	0
	2609	1	0,8179	0,7012	0,5019	0,7325	0	30	4	0	0	0
	2616	1	0,8339	0,6821	0,4999	0,7302	0	33	2	0	0	0
	2618	1	0,8515	0,6575	0,5253	0,7364	0	36	0	0	0	0
HEXAGON	44001	1	0,6843	0,7636	0,5793	0,7418	0	0	24	0	0	0
	45516	1	0,7140	0,7616	0,5339	0,7341	0	9	18	0	0	0
	45802	1	0,7288	0,7606	0,5319	0,7369	0	12	16	0	0	0
	46009	1	0,7452	0,7571	0,5298	0,7394	0	15	14	0	0	0
	46154	1	0,7611	0,7518	0,5337	0,7434	0	18	12	0	0	0
	46250	1	0,7758	0,7465	0,5257	0,7428	0	21	10	0	0	0
	46310	1	0,7910	0,7379	0,5296	0,7456	0	24	8	0	0	0
	46344	1	0,8087	0,7253	0,5216	0,7437	0	27	6	0	0	0
	46361	1	0,8213	0,7134	0,5314	0,7470	0	30	4	0	0	0
	46365	1	0,8112	0,7105	0,5091	0,7360	0	32	0	2	0	0
	46368	1	0,8394	0,6954	0,5058	0,7371	0	33	2	0	0	0
	46369	1	0,8322	0,6963	0,4947	0,7317	0	34	0	1	0	0
	46370	**1**	**0,8504**	**0,6785**	**0,5488**	**0,7502**	**0**	**36**	**0**	**0**	**0**	**0**
OCTAGON	87753	1	0,6838	0,7671	0,5734	0,7406	0	0	24	0	0	0
	88388	1	0,6859	0,7686	0,5557	0,7357	0	3	22	0	0	0
	88886	1	0,6971	0,7684	0,5360	0,7320	0	6	20	0	0	0
	89268	1	0,7120	0,7673	0,5339	0,7349	0	9	18	0	0	0
	89554	1	0,7270	0,7657	0,5319	0,7377	0	12	16	0	0	0
	89761	1	0,7429	0,7626	0,5240	0,7381	0	15	14	0	0	0
	89906	1	0,7593	0,7586	0,5101	0,7363	0	18	12	0	0	0
	90002	1	0,7747	0,7531	0,5081	0,7379	0	21	10	0	0	0
	90062	1	0,7898	0,7451	0,4943	0,7344	0	24	8	0	0	0
	90096	1	0,8065	0,7342	0,4981	0,7370	0	27	6	0	0	0
	90113	1	0,8202	0,7226	0,4902	0,7342	0	30	4	0	0	0
	90120	1	0,8375	0,7064	0,4881	0,7331	0	33	2	0	0	0
	90122	1	0,8491	0,6905	0,5135	0,7408	0	36	0	0	0	0
	95169	1	0,6724	0,7672	0,5595	0,7330	3	0	23	0	0	0

(Continue…)

	#solution	d_δ [−]	d_φ[−]	d_M[−]	d_{CI}[−]	OD [−]	M_1	M_2	M_3	M_4	M_5	M_6
CIRCLE	131505	1	0,6810	0,7677	0,5676	0,7381	0	0	24	0	0	0
	132638	1	0,6988	0,7674	0,5301	0,7302	0	6	20	0	0	0
	133306	1	0,7295	0,7653	0,5143	0,7320	0	12	16	0	0	0
	133513	1	0,7471	0,7612	0,5063	0,7325	0	15	14	0	0	0
	133658	1	0,7625	0,7572	0,4984	0,7324	0	18	12	0	0	0
	133754	1	0,7770	0,7524	0,4905	0,7318	0	21	10	0	0	0
	133814	1	0,7908	0,7464	0,4884	0,7327	0	24	8	0	0	0
	133848	1	0,8055	0,7374	0,4805	0,7309	0	27	6	0	0	0
	133874	1	0,8479	0,6962	0,4900	0,7334	0	36	0	0	0	0

Table 5.8 - Results of the desirability function for optimal solution and "winners" of the three buildings. The optimal solution is in **bold**

Once the analysis based on the desirability function is carried out considering the same weight of the four response variables, the parametric analysis is performed as well with the 4096 combinations of Table 4.3. The results for the three buildings are shown in Figure 5.13 in terms of probability of occurrence.

Regarding the 126-m tall building, a total of 1305 “winners” have been selected and among these the geometrical solutions with greatest probability of occurrence are in descending order: #4908 in 3528 cases, #2476 in 3405 cases, #44 in 3318 cases and #7340 in 3312 cases, as evident in Figure 5.13a. All of them correspond to the uniform-angle diagrid pattern made up of triangular units of three intra-module floors with octagonal, hexagonal, square and circular plan, respectively. Of course, also in this case, most of “winners” are varying-angle geometries. Specifically, 904 of them have a maximum diagonal inclination at base module lower than 72° corresponding to four intra-module floors, whereas it is lower than 76° and 78°, corresponding to five and six intra-module floors, respectively for 316 and 77 structures. For the latter the probability of occurrence is lower than 244. Finally, the uniform-angle pattern turns out to be the optimal one in 93% of cases (3808 out of 4096 combinations). Note that the geometrical solutions with greater number of modules made up of one intra-module floor are not among the “winners” due to high construction complexity and greatest structural mass.

As far as the 210-m tall building is concerned, similar considerations can be made. In particular, the first four geometries that result being the most preferable ones among 6805 “winners” in most combinations, as shown in Figure 5.13b, are in descending order: #41107 in 3617 cases, #1391 in 3465 cases, #21249 in 3377 cases and #60965 in 3193 cases. These solutions are referred to the uniform-angle diagrid pattern made up of triangular units of two intra-module floors with octagonal, square, hexagonal and circular plan shape, respectively. Also in this case, most of "winners" among varying-angle structures (3937 out of 6805) are made up of lower modules composed by a maximum of four intermediate floors, whereas the remaining 2857 structures are characterized by steeper diagonal at the base. Note that in 272 cases the one intra-module floor geometry results to be "winner" when greater weight is given to the top torsional rotation. In this case, 95.90% of the combinations returns the uniform-angle pattern as the optimal geometry.

Regarding the 252-m tall building, the parametric analysis returns 14746 "winners" out of 175008 diagrid structures. It is found that the four peaks relative to each floor plan shape, as shown in Figure 5.13c, correspond to #46361, #90122, #87753 and #131505 solutions. These structures result to be preferable in 3480, 2840, 2520 and 2392 cases, respectively. Moreover, it can be noted that #46361 solution has a varying-angle pattern made up of modules constituted by two and three floors ($M_2 = 30, M_3 = 4, M_j = 0$ for $j \neq 1,4,5,6$), whereas the other three geometries are referred to the uniform-angle population. Specifically, #90122 is the square structure made up of two intra-module floors, #87753 is the octagonal structure made up of three intra-module floors and #131505 is the circular structure made up of three intra-module floors. Also in this case, varying-angle structures with steep diagonals at the base lower than 72° are preferable in most combinations. In this case, 85.55% of the combinations returns the uniform-angle pattern as the optimal geometry.

Finally, it can be concluded that the influence of the weight exponent is very slight as in most combinations the most desirable geometry is always the same, i.e. the two intra-module floors geometry for tall buildings with slenderness greater than 5 and the three intra-module floors one for lower slenderness. Moreover, it can be observed that the shift from three intra-module floors for the 126-m tall building to two intra-module floors for the other three buildings is caused by the simultaneous minimization of the four response variables. In particular, it was found that the top lateral deflection influences the selection of the optimal solution for less slender structure, whereas the effect disappears for slender structure.

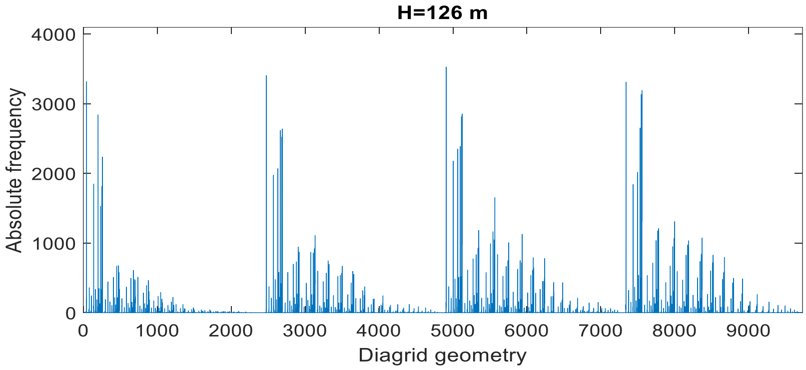

(a)

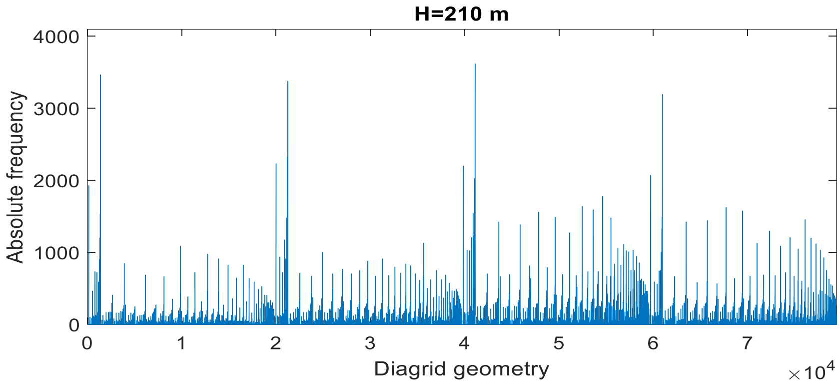

(b)

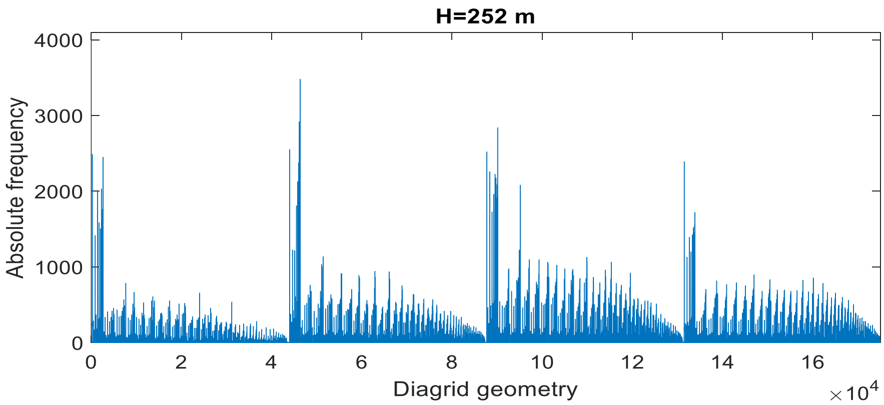

(c)

Figure 5.13 - Results of the parametric analysis in terms of probability of occurrence considering 4096 combinations: (a) the 126-m tall building with 9728 geometries (b) the 210- tall building with 79432 geometries (c) the 252-m tall building with 175008 geometries

5.4. COMPUTATIONAL COST

In case of varying-angle structures it has been found that the number of geometries to be analysed through the strength- and stiffness-based preliminary design and the desirability function is huge, especially for the 252-m tall building. In fact, based on the values reported in Table 5.1, it is clear that all the analyses have lasted a significant time and therefore the concept of computational cost has to be introduced. Now, attention is paid on how much time the preliminary design occurs. Figure 5.14 shows graphically the time needed to carry out the preliminary design of each geometry. It is evident again that the trend is mainly influenced by the diagonal inclination rather by the floor plan shape since it is repetitive. Moreover, it can be seen that the time increases with the number of modules made up of only one intra-module floor as a higher number of diagonals has to be checked in terms of strength and stiffness. In particular, the graphs related to the 210- and 252-m tall buildings show that the uniform-angle diagrid solutions with one intra-module floor represent a particular condition since the preliminary design takes an outlier time. Specifically, in the case of the 60-story building the #19858, #39716, #59574 and #79432 solutions have been analysed respectively in 135, 49, 45 and 41 seconds, whereas in the case of the 72-story building the #43752, #87504, #131256 and #175008 solutions have been analysed respectively in 213, 242, 219 and 244 seconds. Note that all these geometries are made up of one intra-module floor, demonstrating their unsatisfactory performance.

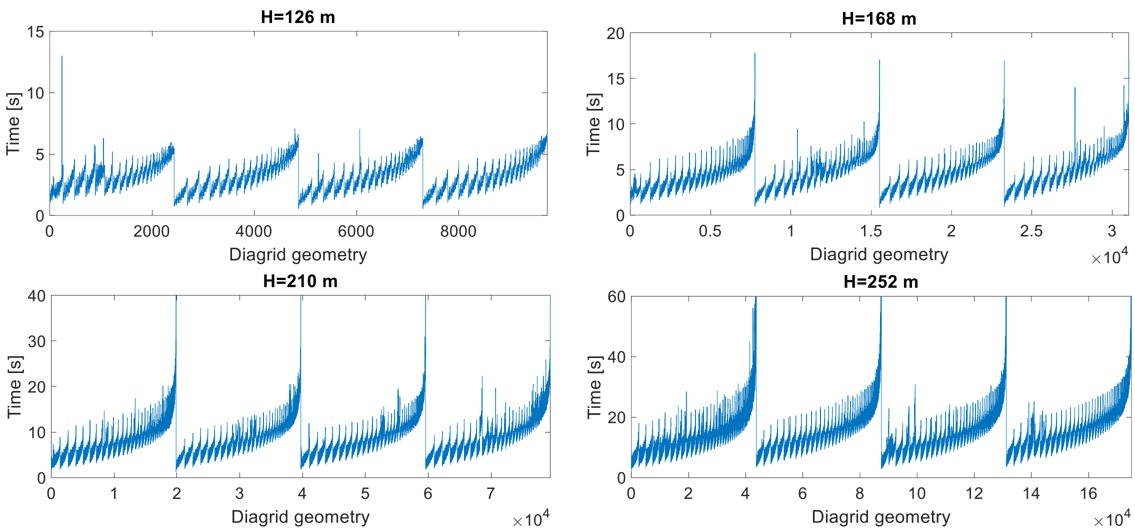

Figure 5.14 – Computational cost of the preliminary design for each diagrid geometry and for each building height

The main aspect that has to be pointed out is related to the effect of the building height. The results are reported in Table 5.9: the second and third columns are related to the maximum and the minimum values of time occurred, the fourth column is referred to the mean value and the remaining two columns are referred to the total time needed to perform the preliminary design for a given building height, changing diagonal inclination and floor plan shape. From the fourth column it can be noted that an entire diagrid structure is designed in the preliminary stage according to stiffness and strength criterion on average around 3, 5, 8 and 15 seconds for the 126-, 168-, 210- and 252-m tall buildings, respectively. This aspect highlights the computational speed of the preliminary design since these values are referred to an analysis that performs hundreds and thousands of iterations for each structure. Regarding the total time needed to perform the analysis, in case of the 72-story tall building, the preliminary design seems to take a long time, almost one month, because the number of analysed diagrid structures is very large, namely 175008 structures. Moreover, from the values of total time, it is found that the transition from one tall building to the slender one the total time increases of about from 4 to 4.7 times. For each height of the building the coefficient of variation (CV) among all geometries has been assessed and it is found that it is equal to 37.06%, 38.60%, 44.35% and 71.65% for the 36-, 48-, 60- and 72-story tall buildings, respectively. However, the required time to perform the preliminary design depends on specifications of the employed computer. In this case a computer, characterized by Intel Core i3 CPU 2.40 GHz as processor, has been used.

H [m]	max [s]	min [s]	mean [s]	total	
				[h]	[gg]
126	12,98	0,532	3,09	8	0,35
168	17,78	0,858	4,54	39	1,63
210	135,04	1,369	8,25	182	7,59
252	244,24	2,861	14,66	713	30

Table 5.9 – Computational cost of the preliminary design for each building height

The results demonstrate the efficiency of the matrix-based method (MBM) for the preliminary design of diagrid structures as it is able to analyse many structures in limited time. Conversely, if this study had been carried out manually or within a Finite Element Method (FEM) environment, it would have been much more difficult. However, once the optimal geometry is identified, FEM is necessary to design the structure in detail

Chapter 6

6. CONCLUSIONS

This Thesis investigates the role of some geometrical features, e.g. diagonal inclination and floor plan shape, in the preliminary design stage of a diagrid structure, expected to exhibit efficient structural behaviour (in terms of lateral and torsional stiffness), lightness and ease of construction. To this purpose, the procedure developed in this work consisted of a preliminary structural analysis by means of the matrix-based method (MBM) and a posteriori multi-response optimization process based on the desirability function approach. In particular, once strength- and stiffness-based preliminary design has been performed for each diagrid geometry, the four response variables, i.e. top lateral deflection, top torsional rotation, structural mass and complexity index, have been assessed. The complexity index (CI) is a parameter referred to the construction complexity evaluated in function of number of nodes, number of diagonals, number of diagonals with length greater than 12 m, number of different diagonal cross-sections and number of different diagonal lengths. After, the desirability function approach has been applied. It consists into the evaluation of the overall desirability (OD) for each diagrid geometry by combining the individual desirability values related to each response variable. Finally, it was possible to select the optimal diagrid geometry as the one with the greatest value of the overall desirability (OD).

This methodology has been applied to a set of uniform- and varying-angle diagrid structures, by considering firstly the four response variables with the same weight. In order to point out the main outcomes, it is necessary to distinguish the populations out of which the optimal geometry was selected, namely unifom- and varying-angle diagrid structures.

In both cases, it is evident that the influence of the floor plan shape is almost negligible, whereas the diagonal inclination has a major effect on the selection of the least and the most desirable geometries. As a matter of fact, it was found that the worst geometries are the ones with very shallow or very steep diagonals, because of excessive lateral displacement under wind loads, large amount of structural mass and excessive torsional rotation.

Regarding the best geometry, in the case of the uniform-angle population, the optimal diagrid geometry is always provided by diagonals with inclination around 65°, corresponding to diagonals spanning over three floors per module. This result was found to be independent from the height of the building. Conversely, in case of the varying-angle population, the optimal diagrid geometries are found towards shallower diagonals around 55°, corresponding to diagonals including two intra-module floors. This difference is due to the following reasons. Firstly, the desirability function approach minimizes simultaneously several response variables, which are taken into account differently when considering the uniform- or varying-angle population. Secondly, the variation of the OD value between geometries with two and three intra-module floors is almost negligible, as lower as 2%, therefore both solutions can be considered optimal in both populations. Lastly, in the varying-angle population, the maximum diagonal inclination is about 78°, corresponding to diagonals spanning over six floors, whereas in the uniform-angle population steeper diagonals (83°), corresponding to twelve intra-module floors, were also considered. Therefore, the reduction of the maximum diagonal angle in the varying-angle population has led to a slight preference towards diagrid structures made up of two intra-module floors, providing a better torsional behaviour. Moreover, considering a wider population led to different values of the individual desirability for the top torsional rotation, the structural mass and the complexity index.

Further investigation has been carried out by performing the parametric analysis. Based on the results, although the optimal geometry is always the same for most weight combinations, in other cases the optimal diagrid solution is different as it depends on the weight given to each response variable. For this reason, it is important to define the importance of each parameter and the choice is expected to the designer.

Some considerations on the advantages and limits of the proposed methodology can also be made. Firstly, the procedure employed, i.e. the MBM coupled with the desirability function, allows to analyse a wide population of structures in relatively short time and within the same computational environment. As a matter of fact, in this Thesis a total of

295304 diagrid structures have been investigated in two months and a half considering both uniform- and varying-angle structures. Both the input phase, pre-processing, analysis and post-processing of data has been entirely carried out in Matlab, without the aid of additional external softwares. Conversely, other methodologies available nowadays, such as the Finite Element Method (FEM), do not ensure the same computational cost as they would take much longer time. Moreover, they often require the user to have specific codes to be developed to have a proper interface with the FE software. All these aspects represent one of the most significant advantages of the proposed methodology.

However, there are also some limitations. As a matter of fact, the MBM is a modular method based on simplifications that lead to neglect the interstory drifts, and it is based on the linear elastic analysis, therefore it neglects the non-linear and dynamic behaviour of the structure. Although this procedure is valid for the preliminary design, the applicability of this method to further design stages might be not recommended. As far as the limitation of the desirability function is concerned, it was found that the optimal diagrid geometry depends on the analysed population since this approach is a post-optimization process based on the comparison of all structures.

Finally, the proposed procedure can also be generalized in future research. In this Thesis attention has been paid on specific diagrid structures with certain geometrical parameters, i.e. diagonal inclination, floor plan shape and building height, in order to guarantee structural performance, in terms of top lateral deflection and top torsional rotation, lightness and constructability. Of course, the designer or the researcher is totally free to choose other features to be studied. As an example, it is possible to consider not only cylindrical envelopes for the exterior of the building, but also different shapes obtained from tapering, twisting and tilting modifications. Since the geometric configuration of the form can strongly influence the system's efficiency [51], this is expected to have a certain influence on the results. Similarly, other or different response variables can also be chosen to be fed to the desirability function. The choice can fall on several variables, depending on aesthetical, economical, energetical and architectural considerations. Moreover, further study can be done by coupling the desirability function approach with the Genetic Algorithm, remembering that both are used to investigate the optimal diagrid geometry. In particular, the desirability function approach is a multi-response optimization process that selects the optimal geometry by comparing the OD values of different individuals in a population. Conversely, the Genetic Algorithm identifies the optimal solution by combinations and alterations of initial geometrical parameters from a starting population until reaching the convergence towards the optimal one. In order to coupled them, one could then use the OD value as objective function of a Genetic Algorithm environment, where several response variables are then taken into account simultaneously.

In conclusion, it can be said that the computational procedure presented here for the selection of the optimal diagrid geometry, based on the MBM and the desirability function approach, is an efficient, innovative and easy way to treat the problem. It also represents a valid tool for designers and researchers to design diagrid structures in the preliminary stage.

BIBLIOGRAPHY

[1] B. S. Smith and A. Coull, Tall building structures: analysis and design, 1991.

[2] M. M. Ali and K. S. Moon, “Structural developments in tall buildings: current trends and future prospect,” *Architectural Science Review,* vol. 50, no. 3, pp. 205-223, 2007.

[3] M. M. Ali and K. S. Moon, “Advances in structural system for tall buildings: emerging developments for contemporary urban giants,” *Buildings,* 2018, 8, 104.

[4] K. S. Moon, J. J. Connor and J. E. Fernandez, “Diagrid structural systems for tall buildings: characteristics and methodology for preliminary design,” *The Structural design of tall and Special Buildings 16.2,* pp. 205-230, 2007.

[5] S. Korsavi and M. R. Maqhareh, “The evolutionary process of diagrid structure towards architectural, structural and sustainability concepts: reviewing case studies,” *Journal of Architectural Engineering Technology,* vol. 2, no. 2, pp. 1-11, 2014.

[6] D. Munro, “Swiss Re’s building, London,” *Nyheter om Stalbyggnad,* pp. 36-43, 2004.

[7] R. Plank, “Swiss Re London,” *Architecture Steel Stahl Acier,* pp. 1-16, 2005.

[8] A. Rahimian and Y. Eilon , “New York's Hearst Tower,” *Structure Magazine February,* pp. 25-29, 2006.

[9] A. Rahimian and Y. Eilon, "Hearst Headquarters: innovation and heritage in harmony," in *CTBUH 8th World Congress*, 2008.

[10] D. Scaramozzino, G. Lacidogna and A. Carpinteri, "New trends towards enhanced structural efficiency and aesthetic potential in tall buildings: the case of Diagrids," *Applied Sciences,* pp. 10 (11), 3917, 2020.

[11] C. Liu, Q. Li, Z. Lu and H. Wu, "A review of the diagrid structural system for tall buildings," *Struct Design Tall Spec Build.,* 2018;27:e1445.

[12] E. Asadi and H. Adeli, "Diagrid: An innovative, sustainable, and efficient structural," *Struct Design Tall Spec. Build.,* 2017;26:e1358.

[13] S. Premdas and M. Sirajuddin, "Diagrid structural system for tall buildings: state of the art review," *International Research Journal of Engineering and Technology (IRJET),* vol. 6, pp. 3406-3410, 2019.

[14] G. M. Montuori, E. Mele, G. Brandonisio and A. De luca, "Design criteria for diagrid tall buildings: Stiffness versus strength," *Struct. Design Tall Spec. Build.,* vol. 23, pp. 1294-1314, 2014.

[15] K. S. Moon, "Sustainable structural engineering strategies for tall buildings," *Struct. Design Tall Spec. Build.,* vol. 17, pp. 895-914, 2008.

[16] G. M. Montuori, E. Mele, G. Brandonisio and A. De Luca, "Secondary bracing systems for diagrid structures in tall buildings," *Eng. Struct.,* vol. 75, pp. 477-488, 2014.

[17] E. Mele, "Diagrid: The renaissance of steel structures for tall buildings geometry, design, behaviour," *Ce/Papers,* vol. 1, pp. 4437-446, 2017.

[18] E. Mele, M. Imbimbo and V. Tomei, "The effect of slenderness on the design of diagrid structures," *Int. J. High Rise Build.,* vol. 8, pp. 83-94, 2019.

[19] W. Guo and J. Teng, “Mechanical property research on high-rise diagrid tube,” *Journal of Xi'an Univ. Archit. Technol. (Natural Science Edition),* 2010, 42(2), 174.

[20] C. Liu and K. Ma, “Calculation model of the lateral stiffness of high-rise diagrid tube structures based on the modular method,” *Struct. Design Tall Spec. Build.,* 2017;26:e1333.

[21] G. Lacidogna, D. Scaramozzino and A. Carpinteri, “A matrix-based method for the structural analysis of diagrid systems,” *Eng. Struct.,* pp. 340-352, 2019.

[22] X. J. Zhou, L. Chen and H. Qu, “Effects of layout of braces for multistory and high-rise steel structures on lateral stiffness of frames,” *Steel Construction,* vol. 18(4), pp. 51-54, 2003 (in Chinese).

[23] C. Zhang, F. Zhao and Y. Liu, “Diagrid tube structures composed of straight diagonals with gradually varying angles,” *Struct. Design Tall Spec. Build.,* vol. 21, pp. 283-295, 2012.

[24] F. Zhao and C. Zhang, “Diagonal arrangements of diagrid tube structures for preliminary design,” *Struct. Design Tall Spec. Build.,* vol. 24, pp. 159-175, 2015.

[25] G. M. Montuori, E. Mele, G. Brandonisio and A. De Luca, “Geometrical patterns for diagrid buildings: Exploring alternative design strategies from the structural point of view,” *Eng. Struct.,* vol. 71, pp. 112-127, 2014.

[26] G. Angelucci and F. Mollaioli, “Diagrid structural system for tall buildings: Changing pattern configuration through topological assessments,” *Struct. Design Tall Spec. Build.,* 2017;26:e:1396.

[27] V. Tomei, M. Imbimbo and E. Mele, "Optimization of structural patterns for tall buildings: The case of diagrid," *Eng. Struct.,* vol. 171, pp. 280-297, 2018.

[28] S. Mirniazmandan, M. Alaghmandan, F. Barazande and E. Rahimianzarif, "Mutual effect of geometric modifications and diagrid structure on structural optimization of tall buildings," *Archit. Sci. Rev.,* vol. 61, no. 6, pp. 371-383, 2018.

[29] G. Lacidogna, D. Scaramozzino and A. Carpinteri, "Influence of the geometrical shape on the structural behavior of diagrid tall buildings under lateral and torque actions," *Dev. Built. Environ.,* 2020, 2, 100009.

[30] G. Lacidogna, D. Scaramozzino and A. Carpinteri, "Optimization of diagrid geometry based on the desirability function approach," *Curved and Layer. Struct.,* vol. 7, pp. 139-152, 2020.

[31] A. Ardekani, I. Dabbaghchian, M. Alaghmandan, M. Golabchi, S. M. Hosseini and S. R. Mirghaderi, "Parametric design of diagrid tall buildings regarding structural efficiency," *Archit. Sci. Rev.,* vol. 63:1, pp. 87-102, 2020.

[32] F. Cascone, D. Faiella, V. Tomei and E. Mele, "A Structural Grammar Approach for the Generative Design of Diagrid-Like Structures," *Buildings,* 2021, 11, 90.

[33] T. Orhan and K. Taskin, "Automated topology design of high-rise diagrid buildings by genetic algorithm optimization," *Struct. Design Tall Spec. Build.,* 2021;30:e1853.

[34] Ashtari¸P., R. Karami and S. Farahmand-Tabar, "Optimum geometrical pattern and design of real-size diagrid structures using accelerated fuzzy-genetic algorithm with bilinear membership function," *Appled Soft Computing,* 2021, 110, 107646.

[35] B. Ekici, Z. T. Kazanasmaz, M. Turrin, M. F. Tasgetiren and I. S. Sariyildiz, "Multi-zone optimisation of high-rise buildings using artificial

intelligence for sustainable metropolises. Part 1: Background, methodology, setup, and machine learning results," *Solar energy,* vol. 224, pp. 373-389, 2021.

[36] B. Ekici, Z. T. Kazanasmaz, M. Turrin, M. F. Tasgetiren and I. Sariyildiz, "Multi-zone optimisation of high-rise buildings using artificial intelligence for sustainable metropolises. Part 2: Optimisation problems, algorithms, results, and method validation," *Solar Energy,* vol. 224, pp. 309-326, 2021.

[37] Consiglio Nazionale delle Ricerche, Istruzioni per la valutazione delle azioni e degli effetti del vento sulle costruzioni CNR-DT 207/2008.

[38] P. Mendis, T. Ngo, N. Haritos, A. Hira, B. Samali and J. Cheung, "Wind loading on tall buildings," *EJSE International,* pp. 41-53, 2007.

[39] L. Rosa, G. Tomasini, A. Zasso and A. Aly, "Wind-induced dynamics and loads in a prismatic slender building: A modal approach based on unsteady pressure measurements," *J. Wind Eng. Ind. Aerodyn.,* Vols. 107-108, pp. 118-130, 2012.

[40] ASCE, Minimum Design Loads for Buildings and Other Structures, American Society of Civil Engineers.

[41] E. Mele, M. Toreno, G. Brandonisio and A. De Luca, "Digrid structures for tall buildings: case studies and design considerations," *Struct. Design Tall Spec. Build.,* vol. 23, pp. 124-145, 2014.

[42] The European Union Per Regulation, EN 1993-1-1: Eurocode 3: Design of steel structures.

[43] A. P. Bazant and L. Cedolin, Stability of structures: elastic, inelastic, fracture and damage theories, World Scientific, 2010.

[44] A. Carpinteri, Advanced Structural Mechanics, Taylor & Francis Group, 2017.

[45] C. Bernuzzi, Progetto e verifica delle strutture in acciaio, Hoepli, 2011.

[46] Scia Engineer, Profile Library Checked Sections, 2010.

[47] E. C. Harrington, "The desirability function," *Ind. Qual. Control,* vol. 4, pp. 494-498, 1965.

[48] G. C. Derringer and R. Suich, "Simultaneous optimization of several response variables," *J. Qual. Technol.,* vol. 12, pp. 214-219, 1980.

[49] L. Vera Candioti, M. M. De Zan, M. S. Camara and H. Goicoechea, "Experimental design and multiple response optimization. Using the desirability function in analytical methods development," *Talanta,* vol. 124, pp. 123-138, 2014.

[50] D. Scaramozzino, Elastic Lattice Models: From Proteins to Diagrid Tall Buildings (Doctoral Dissertation), Turin, 2021.

[51] K. S. Moon, "Sustainable Structural Design of Contemporary Tall Buildings of Various Forms," *CTBUH 9th World Congress,* 2012.

[52] N. Gangasudan and H. Mallikaranchchi, "Predicting Wind Response of Tall Buildings Using Fluid-Structure Interaction," in *MERCon*, 2018.

[53] M. M. Ali and K. S. Moon, "Art of the Skyscraper: The genius of Fazlur Khan," *Rizzoli International Publications: New York,* 2001.

ANNEX A

Table 1. CHS cross-sections (diameter × thickness, in mm) adopted for the twenty-four uniform-angle diagrid patterns based on the strength- and stiffness-based preliminary design, for the square building with $N = 36$. Each cross-section refers to a specific diagrid module in the building. Diagrid modules are ordered from the top to the bottom, i.e. module no.1 is the top module.

Diagrid module no.	S1	S2	S3	S4	S6	S12
1	108 × 28	88.9 × 22.2	82.5 × 20	82.5 × 22.2	101.6 × 20	168.3 × 60
2	127 × 32	114.3 × 28	114.3 × 32	127 × 30	139.7 × 36	298.5 × 80
3	139.7 × 45	127 × 45	139.7 × 36	152.4 × 40	168.3 × 60	406.4 × 100
4	152.4 × 45	139.7 × 45	152.4 × 40	159 × 60	193.7 × 55	
5	168.3 × 60	152.4 × 45	168.3 × 60	177.8 × 55	219.1 × 65	
6	168.3 × 60	159 × 60	177.8 × 55	193.7 × 60	244.5 × 65	
7	177.8 × 55	168.3 × 60	193.7 × 50	219.1 × 55		
8	193.7 × 50	177.8 × 55	219.1 × 50	244.5 × 60		
9	193.7 × 50	193.7 × 50	219.1 × 55	244.5 × 65		
10	219.1 × 50	193.7 × 60	219.1 × 65			
11	219.1 × 50	219.1 × 50	244.5 × 60			
12	219.1 × 50	219.1 × 55	244.5 × 65			
13	219.1 × 55	219.1 × 65				
14	219.1 × 65	244.5 × 60				
15	244.5 × 60	244.5 × 60				
16	244.5 × 60	244.5 × 65				
17	244.5 × 60	244.5 × 80				
18	244.5 × 60	244.5 × 90				
19	244.5 × 70					
20	244.5 × 80					
21	267 × 80					
22	267 × 80					
23	267 × 80					
24	267 × 80					
25	267 × 90					
26	267 × 100					
27	273 × 100					
28	298.5 × 80					
29	298.5 × 80					
30	298.5 × 80					
31	298.5 × 90					
32	298.5 × 90					
33	323.9 × 90					
34	323.9 × 90					
35	323.9 × 90					
36	323.9 × 90					

Table 2. CHS cross-sections (diameter × thickness, in mm) adopted for the twenty-four uniform-angle diagrid patterns based on the strength- and stiffness-based preliminary design, for the hexagonal building with $N = 36$. Each cross-section refers to a specific diagrid module in the building. Diagrid modules are ordered from the top to the bottom, i.e. module no.1 is the top module.

Diagrid module no.	H1	H2	H3	H4	H6	H12
1	101.6 × 28	82.5 × 22.2	82.5 × 17.5	82.5 × 22.2	101.6 × 20	177.8 × 60
2	127 × 30	114.3 × 28	114.3 × 30	127 × 30	139.7 × 36	298.5 × 100
3	139.7 × 36	127 × 32	139.7 × 36	139.7 × 50	168.3 × 60	457 × 90
4	152.4 × 40	139.7 × 36	152.4 × 40	159 × 50	193.7 × 50	
5	159 × 45	152.4 × 40	159 × 60	177.8 × 55	219.1 × 65	

6	168.3 × 60	159 × 45	168.3 × 60	193.7 × 60	244.5 × 65	
7	177.8 × 55	168.3 × 60	193.7 × 50	219.1 × 50		
8	177.8 × 55	177.8 × 55	219.1 × 60	244.5 × 60		
9	193.7 × 50	193.7 × 50	219.1 × 55	244.5 × 60		
10	193.7 × 50	193.7 × 55	219.1 × 65			
11	219.1 × 50	219.1 × 50	244.5 × 60			
12	219.1 × 50	219.1 × 50	244.5 × 70			
13	219.1 × 50	219.1 × 65				
14	219.1 × 50	244.5 × 60				
15	219.1 × 65	244.5 × 60				
16	244.5 × 60	244.5 × 65				
17	244.5 × 60	244.5 × 80				
18	244.5 × 60	244.5 × 90				
19	244.5 × 60					
20	244.5 × 65					
21	244.5 × 80					
22	267 × 80					
23	267 × 80					
24	267 × 80					
25	267 × 80					
26	267 × 90					
27	273 × 100					
28	273 × 100					
29	298.5 × 80					
30	298.5 × 80					
31	298.5 × 80					
32	298.5 × 90					
33	298.5 × 100					
34	298.5 × 100					
35	323.9 × 90					
36	323.9 × 90					

Table 3. CHS cross-sections (diameter × thickness, in mm) adopted for the twenty-four uniform-angle diagrid patterns based on the strength- and stiffness-based preliminary design, for the octagonal building with N = 36. Each cross-section refers to a specific diagrid module in the building. Diagrid modules are ordered from the top to the bottom, i.e. module no.1 is the top module.

Diagrid module no.	O1	O2	O3	O4	O6	O12
1	101.6 × 22.2	82.5 × 20	82.5 × 17.5	82.5 × 22.2	101.6 × 20	193.7 × 55
2	127 × 30	114.3 × 28	114.3 × 28	127 × 30	139.7 × 40	323.9 × 90
3	139.7 × 36	127 × 30	139.7 × 36	139.7 × 50	177.8 × 55	457 × 100
4	152.4 × 40	139.7 × 36	152.4 × 40	159 × 50	193.7 × 60	
5	159 × 45	152.4 × 40	159 × 50	177.8 × 55	219.1 × 65	
6	168.3 × 60	159 × 45	177.8 × 55	193.7 × 55	244.5 × 70	
7	168.3 × 60	168.3 × 60	193.7 × 50	219.1 × 55		
8	177.8 × 55	177.8 × 55	219.1 × 50	219.1 × 65		
9	193.7 × 50	193.7 × 50	219.1 × 50	244.5 × 65		
10	193.7 × 50	193.7 × 55	219.1 × 65			
11	193.7 × 60	219.1 × 50	244.5 × 60			
12	219.1 × 50	219.1 × 50	244.5 × 70			
13	219.1 × 50	219.1 × 60				
14	219.1 × 50	244.5 × 60				
15	219.1 × 55	244.5 × 60				
16	219.1 × 70	244.5 × 65				
17	244.5 × 60	244.5 × 70				

18	244.5 × 60	244.5 × 90				
19	244.5 × 60					
20	244.5 × 65					
21	244.5 × 70					
22	244.5 × 90					
23	267 × 80					
24	267 × 80					
25	267 × 80					
26	267 × 80					
27	267 × 90					
28	273 × 100					
29	273 × 100					
30	298.5 × 80					
31	298.5 × 80					
32	298.5 × 80					
33	298.5 × 90					
34	298.5 × 100					
35	298.5 × 100					
36	323.9 × 90					

Table 4. CHS cross-sections (diameter × thickness, in mm) adopted for the twenty-four uniform-angle diagrid patterns based on the strength- and stiffness-based preliminary design, for the circular building with $N = 36$. Each cross-section refers to a specific diagrid module in the building. Diagrid modules are ordered from the top to the bottom, i.e. module no.1 is the top module.

Diagrid module no.	C1	C2	C3	C4	C6	C12
1	101.6 × 20	82.5 × 20	82.5 × 17.5	82.5 × 22.2	101.6 × 22.2	193.7 × 55
2	127 × 30	108 × 30	114.3 × 28	127 × 30	139.7 × 45	323.9 × 90
3	139.7 × 36	127 × 30	139.7 × 36	139.7 × 50	177.8 × 60	508 × 100
4	152.4 × 40	139.7 × 36	152.4 × 40	159 × 50	219.1 × 50	
5	152.4 × 45	152.4 × 40	159 × 50	177.8 × 55	219.1 × 70	
6	159 × 60	159 × 45	168.3 × 60	193.7 × 55	244.5 × 70	
7	168.3 × 60	168.3 × 60	193.7 × 50	219.1 × 50		
8	177.8 × 55	177.8 × 55	193.7 × 60	219.1 × 70		
9	193.7 × 50	193.7 × 50	219.1 × 50	244.5 × 65		
10	193.7 × 50	193.7 × 50	219.1 × 65			
11	193.7 × 55	219.1 × 50	244.5 × 60			
12	219.1 × 50	219.1 × 50	244.5 × 65			
13	219.1 × 50	219.1 × 55				
14	219.1 × 50	219.1 × 70				
15	219.1 × 50	244.5 × 60				
16	219.1 × 60	244.5 × 60				
17	244.5 × 60	244.5 × 70				
18	244.5 × 60	244.5 × 80				
19	244.5 × 60					
20	244.5 × 60					
21	244.5 × 65					
22	244.5 × 80					
23	244.5 × 90					
24	267 × 80					
25	267 × 80					
26	267 × 80					
27	267 × 80					
28	267 × 90					

29	267 × 100					
30	273 × 100					
31	298.5 × 80					
32	298.5 × 80					
33	298.5 × 80					
34	298.5 × 90					
35	298.5 × 100					
36	323.9 × 90					

Table 5. CHS cross-sections (diameter × thickness, in mm) adopted for the twenty-four uniform-angle diagrid patterns based on the strength- and stiffness-based preliminary design, for the square building with $N = 48$. Each cross-section refers to a specific diagrid module in the building. Diagrid modules are ordered from the top to the bottom, i.e. module no.1 is the top module.

Diagrid module no.	S1	S2	S3	S4	S6	S12
1	139.7 × 36	101.6 × 20	82.5 × 22.2	88.9 × 22.2	101.6 × 30	177.8 × 60
2	159 × 45	114.3 × 32	114.3 × 36	127 × 30	152.4 × 45	323.9 × 90
3	193.7 × 55	139.7 × 45	139.7 × 36	152.4 × 40	193.7 × 55	508 × 100
4	219.1 × 50	152.4 × 45	152.4 × 40	159 × 60	219.1 × 65	660 × 90
5	244.5 × 60	159 × 50	168.3 × 60	193.7 × 50	244.5 × 90	
6	244.5 × 65	177.8 × 60	177.8 × 55	219.1 × 50	267 × 100	
7	244.5 × 70	193.7 × 50	193.7 × 55	219.1 × 60	298.5 × 90	
8	244.5 × 80	193.7 × 55	219.1 × 50	244.5 × 60	323.9 × 100	
9	244.5 × 90	193.7 × 60	219.1 × 60	244.5 × 80		
10	267 × 90	219.1 × 60	219.1 × 70	267 × 80		
11	267 × 90	219.1 × 60	244.5 × 65	267 × 100		
12	267 × 90	219.1 × 65	244.5 × 70	298.5 × 80		
13	267 × 100	244.5 × 65	267 × 80			
14	298.5 × 90	244.5 × 70	267 × 80			
15	298.5 × 100	244.5 × 80	267 × 100			
16	298.5 × 100	244.5 × 90	273 × 100			
17	298.5 × 100	267 × 90				
18	323.9 × 90	267 × 100				
19	355.6 × 90	267 × 100				
20	355.6 × 100	273 × 100				
21	368 × 100	298.5 × 80				
22	368 × 100	298.5 × 90				
23	368 × 100	323.9 × 90				
24	368 × 100	323.9 × 100				
25	406.4 × 100					
26	419 × 100					
27	457 × 90					
28	457 × 90					
29	457 × 90					
30	457 × 90					
31	457 × 100					
32	508 × 90					
33	508 × 100					
34	508 × 100					
35	508 × 100					
36	508 × 100					
37	559 × 90					
38	610 × 90					
39	610 × 90					

40	610 × 90					
41	610 × 100					
42	610 × 100					
43	660 × 90					
44	660 × 90					
45	660 × 100					
46	660 × 100					
47	660 × 100					
48	660 × 100					

Table 6. CHS cross-sections (diameter × thickness, in mm) adopted for the twenty-four uniform-angle diagrid patterns based on the strength- and stiffness-based preliminary design, for the hexagonal building with N = 48. Each cross-section refers to a specific diagrid module in the building. Diagrid modules are ordered from the top to the bottom, i.e. module no.1 is the top module.

Diagrid module no.	H1	H2	H3	H4	H6	H12
1	127 × 36	88.9 × 22.2	82.5 × 20	88.9 × 25	108 × 30	193.7 × 55
2	152.4 × 45	114.3 × 30	114.3 × 32	127 × 32	159 × 45	355.6 × 100
3	168.3 × 60	127 × 40	139.7 × 36	152.4 × 45	219.1 × 50	559 × 90
4	193.7 × 55	139.7 × 45	152.4 × 40	168.3 × 60	244.5 × 60	711 × 100
5	219.1 × 55	152.4 × 45	159 × 60	193.7 × 50	267 × 80	
6	219.1 × 70	159 × 50	177.8 × 55	193.7 × 60	273 × 100	
7	244.5 × 60	177.8 × 55	193.7 × 50	219.1 × 65	323.9 × 90	
8	244.5 × 60	177.8 × 60	219.1 × 50	244.5 × 65	355.6 × 90	
9	244.5 × 70	193.7 × 55	219.1 × 60	267 × 80		
10	244.5 × 70	219.1 × 50	219.1 × 70	267 × 90		
11	267 × 80	219.1 × 55	244.5 × 65	298.5 × 80		
12	267 × 80	219.1 × 60	244.5 × 80	298.5 × 90		
13	267 × 80	244.5 × 60	267 × 80			
14	267 × 90	244.5 × 65	267 × 90			
15	298.5 × 80	244.5 × 70	298.5 × 80			
16	298.5 × 90	244.5 × 80	298.5 × 90			
17	298.5 × 90	267 × 80				
18	298.5 × 90	267 × 90				
19	298.5 × 100	267 × 100				
20	323.9 × 90	267 × 100				
21	355.6 × 90	298.5 × 90				
22	355.6 × 100	298.5 × 90				
23	355.6 × 100	323.9 × 100				
24	355.6 × 100	323.9 × 100				
25	368 × 100					
26	368 × 100					
27	406.4 × 100					
28	419 × 100					
29	419 × 100					
30	419 × 100					
31	457 × 90					
32	457 × 90					
33	508 × 90					
34	508 × 90					
35	508 × 90					
36	508 × 90					
37	508 × 100					

38	508 × 100					
39	559 × 90					
40	559 × 90					
41	559 × 90					
42	559 × 100					
43	559 × 100					
44	610 × 90					
45	610 × 90					
46	610 × 100					
47	610 × 100					
48	660 × 90					

Table 7. CHS cross-sections (diameter × thickness, in mm) adopted for the twenty-four uniform-angle diagrid patterns based on the strength- and stiffness-based preliminary design, for the octagonal building with N = 48. Each cross-section refers to a specific diagrid module in the building. Diagrid modules are ordered from the top to the bottom, i.e. module no.1 is the top module.

Diagrid module no.	O1	O2	O3	O4	O6	O12
1	127 × 30	82.5 × 25	82.5 × 20	88.9 × 25	108 × 30	193.7 × 60
2	152.4 × 40	114.3 × 30	114.3 × 32	127 × 32	159 × 45	355.6 × 100
3	159 × 60	127 × 36	139.7 × 36	152.4 × 45	219.1 × 50	559 × 100
4	193.7 × 50	139.7 × 40	152.4 × 40	168.3 × 60	244.5 × 60	1620 × 40
5	219.1 × 50	152.4 × 45	159 × 60	177.8 × 60	244.5 × 90	
6	219.1 × 65	159 × 60	177.8 × 55	219.1 × 55	298.5 × 90	
7	219.1 × 65	177.8 × 55	193.7 × 50	219.1 × 60	323.9 × 90	
8	219.1 × 70	177.8 × 60	219.1 × 50	244.5 × 65	368 × 100	
9	244.5 × 65	193.7 × 55	219.1 × 55	244.5 × 80		
10	244.5 × 65	219.1 × 50	244.5 × 60	267 × 100		
11	244.5 × 90	219.1 × 55	244.5 × 60	267 × 100		
12	244.5 × 90	219.1 × 60	244.5 × 80	298.5 × 100		
13	244.5 × 90	219.1 × 65	244.5 × 90			
14	244.5 × 90	244.5 × 65	267 × 90			
15	267 × 90	244.5 × 65	273 × 100			
16	298.5 × 80	244.5 × 80	298.5 × 90			
17	298.5 × 80	244.5 × 90				
18	298.5 × 80	267 × 90				
19	298.5 × 80	267 × 90				
20	298.5 × 100	267 × 100				
21	323.9 × 90	273 × 100				
22	355.6 × 90	298.5 × 90				
23	355.6 × 90	323.9 × 90				
24	355.6 × 90	323.9 × 100				
25	355.6 × 90					
26	355.6 × 100					
27	368 × 100					
28	406.4 × 90					
29	406.4 × 100					
30	406.4 × 100					
31	406.4 × 100					
32	419 × 100					
33	419 × 100					
34	457 × 100					

35	508 × 90					
36	508 × 90					
37	508 × 90					
38	508 × 100					
39	508 × 100					
40	559 × 90					
41	559 × 90					
42	559 × 90					
43	559 × 90					
44	559 × 100					
45	610 × 90					
46	610 × 90					
47	610 × 90					
48	610 × 100					

Table 8. CHS cross-sections (diameter × thickness, in mm) adopted for the twenty-four uniform-angle diagrid patterns based on the strength- and stiffness-based preliminary design. for the circular building with $N = 48$. Each cross-section refers to a specific diagrid module in the building. Diagrid modules are ordered from the top to the bottom, i.e. module no.1 is the top module.

Diagrid module no.	C1	C2	C3	C4	C6	C12
1	114.3 × 32	82.5 × 22.2	82.5 × 17.5	101.6 × 20	114.3 × 28	219.1 × 50
2	152.4 × 40	114.3 × 30	114.3 × 30	127 × 36	159 × 50	406.4 × 90
3	159 × 60	127 × 32	139.7 × 36	152.4 × 50	219.1 × 55	610 × 90
4	193.7 × 50	139.7 × 40	152.4 × 40	177.8 × 55	244.5 × 65	1820 × 36
5	193.7 × 55	152.4 × 45	159 × 60	193.7 × 50	267 × 80	
6	219.1 × 60	159 × 50	177.8 × 55	219.1 × 55	298.5 × 80	
7	219.1 × 65	177.8 × 55	193.7 × 50	219.1 × 65	323.9 × 100	
8	219.1 × 70	177.8 × 60	219.1 × 55	244.5 × 70	368 × 100	
9	244.5 × 65	193.7 × 55	219.1 × 60	244.5 × 80		
10	244.5 × 65	193.7 × 60	244.5 × 60	267 × 100		
11	244.5 × 70	219.1 × 55	244.5 × 65	273 × 100		
12	244.5 × 90	219.1 × 55	244.5 × 80	298.5 × 100		
13	244.5 × 90	219.1 × 65	267 × 80			
14	244.5 × 90	244.5 × 65	267 × 90			
15	267 × 80	244.5 × 65	273 × 100			
16	267 × 100	244.5 × 70	298.5 × 80			
17	298.5 × 80	244.5 × 90				
18	298.5 × 80	267 × 90				
19	298.5 × 80	267 × 100				
20	298.5 × 80	273 × 100				
21	298.5 × 100	298.5 × 80				
22	323.9 × 90	298.5 × 90				
23	355.6 × 90	323.9 × 90				
24	355.6 × 90	323.9 × 90				
25	355.6 × 90					
26	355.6 × 90					
27	355.6 × 100					
28	368 × 100					
29	406.4 × 90					
30	406.4 × 100					
31	406.4 × 100					

32	406.4 × 100					
33	419 × 100					
34	457 × 90					
35	457 × 90					
36	457 × 100					
37	457 × 100					
38	457 × 100					
39	508 × 90					
40	508 × 100					
41	508 × 100					
42	508 × 100					
43	508 × 100					
44	559 × 90					
45	559 × 100					
46	610 × 90					
47	610 × 90					
48	610 × 100					

Table 9. CHS cross-sections (diameter × thickness, in mm) adopted for the twenty-four uniform-angle diagrid patterns based on the strength- and stiffness-based preliminary design, for the square building with $N = 60$. Each cross-section refers to a specific diagrid module in the building. Diagrid modules are ordered from the top to the bottom, i.e. module no.1 is the top module.

Diagrid module no.	S1	S2	S3	S4	S6	S12
1	2220 × 40	114.3 × 30	101.6 × 30	108 × 28	114.3 × 32	193.7 × 55
2	2220 × 40	139.7 × 40	139.7 × 45	139.7 × 50	177.8 × 55	368 × 100
3	2220 × 40	168.3 × 60	159 × 45	177.8 × 55	219.1 × 70	559 × 100
4	2220 × 40	193.7 × 55	177.8 × 60	219.1 × 55	244.5 × 90	1820 × 36
5	2220 × 40	219.1 × 55	219.1 × 55	219.1 × 70	298.5 × 80	2220 × 40
6	2220 × 40	219.1 × 70	219.1 × 60	244.5 × 70	323.9 × 100	
7	2220 × 40	244.5 × 60	244.5 × 60	244.5 × 90	368 × 100	
8	2220 × 40	244.5 × 70	244.5 × 70	267 × 100	419 × 100	
9	2220 × 40	244.5 × 80	244.5 × 90	298.5 × 100	508 × 90	
10	2220 × 40	267 × 80	267 × 100	323.9 × 100	559 × 90	
11	2220 × 40	267 × 80	273 × 100	355.6 × 90		
12	2220 × 40	267 × 100	298.5 × 100	406.4 × 90		
13	2220 × 40	298.5 × 90	323.9 × 100	406.4 × 100		
14	2220 × 40	298.5 × 90	323.9 × 100	457 × 90		
15	2220 × 40	298.5 × 100	368 × 100	457 × 100		
16	2220 × 40	323.9 × 100	406.4 × 90			
17	2220 × 40	355.6 × 90	419 × 100			
18	2220 × 40	355.6 × 100	457 × 90			
19	2220 × 40	368 × 100	457 × 100			
20	2220 × 40	368 × 100	508 × 90			
21	2220 × 40	406.4 × 100				
22	2220 × 40	419 × 100				
23	2220 × 40	457 × 90				
24	2220 × 40	457 × 100				
25	2220 × 40	508 × 90				
26	2220 × 40	508 × 90				
27	2220 × 40	559 × 100				
28	2220 × 40	559 × 100				

29	2220 × 40	610 × 90				
30	2220 × 40	610 × 90				
31	2220 × 40					
32	2220 × 40					
33	2220 × 40					
34	2220 × 40					
35	2220 × 40					
36	2220 × 40					
37	2220 × 40					
38	2220 × 40					
39	2220 × 40					
40	2220 × 40					
41	2220 × 40					
42	2220 × 40					
43	2220 × 40					
44	2220 × 40					
45	2220 × 40					
46	2220 × 40					
47	2220 × 40					
48	2220 × 40					
49	2220 × 40					
50	2220 × 40					
51	2220 × 40					
52	2220 × 40					
53	2220 × 40					
54	2220 × 40					
55	2220 × 40					
56	2220 × 40					
57	2220 × 40					
58	2220 × 40					
59	2220 × 40					
60	2220 × 40					

Table 10. CHS cross-sections (diameter × thickness, in mm) adopted for the twenty-four uniform-angle diagrid patterns based on the strength- and stiffness-based preliminary design, for the hexagonal building with N = 60. Each cross-section refers to a specific diagrid module in the building. Diagrid modules are ordered from the top to the bottom, i.e. module no.1 is the top module.

Diagrid module no.	H1	H2	H3	H4	H6	H12
1	168.3 × 60	108 × 30	101.6 × 28	108 × 30	114.3 × 36	219.1 × 60
2	219.1 × 60	139.7 × 36	139.7 × 40	139.7 × 50	177.8 × 60	406.4 × 90
3	244.5 × 70	152.4 × 50	159 × 45	177.8 × 60	219.1 × 70	610 × 100
4	267 × 90	168.3 × 60	177.8 × 55	219.1 × 60	267 × 80	2020 × 40
5	298.5 × 80	193.7 × 50	219.1 × 55	219.1 × 70	298.5 × 100	2220 × 40
6	323.9 × 90	219.1 × 55	219.1 × 60	244.5 × 80	323.9 × 100	
7	323.9 × 100	219.1 × 65	244.5 × 60	244.5 × 90	406.4 × 90	
8	355.6 × 90	219.1 × 70	244.5 × 70	273 × 100	457 × 90	
9	355.6 × 100	244.5 × 65	244.5 × 90	298.5 × 90	559 × 90	
10	368 × 100	244.5 × 80	267 × 100	323.9 × 100	559 × 100	
11	406.4 × 100	244.5 × 90	298.5 × 80	355.6 × 90		
12	406.4 × 100	267 × 80	298.5 × 90	406.4 × 100		
13	406.4 × 100	298.5 × 80	323.9 × 90	419 × 100		
14	419 × 100	298.5 × 80	355.6 × 90	457 × 100		
15	508 × 100	298.5 × 100	406.4 × 90	508 × 100		

16	508 × 100	323.9 × 90	406.4 × 100			
17	508 × 100	355.6 × 90	457 × 90			
18	508 × 100	355.6 × 90	457 × 90			
19	559 × 100	355.6 × 100	508 × 90			
20	610 × 90	368 × 100	508 × 90			
21	660 × 90	406.4 × 100				
22	660 × 90	419 × 100				
23	660 × 90	457 × 90				
24	660 × 90	457 × 100				
25	660 × 100	508 × 90				
26	711 × 100	508 × 90				
27	1820 × 36	559 × 90				
28	1820 × 36	559 × 100				
29	1820 × 40	610 × 90				
30	1820 × 40	610 × 90				
31	2020 × 36					
32	2020 × 40					
33	2220 × 40					
34	2220 × 40					
35	2220 × 40					
36	2220 × 40					
37	2220 × 40					
38	2220 × 40					
39	2220 × 40					
40	2220 × 40					
41	2220 × 40					
42	2220 × 40					
43	2220 × 40					
44	2220 × 40					
45	2220 × 40					
46	2220 × 40					
47	2220 × 40					
48	2220 × 40					
49	2220 × 40					
50	2220 × 40					
51	2220 × 40					
52	2220 × 40					
53	2220 × 40					
54	2220 × 40					
55	2220 × 40					
56	2220 × 40					
57	2220 × 40					
58	2220 × 40					
59	2220 × 40					
60	2220 × 40					

Table 11. CHS cross-sections (diameter × thickness, in mm) adopted for the twenty-four uniform-angle diagrid patterns based on the strength- and stiffness-based preliminary design, for the octagonal building with N = 60. Each cross-section refers to a specific diagrid module in the building. Diagrid modules are ordered from the top to the bottom, i.e. module no.1 is the top module.

Diagrid module no.	O1	O2	O3	O4	O6	O12
1	152.4 × 50	108 × 28	101.6 × 25	108 × 28	114.3 × 36	219.1 × 70
2	193.7 × 60	139.7 × 36	139.7 × 40	139.7 × 45	193.7 × 50	406.4 × 100

3	219.1 × 70	152.4 × 50	159 × 45	177.8 × 55	244.5 × 60	660 × 90
4	244.5 × 80	168.3 × 60	177.8 × 55	219.1 × 55	267 × 90	2220 × 40
5	267 × 90	193.7 × 50	219.1 × 50	244.5 × 60	298.5 × 90	2220 × 40
6	298.5 × 80	219.1 × 60	219.1 × 60	244.5 × 80	355.6 × 90	
7	298.5 × 90	219.1 × 65	219.1 × 70	267 × 90	368 × 100	
8	298.5 × 90	219.1 × 70	244.5 × 70	273 × 100	457 × 100	
9	323.9 × 90	244.5 × 65	244.5 × 80	298.5 × 100	508 × 100	
10	323.9 × 90	244.5 × 90	267 × 100	323.9 × 100	610 × 90	
11	355.6 × 100	244.5 × 90	267 × 100	355.6 × 100		
12	355.6 × 100	267 × 90	298.5 × 100	406.4 × 90		
13	355.6 × 100	267 × 100	323.9 × 90	457 × 90		
14	368 × 100	298.5 × 80	323.9 × 100	457 × 90		
15	406.4 × 90	298.5 × 80	355.6 × 100	508 × 90		
16	457 × 90	323.9 × 90	406.4 × 90			
17	457 × 90	323.9 × 100	419 × 100			
18	457 × 90	355.6 × 90	457 × 100			
19	457 × 90	355.6 × 90	457 × 100			
20	508 × 90	368 × 100	508 × 100			
21	508 × 100	406.4 × 90				
22	559 × 100	419 × 100				
23	559 × 100	419 × 100				
24	559 × 100	457 × 100				
25	559 × 100	457 × 100				
26	610 × 90	508 × 90				
27	610 × 100	508 × 100				
28	660 × 100	508 × 100				
29	660 × 100	559 × 100				
30	660 × 100	610 × 90				
31	660 × 100					
32	711 × 100					
33	1620 × 40					
34	1820 × 36					
35	1820 × 36					
36	1820 × 40					
37	2020 × 36					
38	2020 × 36					
39	2020 × 40					
40	2020 × 40					
41	2020 × 40					
42	2220 × 40					
43	2220 × 40					
44	2220 × 40					
45	2220 × 40					
46	2220 × 40					
47	2220 × 40					
48	2220 × 40					
49	2220 × 40					
50	2220 × 40					
51	2220 × 40					
52	2220 × 40					
53	2220 × 40					
54	2220 × 40					
55	2220 × 40					

56	2220 × 40					
57	2220 × 40					
58	2220 × 40					
59	2220 × 40					
60	2220 × 40					

Table 12. CHS cross-sections (diameter × thickness, in mm) adopted for the twenty-four uniform-angle diagrid patterns based on the strength- and stiffness-based preliminary design, for the circular building with $N = 60$. Each cross-section refers to a specific diagrid module in the building. Diagrid modules are ordered from the top to the bottom, i.e. module no.1 is the top module.

Diagrid module no.	C1	C2	C3	C4	C6	C12
1	139.7 × 50	108 × 28	101.6 × 25	108 × 30	127 × 30	244.5 × 60
2	193.7 × 55	139.7 × 36	139.7 × 40	139.7 × 50	193.7 × 50	419 × 100
3	219.1 × 65	152.4 × 45	159 × 45	177.8 × 60	244.5 × 65	660 × 100
4	244.5 × 70	159 × 60	177.8 × 55	219.1 × 60	267 × 100	2220 × 40
5	244.5 × 90	193.7 × 50	219.1 × 50	219.1 × 70	298.5 × 100	2220 × 40
6	273 × 100	219.1 × 50	219.1 × 65	244.5 × 80	355.6 × 100	
7	273 × 100	219.1 × 65	244.5 × 60	267 × 80	406.4 × 90	
8	298.5 × 80	219.1 × 70	244.5 × 80	273 × 100	457 × 100	
9	298.5 × 100	244.5 × 65	244.5 × 90	298.5 × 100	559 × 90	
10	298.5 × 100	244.5 × 80	273 × 100	323.9 × 100	610 × 90	
11	323.9 × 90	244.5 × 90	298.5 × 80	355.6 × 90		
12	355.6 × 90	267 × 80	298.5 × 100	406.4 × 100		
13	355.6 × 90	267 × 100	323.9 × 100	457 × 90		
14	355.6 × 90	298.5 × 80	355.6 × 90	457 × 100		
15	355.6 × 100	298.5 × 80	368 × 100	508 × 100		
16	406.4 × 100	298.5 × 100	406.4 × 90			
17	419 × 100	323.9 × 100	419 × 100			
18	419 × 100	355.6 × 90	457 × 90			
19	419 × 100	355.6 × 90	457 × 100			
20	457 × 90	355.6 × 100	508 × 90			
21	508 × 90	406.4 × 90				
22	508 × 100	406.4 × 100				
23	559 × 90	419 × 100				
24	559 × 90	457 × 90				
25	559 × 90	457 × 100				
26	559 × 90	508 × 90				
27	559 × 100	508 × 100				
28	610 × 100	559 × 90				
29	660 × 90	559 × 100				
30	660 × 90	610 × 90				
31	660 × 90					
32	660 × 100					
33	660 × 100					
34	711 × 100					
35	1620 × 40					
36	1620 × 40					
37	1620 × 40					
38	1820 × 36					
39	1820 × 40					
40	1820 × 40					
41	1820 × 40					
42	1820 × 40					

43	2020 × 36					
44	2020 × 40					
45	2220 × 40					
46	2220 × 40					
47	2220 × 40					
48	2220 × 40					
49	2220 × 40					
50	2220 × 40					
51	2220 × 40					
52	2220 × 40					
53	2220 × 40					
54	2220 × 40					
55	2220 × 40					
56	2220 × 40					
57	2220 × 40					
58	2220 × 40					
59	2220 × 40					
60	2220 × 40					

Table 13. CHS cross-sections (diameter × thickness, in mm) adopted for the twenty-four uniform-angle diagrid patterns based on the strength- and stiffness-based preliminary design, for the square building with $N = 72$. Each cross-section refers to a specific diagrid module in the building. Diagrid modules are ordered from the top to the bottom, i.e. module no.1 is the top module.

Diagrid module no.	S1	S2	S3	S4	S6	S12
1	2220 × 40	127 × 45	127 × 32	127 × 30	127 × 40	267 × 80
2	2220 × 40	159 × 50	159 × 60	159 × 50	219.1 × 55	508 × 90
3	2220 × 40	219.1 × 55	193.7 × 55	219.1 × 55	244.5 × 90	1820 × 40
4	2220 × 40	244.5 × 60	219.1 × 65	244.5 × 70	298.5 × 80	2220 × 40
5	2220 × 40	244.5 × 80	244.5 × 80	267 × 80	355.6 × 90	2220 × 40
6	2220 × 40	267 × 90	267 × 80	273 × 100	406.4 × 100	2220 × 40
7	2220 × 40	267 × 100	273 × 100	323.9 × 90	457 × 100	
8	2220 × 40	298.5 × 80	298.5 × 80	323.9 × 100	559 × 90	
9	2220 × 40	298.5 × 90	323.9 × 90	406.4 × 90	610 × 100	
10	2220 × 40	323.9 × 90	355.6 × 90	406.4 × 100	660 × 100	
11	2220 × 40	323.9 × 100	368 × 100	457 × 100	1820 × 36	
12	2220 × 40	355.6 × 90	406.4 × 100	508 × 100	1820 × 40	
13	2220 × 40	406.4 × 90	419 × 100	559 × 100		
14	2220 × 40	406.4 × 90	457 × 90	610 × 90		
15	2220 × 40	419 × 100	508 × 100	610 × 100		
16	2220 × 40	457 × 90	559 × 90	660 × 90		
17	2220 × 40	508 × 90	610 × 90	1620 × 40		
18	2220 × 40	508 × 90	610 × 90	1620 × 40		
19	2220 × 40	508 × 100	660 × 90			
20	2220 × 40	559 × 90	660 × 90			
21	2220 × 40	610 × 90	660 × 100			
22	2220 × 40	610 × 90	711 × 100			
23	2220 × 40	660 × 90	1620 × 40			
24	2220 × 40	660 × 90	1820 × 40			
25	2220 × 40	660 × 100				
26	2220 × 40	711 × 100				
27	2220 × 40	1620 × 40				
28	2220 × 40	1620 × 40				
29	2220 × 40	1820 × 36				

30	2220 × 40	1820 × 40				
31	2220 × 40	2020 × 36				
32	2220 × 40	2020 × 36				
33	2220 × 40	2220 × 40				
34	2220 × 40	2220 × 40				
35	2220 × 40	2220 × 40				
36	2220 × 40	2220 × 40				
37	2220 × 40					
38	2220 × 40					
39	2220 × 40					
40	2220 × 40					
41	2220 × 40					
42	2220 × 40					
43	2220 × 40					
44	2220 × 40					
45	2220 × 40					
46	2220 × 40					
47	2220 × 40					
48	2220 × 40					
49	2220 × 40					
50	2220 × 40					
51	2220 × 40					
52	2220 × 40					
53	2220 × 40					
54	2220 × 40					
55	2220 × 40					
56	2220 × 40					
57	2220 × 40					
58	2220 × 40					
59	2220 × 40					
60	2220 × 40					
61	2220 × 40					
62	2220 × 40					
63	2220 × 40					
64	2220 × 40					
65	2220 × 40					
66	2220 × 40					
67	2220 × 40					
68	2220 × 40					
69	2220 × 40					
70	2220 × 40					
71	2220 × 40					
72	2220 × 40					

Table 14. CHS cross-sections (diameter × thickness, in mm) adopted for the twenty-four uniform-angle diagrid patterns based on the strength- and stiffness-based preliminary design, for the hexagonal building with N = 72. Each cross-section refers to a specific diagrid module in the building. Diagrid modules are ordered from the top to the bottom, i.e. module no.1 is the top module.

Diagrid module no.	H1	H2	H3	H4	H6	H12
1	2220 × 40	127 × 36	114.3 × 36	127 × 30	127 × 45	323.9 × 100
2	2220 × 40	152.4 × 50	159 × 50	159 × 50	219.1 × 65	711 × 100

3	2220 × 40	193.7 × 50	193.7 × 50	219.1 × 55	267 × 80	2220 × 40
4	2220 × 40	219.1 × 55	219.1 × 55	244.5 × 70	298.5 × 90	2220 × 40
5	2220 × 40	219.1 × 70	244.5 × 70	267 × 80	355.6 × 100	2220 × 40
6	2220 × 40	244.5 × 80	244.5 × 80	273 × 100	406.4 × 100	2220 × 40
7	2220 × 40	267 × 80	267 × 90	298.5 × 100	508 × 90	
8	2220 × 40	267 × 80	273 × 100	323.9 × 100	559 × 100	
9	2220 × 40	273 × 100	298.5 × 100	406.4 × 90	660 × 100	
10	2220 × 40	298.5 × 90	323.9 × 100	406.4 × 100	660 × 100	
11	2220 × 40	298.5 × 90	368 × 100	508 × 90	1820 × 40	
12	2220 × 40	323.9 × 90	406.4 × 90	508 × 100	2020 × 36	
13	2220 × 40	355.6 × 100	419 × 100	610 × 90		
14	2220 × 40	355.6 × 100	457 × 90	610 × 90		
15	2220 × 40	406.4 × 100	508 × 100	660 × 90		
16	2220 × 40	406.4 × 100	559 × 90	711 × 100		
17	2220 × 40	457 × 90	559 × 100	1820 × 36		
18	2220 × 40	457 × 90	610 × 90	1820 × 40		
19	2220 × 40	508 × 90	660 × 90			
20	2220 × 40	508 × 100	660 × 90			
21	2220 × 40	559 × 100	711 × 100			
22	2220 × 40	559 × 100	711 × 100			
23	2220 × 40	610 × 100	1820 × 40			
24	2220 × 40	610 × 100	2020 × 36			
25	2220 × 40	660 × 100				
26	2220 × 40	660 × 100				
27	2220 × 40	711 × 100				
28	2220 × 40	711 × 100				
29	2220 × 40	1820 × 36				
30	2220 × 40	1820 × 40				
31	2220 × 40	2020 × 36				
32	2220 × 40	2020 × 36				
33	2220 × 40	2220 × 40				
34	2220 × 40	2220 × 40				
35	2220 × 40	2220 × 40				
36	2220 × 40	2220 × 40				
37	2220 × 40					
38	2220 × 40					
39	2220 × 40					
40	2220 × 40					
41	2220 × 40					
42	2220 × 40					
43	2220 × 40					
44	2220 × 40					
45	2220 × 40					
46	2220 × 40					
47	2220 × 40					
48	2220 × 40					
49	2220 × 40					
50	2220 × 40					
51	2220 × 40					
52	2220 × 40					
53	2220 × 40					
54	2220 × 40					
55	2220 × 40					

56	2220 × 40					
57	2220 × 40					
58	2220 × 40					
59	2220 × 40					
60	2220 × 40					
61	2220 × 40					
62	2220 × 40					
63	2220 × 40					
64	2220 × 40					
65	2220 × 40					
66	2220 × 40					
67	2220 × 40					
68	2220 × 40					
69	2220 × 40					
70	2220 × 40					
71	2220 × 40					
72	2220 × 40					

Table 15. CHS cross-sections (diameter × thickness, in mm) adopted for the twenty-four uniform-angle diagrid patterns based on the strength- and stiffness-based preliminary design, for the octagonal building with N = 72. Each cross-section refers to a specific diagrid module in the building. Diagrid modules are ordered from the top to the bottom, i.e. module no.1 is the top module.

Diagrid module no.	O1	O2	O3	O4	O6	O12
1	2220 × 40	127 × 32	114.3 × 32	127 × 30	127 × 45	419 × 100
2	2220 × 40	152.4 × 50	159 × 50	159 × 50	219.1 × 65	2220 × 40
3	2220 × 40	177.8 × 60	193.7 × 50	219.1 × 55	267 × 80	2220 × 40
4	2220 × 40	219.1 × 50	219.1 × 55	244.5 × 70	298.5 × 90	2220 × 40
5	2220 × 40	219.1 × 65	244.5 × 70	267 × 80	355.6 × 100	2220 × 40
6	2220 × 40	244.5 × 80	244.5 × 80	273 × 100	419 × 100	2220 × 40
7	2220 × 40	244.5 × 90	267 × 90	298.5 × 90	457 × 100	
8	2220 × 40	267 × 90	273 × 100	355.6 × 90	610 × 90	
9	2220 × 40	267 × 100	298.5 × 90	368 × 100	610 × 100	
10	2220 × 40	298.5 × 90	323.9 × 100	419 × 100	711 × 100	
11	2220 × 40	298.5 × 90	355.6 × 90	457 × 90	1620 × 40	
12	2220 × 40	323.9 × 90	406.4 × 100	559 × 90	2220 × 40	
13	2220 × 40	355.6 × 90	406.4 × 100	559 × 100		
14	2220 × 40	355.6 × 100	457 × 90	610 × 100		
15	2220 × 40	368 × 100	457 × 100	610 × 100		
16	2220 × 40	406.4 × 100	559 × 90	711 × 100		
17	2220 × 40	419 × 100	559 × 100	711 × 100		
18	2220 × 40	457 × 90	610 × 90	1820 × 40		
19	2220 × 40	457 × 100	610 × 100			
20	2220 × 40	508 × 100	660 × 100			
21	2220 × 40	559 × 90	711 × 100			
22	2220 × 40	559 × 100	1620 × 40			
23	2220 × 40	610 × 90	1820 × 36			
24	2220 × 40	610 × 100	2020 × 36			
25	2220 × 40	610 × 100				
26	2220 × 40	660 × 100				
27	2220 × 40	660 × 100				
28	2220 × 40	711 × 100				
29	2220 × 40	1620 × 40				
30	2220 × 40	1820 × 40				
31	2220 × 40	1820 × 40				

32	2220 × 40	2020 × 36				
33	2220 × 40	2020 × 36				
34	2220 × 40	2220 × 40				
35	2220 × 40	2220 × 40				
36	2220 × 40	2220 × 40				
37	2220 × 40					
38	2220 × 40					
39	2220 × 40					
40	2220 × 40					
41	2220 × 40					
42	2220 × 40					
43	2220 × 40					
44	2220 × 40					
45	2220 × 40					
46	2220 × 40					
47	2220 × 40					
48	2220 × 40					
49	2220 × 40					
50	2220 × 40					
51	2220 × 40					
52	2220 × 40					
53	2220 × 40					
54	2220 × 40					
55	2220 × 40					
56	2220 × 40					
57	2220 × 40					
58	2220 × 40					
59	2220 × 40					
60	2220 × 40					
61	2220 × 40					
62	2220 × 40					
63	2220 × 40					
64	2220 × 40					
65	2220 × 40					
66	2220 × 40					
67	2220 × 40					
68	2220 × 40					
69	2220 × 40					
70	2220 × 40					
71	2220 × 40					
72	2220 × 40					

Table 16. CHS cross-sections (diameter × thickness, in mm) adopted for the twenty-four uniform-angle diagrid patterns based on the strength- and stiffness-based preliminary design, for the circular building with $N = 72$. Each cross-section refers to a specific diagrid module in the building. Diagrid modules are ordered from the top to the bottom, i.e. module no.1 is the top module.

Diagrid module no.	C1	C2	C3	C4	C6	C12
1	2220 × 40	127 × 30	114.3 × 32	127 × 30	139.7 × 36	2220 × 40
2	2220 × 40	152.4 × 50	159 × 50	159 × 60	219.1 × 70	2220 × 40
3	2220 × 40	177.8 × 60	193.7 × 50	219.1 × 60	267 × 90	2220 × 40
4	2220 × 40	219.1 × 50	219.1 × 55	244.5 × 80	298.5 × 100	2220 × 40
5	2220 × 40	219.1 × 65	244.5 × 70	267 × 90	368 × 100	2220 × 40

6	2220 × 40	244.5 × 70	244.5 × 80	298.5 × 80	419 × 100	2220 × 40
7	2220 × 40	244.5 × 90	267 × 90	298.5 × 100	508 × 90	
8	2220 × 40	267 × 80	273 × 100	355.6 × 90	610 × 90	
9	2220 × 40	267 × 100	298.5 × 90	406.4 × 90	660 × 90	
10	2220 × 40	298.5 × 80	323.9 × 100	419 × 100	1620 × 40	
11	2220 × 40	298.5 × 90	355.6 × 90	457 × 100	1820 × 40	
12	2220 × 40	298.5 × 100	406.4 × 90	559 × 90	2020 × 40	
13	2220 × 40	355.6 × 90	406.4 × 100	610 × 90		
14	2220 × 40	355.6 × 100	419 × 100	610 × 100		
15	2220 × 40	368 × 100	508 × 90	660 × 90		
16	2220 × 40	406.4 × 100	508 × 100	711 × 100		
17	2220 × 40	419 × 100	559 × 100	1620 × 40		
18	2220 × 40	457 × 90	610 × 100	1820 × 36		
19	2220 × 40	457 × 100	660 × 90			
20	2220 × 40	508 × 90	660 × 100			
21	2220 × 40	559 × 90	711 × 100			
22	2220 × 40	559 × 100	1620 × 40			
23	2220 × 40	610 × 90	1820 × 36			
24	2220 × 40	610 × 100	1820 × 40			
25	2220 × 40	660 × 90				
26	2220 × 40	660 × 100				
27	2220 × 40	711 × 100				
28	2220 × 40	1620 × 40				
29	2220 × 40	1820 × 36				
30	2220 × 40	1820 × 36				
31	2220 × 40	1820 × 40				
32	2220 × 40	2020 × 36				
33	2220 × 40	2020 × 36				
34	2220 × 40	2020 × 40				
35	2220 × 40	2220 × 40				
36	2220 × 40	2220 × 40				
37	2220 × 40					
38	2220 × 40					
39	2220 × 40					
40	2220 × 40					
41	2220 × 40					
42	2220 × 40					
43	2220 × 40					
44	2220 × 40					
45	2220 × 40					
46	2220 × 40					
47	2220 × 40					
48	2220 × 40					
49	2220 × 40					
50	2220 × 40					
51	2220 × 40					
52	2220 × 40					
53	2220 × 40					
54	2220 × 40					
55	2220 × 40					
56	2220 × 40					
57	2220 × 40					

58	2220 × 40					
59	2220 × 40					
60	2220 × 40					
61	2220 × 40					
62	2220 × 40					
63	2220 × 40					
64	2220 × 40					
65	2220 × 40					
66	2220 × 40					
67	2220 × 40					
68	2220 × 40					
69	2220 × 40					
70	2220 × 40					
71	2220 × 40					
72	2220 × 40					